UNDERSTANDING THE VIRAL-HOST INTERACTIONS OF NEWLY EMERGED AND HIGHLY PATHOGENIC HUMAN CORONAVIRUSES

NG OI WING

(B.Sc.(Hons.), NTU)

A THESIS SUBMITTED
FOR THE DEGREE OF DOCTOR OF PHILOSOPHY

DEPARTMENT OF MICROBIOLOGY

NATIONAL UNIVERSITY OF SINGAPORE

2015

DECLARATION

I hereby declare that this thesis is my original work and it has been written by me in its entirety. I have duly acknowledged all the sources of information which have been used in the thesis.

This thesis has also not been submitted for any degree in any university previously.

Ng Oi Wing

24 July 2015

ACKNOWLEDGEMENTS

Firstly, I would like to express my greatest gratitude to my supervisor, A/Prof Tan Yee Joo. This work would not have been possible without her invaluable mentorship, scientific insights and advice. Sincere thanks to her for the patience and guidance in supervising me through my PhD studies. The support and opportunities that she has given me in the past 4 years have greatly broadened my scientific learning and helped me mature as a scientist.

I would like to acknowledge members of my thesis advisory committee, A/Prof Vincent Chow and Dr Zhang Yongliang, for their time in attending our meetings as well as their constructive suggestions for my PhD projects. I would also like to thank our collaborators, Professor Malik Peiris, Dr Leo Poon and Cythia Leung from the University of Hong Kong for their help in the generation of the SARS escape mutant viruses. For the SARS T cell study, I would like to acknowledge Professor Antonio Bertoletti from DUKE-NUS Graduate Medical School for his expertise and Dr Leong Hoe Nam from the Singapore General Hospital for providing the patient blood samples. In addition, I would like to extend my thanks to the lab members of the AB lab, especially Dr Anthony Tan and Adeline Chia for their great help and input into the project.

Not forgetting the many people within NUS who has helped me in one way or another throughout this PhD journey. Sincere thanks to Dr Paul Hutchinson and Guo Wei from the Flow Cytometry Unit, Center of Life Sciences (CeLs), for their expertise and guidance in my flow cytometry experiments; Shu Ying and Weian from the Confocal Microscopy Unit, Yong Loo Lin School of Medicine, for their help in the confocal microscopy work and Benson for his time in helping me with the irradiation of cells

despite his busy schedule. I would also like to extend my thanks to the departmental staff from the Department of Microbiology who have provided me assistance in various ways.

To all members of the TYJ lab, both past and present, thank you all for the companionship, advice, encouragement and friendship. There have been ups and downs in the past 4 years, and words can't describe how much I appreciate each and every one of you for being an important part of this journey. To past members Sandy, Megha and Hwee Teng who have taught me many things and helped me settle into the lab since the start of my PhD studies, thank you for being such great colleagues and friends, for the inspiration and support. To present members Ching Wooen and Vanessa, thank you both for the continuous encouragement, advice and help throughout the years, especially in the final stretch. Not forgetting others including Jude, Bhaskar, Chee Keng, Jianping, Bernard, Subha and James, thank you all for your kindness and willingness to help each time I have questions or doubts.

I would like to express my deepest gratitude to my parents and siblings for their support and understanding that have allowed me to focus on my PhD studies. Last but not least, my heartfelt appreciation to my fiancé, Youyi, for being my pillar of strength and for his never-ending support and encouragement.

TABLE OF CONTENTS

SUMMARY

Newly emerged zoonotic coronaviruses cause severe diseases in humans and pose significant public health threats and challenges. In the past 12 years, we saw the emergences of two highly pathogenic human coronaviruses, the Severe Acute Respiratory Syndrome coronavirus (SARS-CoV) and the Middle East Respiratory Syndrome coronavirus (MERS-CoV), which are characterized by severe lower respiratory tract infections and high mortality rates. With the possible re-emergence of SARS-CoV and the ongoing MERS epidemic in Middle East, the availability of treatments and vaccines for these highly pathogenic viruses is of great urgency. In this thesis, we focused on the understanding of viral-host interactions in SARS-CoV and MERS-CoV, which is important for identifying potential drug targets and developing antiviral strategies.

In the first part of this thesis, we characterized two monoclonal antibodies (mAbs), 1A9 and 1G10, which bind to the SARS-CoV Spike (S) protein at two separate novel epitopes located within the highly conserved S2 domain. These mAbs possess broadly-neutralizing effects on infection of human SARS-CoV, zoonotic civet SARS-CoV and bat SARS-like-CoV strains *in vitro*. Through generating escape mutants, a substitution of aspartic acid (D) at residue 1128 with alanine (A) as found in escape mutants led to decrease in mAb 1A9 binding and resistance to mAb 1A9 neutralization. Furthermore, the D1128A mutation exerted no effects on the fundamental processing of S protein, suggesting that the escape virus retained similar property as wild-type virus. This work provided support for the usage of these mAbs in combination passive immunotherapy for SARS treatment. It also provided new information on two novel

neutralizing epitopes on SARS-CoV S protein, opening new avenues for the design of a universal SARS vaccine.

In the second study, we identified memory T cell responses from 3 SARS-convalescent individuals who recovered from SARS ranging from 9 to 11 years ago. We carried out in-depth characterizations of two SARS-specific $CD8^+$ T cell responses targeting the SARS-CoV membrane (M) and the nucleocapsid (N) protein and showed that these $CD8^+$ T cell responses persisted up to 11 years post-infection, indicating their long-lived nature. These $CD8^+$ T cell epitopes are fully conserved among human and civet SARS-CoVs and bat SARS-like-CoVs, indicating the cross-protection of the T cell responses. This information is important for our understanding of cellular immune responses in SARS-CoV infections and has implications on the design of effective SARS vaccines.

In the last part, we investigated the effects of the MERS-CoV N protein on cellular activities and functions in comparison to the SARS-CoV N protein. It was found that the MERS-CoV N protein shared some common properties as the SARS-CoV N protein. A specific viral-host interaction of MERS-CoV N protein and the host protein eukaryotic elongation factor 1 alpha (eEF1A) was demonstrated and this was found to have significant effects on cellular processes including translation and F-actin bundling. This study shed light into the possible roles of MERS-CoV N protein in virus replication and pathogenesis, and can be applicable in developing antiviral strategies targeting the N protein for effective treatment of MERS.

LIST OF TABLES

LIST OF FIGURES

ABBREVIATIONS

2’O-MTase	Nucleoside-2’-O-methyltransferase
3CLpro	3C-like proteinase
ACE2	Angiotensin-converting enzyme 2
ADCC	Antibody-dependent cellular cytotoxicity
ADCP	Antibody-dependent cellular phagocytosis
ARDS	Acute respiratory distress syndrome
BSL	Biosafety level
CAR	Chimeric antigen receptor
CDC	Complement-dependent cytotoxicity
CHO	Chinese hamster ovary
Co-IP	Co-immunoprecipitation
CPE	Cytopathic effect
CTL	Cytotoxic T lymphocyte
DAPI	4',6-diamidino-2-phenylindole
DC-SIGN	Dendritic cell-specific ICAM-3 grabbing non-integrin
DHFR	Dihydrofolate reductase
DMEM	Dulbecco’s modified Eagle’s medium
DMSO	Dimethyl sulfoxide
DMV	Double-membrane vesicle
DPP4	Dipeptidyl peptidase 4
DTT	Dithiothreitol
dsRNA	Double-stranded RNA
EBV	Epstein-Barr virus
EBV-LCL	Epstein-Barr virus-transformed lymphoblastoid B cell line
E. coli	*Escherichia coli*
EDTA	Ethylenediaminetetraacetic acid
eEF1A	Eukaryotic elongation factor 1 alpha
ELISA	Enzyme-linked immunosorbent assay
ELISpot	Enzyme-linked immunospot
ER	Endoplasmic reticulum
ERGIC	ER-Golgi intermediate compartment
ExoN	Exonuclease
FACS	Fluorescence-activated cell sorting
FBS	Fetal bovine serum
FCS	Fetal calf serum
FITC	Fluorescein isothiocyanate
GST	Gluthathione S-transferase
HBSS	Hank's Balanced Salt Solution
HCoV	Human coronavirus
HBV	Hepatitis B virus
HCV	Hepatitis C virus
HA	Hemagglutinin
HAT	Human airway tryptase
HE	Hemagglutinin-easterase
HEK	Human embryonic kidney

HIV	Human Immunodeficiency Virus
HLA	Human Leukocyte Antigen
ICS	Intracellular cytokine staining
IFN	Interferon
IL	Interleukin
IP	Immunoprecipitation
IPTG	Isopropyl β-D-thiogalactopyranoside
LB	Luria-Bertani media
LSECtin	Liver and lymph node sinusoidal endothelial cell C-type lectin
mAbs	Monoclonal antibodies
MERS	Middle East Respiratory Syndrome
MERS-CoV	Middle East Respiratory Syndrome coronavirus
MHV	Mouse hepatitis virus
MLV	Murine leukemia virus
NES	Nuclear export signal
NLS	Nuclear localization signal
NP40	Nonidet P-40
NSP	Non-structural protein
N7-Mtase	(Guanine)-N7-methyltransferase
ORFs	Open reading frames
PBMCs	Peripheral blood mononuclear cells
PBS	Phosphate buffered saline
PE	Phycoerythrin
PerCP	Peridinin chlorophyll protein
PFA	Paraformaldehyde
PLpro	Papain-like proteinase
PHA	Phytohemagglutinin
PHB	Prohibitin
PMA	Phorbol 12-myristate 13-acetate
PMSF	Phenylmethylsulfonyl fluoride
RBD	Receptor-binding domain
RdRp	RNA-dependent RNA polymerase
RNAi	RNA interference
RTC	Replication-transcription complex
SARS	Severe Acute Respiratory Syndrome
SARS-CoV	Severe Acute Respiratory Syndrome coronavirus
SDS-PAGE	Sodium dodecyl sulfate polyacrylamide gel electrophoresis
SFU	Spot-forming unit
S-pp	S-pseudotyped virus particle
ssRNA	single-stranded RNA
SUD	SARS unique domain
SL-CoVs	SARS-like coronaviruses
TB	Terrific broth medium
TCR	T cell receptor
$TCID_{50}$	50% Tissue Culture Infective Dose
TGEV	Transmissible gastroenteritis virus
TMPRSS2	Transmembrane protease serine 2
TPase	Triphosphase

TTSP	Transmembrane serine protease
WB	Western blot
WT	Wild-type
VSV-G	Vesicular stomatitis virus G protein

LIST OF JOURNAL ARTICLES

1) **Ng OW**, Keng CT, Leung CS, Peiris JS, Poon LL, Tan YJ. Substitution at aspartic acid 1128 in the SARS coronavirus spike glycoprotein mediates escape from a S2 domain-targeting neutralizing monoclonal antibody. PLoS One. 2014 Jul 14;9(7):e102415. doi:10.1371/journal.pone.0102415. eCollection 2014.

2) Dang VT, Mandakhalikar KD, **Ng OW**, Tan YJ. A simple methodology for conversion of mouse monoclonal antibody to human-mouse chimeric form. Clin Dev Immunol. 2013;2013:716961. doi: 10.1155/2013/716961. Epub 2013 Sep 2.

LIST OF CONFERENCE PRESENTATIONS

1) NUS Yong Loo Lin School of Medicine 4th Annual Graduate Scientific Congress, Singapore, 11th March 2014

   Poster presentation titled "Substitution at Aspartic Acid 1128 in the SARS Coronavirus Spike Glycoprotein Mediates Escape from a S2 Domain-Targeting Neutralizing Monoclonal Antibody"

2) The Macrae Foundation XVI International Symposium on Respiratory Viral Infections, Seoul, South Korea, 13 – 16th March 2014

   Oral Presentation titled "Substitution at Aspartic Acid 1128 in the SARS Coronavirus Spike Glycoprotein Mediates Escape from a S2 Domain-Targeting Neutralizing Monoclonal Antibody"

3) NUS Yong Loo Lin School of Medicine 5th Annual Graduate Scientific Congress, Singapore, 27th January 2015

   Poster presentation titled "Characterization of SARS-CoV $CD8^+$ T cell Responses against the Membrane and Nucleocapsid proteins in SARS-recovered individual"

4) 12th NUS-Nagasaki Joint Symposium: Innovations and Insights in Infection and Immunity, Singapore, 11th-12th June 2015

   Poster presentation titled "Characterization of SARS-CoV $CD8^+$ T cell Responses against the Membrane and Nucleocapsid proteins in SARS-recovered individual"

CHAPTER 1: INTRODUCTION

1.1 Coronaviruses as Emerging Zoonoses

Emerging viral infections present major threats to the public health. Majority of newly emerged viruses are zoonoses, which are infectious diseases in animals but can be transmitted to humans when the pathogen acquires the ability to switch host into humans [1]. Coronaviruses cause a wide range of diseases in animal hosts, including livestock and domestic animals such as chickens, cows, pigs and cats, and have the ability to cause severe diseases, including severe gastroenteritis, respiratory tract infections, peritonitis, hepatitis, nephritis and encephalitis [2]. They are also highly diversed and are capable of frequent interspecies jumping [3]. Human coronaviruses (HCoVs), HCoV-229E and HCoV-OC43, are the first two identified coronaviruses that are capable of infecting humans and are common causes of mild and self-limiting upper respiratory tract illnesses [2]. In 2003, the Severe Acute Respiratory Syndrome coronavirus (SARS-CoV), a zoonotic virus that has overcome the species barrier to infect humans, emerged as a highly pathogenic coronavirus capable of causing severe respiratory syndrome in human. HCoV-NL63 and HCoV-HKU1, which cause mild upper respiratory tract disease similar to that described for HCoV-229E and HCoV-OC43, were subsequently discovered in 2004 and 2005 respectively after the SARS epidemic. In 2012, another highly pathogenic human coronavirus, the Middle East Respiratory Syndrome coronavirus (MERS-CoV), was identified. Similar to SARS-CoV, MERS-CoV was found to originate from zoonotic source(s). The 2003 SARS epidemic and the recent emergence of MERS-CoV significantly highlight the problems and threats that cross-species transmissions of zoonotic coronaviruses pose to the human population at large.

1.2 Overview of Severe Acute Respiratory Syndrome Coronavirus

Severe Acute Respiratory Syndrome (SARS) first emerged 12 years ago as a highly contagious infectious disease. The initial cases of SARS first appeared in the Guangdong Province of China in late 2002. In February 2003, an individual, who contacted SARS in Guangdong, travelled to Hong Kong where he transmitted the disease to others, leading to an outbreak in Hong Kong as well as the global dissemination of the disease. In the span of 4 months, SARS had spread widely to 25 countries across 5 continents, causing global panic as well as drastic public health measures to contain the spread of the disease [4]. The causative agent of SARS was identified as a then novel coronavirus, termed SARS coronavirus (SARS-CoV) [5]. Through concerted global efforts and effective measures such as rapid diagnosis of infected patients, efficient contact tracing, patient isolation, quarantines and air travel restrictions, SARS was successfully curbed and the SARS epidemic was declared over on 5 July 2003. By then, SARS had affected a total of 8098 people globally including 774 deaths, a fatality rate of around 10% [4]. Subsequently, four sporadic SARS cases were reported in Guangdong in the period December 2003 to January 2004, as well as 3 lab-acquired SARS cases in 2004, with no secondary human-to-human transmission [6]. Since then, there has been no report of human SARS cases.

The main route of transmission of the SARS-CoV is believed to be air droplets, although the fecal-oral route has also been suggested and transmission was often facilitated by close contact with infected patients [7]. The incubation of SARS-CoV infection ranged from 2 to 14 days, with infected individuals exhibiting a wide clinical course characterized by lower respiratory tract infection with symptoms such as fever, chills, myalgia, cough, headache, and dyspnea [8]. Extrapulmonary symptoms were also

observed with progressive infection including watery diarrhea as well as hematologic changes such as lymphopenia and elevated cytokines and chemokines levels [9]. Terminal events were mainly associated with severe respiratory failure such as acute respiratory distress syndrome (ARDS), and in some cases, multiple organ failures including hepatic dysfunction, kidney failures and cardiac dysfunction [10,11]. The risk of infection increases significantly with age and pre-existing co-morbid conditions correlated with high death rate [11]. Supportive treatment was the main form of treatment for managing SARS during the SARS epidemic. Other treatment regimens utilized included antiviral drugs such as ribavirin, lopinavir and ritonavir, interferon, corticosteroids treatment and convalescent plasma administration [10]. However, due to a lack of randomized control trials, effectiveness of these antiviral therapies was not evaluated. Till today, there remain an absence of approved, effective treatment and vaccine for SARS.

1.3 Virology of SARS-CoV

The SARS-CoV is classified in the genus *betacoronavirus* (lineage B), family *Coronaviridae* and order *Nidovirales*. It is an enveloped, positive-sense and single-stranded RNA virus of a genome of approximately 29.7 kb, encoding 16 non-structural proteins (nsps), 4 structural proteins and 8 accessory proteins (Figure 1.1A). Each virion particle is approximately 100 nm and is composed of a lipid bilayer studded by the structural membrane (M), envelope (E) and spike (S) proteins enclosing the helical nucleocapsid, which is formed by the association of the viral RNA with the structural nucleocapsid (N) protein (Figure1.1B) [12].

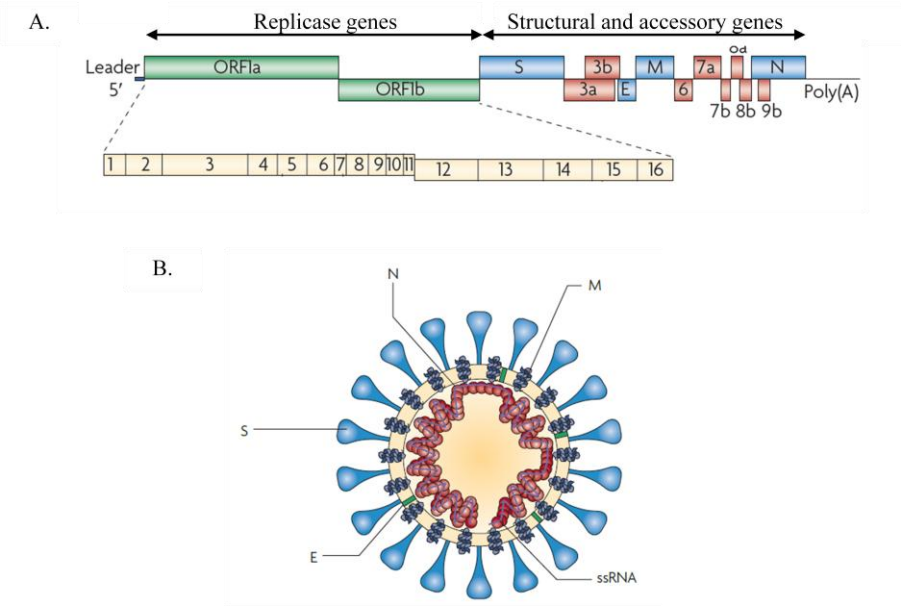

Figure 1.1. Genome and virion structure of SARS-CoV. (A) Schematic diagram of genome organization of SARS-CoV. The 5' end ORF1a and 1b (in green) encodes for a large replicase polyprotein that is cleaved to give rise to 16 nsps (in yellow). The 3' end of the genome encodes for 4 structural proteins spike (S), envelope (E), membrane (M) and nucleocapsid (N) (in blue), as well as 8 accessory proteins 3a, 3b, 6, 7a, 7b, 8a, 8b and 9b (in red). (B) Schematic diagram of the SARS-CoV virion particle. Figures adapted from Perlman *et al* [12].

Like all coronaviruses, the life cycle of SARS-CoV begins upon binding to host cell receptor and entry into host cell, releasing the viral genome into the cytoplasm. Two open reading frames, ORF1a and ORF1b, located at the 5' end of the viral genome are first translated into 2 replicase polyproteins, pp1a and pp1ab, which are subsequently cleaved to give rise to 16 nsps [13] . These viral proteins, together with host cellular proteins, assemble into replication-transcription complexes (RTCs) within endoplasmic reticulum (ER)-derived membrane-bound vesicles, where viral transcription and replication process occur [14,15]. The purpose of these membrane-bound RTCs remains uncertain, but it is likely to create a protected microenvironment for efficient viral replication and viral protein interaction to prevent the activation of host cell anti-viral

defense mechanisms [14]. Viral RNA replication occurs with the synthesis of genome-length or subgenome-length minus-sense RNAs, which serves as the templates for plus-sense genomic and subgenomic mRNA synthesis [16]. Subgenomic mRNAs are translated into structural and accessory proteins. The structural S, M and E proteins localize to the ER and migrate to ER-Golgi intermediate compartment (ERGIC), where they assemble with viral nucleocapsids that are formed by the encapsidation of full-length viral genomes by the structural N protein. The assembled proteins then bud off from the ERGIC to form progeny virion particles, which are transported to the plasma membrane in smooth-walled vesicles to be released out to the cell by exocytosis [13].

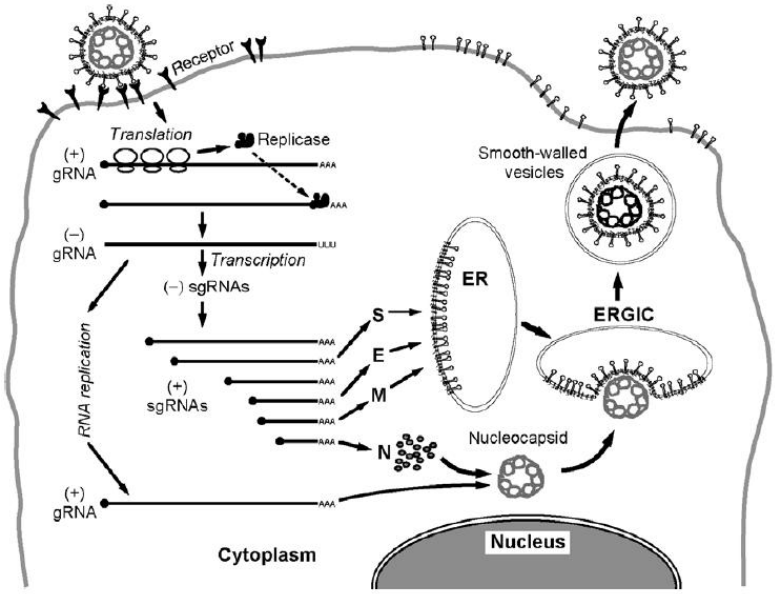

Figure 1.2. The life cycle of SARS-CoV. gRNA: genomic RNA; sgRNA: subgenomic RNA. Figure adapted from Master *et al*. [13]

1.3.1 Non-Structural Proteins

The replicase gene make up about 2/3 of the entire SARS-CoV genome (22,000 nucleotides) at the 5' terminal end [17]. Translation of the replicase gene gives rise to two large replicase polyproteins, pp1a and pp1ab, encoded by two partially overlapping open-reading frames, ORF1a and ORF1a/b respectively [18]. The translation of ORF1a occurs typically, terminating at the 1a stop codon, resulting in the generation of polyprotein pp1a of 486kDa; however, the presence of certain RNA signals located before the 1a stop codon can direct elongating ribosomes into an alternative reading frame, bypassing the 1a stop codon and resulting in the continual translation of ORF1b and the generation of polyprotein pp1ab of 790kDa [19]. This mechanism of ribosome directing is known as programmed -1 ribosomal frameshifting, and has been demonstrated to be important in coronaviral RNA synthesis and replication [20]. Pp1a and pp1ab are subsequently enzymatically processed and cleaved by viral-encoded proteases to generate 16 nsps (Figure 1.3). Nsp1 to 11 are derived from the cleavage of pp1a while nsp12 to 16 are derived from that of pp1b. Cleavage of the polyproteins is achieved by two SARS-CoV-encoded proteases, the papain-like proteinase (PLpro) of nsp3 and the 3C-like proteinase (3CLpro) of nsp5 [21]. The 16 nsps then assemble into RTCs in the double-membrane vesicles (DMVs) where they play critical and essential roles in viral genome transcription and replication. A summary of the characteristics and functions of each nsp is provided in Table 1.1.

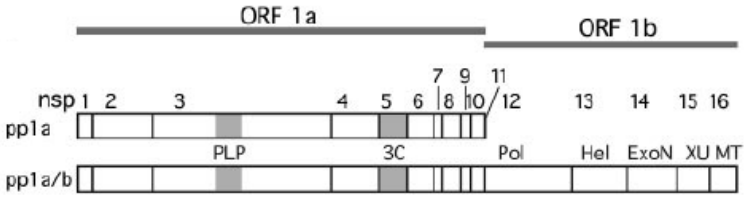

Figure 1.3. Structure of the SARS-CoV replicase proteins pp1a and pp1ab. The replicase proteins are enzymatically cleaved to yield nsps 1-16. Figure adapted from Wathelet et al [19].

Table 1.1. Summary of characterization and functions of SARS-CoV nsps

PROTEIN	CHARACTERISTICS AND STRUCTURE	FUNCTIONS
NSP1	- 20 kDa protein of 179 residues in length - Possesses a complex β-barrel fold structure mixed with helixes [22] - Localization in cytoplasm of infected cells [23] - Unique to SARS-CoV as it showed no significant sequence similarities with any other viral proteins [17]	- Suppresses host gene expression by inhibiting eukaryotic translation - Functions as an interferon (IFN) antagonist and suppresses expression of innate immune genes [24,25,26] - Promotes host mRNA degradation, but not coronavirus RNA degradation [25] - Inhibits antiviral signal transduction [19]
NSP2	- 65kDa protein - Crystallographic structure of C terminal nsp2 resolved, but not the full length protein [27]	- Dispensable for viral replication [28] - Interacts with host cell proteins, prohibitin 1 (PHB1) and PHB2 [29] - Role(s) in coronavirus replication and/or pathogenesis remains largely unknown
NSP3	- Protein of 1922 residues, the largest among all nsps - A glycosylated, transmembrane, multi-domain protein, consisting of a highly conserved N-terminal domain, a catalytically active ADP-ribose-1”-phosphatase domain, a SARS Unique domain (SUD), a ubiquitin-like domain, a catalytically active papain-like protease (PLpro) domain, a nucleic acid-binding domain, a marker domain known as G2M, two double-pass transmembrane domains, a metal-binding domain and a Y domain [30] - 3D structures of some domains resolved by NMR spectroscopy or X-ray crystallography [31] - Localization at ER membrane with domains residing in the cytosol [32]	- Functions as a PLpro for the cleavage at nsp1/2, nsp2/3 and nsp3/4 cleavage sites, giving rise to the individual nsps [33] - ADP-ribose-1”-phosphatase domain possibly play a role in the synthesis of viral subgenomic RNAs [34] - SUD could be involved in altering apoptotic and signaling pathways in infected cells [35] - Nucleic acid-binding domain acts as a nucleic acid chaperone [36] - Forms the anchor of the viral replication complex to the membrane of double-membrane vesicles together with nsp 4 and 6 [37]

PROTEIN	CHARACTERISTICS AND STRUCTURE	FUNCTIONS
NSP4	- 56 kDa protein of 500 amino acids - Consists of four transmembrane domains - Localizes at the ER membranes [38]	- Forms the anchor of the viral replication complex to the membrane of double-membrane vesicles with nsp 3 and 6 [37]
NSP5	- 34kDa protein - Contains three conserved domains: two domains from the N-terminal form a chymotrypsin-like structure, while the third domain is required for dimerization - 3D structure has been resolved using X-ray crystallography - Enzymatically active form exists as a homodimer [39]	- Functions as the 3C-like (3CL) protease, also known as main protease (Mpro), required for the cleavages of pp1a and pp1ab into nsps - Indispensable for viral replication [21] - Capable of inducing mitochondrial-mediated apoptosis [40]
NSP6	- Protein of 287 amino acids - Contains six transmembrane domains with a long C-terminal tail exposed in the cell cytosol [41,42]	- Forms the anchor of the viral replication complex to the membrane of double-membrane vesicles with nsp 3 and 4 [37] - Capable of inducing autophagy [43]
NSP7	- 10 kDa protein of 83 amino acids - NMR structure of nsp7 and crystal structure of nsp7/nsp8 hexadecamer have been determined [44,45]	- Interacts with nsp8 to form a hexadecamer complex, which bind double-stranded RNA (dsRNA) and extends RNA templates - Possibly functions as a factor that enhances transcription efficiency of RNA-dependent RNA polymerase (RdRp) activity of nsp8 [44,46]
NSP8	- 22 kDa protein consisting of 197 amino acids - Well-conserved among coronaviruses with approximately 66% amino acid sequence similarity - Crystallography study showed that nsp8 exists as an octamer, which interacts with eight other molecules of nsp7 to form a hexadecamer with a hollow ring structure [44]	- Possesses RNA-dependent RNA polymerase (RdRp) activity with low processing rate and low fidelity, possibly functions as a primase which synthesize primers to be utilized by nsp12 RdRp for RNA replication [47] - Interacts with SARS-CoV accessory protein ORF6, but function of this interaction remains unknown [48]

PROTEIN	CHARACTERISTICS AND STRUCTURE	FUNCTIONS
NSP9	- 12 kDa proteins consisting of 112 residues - Each molecule composed of seven beta strands and one alpha helix - Several crystallographic nsp9 dimer structures have been reported with different dimer interfaces [49,50,51]	- Binds single-stranded RNA (ssRNA) without sequence specificity, engages other proteins of the replicase complex to mediate viral RNA transcription and replication [49] - Interacts with the replicase complex via binding to nsp8 [51] - Necessary for viral replication and viability [52]
NSP10	- Protein of 139 amino acids in length - Highly conserved in coronaviruses - Crystal structure of nsp10 monomer revealed α-helices and β-strands, consisting of two zinc ion-binding motifs - 12 subunits of nsp10 assemble to from a dodecamer [53,54] - Crystal structure of nsp10 complexed with nsp16 resolved [55]	- Proposed to be a viral transcription factor due to its zinc ion binding property [54] - Interacts with nsp14 and activates nsp14 exoribonuclease activity [56,57] - Binds nsp16 and acts as a stimulatory factor for nsp16 2'-O methyltransferase (2'-O MTase) activity [58]
NSP11	- A short 13 amino acid residue peptide region [54]	- Function unknown
NSP12	- 102 kDa protein of 932 amino acids - Most conserved protein in coronaviruses and in nidoviruses - 2/3 of the protein at its C terminal end contains the RdRp domain responsible for RdRp enzymatic activity - N terminal end may consist of other domains of currently unknown functions [59,60]	- Exhibits primer-dependent RdRp activity for the replication and transcription of full-length genomic and subgenomic viral RNA [61] - Interacts directly with nsp7/8 complex, which increases RNA binding activity and confers RNA processivity to nsp12 [47]
NSP13	- 66.5 kDa protein - N terminal end contains zinc ion-binding domain, which is important for the protein's helicase activity	- Exhibits NTPase/RNA helicase activity which utilizes energy from nucleotide hydrolysis to unwind dsRNA into ssRNA during RNA transcription [64] - Interacts with nsp12 in the viral replication complex

PROTEIN	CHARACTERISTICS AND STRUCTURE	FUNCTIONS
	- C terminal end contains domain responsible for helicase activity [62,63]	and interaction enhances nsp13 helicase activity [65] - Indispensable for coronavirus replication and survival in infected cells [66] - Exhibits RNA 5' triphosphase (TPase) activity *in vitro*, but a direct role of nsp13 in RNA capping is yet to be established [64]
NSP14	- 60 kDa protein of 527 amino acids - Binds metal ions such as Mg^{2+}, which acts as co-factor to nsp14 enzyme activity [67] - Contains two functional domains, the exonuclease (ExoN) and guanine-N7-methyltransferase (N7-Mtase) domains, and amino acids 62-527 are critical for both activities [68] - Crystal structure not available	- Exhibits 3'-5' ExoN activity, belongs to the DEDD superfamily of exonucleases - Proposed to function in viral RNA proof-reading, repair and recombination to maintain the integrity of the large and long coronavirus genomic RNA [69] - SARS-CoV containing mutation at nsp14 ExoN active site was able to replicate but exhibited high mutation rates [70] - ExoN activity enhanced through interaction with nsp10 [71] - Also a N7-MTase involved in the N7-methylguanosine (m7G) capping of viral RNA, which is essential for viral replication [68]
NSP15	- 38.5 kDa protein of 346 amino acids - Unique to nidoviruses - Crystal structure of nsp15 monomer revealed 3 extended domains: a 60 aa N-terminal domain, a 128 aa central domain and a 153 aa C-terminal domain. - C-terminal domain contains the endoribonuclease active site - Capable of forming a hexamer although biological relevance of the hexamer has yet to be established [72,73]	- Exhibits endoribonuclease activity and cleave preferentially 5' to uridylates in dsRNA, requiring Mn^{2+} as co-factor [74,75,76] - Actual biological role in viral replication unknown

PROTEIN	CHARACTERISTICS AND STRUCTURE	FUNCTIONS
NSP16	- 300 amino acids in length - Crystal structure solved in complex with nsp10 [77,78]	- Exhibits nucleoside-2'-O-methyltransferase (2'O-MTase) activity, which adds a methyl group at the 2'O position of the first nucleotide of the SARS-CoV genomic mRNA, forming a cap-1 structure [79,80] - Interacts with nsp10, in which interaction activates 2'O-MTase activity of nsp16 [77,78]

1.3.2 Structural Proteins

Like other coronaviruses, the SARS-CoV genome encodes for 4 structural proteins, namely the spike (S), envelope (E), membrane (M) and the nucleocapsid (N) proteins. Unlike some betacoronaviruses, the SARS-CoV lacks the gene to encode for a fifth structural protein, the hemagglutinin-easterase (HE) protein [81]. The generation of structural proteins is a result from the translation of viral subgenomic RNAs. Structural proteins play important roles in the assembly and formation of virion particles. Through the co-infection of insect cells using recombinant baculoviruses expressing the viral structural proteins, it has been shown that the E and M proteins are necessary and sufficient for the efficient formation of SARS-CoV virus-like particles (VLPs) [82]. In contrary, another group showed that the N and M proteins are required for this efficient VLP formation through the co-transfection of plasmids expressing SARS-CoV structural proteins into human embryonic kidney (HEK) 293T cells [83,84]. More recently, it was demonstrated that the expression of both E and N proteins with M protein is key to the efficient assembly and egress of SARS-CoV VLPs in transfected Vero E6 cells [85].

1.3.2.1 Envelope Protein

The SARS-CoV E protein is an integral membrane protein of a small size of 76 amino acids in length [86]. It is a glycosylated protein that co-localizes to the ERGIC region [87,88,89], where it interacts directly with the M protein for viral assembly and formation [90,91]. It has been recently demonstrated that the E protein can also interact with N protein, although this interaction is not directly involved in virus assembly and budding unlike the E/M interaction [92]. The N-terminal end of the SARS-CoV E protein contains a short hydrophilic region of 7-9 amino acids and a longer 21-29 amino acid

hydrophobic region followed by a hydrophilic C-terminal tail, forming an ion channel in the lipid bilayer of the virion particle [93,94]. Ion channels encoded by viruses, also known as viroporins, play important roles in virus morphogenesis, entry, trafficking, maturation and virulence [95,96]. While the SARS-CoV E protein is not completely essential in the generation of infectious viral particles, it has been demonstrated to be a virulence determinant, as the deletion of the E gene from the SARS-CoV genome resulted in an attenuated virus [88,97]. Virus fitness and pathogenesis is further shown to be linked to the E protein ion channel activity [98]. The SARS-CoV E protein is also involved in the regulation of cell stress response as well as the induction of apoptosis [99,100]. E protein ion channel activity could be inhibited by amantadine and hexemethylene amiloride, with the latter able to inhibit viral replication, indicating the potential of targeting the E protein as an antiviral strategy [101,102].

1.3.2.2 Membrane Protein

The SARS-CoV M protein is the most abundant structural protein in the virus particle. It is a transmembrane glycoprotein of 221 amino acids which consists of an N-terminal ectodomain with a single N-glycosylation site, three transmembrane hydrophobic domains and a long cytosolic C-terminus [86,103]. The M protein is an essential protein in the assembly, formation and budding of coronavirus particles through its ability to interact with all other structural proteins including E, N and S protein [104]. The M protein co-localizes predominantly at the Golgi apparatus, where interactions with other structural proteins occur, although localization at the ER compartment as well as plasma membranes is also possible [105,106]. The C-terminal end of the M protein (amino acid residues 197-221) was determined to be the site of interaction with residues

351-422 of the N protein [84,107]. The C-terminal region, in particular the tyrosine at residue 195, is also necessary for the interaction and Golgi-retention of S proteins [108,109]. The M protein resides mainly in the ER membrane and is able to interact with two transmembrane domains (residues 11-33 and residues 37-59) of the E protein [91]. In addition, it is capable of self-assembly and this was shown to be important in the formation of VLPs [110]**.** Besides its role in virus assembly, the M protein is capable in inducing apoptosis via the Akt signaling pathway [111,112] and in suppressing innate antiviral response by inhibiting type 1 interferon (IFN) production [113,114]. It is also reported that the M protein suppresses NF-kB activation and COX-2 expression, leading to decreased antiviral inflammatory response [115]. The M protein also plays a role in inducing B cell and T cell immunity during viral infection (see later section 1.8).

1.3.2.3 Nucleocapsid Protein

The primary function of the SARS-CoV N protein is to package the single-stranded positive-sense viral RNA into a ribonucleocapsid complex, which constitutes the template essential for replication of viral genomic information [104]. The SARS-CoV N protein is a 46kDa phosphoprotein of 422 amino acids that shares a sequence homology of around 20-30% with other coronavirus N proteins [86]. It predominantly localize in the cell cytoplasm, although rare occasions of nuclear localization could be observed in transfected cells [116]. It contains 3 nuclear localization signals (NLSs), NLS1, NLS2 and NLS3, and hence believed to be able to shuttle between cytoplasm and nucleus/nucleolus [117]. However, how localization of the protein is regulated remains unknown. The N protein undergoes various post-translationally modifications, including phosphorylation, acetylation and sumotylation [118,119,120].

There are 2 structured and ordered domains within the N protein, namely the N-terminal domain (NTD, residues 45-181) and the C-terminal domain (CTD, residues 248–365), which are interspersed with intrinsically disordered (ID) regions [121]. The NTD functions mainly to bind RNA [122,123], while the CTD functions as a domain for N protein oligomerization and self-association, necessary for the formation of the viral capsid which forms an external protection for the viral genome [124,125]. The CTD is also capable in associating with RNA and at a higher affinity compared to the NTD, suggesting that the involvement of both domains in viral RNA packaging [125]. The ID regions also have fundamental roles in RNA-packaging. For instance, the central ID region has RNA-binding affinity and exists in an extended conformation, thereby allowing maximum interaction of the N protein with RNA [126]. In addition, the SR-rich region of the central ID region is thought to be the site of multiple phosphorylation and therefore an important region in regulating RNA binding [120]. The N protein is also involved in the efficient formation, trafficking and release of viral particles through its association with other viral structural proteins, including the M and E proteins [84,85,92].

The SARS-CoV N protein is capable of interacting with numerous host cell proteins and is therefore believed to function not only as the building block of the viral ribonucleocapsid, but also as a major modulator of host cell responses and viral pathogenesis. A study by Zhang *et al* demonstrated the ability of both the NTD (residues 86-96) and the CTD (residues 341-422) of the N protein to activate and upregulate IL-6 gene expression, possibly through the direct or indirect binding of the transcriptional factor NF-κB regulatory element on the IL-6 promoter [127]. This provides a possible explanation to the increased IL-6 levels, inflammatory responses and cytokine storms observed in SARS patients. In line with this, another study showed that residues 136-204

of the SARS-CoV N protein activate the expression of COX-2, another pro-inflammatory molecule, through direct binding to C/EBP and NF-κB regulatory elements on the COX-2 promoter using chromatin immunoprecipitation and electrophoresis mobility shift assays [128]. However, a study carried out by He *et al*, using an enzyme-linked immunosorbent assay (ELISA)-based detection technique and an *in vitro* inducible-vector assay, found that the SARS-CoV N protein does not activate NF-κB pathway, but activates the AP-1 signalling transduction pathway [129]. Like other SARS-CoV protein including the M, nsp1, nsp3, nsp7, nsp15 and accessory 3b and 6 proteins, the N protein is an IFN antagonist capable of inhibiting IFN-β synthesis and the CTD (residues 281-365) was found to be involved in this function [130,131]. The SARS-CoV N protein also promotes the TGF-β-induced expression of PAI-1, a fibrotic promoter, possibly explaining the cause of SARS-induced lung injury and fibrosis [132]. More recently, the SARS-CoV N protein has been shown to be a suppressor of RNA interference (RNAi) process involved in post-transcriptional gene silencing in mammalian cells, thereby preventing host cell antiviral immune response [133].

The deregulation of host cell cycle is a common strategy adopted by viruses to enhance their own replication and survival. For the SARS-CoV, the N protein has been shown to cause cell cycle arrest at the S phase through the interaction and inhibition of the cyclin-dependent kinase (CDK) complex, as demonstrated by the exogenous expression of N protein in COS-1 and Huh-7 cells [134]. This is confirmed in SARS-CoV-infected cells, where the protein levels of cyclin A, CDK2 and P-p27 are found to be down-regulated, indicating that the ability of the N protein to cause cell cycle arrest is a physiological phenomenon during infection [134]. It is postulated that the blockage of S phase in the cell cycle allows genomic replication of SARS-CoV as well as assembly and

budding of progeny viral particles. It has also been reported that the N protein is capable of inducing apoptosis. For instance, in the absence of growth factors, the N protein up-regulated p38 MAPK pathway and activated caspase 3 and 7 activity in COS-1 monkey kidney cells [135]. The SARS-CoV M protein has also been shown to enhance N protein-induced apoptosis in human pulmonary fibroblast cells *in vitro* [136]. The upstream initiators of N protein-induced apoptosis remain to be identified. However, through the binding to Smad3, the SARS-CoV N protein is capable in attenuating TGF-β-induced apoptosis, which could be a mechanism employed by the virus to inhibit apoptosis in early stages of infection to favour virus packaging and replication [132].

The SARS-CoV N protein has been suggested to regulate cell stress responses that result from viral infections. It was shown that the N protein can suppress host cell translation through its direct interaction with eukaryotic elongation factor 1 alpha (eEF1A), a major translation factor in mammalian cells [137]. Moreover, this interaction inhibits cytokinesis through reduction of F-actin bundling, which leads to decreased cell proliferation and formation of multinucleated syncytia in macrophages as observed in late-phase SARS-CoV infection. In addition, the SARS-CoV N protein binds to human cellular heterogeneous nuclear ribonucleoprotein A1 to form a complex essential for transcription and replication of viral RNA [138]. The N protein is also a major immunogenic antigen capable of eliciting antibody and T cell responses in infected individuals [139,140,141,142]. The early detection of N protein in SARS patients' sera allows it to be used as an early diagnostic marker for SARS-CoV infection [143,144].

1.3.2.4 Spike Protein

Coronaviruses are named for their characteristic crown-like appearance, which is a result of the presence of surface spikes or peplomers on the viral particles. By scanning electron microscopy, the SARS-CoV peplomer dimensions and shape have been defined [145]. Each peplomer is composed of a trimer of the S protein, a type 1 glycoprotein of 1255 amino acids in length [86,146]. Each S protein consists of 2 functional subunits, namely the N-terminal S1 subunit (amino acid residues 14-679) and the C-terminal S2 subunit (amino acid residues 680-1255) [147]. A schematic diagram of the S protein is provided in Figure 1.4. Structurally, the S1 domain is presented as the globular head with receptor-binding capability, while the S2 domain is presented at the stalk portion of the spike, embedded within the viral membrane [148]. The S protein functions primarily for viral attachment and entry into host cells, and is the principal determinant of host range and tropism [149].

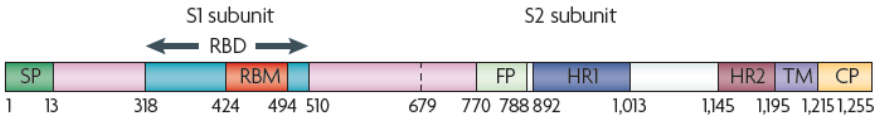

Figure 1.4. Schematic of the SARS-CoV S protein. Numbers are indicative of amino acid residues on the S protein from the N- to C-terminus. SP, signal peptide; RBD, receptor-binding domain; RBM, receptor-binding motif; FP, fusion peptide; HR1, heptad repeat 1; HR2, heptad repeat 2; TM, transmembrane domain; CP, cytoplasmic tail. Figure adapted from Du *et al.*[147].

The S1 subunit is important in viral attachment to host cell receptor, which is determined to be a metallopeptidase, the angiotensin-converting enzyme 2 (ACE2), for the SARS-CoV [150]. A 193 region corresponding to residues 318 to 510 within the S1 subunit, known as the receptor-binding domain (RBD), is sufficient for the interaction with the ACE2 receptor, and an amino acid substitution at residue 454 abolished binding

to ACE2, indicating the importance of this residue in association with the receptor [151]. It was further demonstrated by Chakraborti *et al* that mutations of ten residues (K390, R426, D429, T431, I455, N473, F483, Q492, Y494, R495) within the RBD significantly reduced binding to ACE2 [152]. The structure of the RBD-ACE2 complex has been resolved and the region in direct contact with ACE2 is mapped to be residues 424 to 494 [153]. Using Chinese hamster ovary (CHO) cells that were transduced with a human lung cDNA library using retroviral vectors, soluble SARS-CoV S protein is also found to bind to human cellular lectin CD209L (also known as DC-SIGNR, DC-SIGN2 or L-SIGN), which is possibly an alternative receptor for SARS-CoV in addition to ACE2 [154]. It was shown that CD209L can mediate infection by SARS-CoV, but at a lower efficiency compared to human ACE2. Other studies have also demonstrated the ability of S protein to bind to the dendritic cell-specific ICAM-3 grabbing non-integrin (DC-SIGN) on dendritic cells [155,156]. Interestingly, dendritic cells were not susceptible to SARS-CoV infection, suggesting that DC-SIGN does not function as a receptor for SARS-CoV. However, dendritic cells were able to transfer the virus to other susceptible cells, which could be a mechanism employed by SARS-CoV to disseminate viruses and sustain a continuous and persistent infection in its host. The S protein is also shown to interact with another lectin, LSECtin (liver and lymph node sinusoidal endothelial cell C-type lectin) to enhance viral infection in conjunction with DC-SIGNR in hepatocytes [157].

The SARS-CoV S protein is a type I fusion protein and shares the same basic fusion mechanism as other type I viral fusion proteins such as gp160 of Human Immunodeficiency Virus (HIV) and the hemagglutinin (HA) protein of Influenza A virus [158]. The S2 subunit contains the putative fusion peptide and two heptad repeat regions, HR1 and HR2, important for the fusion process with target cells [159,160]. Upon the

association of the RBD with the ACE2 receptor, the conformational change of the S2 is triggered, resulting in the insertion of the fusion peptide into the target cell membrane and the association of HR1 and HR2 to form a stable six-helical bundle fusion core structure [159]. This brings the viral membrane to close proximity to the target cell, facilitating membrane fusion and viral entry [161,162]. The site of interaction between HR1 and HR2 is mapped to residues 914-949 of the HR1 region and residues 1148-1185 of the HR2 region [163] . The resolution of the crystal structure of the SARS-CoV HR1-HR2 fusion core showed high structural similarity to that of the murine coronavirus, mouse hepatitis virus (MHV) [164], and the alignment of S2 domains among different coronaviruses revealed high sequence identity, indicating the highly conserved nature of the fusion process in coronaviruses [165]. On the other hand, different species of coronaviruses show great sequence variability within the S1 domain, which results in a wide range of tissue tropisms via a variety of cellular receptors.

Many viral fusion proteins undergo proteolytic cleavage for productive viral entry into host cells. Proteolytic cleavage is thought to occur near the position of the fusion peptide, a non-polar region of 15-25 amino acid residues long that is capable of interacting and inserting into cell membrane to trigger fusion [166]. Similar to the Influenza A virus, SARS-CoV entry is inhibited by lysosomotropic agents, suggesting the need for an acidic pH to trigger SARS-CoV S fusion [155,167]. Inhibition of endosomal cysteine protease, cathepsin L, has been shown to be able to inhibit SARS-CoV infection [168] and its cleavage site on S protein was reported to be T678, close to the S1/S2 boundary [169]. Nonetheless, fusion can occur in the absence of acidic pH with the addition of trypsin [170]. Trypsin was implicated in fusion activation through sequential cleavage of S protein at 2 sites, the first at R667 and the second at R797 [171]. Elastase

was also shown to be able to activate fusion via cleavage at position residue 795 [172]. Studies have also shown that the SARS-CoV S protein is capable of fusion through activation by host cell exogenous proteases present in the lung lumen, such as transmembrane protease serine 2 (TMPRSS2) and human airway tryptase (HAT), which are members of the type II transmembrane serine protease family (TTSPs) [173]. It was demonstrated that TMPRSS2 cleaves the S protein at multiple sites in S2 subunit, resulting in cell-cell and virus-cell fusion, although the precise cleavage sites have not been determined [174], while HAT cleaves SARS-CoV S protein specifically at residue R667 [175]. The inhibition of TTSPs partially prevents SARS-CoV infection of HeLa cells expressing ACE2, while the dual inhibition of TTSPs and cathepsin L efficiently blocked viral entry and infection [176]. Taking all together, it is likely that viral entry via both cell surface plasma membrane and the endosomes are important for SARS-CoV infection [177].

To date, there is no consensus on the exact location and sequence of SARS-CoV fusion peptide. Using a transmembrane predictor program to predict transmembrane domains within the SARS-CoV S protein, a hydrophobic region of residues 858-886, located at the N terminus of the HR1 region, was predicted to be the fusion peptide of the SARS-CoV S [178]. Subsequently, Sainz *et al* identified another putative fusion peptide at position residues 770-788 through the demonstration of the ability of this region to induce membrane fusion of lipid vesicles [179]. Madu *et al* identified another region, residues 798-815, to be the fusion peptide through mutagenesis followed by cell-cell fusion assay and pseudovirus assays, and showed that residues L803, L804 and F805 are especially important for membrane fusion [180]. According to a predictive quaternary structure of SARS-CoV, the position and the structure of this region (residues 798-815)

is strongly suggestive of its function as a viral fusion peptide [181]. A short region of aromatic amino-acids, known as the juxtamembrane domain (residues 1193 to 1199), located proximal to the transmembrane domain (TMD) of S, has also been implicated in the fusion process, as single alanine subsititutions and Y1188A/Y1191A mutations within the domain significantly reduced S-mediated cell-cell fusion [182]. Using the murine leukemia virus (MLV)-based pseudotyping system to generate SARS pseudoviral particles, the TMD itself (residues 1194 to 1227) was found to play a role in viral fusion and entry, as the replacement of the SARS-CoV TMD with that of the Vesicular stomatitis virus G protein (VSV-G) resulted in a marked decrease of fusion activity [183]. Both the tryptophan-rich and cysteine-rich regions of the SARS-CoV S TMD are found to be important in S-mediated cell fusion [184,185]. The cytoplasmic tail located at the C-terminal end of S protein is not necessary for fusion, but it contains the dibasic KxHxx-$_{COOH}$ motif which functions for the retaining of S protein in the ERGIC and for the interaction and co-localization with the SARS-CoV M protein in the ERGIC, contributing to efficient virus assembly and production [109].

Besides its role in virus entry, numerous studies focus on the delineation of the effects of SARS-CoV S protein on host response. The SARS-CoV was shown to be able to activate NF-κB in human peripheral blood monocyte macrophages *in vitro* [186], and it was further demonstrated to upregulate chemokine (C-C motif) ligand 2 (CCL2) through its interaction with ACE2 receptor, resulting in severe inflammatory lung injuries as observed in SARS patients [187]. The SARS-CoV S protein is also a major antigenic determinant in eliciting neutralizing antibody production in infected individuals [188]. S-specific neutralizing antibodies recognize epitopes within the RBD, thereby inhibiting viral association with ACE2 receptor and preventing infection; alternatively, they target

epitopes within the S2 domain to neutralize viral infection through the inhibition of S-mediated viral-cell fusion [189]. Moreover, S protein is capable of generating both $CD8^+$ and $CD4^+$ T cell responses as observed in infected SARS-patients as well as in animal models infected with the virus, indicating its role in eliciting host immune response necessary for the protection against SARS-CoV infections [140,190,191,192].

Because of its receptor-recognition and ability to mediate viral attachment and entry into host cells for infection to occur, the S protein is an important target in the development of antiviral therapeutics and vaccines against the SARS-CoV. Peptides capable of inhibiting S-ACE2 interaction [193,194], preventing the cleavage of S protein [168,195] and blocking the HR1-HR2 fusion core formation [196,197] have been described to effectively inhibit SARS-CoV infections. Numerous natural compounds and small molecules have also been studied for their abilities to block SARS-CoV viral entry and infection using high-throughput screening methods [198,199]. For instance, the compound extracted from natural herbs, emodin, is able to block the interaction of S and ACE2, thereby inhibiting viral entry and infection of SARS pseudoviral particles in Vero E6 cells [200]. However, the antiviral capabilities of these agents were mostly tested *in vitro*, *in vivo* work involving animal models is needed to further evaluate their effects. Neutralizing antibodies specific against S protein are also potential prophylactic and therapeutic agents for preventing and treating SARS-CoV infections. Neutralizing monoclonal antibodies (mAbs) could be generated by various methods, including the immunization of mouse models with whole inactivated SARS-CoV virus, full-length or partial region of the S protein [201,202], and the screening for mAbs directly from B cells of SARS-infected individuals [203].

The development of effective SARS-CoV vaccine is crucial in the event of a re-emergence of SARS-CoV or SARS-like coronaviruses (SL-CoVs) from zoonotic sources. Vaccines development for SARS-CoV largely focuses on eliciting neutralizing antibodies and T cell responses against the SARS-CoV S protein, since the SARS-CoV S protein is a major antigen in inducing protective immunity. The immunization of mice and rabbits with inactivated SARS-CoV vaccine elicited high production of neutralizing antibodies that recognize S protein, especially the RBD region, suggesting that the RBD is the major neutralization determinant in the inactivated vaccine [204]. The administration of a viral vector-based subunit vaccine, a modified vaccinia virus Ankara-based recombinant SARS-S vaccine in ferrets elicited effective neutralizing antibodies production but this was accompanied with enhanced hepatitis during SARS-CoV infection [205]. Another promising subunit vaccine candidate, a recombinant adeno-associated virus expressing the RBD of SARS-CoV S, administered via the intranasal route, was able to induce strong specific pulmonary humoral and cytotoxic T lymphocyte (CTL) responses and protected vaccinated mice from SARS-CoV challenge [206]. SARS-CoV S DNA vaccines resulted in the generation of robust antigen-specific memory $CD4^+$ and $CD8^+$ T cell responses and neutralizing antibodies in mouse models [207,208]. Protein-based vaccines, such as recombinant proteins of the SARS-CoV S protein and the RBD expressed in mammalian cells, also elicited potent neutralizing antibody responses that protect against SARS-CoV challenges in animal models [209,210,211].

1.3.3 Accessory Proteins

In addition to the replicase and structural proteins, the SARS-CoV genome also encodes for eight accessory proteins, namely the 3a, 3b, 6, 7a, 7b, 8a, 8b, and 9b proteins,

with ORFs are interspersed among the structural genes at the C-terminal end of the SARS-CoV genome (Figure 1.6) [212,213]. While the amino acid sequences of the replicase and structural proteins of SARS-CoV share certain levels of homology with other coronaviruses, the accessory proteins of SARS-CoV do not show significant sequence similarity with viral proteins of other coronaviruses and are thus unique to SARS-CoV [81]. Coronaviruses accessory proteins, including that of SARS-CoV, are dispensable for viral replication and viability [214,215,216]. However, these proteins are believed to play important roles in viral pathogenesis and confer biological advantages to the virus during infections through the modulation of a variety of cellular processes, including cell proliferation, signal transduction pathways and programmed cell death [217]. Extensive work has been done by various research groups in characterizing and understanding the functions of each SARS-CoV accessory protein. A summary of the characteristics and functions of the SARS-CoV accessory proteins is provided in Table 1.2.

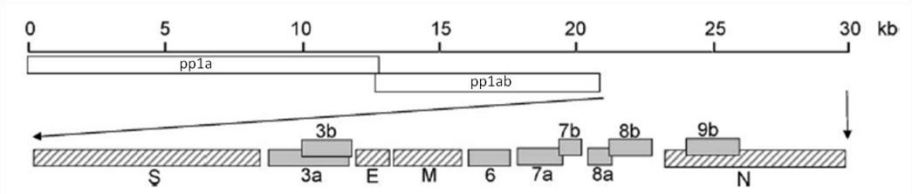

Figure 1.5. Schematic diagram indicating the positions of accessory proteins ORF 3a, 3b, 6, 7a, 7b, 8a, 8b and 9b in the SARS-CoV genome, as highlighted in grey. Pp1a and pp1ab represent the replicase polyproteins; S, E, M and N represent the SARS-CoV structural spike, envelope, membrane and nucleocapsid proteins. Diagram adapted from Tan *et al.* [212]

Table 1.2. Summary of characterization and functions of SARS-CoV accessory proteins

PROTEIN	CHARACTERISTICS AND STRUCTURE	FUNCTIONS
3a	- Comprises of 274 amino acid residues, the largest of all SARS-CoV accessory proteins - Present in a 31-kDa unglycosylated form as well as a 37-kDa O-gylcosylated form [218] - A minor structural protein present on viral envelope [219] - Localization in plasma membrane and in cytoplasm with the highest concentration in Golgi apparatus [220,221,222] - Consists of an N-terminal domain made up of three transmembrane domains; a central domain that is able to interact with 5'UTR of SARS-CoV genome and a hydrophilic C-terminal domain [223,224] - Undergoes oligomerization to form homodimers and homotetramers [225] - Interacts with SARS-CoV M, S, E, and 7a proteins [226] - Structure currently unknown	- Capable in triggering humoral and cellular adaptive immune responses in SARS-infected individuals and in mouse models [142,221,227] - Activates NF-κB and JNK pathway, resulting in upregulation of RANTES and IL-8 [228] - Down-regulates type I IFN receptors and triggers the PERK pathway which induces ER stress [229] - Forms an ion channel that may function to promote viral release and apoptosis [225,230] - C-terminal domain capable of causing G1 cell cycle arrest by inhibiting cyclin D3 [231] - C-terminal domain important for internalization of viral proteins such as the S protein into intracellular components, facilitating assembly of viral particles [223] - Non-essential for viral replication [216] - Induces apoptosis in transfected cells [232,233]
3b	- Comprises of 154 amino acid residues - Translated from ORF3 (similar to that for 3a protein) via an internal ribosomal entry mechanism [234] - Localizes in nucleolus and mitochondria [235,236,237] - Structure currently unknown	- Induces antibody production as antibodies against 3b protein have been detected in SARS-infected patients [238] - Capable of inducing apoptosis and necrosis [239] - Contributes to inhibition of host antiviral response by the downregulation of type-I IFN such as IFN-β [240] - Induces G0/G1 cell cycle arrest [241] - Non-essential for viral replication [216]

6	- 63 amino acid residues in length - Subcellular localization in Golgi apparatus and ER - Incorporated into VLPs when co-expressed with SARS-CoV structural S, E and M proteins [242] - Consists of an amphipathic N-terminal portion (aa 1-40) and a polar C-terminal region - Residues 2-37 of N-terminal region form α-helical structure and is embedded in cellular membrane, while the C-terminal region contains the protein internalization signal (aa 49-52) and the ER export signal [243] - Structure currently unknown	- Non-essential for viral replication [216] but mutation resulted in lower viral titres during initial infection compared to wild-type [244]
7a	- Consists of 122 residues - Type I transmembrane protein, consisting of a lumenal domain, transmembrane domain and C-terminal tail. - Localization in perinuclear region - Lumenal domain consists of a compact seven-stranded beta structure [245]	- Interacts with M and N proteins and is incorporated into viral particles [246] - Also interacts with S and 3a protein, but interactions are non-essential for incorporation into viral particles [222,246] - Induces apoptosis via caspase-dependent pathway [247] - Inhibits cellular protein synthesis and activates p38 mitogen-activated protein kinase [248] - Induces cell cycle arrest [249] - Enhances production of pro-inflammatory cytokines [228] - Dispensable for viral replication [216]
7b	- An integral membrane protein of 44 amino acids - Localizes in Golgi apparatus [250] - Structure unknown	- Detection of anti-7a antibody in sera of SARS patients [238] - Dispensable for viral replication [216] - Biological functions unknown

8a and 8b	- Derived from the translation of ORF8a and 8b, which are the result of a 29-nucleotide deletion in the ORF8ab from the early to late phase of the SARS epidemic - 8a protein is 39 residues and 8b protein is 84 residues in length [251] - 8a protein localizes in mitochondria [252] - 8b protein localizes in nucleus and cytoplasm [253] - Crystal structures unsolved	- 8a protein interacts with S protein while 8b interacts with M, E, 3a and 7a proteins. 8b protein also downregulates E protein level [254] - 8a protein induces apoptosis and promotes viral replication [253] - 8b protein binds to monoubiquitin and polyubiquitin and is rapidly degraded by proteasomes in mammalian cells [255] - Overexpression of 8b proteins induces DNA synthesis [253]
9b	- 98-residue protein - Expressed from an internal ORF located within the N gene - Localizes at ER [256] - Crystal structure shows a dimeric tent-like structure consisting of an amphipathic surface with a central hydrophobic cavity [257]	- Anti-9b antibodies were detected in sera of convalescent patients [258] - Exact biological function unknown, but proposed to contribute to virus assembly as a membrane-attachment point for other viral proteins [257]

1.4 Zoonotic Origin of SARS-CoV

Evidence has shown that SARS-CoV is a zoonotic virus that has crossed the species barrier to infect humans. Small animals such as palm civets (*Paguma larvata*) and raccoon dogs (*Nyctereutes procynonoides*) sold in live-animal wet markets in Guangdong Province of Southern China were the immediate source(s) of the virus transmitted to humans during the 2003 SARS outbreak [251]. Sporadic SARS cases that occurred in late 2003 were also traced to be associated with preparation and consumption of palm civet meat [259]. The full-length genome of the SARS-CoV isolated from these animals shared 99.8% sequence homology with the human SARS-CoV, indicating the viruses are closely related [251]. For cross-species transmission to occur, the virus needs to adapt to its new host in numerous ways, the first and most important determinant being the ability to recognize the new host cell receptor. Sequence analysis of the S genes from human and civet SARS-CoV isolates revealed 2 critical mutations at residues 479 and 487 that resulted in a more efficient binding to the human ACE2 receptor compared to the civet ACE2 receptor, leading to a civet-to-human transmission [260,261]. The SARS-CoV isolates in the 2003 SARS epidemic possessed a threonine residue at position 487, which conferred strong binding of S to human ACE2. On the other hand, the isolates from the 2003-2004 sporadic SARS outbreaks with no human-to-human transmission contained a serine residue at position 487 [262]. This indicates the importance of the mutation at this position in the adaptation of SARS-CoV in human.

Numerous observations suggest that palm civets and other small animals are merely conduits for SARS-CoV transmission to humans rather than the natural wild-life reservoir harbouring the virus. Firstly, viral RNA detection and anti-SARS sera were only

detected in civets from marketplace but not in the farmed or wild-life civets, indicating that palm civets are not widely infected by SARS-CoV [263]. In addition, sequence comparison of various civet SARS-CoV isolates revealed high non-synonymous/synonymous nucleotide substitution ratio, indicating ongoing mutation and evolving process of the virus in civets, further suggesting that palm civets are unlikely the natural reservoir of the virus [264]. High prevalence of anti-SARS-CoV antibodies was detected in serological surveys involving people not infected with SARS-CoV but work in retail business of palm civets and wild animals, suggesting that cross-transmissions of a precursor SARS-CoV probably occurred before the actual SARS epidemic [251].

In 2005, the identification of RNA sequences of SARS-like coronaviruses (SL-CoVs) (Rf1 and Rp3 strains) and the detection of anti-SARS-N antibodies in Chinese horseshoe bat species in the genus *Rhinolophus* were reported [265,266]. This is an important step in identifying bats as the natural reservoirs of SARS-CoV. Analysis of non-synonymous/synonymous nucleotide substitution ratio of bat SL-CoVs indicated the absence of positive selection pressure [267], suggesting that SL-CoVs have evolved in bat hosts for a long period of time. These bat SL-CoVs are highly similar to human and civet SARS-CoVs with high sequence homology ranging between 88 to 92% [265,266]. Notably, the variations of S gene sequence identity hovered between 76 to 78%, with greater sequence differences in the S1 domain (68%) compared to the S2 domain (92 to 96%). Unlike human and civet SARS-CoVs which utilize the human and civet ACE2 receptors for viral entry, these bat SL-CoVs do not do so via the bat ACE2 receptor. However, the replacement of the RBD of the bat SL-CoV S protein with that of the human SARS-CoV S protein was sufficient to enable infection of cells through the ACE2 receptor [268]. Efforts in cultivating these bat SL-CoVs in culture have so far been futile

and their cellular receptor remains unknown. Following this, a diversity of bat SL-CoVs have been identified not only in China, but also in other parts of the world including European, African and South East Asian countries [269]. The inability of these bat SL-CoV S proteins to use ACE2 as cellular receptor suggests that they are unlikely the direct progenitor of SARS-CoV. Nonetheless, two models of SARS-CoV emergence have been initially proposed: (1) an initial cross-species jump of SL-CoV from bats to civets, followed by another jump from civets to humans; (2) direct transmission of SL-CoV from bats to humans, followed by numerous bi-directional transmissions between human and civets [270].

More recently in 2013, the identification of bat SL-CoV (RsSHC014 and Rs3367 strains) sequences in Chinese horseshoe bats with high sequence identity between 85 to 96% to human SARS-CoV, especially in RBD region, strongly supported that a direct transmission from bats to human is plausible [271]. This study also reported the successful isolation of a first live bat SL-CoV (WIV1) from Vero E6 cells, and WIV1 was shown to be able to infect and replicate in cells expressing ACE2 receptors of human, civets and bat origin, demonstrating its ability in infecting bats, civets and human. This further gives important evidence that bat coronaviruses present a significant threat to the public health. The re-emergence of SARS in humans remains a possibility with the continual persistence of SL-CoVs in animal hosts and reservoirs.

1.5 Overview of Middle East Respiratory Syndrome Coronavirus

Before SARS-CoV emerged, only two coronaviruses, HCoV-229E and HCoV-OC43, were known to infect humans. Soon after the SARS epidemic, two more human coronaviruses, HCoV-HKU1 and HCoV-NL63, were discovered. Nearly a decade after the SARS epidemic, another novel coronavirus, the sixth known to infect humans, emerged in the Middle East. This virus was first identified and isolated in June 2012 from a Saudi male patient in Jeddah, Saudi Arabia, who passed away from the infection presenting acute pneumonia and renal failure [272]. The virus was first provisionally named HCoV-EMC and later renamed the Middle East Respiratory Syndrome Coronavirus (MERS-CoV) [273]. Unlike the HCoV-229E, HCoV-OC43, HCoV-HKU1 and HCoV-NL63 which cause mild and self-limiting upper respiratory tract infections, MERS-CoV, together with SARS-CoV, is classified as highly pathogenic human coronaviruses as they cause serious lower respiratory tract infections as well as extrapulmonary manifestations which could be fatal. As of 15th July 2015, a total number of 1,368 laboratory-confirmed MERS cases were reported with at least 489 deaths [274]. A majority of the reported cases occurred in the Middle East, with the most number in Saudi Arabia, and all cases outside the Middle East, including Europe, North American, Africa and Asia, were linked to travel histories to the Middle Eastern countries [275]. Human-to-human transmissions of MERS-CoV have been described in family clusters that resulted from close contact with the infected index case and in healthcare settings between healthcare workers and patients [276,277]. Otherwise, MERS-CoV is incapable of sustained human-to-human transmission, unlike SARS-CoV that is well-adapted to transmission between humans. Based on current data, MERS-CoV is considered more virulent compared to SARS-CoV, as reflected from its higher mortality rate of over 35%

compared to 10% of SARS-CoV [278]. However, the high mortality rate of MERS-CoV could be an overestimate due to the lack of report of asymptomatic and mild cases. While the SARS epidemic occurred swiftly and was effectively brought to an end after 4 months of intensive public health efforts, the MERS-CoV has persisted for more than 3 years and the number of affected individuals continues to escalate.

MERS presents as a lower respiratory tract infection with symptoms including high fever, cough and dyspnea as well as extrapulmonary symptoms such as nausea, diarrhea and vomiting [278]. The incubation period of MERS-CoV infection is estimated to range from 1.9 to 14.7 days with symptom onset usually occurring by day 12 [276,279]. Infection can develop into severe complications such as severe pneumonia, ARDS and respiratory failure as well as other systemic manifestations including hepatic dysfunction, pericarditis and acute renal failure [279,280]. Mild and asymptomatic infections have been observed, while severe cases were commonly seen in elderly patients with co-morbidities, such as diabetes mellitus, chronic renal disease, chronic cardiac disease and pulmonary disease [276,279,280,281]. It was also found that males above 50 years of age with multiple co-morbidities were associated with a higher mortality rate [282].

Currently, there are no standardized treatment or approved therapeutic drugs and vaccines available for MERS-CoV infections. As with the case of SARS, supportive care is the main form of treatment for MERS patients. While randomized controlled trials to prove efficacies of existing antiviral drugs for MERS treatment are not available, numerous studies have identified antiviral agents in controlling MERS-CoV infection through *in vitro* and *in vivo* approaches. These include broad-specturm antivirals such as interferons, ribavarin and cyclophilin inhibitors, which also exhibit antiviral activities for

SARS-CoV [283,284]. Other existing drugs with potential anti-MERS-CoV activities include mycophenolic acid, lopinavir-ritonavir combination and chloroquine [285,286].

1.6 Virology of MERS-CoV

Same as the SARS-CoV, the MERS-CoV belongs to the genus *betacoronavirus*, family *Coronaviridae* and order *Nidovirales*. While SARS-CoV belongs to lineage B of the *betacoronavirus* genus, MERS-CoV is the first coronavirus in *betacoronavirus* lineage C capable in infecting human. Like all nidoviruses, MERS-CoV is a positive-sense, single-stranded RNA virus of approximately 30kb genome size. Its genome encodes for 16 nsps, 4 structural proteins and at least 4 accessory proteins (Figure 1.6).

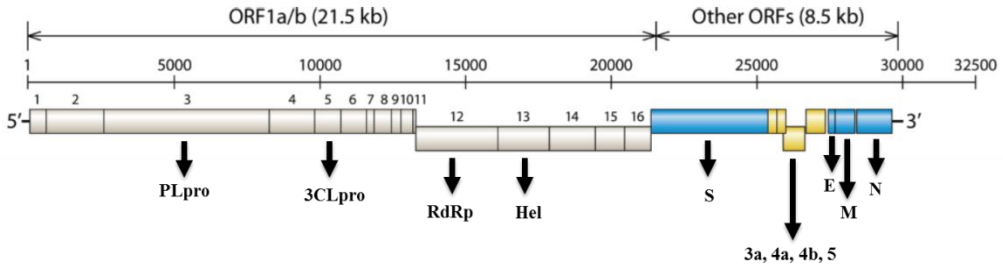

Figure 1.6. Genomic arrangement of MERS-CoV. ORF1a/b gives rise to nsps 1 to 16 (light grey), while the 3' ORFs give rise to structural (blue) and accessory (yellow) proteins. Abbreviations: PLpro (nsp3), papain-like protease; 3CLpro (nsp5), 3C-like protease; RdRp (nsp12), RNA-dependent RNA polymerase; Hel (nsp13), helicase; S, spike; E, envelope; M, membrane, N, nucleocapsid. Figure modified from Chan *et al* [287].

As MERS-CoV is a new virus, work on dissecting the functions of individual viral protein is still ongoing. Nonetheless, the putative roles of the viral proteins could be derived based on analogy to other coronavirus proteins, such as that of SARS-CoV. Genomic analysis of the MERS-CoV genome revealed similarities to SARS-CoV and other coronaviruses. 2/3 of the genome from the 5' proximal end consists of the ORF1a

and ORF1b that encode for the replicase polyproteins pp1a (4391 amino acids) and pp1ab (7078 amino acids), with the latter translated *via* a ribosomal frameshifting at the end of ORF1a. The remaining 1/3 of the genome downstream of the ORF1b encodes for the structural S, E, M and N proteins as well as accessory protein 3, 4a, 4b, and 5 [288].

The replicase polyproteins pp1a and pp1ab are cleaved into 16 nsps by the PLpro (nsp3) and the 3CLpro (nsp5) [288,289]. Nsps play critical roles in viral genome transcription and replication, as well as other regulatory functions in viral replication and pathogenesis [23]. The MERS-CoV nsp3 protein, in addition to its protease activity, is also a viral deubiquitinating enzyme, like that of SARS-CoV, and acts as an IFN antagonist by interfering with the IFN regulatory factor 3 (IRF3) pathway [290,291]. Although the MERS-CoV and SARS-CoV PLpro process similar substrates, they exhibit distinct catalytic efficiencies, suggesting fundamental differences between the two viruses [292]. The MERS-CoV nsp5 3CLpro has been shown to be activated by ligand-induced dimerization [293]. Using a cleavage site prediction method, 11 canonical sites downstream of nsp4, which are conserved within coronaviruses, were predicted for 3CLpro, which is in agreement with the understanding that 3CLpro cleaves downstream of nsp4 to yield nsp4 to nsp16 [294]. However, 3 non-canonical cleavage sites upstream of nsp4 were identified and experimentally confirmed, suggesting a novel role for MERS-CoV 3CLpro processing of pp1a and pp1ab [294].

The MERS-CoV structural S protein is 1353 amino acids in length and is a type I transmembrane glycoprotein and a type I fusion protein that assembles into trimers, constituting the spike peplomers on the surface of the viral particle [295]. Same as the S protein of other coronaviruses, it is composed of the N-terminal S1 domain and C-

terminal S2 domain and is the main determinant of host cell tropism through its function to mediate viral attachment and entry into host cells during viral infection [296]. The N-terminal S1 domain (residues 1-751) is responsible for attachment and binding to the host cell receptor, while the C-terminal S2 domain (residues 752-1353) mediates viral-cell membrane fusion during the viral entry process (Figure 1.7). The host cell receptor utilized by the MERS-CoV was identified to be the dipeptidyl peptidase 4 (DPP4) molecule, also known as CD26 [297]. The RBD within the S1 subunit important for interaction with DPP4 receptor was mapped to be a 231-residue region at amino acids 358 to 588 [298]. As with all coronaviruses, the S protein is a major antigenic determinant in eliciting high levels of neutralizing antibodies, which can inhibit viral entry and neutralize MERS-CoV infections [299,300]. Upon receptor binding and recognition, the MERS-CoV S protein is activated for membrane fusion through the cleavage into S1 and S2 subunits by several host cell proteases, including TMPRSS2, cathepsin and furin [301,302]. Protease inhibitors, such as inhibitors of TMPRSS2 and furin, are potential treatment options for MERS-CoV infection as they have been demonstrated to be able to block MERS-CoV cell entry via the inhibition of cell-cell fusion [303,304].

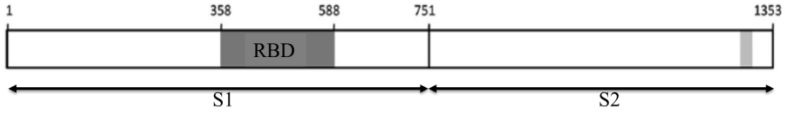

Figure 1.7. Schematic drawing indicating the domains of MERS-CoV S protein. RBD, receptor-binding domain. Figure adapted from Mou *et al* [298].

Besides S protein, the E, M and N proteins make up other 3 critical structural proteins of MERS-CoV, and less information on them is available so far. The MERS-CoV E protein, similar to that of SARS-CoV, consisting of a α-helical structure with a single transmembrane domain and function as ion channels in lipid bilayer [305] and is essential for viral propagation and infectivity [306]. The M protein forms the main component of the viral outer membrane and acts as an IFN antagonist [307], while the N protein package viral RNA during the assembly of virion particles [308].

Thus far, little is known about the MERS-CoV accessory proteins, but like in the case for SARS-CoV and other coronaviruses, they are believed to play crucial roles in viral pathogenesis and regulate viral-host interactions to promote viral replication and survival [213]. It has been shown that accessory protein 4a, 4b and 5 are not essential for viral replication [306] and can potentially function as IFN antagonists [307]. Accessory protein 4a is able to inhibit innate immunity signaling pathway through its binding to dsRNA to suppress PACT-induced activation of retinoic acid-inducible gene 1 (RIG-I) and melanoma differentiation-associated protein 5 (MDA5) [309]. The MERS-CoV ORF4b-encoded accessory protein 4b has also been demonstrated to facilitate viral invasion from innate immunity through the specific inhibition of type I IFN and NF-κB signaling pathways [310]. An additional accessory protein 8, which is believed to be encoded by ORF8b located within the N gene, has no reported function [288].

1.7 Zoonotic Origin of MERS-CoV

It was postulated that a novel episode of interspecies cross-transmission has led to the emergence of MERS-CoV in humans due to the absence of human serological evidence that the virus has been circulating in the general population in Middle East

[311,312]. First evidence that suggests MERS-CoV is a zoonotic agent came from the genomic sequence analysis of MERS-CoV with existing coronaviruses, which revealed close phylogenetic relationship between MERS-CoV with two bat lineage C betacoronaviruses, Ty-BatCoV HKU4 and Pi-BatCoV HKU5, which were identified prior to the emergence of MERS-CoV from the *Tylonycteris pachypus* and *Pipistrellus abramus* bats respectively in Hong Kong [313,314]. Based on the RdRp gene sequence, MERS-CoV shared approximately 90% and 92% sequence identity as BatCoV HKU4 and HKU5 respectively, and the low nonsynonymous/synonymous nucleotide substitution ratios of BatCoV HKU4 and HKU5 suggest that bats are the primary reservoirs of the two viruses [315]. Other related lineage C betacoronaviruses related to MERS-CoV have also been identified from various bat species in many other countries including the Middle East, Africa, Central America and Europe, further indicating the high prevalence of MERS-CoV-related bat coronaviruses worldwide [316,317,318,319,320]. Despite this, none of these batCoV strains are likely the direct ancestor of MERS-CoV, as the genetic similarity of the S gene ranges from 64.6 to 67.4% [315,318]. It has been recently demonstrated by two separate groups that the RBD of BatCoV-HKU4 S protein, similar to MERS-CoV S protein, could recognize both bat and human DPP4, indicating that bat DDP4 is the functional receptor of BatCoV-HKU4 [321,322]. However, batCoV-HKU4 was unable to mediate viral entry into human cells due to its inability to be activated by endogenous human proteases [321]. It has been further shown that the introduction of two mutations in the batCoV-HKU4 S protein, which allow cleavage by human proteases, conferred capability to mediate viral entry into human cells, indicating the importance of these two mutations in the adaptation to human cellular proteases by MERS-CoV [323]. This not only provided further evidence

for the bat origin of MERS-CoV, but also insight into the mechanism of bat-to-human transmission of MERS-CoV.

Intermediate animal hosts, such as civet cats and raccoon dogs, have played a part in the amplification of the SARS-CoV and its interspecies transmission to human [251]. Therefore, efforts have been made to identify intermediate host(s) of MERS-CoV transmission to human. MERS-CoV is capable in replicating in a wide range of mammalian cell lines *in vitro*, including that from human, bat, pig, goal, rabbit, horse, and camel, indicating the ability of MERS-CoV S protein to recognize the DPP4 molecule of different mammals and the wide tissue tropism of the virus [324,325,326,327,328]. Human MERS-CoV infections have been linked to close contacts with camels. Camels were first implicated as the intermediate host of MERS-CoV when high titres of MERS-CoV-neutralizing sera were detected in dromendary camels in Oman, Middle East [329]. Subsequent seroepidemiological studies demonstrated the serological evidence of MERS-CoV infections in camels in various countries in Middle East, including Saudi Arabia, United Arab Emirates, Jordan and Qatar, as well as in other countries such as Egypt, Kenya and Tunisia, indicating the widespread circulation of MERS-CoV or other MERS-CoV-related strains in the dromendary camels [330]. Moreover, antibodies could be detect in archived camel sera from Saudi Arabian camels as early as ten years before the emergence of MERS, and in archived camel serum from camels in Eastern Africa up to 30 years ago, indicating the presence of the MERS-CoV or related viruses long before the MERS-CoV was identified in humans [331,332,333]. It is therefore speculated that the MERS-CoV has been co-circulating at the animal-human interface for a period of time before 2012. The strongest evidence of a direct camel-to-human transmission of MERS-CoV was established when

the virus was isolated from dromendary camels which shared 100% sequence identity as that from MERS patients who developed MERS after close contact with sick camels [334,335]. In addition, seroprevalence of MERS-CoV antibodies was significantly higher in camel-exposed individuals than in the general population, indicating the role that camels play in the transmission of the virus to humans [336].

It is clear now that MERS-CoV is a zoonosis and infection with MERS-CoV or a related virus in camels is not a new occurrence in the Middle East. At this stage, the question of the exact origin(s) of MERS-CoV remains unresolved. It is uncertain whether camels serve as the intermediate amplification host or the natural reservoir of MERS-CoV or related virus strains. Although bats are believed to be the natural hosts of all betacoronaviruses, the detection of anti-MERS-CoV antibodies in archived camel sera more than 30 years ago suggests that MERS-CoV is well-adapted in camels to be circulating in camels for such a long time [333,337]. In support of this, a recent study focusing on the detection of viral genomic RNA in camels revealed 1.6% prevalence of MERS-CoV RNA in the nasal swabs from a total of 7083 camels in United Arab Emirates, and there was absence of obvious clinical symptoms exhibited by the camels [338]. In addition, it has been proposed that other alternative sources involved in MERS-CoV transmission could be present but not identified so far, as a significant number of human MERS cases do not have direct contact with camels [287]. Further surveillance studies in camels and the evolutionary studies of coronaviruses in different animal species would be needed to address these questions.

1.8 Immune Responses against Viral Infections

When encountered with infections, the human body raises immune responses in attempt to clear and destroy the foreign pathogen. Understanding the immune responses against viruses is critical for the development of antiviral treatments and vaccines. There are two forms of immunity – the innate and the adaptive immunity. The innate immunity forms the early barrier to infections, which is usually activated immediately after infection. On the other hand, the adaptive immunity is activated later and is capable of developing an immunological memory that protects the body from future infection from the same or similar pathogen. The adaptive immunity plays an important role in the elimination of viruses during viral infections. There are two arms of the adaptive immunity – the humoral and cellular immunity – of which both are recognized to be important in both the clearance and the pathogenesis of viral infections, including SARS-CoV [191,206,339]. To date, little is known about the immune responses in MERS-CoV-infected individuals due to the limited amount of clinical data and samples available for study. Here, we provide a review of the importance of humoral and cellular immunity in coronavirus infection, with a focus on SARS-CoV, and how this knowledge has been and can be translated to development of potential antiviral strategies for SARS, such as passive immunotherapy, adoptive immunotherapy and vaccines.

1.8.1 Humoral Immunity against SARS-CoV

Humoral immunity involves the secretion of neutralizing antibodies, which possess antiviral properties and are vital in controlling viral diseases. Antibodies function through different mechanisms, namely by (1) inhibition of viral entry, (2) Fc-mediated effector functions and (3) as immunomodulaters. Through direct binding to viral surface

spikes to prevent their interaction with cellular receptors, or through association with cellular receptors and co-receptors to abolish viral engagement, antibodies can inhibit viral entry processes. Alternatively, antibodies can inhibit the fusion process of viral entry by interfering with associated conformation changes through steric hindrance. Cross-linking of virion particles and inhibition of release of progeny virions from cells mediated by antibodies also results in immobilization of viruses and prevent further viral spread [340]. Fc-mediated effector functions of antibodies include antibody-dependent cellular cytotoxicity (ADCC), antibody-dependent cellular phagocytosis (ADCP) and complement-dependent cytotoxicity (CDC), which are responsible for the direct killing of virus-infected cells [341]. In addition, antibodies play a role in immune modulation by inducing and maintaining protective antiviral immunity through the enhancement of primary and memory T cell responses [342,343].

SARS-specific IgG, IgM and IgA antibodies could be detected in SARS patients 10-14 days after the onset of symptoms [344]. While the titres of IgM and IgA peaked during the acute phase of the disease and went below baseline level by day 180, IgG titres were low initially followed by an increase that peaked at week 12 and persisted at day 240 [139]. The longer persistence of IgG antibodies suggests that they are the primary protective humoral immune response against SARS-CoV infections. High SARS-CoV-specific antibody responses have been associated with the clearance of virus and recovery of SARS patients [345]. Seroconversion of SARS-specific IgG antibodies occurred between days 10-20, which coincided with the decrease in SARS-CoV viral load [346]. In an analysis of serum samples collected from 623 SARS patients, SARS-CoV-neutralizing activities were highly attributed to IgG antibodies [347]. The persistence of SARS-CoV IgG neutralizing antibodies persisted up to 2 years post-infection, after which

the levels started to decrease and eventually undetectable at 6 years after recovery [347,348].

Antibodies specific against the SARS-CoV N and S proteins were detected in patients' sera, indicating the antigenicity of these 2 proteins in the natural course of SARS-CoV infection. In studies evaluating humoral immunity in SARS patients, N-specific antibodies were consistently detected in sera of SARS patients, while not all patients produced S-specific antibodies [139]. The strong antigenic property of N protein could be explained by the high abundance of the N protein in SARS-CoV virions and in infected cells, allowing N protein-based assay to be utilized in the serological diagnosis of SARS. However, virus neutralizing activities were mainly attributed to S-specific IgG antibodies [349]. Therefore, the S protein is a target for the induction of neutralizing antibodies for anti-SARS therapeutics as well as in vaccine strategies.

1.8.1.1 Monoclonal Antibodies for SARS-CoV Passive Immunotherapy

Passive immunotherapy using antibodies has been known as an effective antimicrobial strategy for a long time. The recent years of development in technologies involving monoclonal antibody (mAb) production and engineering has allowed the generation of numerous mAbs targeting viruses for which effective treatments and vaccines are inadequate or unavailable, including Hepatitis B and C viruses, HIV, rabies virus, Influenza A virus and the SARS-CoV [350,351]. During the SARS epidemic, treatment of patients using convalescent sera from recovered patients was found effective with no adverse effects, supporting the use of SARS-CoV-targeting antibodies as a means of therapeutic treatment for SARS [352,353]. In addition, since viral loads in the respiratory tract during SARS-CoV infection peaks at day 10 following the onset of

clinical symptoms [354], there is a window sufficient for post-exposure treatment using neutralizing antibodies. These neutralizing antibodies can be administered as a prophylaxis against infection in high-risk individuals such as contacts, healthcare, laboratory personnel as well as the immunocompromised in the event of a SARS outbreak. SARS-CoV-neutralizing mAbs targeting both the S1 and S2 domain of the S protein have been reported. A majority of them bind to the RBD of the S1 domain, which neutralizes viral infection by preventing RBD interaction with the ACE2 receptor [189]. On the other hand, anti-S2 SARS-CoV-neutralizing mAbs are believed to inhibit viral entry by disrupting the viral-cell membrane fusion process. The most potent neutralizing mAbs are those that bind directly to RBD and interfere directly with the receptor binding process. However, under selection pressures during mAb adminstration, virus strains undergo antigenic variations and drifts that result in viral escape from neutralizing mAbs, rendering the mAbs ineffective [355]. A way to circumvent this problem is to make use of a combination of mAbs targeting different antigenic regions to minimize the generation of escape mutants. In a study by ter Meulen *et al.*, two human anti-SARS-CoV mAbs, CR3014 and CR3022, bound to two different epitopes within the RBD of the S1 subunit and CR3022 was able to neutralize the escape mutant of CR3014, providing promising evidence on how a combination of non-competing anti-S1 mAbs can prevent generation of escape mutants [356].

In addition, much focus has been placed on the development of broadly-neutralizing mAbs targeting conserved epitope regions that are involved in highly conserved functions such as the post-attachment fusion process [357], for which mutations during antigenic variations will result in the loss of important function necessary for viral infection and survival. This is especially important in targeting viruses

that arise from heterogeneous pools circulating in animal reservoirs with high antigenic diversity, such as the SARS-CoV. Given the high diversity and prevalence of zoonotic SL-CoVs found in bats, future outbreaks could most likely be caused by a variant strain of SARS-CoV originating from SL-CoVs in bats and/or other intermediate hosts. The development of mAbs for the prophylaxis and therapeutic purposes should therefore target both human SARS-CoV strains and also zoonotic SL-CoV strains. MAbs that target the S2 domain of the SARS-CoV S protein are broadly neutralizing and can confer cross-protection against human SARS-CoV and zoonotic strains of SL-CoVs [188]. A brief summary of anti-SARS-CoV mAbs targeting the S2 domain discovered to date is provided in Table 1.3.

Table 1.3. List of mAbs targeting the S2 domain of the SARS-CoV

MAb Epitope(s) within S2	Origin of mAb	Results and findings	Refs
HR1 and HR2	Humanized mice immunized with S protein ectodomain	- mAbs targeting the highly conserved HR1 and HR2 domains are broadly neutralizing - Combination of anti-S1 and anti-S2 mAbs effective in neutralization compared to individual mAb	[358]
Residues 791-805 of S2 (MAb 5H10)	Humanized mice immunized with *E.coli*-expressed recombinant peptide of S protein	- mAb 5H10 prevented viral fusion and entry but not viral attachment to host cells or cleavage of S - Administration of mAb 5H10 in SARS rhesus models suppressed SARS-CoV-induced pathogenesis - Significant amounts of antibodies detected 2 weeks after administration, suggesting its potential use in prophylaxis and therapeutics	[359]
Residues1023-1189 (ScFv B1)	Generation of a SARS-CoV scFv immune library from convalescent SARS patients, selection using whole SARS-CoV virions	- Using *in vitro* pseudotyped virus neutralization assay, ScFv B1 exhibited inhibitory effects in dose-dependent manner, with IC50 around 12μg/ml	[360]
Residues 787-809	Antibodies screened from convalescent SARS patients using a phage display dodecapeptide library	- Majority of SARS convalescent patients (82.5%) produced antibody against this epitope region, indicating the immunodominance of this epitope site - Plasma from SARS convalescent patients was able to protect SARS-CoV (BJ01) infection in Vero E6 cells - Anti-S2 antibodies not detected in some	[361]

MAb Epitope(s) within S2	Origin of mAb	Results and findings	Refs
		convalescent plasma, indicating that other antibodies targeting other antigenic regions are also necessary for protection - Other epitopes identified in study located in N, S1, E and M proteins	
Residues 1143–1157 located within HR2	BALB/c mice immunized using *E-coli* purified recombinant protein of residues 268-1255 of SARS-CoV S protein	- mAbs neutralized SARS-CoV infection of Vero E6 cells in a dose-dependent manner	[362]
Four epitopes at residues 1091-1130, 1111-1130, 1151-1170, 1151-1192	BALB/c mice immunized using E.coli expressed GST-tagged S fragment consisting of amino acids 1029-1192	- mAbs able to neutralize SARS-CoV infection *in vitro* - mAbs inhibited S-induced cell-cell membrane fusion, suggesting that the mAbs neutralized SARS-CoV infection through the inhibition of fusion process	[363]
Residues 789-799	BALB/c mice immunized with recombinant S protein that consists of 6 antigenic regions of the S protein predicted using bioinformatics analysis	- Binding assays were carried out to show mAb binding to S - Neutralization capability of mAb was not investigated	[364]

1.8.2 Cellular Immunity against SARS-CoV

Besides the secretion of antibodies, cellular immunity executed by $CD4^+$ helper T cells and $CD8^+$ cytotoxic T cells plays an equally important role in the control of viral infections. $CD4^+$ helper T cells exhibit several important functions, namely (1) the promotion of B cell activation and antibody production by B cells, including class switching and affinity maturation; (2) promotion of the generation of long-lived antibody-producing plasma cells and B cell memory; (3) induction of optimal antiviral $CD8^+$ T cell responses and generation of memory $CD8^+$ T cells; (4) conferring of antiviral functions through the release of cytokines, direct lysis of virus-infected cells and activation of antigen-presenting cells [365]. On the other hand, $CD8^+$ T cells are mainly responsible for cytotoxic activities through the production of inflammatory and antiviral cytokines and chemokines [366], as well as cytotoxic molecules such as granzymes and perforin which will direct the killing of virus-infected cells through exocytosis [367].

To date, there is limited knowledge on antigen-specific T cell-mediated cellular immunity against SARS-CoV. Nonetheless, several studies using animal models have indicated the importance of T cells in the clearance of SARS-CoV during primary infection and the protection from disease. In a study using senescent BALB/c mice infected with human SARS-CoV Urbani strain, it was found that $CD4^+$ T cells, but not $CD8^+$ T cells, contributed to virus clearance [368]. In another study, infected BALB/c mice with mouse-adapted SARS-CoV strain, MA15, showed robust T cell responses that were necessary and sufficient for virus clearance in the absence of innate immunity, and the adoptive transfer of *in vitro* cultured antiviral T cells significantly improved survival of the infected mice [369]. A further study by the same group showed that memory $CD8^+$

T cells specific against SARS-CoV provided substantial protection against lethal MA15 infection, although $CD4^+$ T cells and antibody production were also necessary for complete protection [370]. In humans, it has been suggested that cellular immunity can play dual roles in the control of virus replication and immunopathogenesis of acute SARS-CoV infection [371]. The delayed development of adaptive immune response and decreased T cell numbers (lymphopenia) had been observed to correlate with prolonged virus clearance and severe disease, indicating the importance of T cell-mediated cellular immune response in disease progression and limitation [372,373,374]. On the other hand, an extreme cellular immune response may result in lung tissue injury by production of cytokines and chemokines that attract large number of neutrophils and macrophages to induce an enhanced production of proinflammatory cytokines, leading to dysregulation of the cytokine network and the exacerbation of disease, as observed in lung tissues during autopsy of SARS victims [354]. In addition, while studies on convalescent SARS patients indicated that SARS-CoV-specific antibody response is short-lived, SARS-CoV-specific memory T cell responses were found to persist up to 6 years after recovery in the absence of antigen, suggesting the long-lived nature and the importance of SARS-CoV-specific T cell immunity [142,375].

1.8.2.1 SARS-CoV Adoptive Immunotherapy and Vaccine Development

SARS-CoV being a novel coronavirus which first emerged in 2003 with no subsequent re-emergence in humans, not much is known about the conference of immunological memory in humans after infection. The delineation of SARS-CoV-specific T cell populations and epitopes from SARS convalescent subjects allows the understanding SARS-specific protective immunity, which can influence the development

of vaccine strategies against the virus, which should target to induce a robust and long-term memory T cell response. From peripheral blood of SARS-recovered patients, memory T cell responses specific against SARS-CoV were detected and numerous T cell epitopes have been mapped in several SARS-CoV proteins, including the structural S, M, N and E proteins, the non-structural replicase polyprotein as well as the accessory proteins. A summary of SARS-CoV-specific $CD4^+$ and $CD8^+$ T cell epitopes identified from SARS-recovered human subjects is provided in Table 1.4. The use of animal models provides a good platform for the evaluation of vaccination options. In a study using transgenic mice, the use of a vaccine regime consisting of a SARS-CoV spike (S) DNA prime and HLA-A*0201 restricted peptides boost successfully elicited HLA-A*0201-restricted S-specific $CD8^+$ T cells, which could protect against infection, giving evidence that such a vaccine could potentially be used in humans [192]. In another study, an immunodominant SARS-specific $CD8^+$ T cell epitope within the SARS-CoV N protein was identified, and naive lymphocytes from healthy individuals engineered to express the T cell receptor (TCR) specific for this epitope exhibited similar properties as the SARS-specific memory $CD8^+$ T cells, indicating the possible use of TCR-redirected T cells for adoptive immunotherapy of the treatment of SARS-CoV infections [142].

Table 1.4. Summary of SARS-specific $CD4^+$ and $CD8^+$ T cell epitopes identified from SARS-recovered human subjects

T cell epitope (residue numbers)	Type of T cell response	HLA-restriction	Method of identification	Refs
(1) STRUCTURAL PROTEINS ***Spike protein***				
1203-1211 978-986	$CD8^+$	HLA-A*0201	- Screening from 8 SARS-recovered patients at 1 year post-infection using peptides spanning the SARS-CoV S protein	[376]
411-420	$CD8^+$	HLA-A*0201	- HLA-A*0201-restricted cytotoxic T lymphocyte (CTL) epitope prediction using BioInformatics and Molecular Analysis Section (BIMAS) HLA Peptide Binding Predictions, followed by evaluation of binding capacity of refolded peptides to HLA-A*0201 molecules in T2 binding assay - Peptides were evaluated for CTL activity in HLA-A2-positive and negative SARS-recovered donors 7-8 months after infection - CTL response verified in HLA-A*0201 transgenic mice after peptide immunization	[377]
958-966	$CD8^+$	HLA-A*0201	- HLA-A*0201-restricted epitopes in S protein predicted based on the presence of HLA-A*0201 binding motifs and the proteasome cleavage sites - T2 binding assay and evaluation of peptide CTL activity in 10 HLA-$A2^+$ SARS-recovered donors - CTL activity of peptide further evaluated in HLA-A2 transgenic mice	[378]

T cell epitope (residue numbers)	Type of T cell response	HLA-restriction	Method of identification	Refs
1042-1050	$CD8^+$	HLA-A*0201	- Prediction of HLA-A*0201 binding peptides within S and N proteins, followed by validation by T2-cell binding assay - Immunogenicity was measured in HLA-A2.1 transgenic mice and *in vitro* vaccination of healthy and SARS-recovered human PBMCs - Memory $CD8^+$ response against peptide detected in SARS-recovered donor more than 1 year post-infection.	[141]
39-54	$CD8^+$	Undetermined	- Identification of SARS-CoV-specific T cell responses in 128 SARS-recovered patients 1 year post-infection using a total of 1843 peptides spanning the entire SARS-CoV proteome in IFNγ ELISpot assays and flow cytometry.	[140]
187-203				
299-316	$CD4^+$			
343-360	$CD8^+$			
411-426	$CD4^+$			
427-449	$CD8^+$			
435-451	$CD4^+$ and $CD8^+$			
512-527	$CD8^+$			
520-537	$CD4^+$			
528-545	$CD8^+$			
536-553	$CD4^+$			
619-637	$CD8^+$			
633-650	$CD4^+$ and $CD8^+$			
649-666	$CD8^+$			
665-681				
672-689				
767-784				
791-808	$CD4^+$			
842-859				
897-913				
918-934				

T cell epitope (residue numbers)	Type of T cell response	HLA-restriction	Method of identification	Refs
970-986				
1082-1097	$CD8^+$			
Membrane protein				
21-44	$CD4^+$ and $CD8^+$	Undetermined	- Screening of PBMCs from SARS-recovered individuals 12-23 months after infection using a total of 30 peptides spanning the entire M protein sequence	[379]
65-91				
117-140				
200-220				
121-135	$CD8^+$	Undetermined	- Identification of SARS-CoV-specific T cell responses in 128 SARS-recovered patients 1 year post-infection using a total of 1843 peptides spanning the entire SARS-CoV proteome in IFNγ ELISpot assays and flow cytometry.	[140]
146-160	$CD4^+$ and $CD8^+$			
161-175				
166-180	$CD8^+$			
176-189				
181-195				
191-205				
196-210	$CD4^+$ and $CD8^+$			
Nucleocapsid protein				
223-231 227-235 317-325	$CD8^+$	HLA-A*0201	- Prediction of HLA-A*0201 binding peptides within S and N proteins, followed by validation by T2-cell binding assay - Immunogenicity was measured in HLA-A2.1 transgenic mice and *in vitro* vaccination of healthy and SARS-recovered human PBMCs -Memory $CD8^+$ response against peptide detected in SARS-recovered donor more than 1 year post-infection.	[141]
41–55	$CD8^+$	Undetermined	- Identification of SARS-CoV-specific memory T cell responses against SARS-CoV N protein and 3a protein in 16 SARS-recovered donors at 6 years post-infection using IFNγ ELISpot,	[142]
101–115	$CD4^+$			
126–140	$CD4^+$			
216-225	$CD8^+$	HLA-B*40:01		

T cell epitope (residue numbers)	Type of T cell response	HLA-restriction	Method of identification	Refs
261–275	$CD8^+$	Undetermined	intracellular cytokine staining (ICS) and flow cytometry	
306–320	$CD4^+$			
326-340	$CD4^+$			
321–335	$CD8^+$			
106-120	$CD8^+$	Undetermined	- Identification of SARS-CoV-specific T cell responses in 128 SARS-recovered patients 1 year post-infection using a total of 1843 peptides spanning the entire SARS-CoV proteome in IFNγ ELISpot assay and flow cytometry	[140]
116-130				
121-135				
211-225				
356-370				
361-375				
Envelope protein				
9 to 26	$CD4^+$ and $CD8^+$	Undetermined	- Screening of PBMCs from individuals who have fully recovered from SARS two years after infection using 9 peptides spanning the E protein sequence	[380]
33 to 49				
40-57				
11-25	$CD8^+$	Undetermined	- Identification of SARS-CoV-specific T cell responses in 128 SARS-recovered patients 1 year post-infection using a total of 1843 peptides spanning the entire SARS-CoV proteome in IFNγ ELISpot assays and flow cytometry	[140]
41-55				
(2) NON-STRUCTURAL REPLICASE PROTEIN				
356-370	$CD8^+$	Undetermined	- Identification of SARS-CoV-specific T cell responses in 128 SARS-recovered patients 1 year post-infection using a total of 1843 peptides spanning the entire SARS-CoV proteome in IFNγ ELISpot assays and flow cytometry	[140]
806-820				
869-883	$CD4^+$			
4170-4186	$CD8^+$			
4486-4500	$CD4^+$			

T cell epitope (residue numbers)	Type of T cell response	HLA-restriction	Method of identification	Refs
4506-4520	$CD8^+$			
4701-4715				
(3) ACCESSORY PROTEINS				
3a (previously known as ORF3)				
6-20	$CD4^+$ and $CD8^+$	Undetermined	- Identification of SARS-CoV-specific memory T cell responses against SARS-CoV N protein and 3a protein in 16 SARS-recovered donors at 6 years post-infection using IFNγ ELISpot, intracellular cytokine staining (ICS) and flow cytometry	[142]
51-65	$CD4^+$			
66-80				
169-210				
206-220				
6-20	$CD4^+$ and $CD8^+$	Undetermined	- Identification of SARS-CoV-specific T cell responses in 128 SARS-recovered patients 1 year post-infection using a total of 1843 peptides spanning the entire SARS-CoV proteome in IFNγ ELISpot assays and flow cytometry	[140]
36-50	$CD8^+$			
121-135				
3b (previously known as ORF4)				
140-154	$CD8^+$	Undetermined		
6 (previously known as ORF7)				
11-25	$CD8^+$	Undetermined		
26-40				
9b (previously known as ORF13)				
46-60	$CD8^+$	Undetermined		
61-75				
81-94				

1.9 Comparison between SARS-CoV and MERS-CoV

Comparing MERS and SARS, many similarities in clinical symptoms can be seen, with severely ill patients usually presenting acute hypoxic respiratory failure. However, important differences exist between the two diseases caused by the two viruses, in terms of disease epidemiology, clinical symptoms presented in patients and virology characteristics. For instance, although both SARS and MERS seem to affect elderlies with similar co-morbidities, diabetes type 2 and chronic renal diseases are significant co-morbidities for MERS [11,381]. Acute renal failure was also more frequently associated with MERS fatality compared to SARS [382]. SARS patients showed diffuse alveolar damage with an exudative phase, a proliferative phase and a final fibrotic phase, while for MERS, there is limited evidence to suggest the development of fibrosis at the end stage ARDS in severe patients [383]. These differences may indicate distinct underlying mechanisms and pathogenesis of the two diseases. A comparison of the SARS-CoV and MERS-CoV is provided in Table 1.5.

Table 1.5. Comparison of SARS-CoV and MERS-CoV

	SARS-CoV	MERS-CoV	Refs
Epidemiology			
Year of identification	2003	2012	[4,251,274, 275,278, 330]
Geographical origin	Southern China, Guangdong Province	Middle East	
Affected regions	Asia, including Mainland China, Hong Kong, Singapore, Taiwan Other countries outside Asia include Canada and United States	Middle East countries including Saudi Arabia, United Arab Emirates (UAE), Jordan and Oman Other regions outside Middle East include Europe, North American, Africa and Asia	
Total number of infected cases	8098 infected cases, 774 deaths	1,368 laboratory-confirmed cases, 489 deaths (as of 15th July 2015)	
Period of epidemic	February to July 2003 Sporadic cases in December 2003 to January 2004	June 2012 to present	
Epidemic center(s) of outbreak	Community-based places, like wildlife animal wet markets and restaurants, hotels, hospitals, airplanes, housing estate with poor sewage system and laboratories	Hospitals and family households	
Fatality rate	10%	>35%	
Intermediate host responsible	Wildlife animals sold in wet markets, such as palm civets and raccoon dogs	Dromendary camels, bats Others?	

	SARS-CoV	MERS-CoV	Refs
for transmission to human			
Natural reservoir	Chinese horseshoe bats	Undetermined, speculated to be bats or camels	
Transmission routes	Close contact, air droplets, fecal-oral	Close contact, air droplets	
Incubation period	2 to 14 days	1.9 to 14.7 days	
Basic reproduction number and transmissibility	0.3-4.1 High transmissibility	0.3-1.3 Low transmissibility	
Clinical characteristics			
Onset of clinical symptoms	Within 12.5 days of infection	Around day 12 after infection	[9,11,276, 279,280, 281,344, 384,385, 386,387]
Clinical symptoms	Persistent fever, dry cough, chills, myalgia, headache, and dyspnea Less common symptoms include sore throat, rhinorrhoea, nausea and vomiting	High fever, nonproductive cough, chills, headache, dyspnea, and myalgia Less common symptoms include sore throat, nausea, vomiting and dizziness	
Extrapulmonary manifestations	Watery diarrhea, tachycardia, bradycardia tachypnoea, hypotension, liver and renal dysfunctions	Diarrhea, abdominal pain, liver and renal dysfunctions, pericarditis, arrhythmias, hypotension	
Biochemical and hematologic findings	Elevated creatine kinase, lactate dehydrogenase and alanine transaminases levels, hyponatremia and hypokalemia Lymphopenia, leukopenia, thrombocytopenia, anemia, elevated cytokines and chemokines levels	Elevated lactate dehydrogenase, creatine kinase and alanine aminotransferase levels Leukopenia, leukocytosis, lymphopenia, lymphocytosis, thrombocytopenia, thrombocytosis	

	SARS-CoV	MERS-CoV	Refs
Fatal complications	ARDS	ARDS, acute renal failure	
Radiological changes	Enlarged lung opacities, predominantly at lung periphery and the lower zone Absence of cavitation, hilar lymphadenopathy or pleural effusion Lesions of fibrocellular intra-alveolar organization with bronchiolitis obliterans organizing pneumonia-like pattern	Enlarged lung opacities Unilateral or bilateral interstitial infiltrates Small pleural effusions and consolidation Distribution of lesions resembling that of organizing pneumonia Radiological findings resemble that of severe pandemic H1N1 influenza infection	
Mean age of infected individuals	39.3±16.8 years	53.5±29.5 years	
Comorbidities associated with severe disease	Asthma and chronic pulmonary disease Cardiovascular and cerebrovascular diseases Diabetes mellitus Cancer Chronic renal disease and chronic liver disease	Diabetes mellitus Chronic renal disease Hypertension Less common comorbidities include chronic cardiac disease and pulmonary diseases, smoking and obesity	
Main form of treatment	Supportive treatment Ventilator support for ARDS Ribavirin and corticosteroid combination treatment Interferon treatment Lopinavir/ritonavir treatment Convalescent plasma administration	Supportive treatment Ventilator support for ARDS Ribavirin and interferon-β treatments	

	SARS-CoV	MERS-CoV	Refs
Virology			
Classification	Order *Nidovirale* Family *Coronaviridae* Genus *betacoronavirus*, lineage B	Order *Nidovirale* Family *Coronaviridae* Genus *betacoronavirus*, lineage C	[147,171, 172,174, 175,297, 302]
Host receptor	ACE2	DPP4	
Host proteases for S protein activation	TMPRSS2, cathepsin L, HAT	TMPRSS2, cathepsin L, furin	
Susceptible cell lines	Limited cell line tropism, including primates cell lines (Vero E6, LLC-MK2, FRhK-4), human liver cell lines (Huh-7, HepG2), human lung cell line (Glc82, Calu-3), and human colon intestinal cell lines (T84 and Colo320)	Wider range of mammalian cell lines from primate (VeroE6, LLC-MK2), bats, porcine, civets and rabbits. Human cell lines include those from respiratory (Calu-3, HFL), gastrointestinal tract (Caco-2), liver (Huh-7) and kidney (HEK 293T and 769P)	[324,325, 388]
Animal models	Rhesus macaques, cynomolgus macaques, ferrets, BALB/c mice, transgenic mice expressing human ACE2 receptor	Rhesus macaques, marmoset, dromedary camels, transgenic mice expressing human DPP4 receptor	[389]
Host immunity			
Innate immunity	SARS-related severe lung injury attributed to the dysregulation of proinflammatory cytokines and chemokines SARS-CoV infection antagonizes IFN production by interfering the activation of IFN downstream signaling pathways	Fatal MERS-CoV infections could be associated with dysregulation of innate immune response coupled with inefficient activation of adaptive immune response *In vitro* studies showed that MERS-CoV infection inhibits and delay IFN induction MERS-CoV infection resulted in a great secretion of type I and III IFNs, in particularly IFN-α, as compared to SARS-	[390,391, 392,393, 394]

	SARS-CoV	MERS-CoV	Refs
		CoV	
Humoral immunity	Virus-specific antibody detectable around day 10-14 after the onset of symptoms IgM and IgA levels peaked during the acute phase of disease and went below baseline level by day 180 IgG titres were low initially followed by an increase that peaked at week 12 and persisted for more than a year	Serum neutralizing antibodies detected on day 12 post-infection in human MERS cases and persist up to a month after onset of symptoms MERS-CoV-specific IgM antibody response mounted before day 16 after onset of symptoms IgG antibody titres peaked at 3 weeks after onset of symptoms and remained elevated up to 5 weeks MERS-CoV-specific antibodies undetectable in MERS victims, suggesting the importance of antibody responses in protection against infection	[287,391, 395,396]
Cellular immunity	Found to persist in convalescent individuals up to 6 years after recovery T cell immunity shown to be important in virus clearance and protection against SARS-CoV infections in animal models	Systematic study of cellular responses in MERS human cases unavailable T cell deficiency associated with persistent infections and inability to clear virus in transgenic mouse models expressing human DPP4; $CD8^+$ T cell responses targeting the MERS-CoV S protein peaked at day 7-10 post-infection and exhibited low level of cross-reactivity to SARS-CoV	[191,369, 397,398]

1.10 Goals of the Project

In response to viral infection, host mechanisms are triggered to raise immune defenses against the viruses. At the same time, viruses have evolved ways to evade host defense system as well as to hijack the host cellular machinery for efficient replication to ensure successful infection and survival. These processes involve the interplay of various viral and host factors. The understanding of these complex viral-host interactions is critical for the identification of drug targets in the development of antiviral strategies. In this thesis, viral-host interactions triggered by SARS-CoV and MERS-CoV are investigated in 3 separate studies/chapters, addressing various viral-host interactions that are involved in host immune responses and viral subversion of host cell machinery.

As neutralizing antibodies play a critical role in protection and clearance of SARS-CoV infections, the use of mAbs as prophylactic and therapeutic agents in passive immunotherapy is a promising antiviral strategy against SARS-CoV. In the first study, our aim is to characterize the interaction of two SARS-CoV-neutralizing mAbs with the SARS-CoV S protein. These mAbs bind to SARS-CoV S at novel epitopes located within the highly conserved S2 domain. Through the generation of escape SARS-CoV mutants using these mAbs, we hope to identify critical residue(s) required for the binding and inhibitory activity of the mAbs, so as to gain a better understanding of the neutralization mechanisms of the mAbs as well as the role of the neutralizing epitopes in S protein function.

The understanding and knowledge on the cellular immunity elicited by SARS-CoV infections is so far limited, and it is uncertain how long memory cellular responses persist in SARS-convalescent patients after recovery from SARS. In the second study, the main objective is to determine the presence of SARS-specific

memory T cell responses in SARS-recovered subjects at 9 to 11 years post-infection. In addition, we further characterized two SARS-specific $CD8^+$ T cell responses that target the M protein and N protein of SARS-CoV by determining the minimal epitope and the HLA class I restriction of the responses. This study provides evidence for the M and N proteins as important targets of the host cellular immune system during the encounter of SARS-CoV infection, and has significant implications in the design and development of vaccines as well as treatment options for SARS.

Being a novel coronavirus, the mechanisms underlying the high pathogenicity of MERS-CoV is currently poorly understood. The comparison of MERS-CoV with the SARS-CoV is important in understanding this new virus, since both viruses belong to the same genus and display some identical clinical features. Further delineation of the viral-host interactions of MERS-CoV and its host can lead to a better understanding of the mechanisms involved in the replication and pathogenesis of the virus and the identification of drug targets and antiviral options. In the third study, the main objective is to investigate similarities and differences between the MERS-CoV and the SARS-CoV N proteins, in terms of cellular activities and functions that have been established for SARS-CoV N protein. Focus is placed in three main aspects: (i) ability to interact with host factor eEF1A; (ii) ability to inhibit cellular protein translation and (iii) to induce actin re-arrangement. Through this study, we aim to gain a better understanding on the role of MERS-CoV N protein in the process of viral infection, replication and pathogenesis.

CHAPTER 2: MATERIALS AND METHODS

2.1 Ascites production

This was performed by the Monoclonal Antibody Unit at Institute of Molecular and Cell Biology (IMCB). Ascites were produced by injecting hybridoma cells into the peritoneal cavities of pristine-primed BALB/c mice. The protocol was approved by the Institutional Animal Care and Use Committee (IACUC) of the Biological Resource Centre, A*Star, Singapore (Protocol Number: 110694). All the procedures were carried out in strict accordance with the recommendations of the National Advisory Committee for Laboratory Animal Research (NACLAR) guidelines in Singapore. All efforts were made to minimize suffering and euthanasia was performed using carbon dioxide.

2.2 Cell lines and virus

Vero E6, HeLa (American Type Culture Collection) and human embryonic kidney (HEK) 293 FT cells (Invitrogen) were grown in Dulbecco's modified Eagle's medium (DMEM [Invitrogen]) supplemented with 10% fetal bovine serum (FBS [Hyclone]), nonessential amino acids (Gibco®) and penicillin (10,000 units/ml)-streptomycin (10mg/ml) solution (Sigma Aldrich). Chinese hamster ovary (CHO) cell line stably expressing the human ACE2, known as CHO-ACE2, was established previously [363], and cultured in the same medium. All cell lines were maintained at $37^{o}C$ with 5% CO_2. The human SARS-CoV strain HKU39849 was used in the generation of escape mutant.

2.3 Purification of monoclonal antibodies

Antibodies were purified from the ascites by using affinity chromatography. Briefly, a 1ml HiTrap Protein G HP beads column (GE Healthcare) was pre-washed

using ~20 ml of 20 mM sodium phosphate buffer, pH 7.0 at a constant flow-rate of 1 ml/min using a peristaltic pump. Five-milliliter of ascites fluids were mixed with equal volume of 40 mM sodium phosphate buffer and passed through a 0.45 µm filter. The filtered ascites fluids were passed through the column at the same flow-rate of 1 ml/min. Extensive washing was performed using the 20 mM sodium phosphate buffer. Elution buffer (0.1 M glycine-HCl, pH 2.7) was then passed through the column at a flow-rate of 1 ml/min and the flow-through was collected at 0.5 ml fractions in 1.5ml microtubes containing 20µl of neutralization buffer (1 M Tris-HCl, pH 9.0). The concentration of the purified monoclonal antibodies in each tube was determined using the Coomassie Plus protein assay reagent (Thermo Scientific).

2.4 Generation of escape mutants

The generation of escape mutants was performed by a previous PhD candidate from our laboratory, Keng Choong Tat, in collaboration with our collaborators from the University of Hong Kong. All work was carried out in a biosafety level 3 (BSL-3) laboratory. Using 50% Tissue Culture Infective Dose ($TCID_{50}$) of 100 of SARS-CoV strain HKU39849 for infection of Vero E6 cells in the presence of different concentrations of mAb 1A9 or 1G10, the concentrations of mAb 1A9 and 1G10 that reduced the virus titres by about 4 logarithms (log) was determined to be 0.25 mg/ml and 0.1 mg/ml respectively and used for the generation of virus escape mutants. Serial dilutions of SARS-CoV ranging from 10^{-1} to 10^{-8} were incubated in the presence of 0.25 mg/ml of mAb 1A9 or 0.1 mg/ml mAb 1G10 for 1 hour at 37 °C and 5 % CO_2. The virus-mAb mixtures were then incubated with Vero E6 cells in a 96-well plate for 1 hour at 37 °C and 5% CO_2, after which the virus-mAb mixtures were removed and the cells were washed twice with medium. The cells were further incubated for 2 days in the presence of mAb 1A9 or 1G10 at concentrations 0.25 mg/ml and 0.1 mg/ml respectively. The supernatant from the

wells containing cells that exhibited cytopathic effect (CPE) at the highest dilution of SARS-CoV was harvested. The percentage CPE was determined by visual counting of floating cells and attached cells. Wells with more than 80% floating cells were considered to have CPE. The harvested supernatant was again incubated in the presence of 0.25 mg/ml of mAb 1A9 or 0.1 mg/ml of mAb 1G10 for 1 hour at 37°C before the virus-mAb mixture was used to infect fresh Vero E6 cells in the presence of mAb 1A9 or 1G10 at concentration 0.25 mg/ml and 0.1 mg/ml respectively. This was performed 3 times. The final virus sample was added to Vero E6 cells in a 6-well plate and incubated for 1 hour at 37°C and 5% CO_2 before the wells were overlaid with agarose containing 0.25 mg/ml mAb 1A9 or 0.1 mg/ml mAb 1G10 and incubated for 3-5 days at 37°C and 5% CO_2. Five plaques were picked using a pasteur pipette for each mAb, freeze-thawed once and further amplified in Vero E6 cells. Neutralization tests were then performed on all the virus clones to confirm that they could escape neutralization by the mAbs.

2.5 TOPO cloning and sequencing

Viral RNA of 5 escape virus clones was isolated using the QIAamp viral RNA mini kit (Qiagen) and converted into cDNA by standard reverse transcription (SuperScript II Reverse Transcriptase, Invitrogen). The cDNA was then amplified by PCR using specific primers targeting the S gene to generate a long fragment (amino acids 1 to 1003) and a short fragment (amino acids 969 to 1255). These gene fragments were cloned into pCR2.1-TOPO vector (Invitrogen) and five colonies were sequenced.

2.6 Construction of plasmids for expression in mammalian cells.

The S gene of the human SARS-CoV HKU39849 strain was obtained from viral RNA after reverse transcription and PCR and cloned into the pXJ3' expression

vector using the BamHI and XhoI restriction sites. To generate plasmids for the expression of mutant S, specific primers were designed for two-round PCR site-directed mutagenesis of wild-type S gene using the Expand High Fidelity PCR System (Roche). The PCR products were then cloned into the pXJ3' expression vector using BamHI and XhoI restriction sites to form pXJ3'-S-N1056K, pXJ3'-S-D1128A, pXJ3'-S-D1128A/N1056K, pXJ3'-S-D1128E and pXJ3'-S-D1128N plasmids. The S genes of human SARS-CoV and MERS-CoV were also separately cloned into the pXJ3'-HA vector using BamHI and XhoI restriction sites.

Plasmids containing the N genes of SARS-CoV and MERS-CoV were synthesized (Genscript) and subcloned into pXJ40-FLAG vector using the BamHI and NotI restriction sites. Specific primers were designed for the construction of the N-terminal MERS-CoV N protein of amino acids 1-195, C-terminal amino acids 196-414, 196-349, 196-312 and 196-285 using the Q5® High-Fidelity DNA Polymerase PCR system (New England Biolabs® Inc). The PCR products were cloned into the pXJ40-FLAG vector using the BamHI and NotI restriction sites. The human eukaryotic elongation factor 1 alpha (eEF1A) gene was cloned into the pXJ40-myc vector, also using the BamHI and NotI restriction sites.

2.7 Transient expression of SARS-CoV proteins in mammalian cells

Cells were plated in 6cm dishes 24 hours prior to transient transfection experiments. Expression plasmids were transiently transfected into cells using Lipofectamine 2000 reagent (Invitrogen) according to manufacturer's protocol. Transient transfection was carried out in DMEM with 10% FBS in the absence of streptomycin and penicillin, and the medium was replaced 6 hours post-transfection with DMEM containing 10% FBS. The cells were harvested at 24 or 48 hours post-transfection by scrapping and cells were spun down by centrifugation and washed

twice with cold 1x phosphate buffered saline (PBS). Cell were then resuspended in lysis buffer (50 mM Tris-HCl[pH 8.0], 150 mM sodium chloride [NaCl], 0.5% Nonidet P-40 [NP40], 0.5% deoxycholic acid, 0.005% sodium dodecyl sulfate [SDS] and 1 mM phenylmethylsulfonyl fluoride [PMSF]) and subjected to freeze-thaw five times followed by spinning down at 13,000 rpm to remove cell debris. Cell lysate protein concentrations were quantitated using the Coomassie Plus protein assay reagent (Thermo Scientific). Cell lysates were subsequently used for Western blot, immunoprecipitation and co-immunoprecipitation experiments.

2.8 Western Blot analysis

Proteins in cell lysates were separated on 7.5%, 10%, 12% or 15% polyacrylamide gels by sodium dodecyl sulfate polyacrylamide gel electrophoresis (SDS-PAGE) and transferred onto nitrocellulose membranes. The membranes were blocked in 5% skimmed milk in tris-buffered saline with 0.05% Tween 20 (TBST) and incubated with primary antibodies overnight at 4^{o}C. The membranes were then washed in TBST before incubation with secondary horseradish peroxidase (HRP)-conjugated antibodies (Pierce) at room temperature for 1 hour. The membranes were washed in TBST again followed by the addition of enhanced chemiluminescence substrate (Pierce) for film development. For loading controls, membranes were re-probed with mouse anti-GAPDH (Santa Cruz Biotechnology) antibody overnight at 4^{o}C, followed by secondary antibody and addition of enhanced chemiluminescence substrate (Pierce) for film development.

2.9 Immunoprecipitation (IP) and co-immunoprecipitation (co-IP)

In IP, mouse mAbs 1A9 and 7G12 were used to pull down wild-type and mutant S proteins in cell lysates for 1 hour at 4^{o}C, followed by the addition of protein A beads (Roche) and incubation at 4^{o}C overnight. The beads were then washed in

lysis buffer three times and subjected to Western blot analysis for the detection of S proteins using the rabbit anti-SΔ1 antibody (binds to amino acids 48-358 of the S1 subunit) [201] as primary antibody and goat anti-rabbit HRP-conjugated antibody (Pierce) as secondary antibody, followed by the addition of enhanced chemiluminescence substrate (Pierce) for film development.

For co-IP of eEF1A and N protein, mouse anti-myc antibody (Santa Cruz Biotechnology) were added to cell lysates for 1 hour at 4^{o}C, followed by the addition of protein A beads (Roche) and incubated at 4^{o}C for 3 hours. The beads were washed in RIPA buffer (50 mM Tris-HCl[pH 8.0], 150 mM NaCl, 0.5% NP40 and 0.5% deoxycholic acid) 5 times and subjected to Western blot analysis using rabbit anti-FLAG antibody (Sigma Aldrich) as primary antibody and HRP Clean-Blot^{TM} IP Detection Reagent (Thermo Scientific) as secondary antibody, followed by the addition of enhanced chemiluminescence substrate (Pierce) for film development. Alternatively, cell lysates were subjected to co-IP using FLAG beads (Sigma Aldrich) for incubation at 4^{o}C for 3 hours. The beads were washed in RIPA buffer 5 times and subjected to Western blot analysis using rabbit anti-myc antibody (Santa Cruz Biotechnology) as primary antibody and HRP Clean-Blot^{TM} IP Detection Reagent (Thermo Scientific) as secondary antibody, followed by the addition of enhanced chemiluminescence substrate (Pierce) for film development.

2.10 Expression and purification of GST-fusion proteins in bacteria

SARS-CoV wild-type and mutant S fragment consisting of amino acids 1030-1188 (S[1030-1188aa]), full length SARS-CoV N, full length and truncated MERS-CoV N proteins were expressed as glutathione-transferase (GST) fusion proteins using the pGEX6p1 vector (GE healthcare). The pGEX6p1 plasmids were separately transformed into *Escherichia coli* (*E. coli*) BL21-DE3 cells (Stratagene).

Single colonies were grown in Terrific Broth (TB) or Luria-Bertani (LB) media in the presence of 100 μg/ml ampicilin at 37°C overnight. The cultures were then inoculated in fresh TB or LB media with ampicilin at a dilution of 1:100 and incubated in a shaker at 37°C. On reaching an optical density at 600nm (OD600nm) of 0.6-0.8, cells were cooled to 16°C and induced with isopropyl *β*-D-thiogalactopyranoside (IPTG) at a final concentration of 0.5 mM and incubated overnight. The bacterial pellets were then collected by centrifugation and resuspended in lysis buffer (10mM Tris-HCl[pH7.4], 150mM NaCl, 1mM ethylenediaminetetraacetic acid [EDTA], 100ug/ml lysozyme, 5mM dithiothreitol [DTT] and 15mM PMSF) and subjected to sonication. 20% sarkosyl was added for the lysis of bacteria expressing the S fragments. The lysates were cleared by centrifugation at 12,000rpm for 30 minutes and incubated with gluthathione (GSH) sepharose beads (GE Healthcare) overnight at 4°C. After washing the beads with washing buffer (10mM Tris-HCl[pH7.4], 150mM NaCl and 1mM EDTA), 10mM reduced gluthathione solution (Sigma Aldrich) was added to the beads for the elution of the GST-fusion proteins. The purified GST-fusion proteins were then subjected to SDS-PAGE on a 12% gel and stained using coomassie blue to visualize size and purity of proteins.

2.11 Enzyme-linked immunosorbent assay (ELISA)

Purified GST-fusion wild-type and mutant (N1056K and D1128A) S proteins (GST-S[1030-1188aa]) were coated onto 96-well ELISA plates (Nunc) overnight at 4°C at 100 ng/well. The wells were blocked in 5% skimmed milk in phosphate-buffered saline with 0.1% Tween 20 (PBST) for 1 hour at room temperature, and primary antibodies mAb 1A9 and mouse anti-GST antibody [Santa Cruz] were added at 4-fold dilutions and incubated at 37°C for 2-3 hours. The wells were then washed in PBST followed by the addition of goat anti-mouse HRP-conjugated antibody

(Pierce) as secondary antibody and incubated at 37^{o}C for 1 hour. Tetramethylbenzidine substrate (Pierce) was then added and reaction was stopped using 0.2M sulphuric acid. Optical density at 450nm (OD450nm) was obtained using an absorbance reader (Tecan Infinite M200). Statistical difference in binding of mAb 1A9 to wild-type S and mutant S was analyzed using unpaired t-test. Significance was indicated by *p* value of <0.01.

2.12 Generation of pseudotyped particles expressing S protein (S-pp)

The ability of SARS-CoV containing mutant S to infect cells and the resulting effect on mAb neutralization in SARS-CoV entry were studied using a pseudotyped virus system. Based on this pseudotyped virus system, replication incompetent lentiviral particles expressing S proteins on the surface and containing the firefly luciferase reporter gene were used in replacement of live SARS-CoVs. Viral entry into permissive cell lines is reflected in the luciferase activity of the infected cells. To generate S-pseudotyped particle (S-pp), lentiviral vector pNL43-R^{-} E^{-}Luc and plasmids expressing S genes were co-transfected in 293 FT cells using Lipofectamine 2000 reagent (Invitrogen) according to manufacturer's protocol in DMEM medium. 48 hours post-transfection, the supernatant was collected and centrifuged at 3000rpm for 5 minutes to remove cell debris. The viral supernatant was then subjected to P24 ELISA (QuickTiter Lentivirus Titer kit, Cells Biolabs) according to manufacturer's protocol to quantify viral titres.

2.13 *In vitro* S-pp neutralization assay

All S-pp neutralization assays were carried out in 24-well plates. CHO-ACE2 cells were grown in 500ul of DMEM+10% FBS per well for 24 hours prior to experiment. In S-pp neutralization assays, 16 ng of S-pp (as quantified using P24 ELISA) were pre-incubated in the absence or presence of mAb 1A9 or mAb 1G10 at

25, 50, 100 and 200 µg/ml for 1 hour at room temperature on a nutator. The mAb-virus or virus-alone mixtures were used to infect CHO-ACE2 cells on 24-well plates and incubated at 37^{o}C for 48 hours. Mab 7G12, a non-neutralizing anti-S1 antibody that binds to the RBD of S [363], was included as a control antibody at 200 µg/ml. At 48 hours post-infection, cells were harvested using the luciferase assay system (Promega) and luciferase expressions of cells were determined according to manufacturer's protocol. Percentages of viral entry were then calculated based on the luciferase readings obtained. All experiments were carried out in triplicates. Statistical differences in viral entry between wild-type and mutant S-pps were determined using unpaired t-test. Significance was indicated by *p* value of <0.01.

2.14 ELISA for S protein quantification in S-pps

S-pps were coated onto 96-well ELISA plates (Nunc) at 16 ng/well (as quantitated by P24 ELISA) overnight at 4^{o}C. The wells were blocked in 5% skimmed milk in PBST containing 0.1% Tween 20, and primary antibodies mAb 7G12 [363] and mouse anti-P24 mAb were added at 4-fold dilutions and incubated at 37^{o}C for 2 hours. The wells were then washed in PBST followed by the addition of goat anti-mouse HRP-conjugated antibody (Pierce) as secondary antibody and incubated at 37^{o}C for 1 hour. Tetramethylbenzidine substrate (Pierce) was added and reaction was stopped using 0.2M sulphuric acid. OD450nm was obtained using an absorbance reader (Tecan Infinite M200). Differences in S protein level in wild-type and mutant D1128A S-pp were evaluated using unpaired t-test. Significance was indicated by *p* value of <0.01.

2.15 Fluorescence-activated Cell Sorting (FACS) analysis for surface expression of S protein

293 FT cells were seeded in 6-cm dishes in DMEM+10%FBS medium 24 hours prior to transfection. The cells were transfected with pXJ3' empty vector, pXJ3'-S and pXJ3'-S-D1128A plasmids using Lipofectamine 2000 reagent (Invitrogen) according to manufacturer's protocol and harvested at 72 hours post-transfection. The cells were detached using the cell dissociation solution (Sigma), washed twice in 1xPBS and incubated with purified mouse mAb 7G12 [363] in 1xPBS containing 1% bovine serum albumin (BSA) for 3 hours at 4^{o}C on a nutator. The cells were washed 3 times using 1xPBS containing 1% BSA and then incubated with fluorescein isothiocyanate (FITC)-conjugated goat anti-mouse IgG (Santa Cruz) secondary antibody for 1 hour at 4^{o}C on the nutator. Cells were washed again 3 times and used immediately for FACS analysis using the CyAn flow cytometer (Beckman Coulter). All FACS data was analyzed using the FlowJo software application.

2.16 Synthetic peptides

A total number of 550 peptides were purchased from Chiron Mimotopes (Victoria, Australia) at purity above 80% and their compositions were confirmed by mass spectrometry analysis. The peptides are 15-mer peptides overlapping by 10 residues spanning the proteome of the SARS-CoV structural S (n=249 peptides), E (n=14 peptides), M (n=43 peptides), N (n=82 peptides) proteins and accessory 3a (n= 53 peptides), 3b (n=29 peptides), 6 (n=11 peptide), 7a (n=23 peptides), 7b (n=7 peptides), 8a (n=6 peptides) and 8b (n=15 peptides) and 9 (n=18 peptides) proteins. The peptides were grouped and pooled into matrices consisting of a total of 118 numeric and alphabetic pools. The matrix peptide pools were designed by Dr Anthony Tan. All peptides were received in lyophilized forms and were diluted at 40

mg/mL in dimethyl sulfoxide (DMSO) and then further diluted in RPMI medium (Gibco®) at working dilutions of 10 mg/mL to 1 mg/mL. Peptide stock solutions were prepared by ex-members of the lab, Janice Oh (for N and 3a peptides) and Dr Ramesh (for other peptides).

2.17 Collection of blood samples from SARS-recovered subjects

A total of three SARS-recovered individuals were enrolled in this study from the Singapore General Hospital, Singapore. All participants were diagnosed with SARS based on clinical examination during the period of 2003, according to World Health Organization's definition of SARS [399]. Blood samples were obtained from them at 9 to 11 years post-infection (9 years post-infection for 2 individuals, 11 years post-infection for 1 individual). One normal subject without any contact history with SARS patients was enrolled as control subject. This study was approved by the Centralized Institutional Review Board of the Singapore Health Services Pte, Ltd. (Singapore).

2.18 PBMC isolation and *in vitro* expansion of SARS-specific T cells

Peripheral blood mononuclear cells (PBMCs) were isolated from fresh heparinized blood by density gradient centrifugation using Ficoll-Paque^{TM} (GE Life Sciences) and resuspended in AIM-V medium (Invitrogen) with 2% pooled human AB serum (AIM-V+2%AB). Cells were either frozen down in liquid nitrogen or used directly for *in vitro* expansion.

For *in vitro* expansion assay, 20% of the PBMCs was first stimulated with 10 μg/ml of all the 15-mer overlapping peptides or 5 μg/ml of a single peptide for 1 hour at 37^{o}C. The cells were then washed 3 times with Hank's Balanced Salt Solution (HBSS [Gibco®]) and added to the remaining 80% PBMC resuspended in AIM-

V+2%AB medium supplemented with interleukin-2 (IL-2) (R&D Systems) at 20 U/ml. The cells were seeded in 24-well plates at 100,000 cells per well and cultured at 37^{o}C for 10 days.

2.19 Anti-human IFNγ ELISpot assay

Anti-human IFNγ enzyme-linked immunospot (ELISpot) assays were performed as previously described [142]. Briefly, 96-well MultiScreen®HTS Filter plates (Millipore) were coated with 5 μg/mL of mouse anti-human IFN-γ mAb (Mabtech) overnight at 4^{o}C, as recommended by the manufacturer. The plates were then washed 5 times with PBS and blocked with AIM-V supplemented with 10% heat-inactivated fetal calf serum (FCS) for 30 minutes at room temperature. A total of 5 x 10^4 *in vitro* expanded PBMCs were seeded per well and incubated in the absence or presence of numeric and alphabetic peptide pools (at final concentration of 5 μg/ml) for 18 hours at 37^{o}C. Negative and positive controls consisted of cells not stimulated with any peptide and cells stimulated with phytohemagglutinin (PHA) respectively. The plates were then washed 5 times with PBS followed by the addition of biotinylated anti-human IFNγ mAb (Mabtech) and incubated at room temperature for 2 hours. The plates were washed again with PBS and streptavidin-alkaline phosphatase reagent (Mabtech) was added at 1:2,000 dilution for incubation at room temperature in the dark for 1 hour. After another round of washes with PBS, alkaline phosphatase substrate 5-bromo-4-chloro-3-indolyl phosphate-nitro blue tetrazolium chloride (BCIP-NBT) (Kirkegaard & Perry Laboratories, Inc.) was added. After 10 to 15 minutes, the colorimetric reaction was stopped by washing in distilled water. The plates were air-dried and spots were counted using an automated ELISPOT reader and the ImmunoSpot software (Cellular Technology, Ltd.). The number of IFNγ-producing cells was expressed in spot-forming units (SFU) per 5 x 10^4 cells. The positive threshold was set at the number of spots at least twice of that observed in

negative controls (cells not stimulated with peptides). The positive peptide responsible for the positive ELISpot results was identified as the common peptide present in both the numberic and alphabetic pools. Intracellular cytokine staining (ICS) was carried out for each positive peptide to confirm the T cell response and to determine the T cell subset ($CD4^+$ or $CD8^+$) responsible for IFNγ production.

2.20 Intra-cellular cytokine staining (ICS) and degranulation assays

In vitro expanded PBMCs (100,000 cells) were incubated in AIM-V+2%AB medium alone (negative control) or with peptides at final concentration of 5 μg/ml for 5 hours or overnight in the presence of brefeldin A. Brefeldin A was used at 10 μg/ml final concentration for 5 hours stimulation or 2 μg/ml final concentration for overnight stimulation. Anti-CD107a-FITC antibody (BD Pharmingen) was also added for assessing $CD8^+$ T cell degranulation. Positive control consisted of T cells incubated in AIM-V+2%AB with 10 ng/ml phorbol 12-myristate 13-acetate (PMA) and 100 ng/ml ionomycin. Following stimulation, the cells were washed 3 to 4 times in HBSS and stained with anti-CD8-phycoerythrin(PE)-Cy7 and anti-CD3-peridinin chlorophyll protein(PerCP)-Cy5.5 (BD Pharmingen) for 30 minutes at 4^oC in the dark. After this, cells were washed in 1xPBS containing 1% BSA and 0.1% azide, fixed and permeabilized using Cytofix/Cytoperm fixation/permeabilization reagent (BD Biosciences) according to manufacturer's protocol. Intracellular staining using anti-IFN-γ-PE (BD Pharmingen) was carried out at 4^oC for 30 minutes in the dark, followed by washing and flow cytometry analysis using the LSR II flow cytometer (BD Biosciences). All FACS data was analyzed using the FACSDiva software application.

2.21 Human Leukocyte Antigen (HLA) restriction of $CD8^+$ T cell responses

The HLA class I phenotype of each SARS-recovered subjects enrolled in current study was determined by PCR amplification and sequencing-based typing method [400], performed by BGI Clinical laboratories (ShenZhen, China). A panel of Epstein-Barr virus (EBV)-transformed lymphoblastoid B cell lines (EBV-LCLs) possessing matching HLA phenotypes as the SARS subjects were used as antigen-presenting cells to determine the HLA restriction of each $CD8^+$ T cell response. T cells were incubated with the EBV-LCL pulsed with the specific peptide, followed by quantification of IFN-γ- and CD107a-expressing $CD8^+$ cells by ICS and flow cytometry as described above. All EBV-LCLs were maintained in R10 media.

2.22 Restimulation of SARS-specific T cells and minimal epitope mapping for $CD8^+$ T cell epitopes

Restimulated SARS-specific $CD8^+$ T cells were used for minimal epitope mapping. For restimulation of SARS peptide-specific T cells, fresh PBMCs from a healthy donor and EBV-LCL consisting of the HLA allele restricting the $CD8^+$ T cell response were used as feeder cells. PBMCs and EBV-LCLs were resuspended in AIM-V+2%AB and R10 media respectively. Specific peptide was added to the EBV-LCL at 1 μg/ml concentration and incubated at 37^{o}C for 1 hour, followed by 3 washes with HBSS. The PBMCs and the peptide-pulsed EBV-LCL were irradiated at 2500 RADs and 4000 RADs respectively. The irradiated cells were washed 3 times in HBSS and added to the *in vitro*-expanded T cells in AIM-V+2%AB supplemented with IL-2 (20 U/ml), IL-7 (10 ng/ml) and IL-15 (10 ng/ml). The cells were then co-cultured at 37^{o}C for 10 days.

The restimulated T cells were then tested with truncated peptides of the 15-mer peptide by IFN-γ ICS as described above for the mapping of the minimal T cell

epitope. For the M29 minimal epitope mapping, a total of 21 peptides (8-mers to 12-mers) that span the M29 region were tested, while for N53, a total of 6 peptides (8-mers to 10-mers) that span the overlapping region of N53 and N54 were used. EBV-LCLs expressing the HLA-B*15:02 and HLA-B*15:25 alleles were used as antigen-presenting cells for M29-specific T cells and N53-specific T cells respectively.

2.23 Immunofluorescence assay (IFA)

293 FT or HeLa cells were seeded on coverslips in 24-well plates 24 hours prior to transient transfection experiment. Transfection with appropriate expression vectors and plasmids was carried out using Lipofectamine 2000 reagent (Invitrogen) according to manufacturer's protocol. 24 hours, 48 hours or 72 hours post-transfection, cells on coverslips were washed with 1xPBS and fixed with 4% paraformaldehyde (PFA) for 10 minutes, followed by washing with 1xPBS again and permeabilized with 0.1% Trition-X in 1xPBS for 10 minutes. The cells were washed and blocked in 1% BSA in 1xPBS for 30 minutes before incubation with primary antibodies, rabbit anti-FLAG (Sigma Aldrich) and mouse anti-eEF1A (Upstate, Milipore) antibodies, for 2 hours at room temperature. After washing to remove unbound antibodies, the cells were incubated with Alexa Fluor® 488-conjugated goat anti-rabbit IgG and Alexa Fluor® 568-conjugated goat anti-mouse IgG (Molecular Probes^{TM}) for 1 hour at room temperature in the dark. For visualization of F-actin, Alexa Fluor® 647-conjugated phalloidin (Molecular Probes^{TM}) was added. The cells were washed and stained with 4',6-diamidino-2-phenylindole (DAPI) dye (Molecular Probes^{TM}) for 5 minutes and mounted onto microscope glass slides using Fluorosave mounting medium (Calbiochem, Merck Chemicals Ltd). Images were obtained using the confocal microscope (Olympus FV1000).

2.24 *In vitro* transcription

In vitro transcription assay was carried out using the MEGAscript® T7 Kit (Ambion) according to manufacturer's protocol. Plasmid DNA containing the firefly luciferase gene was first digested using restriction enzymes to yield the linearized template DNA and then added into the reaction mix for *in vitro* transcription reaction. The resultant luciferase-encoding RNA is purified using the RNeasy mini kit (Qiagen) and was used in subsequent *in vitro* translation experiments.

2.25 *In vitro* translation

In vitro translation assay was done using the rabbit Retic Lysate IVT™ Kit (Ambion). Purified bacterial-expressed GST and GST-fusion SARS-CoV N and MERS-CoV N proteins were first incubated at the appropriate concentrations with the rabbit reticulocyte lysate for 0.5 hour at 30^{o}C, after which the luciferase-encoding RNA and reaction mix were added to the mixture and incubated for another 2 hours at 30^{o}C. 5µl of the mixture was added to 50µl of luciferase substrate (Promega) and luciferase activity was measured using the automated plate reader (Tecan Infinite M200). Statistical differences in luciferase readings between the samples were analysed using unpaired t-test. Significance was indicated by *p* value of <0.01.

CHAPTER 3: CHARACTERIZATION OF SARS CORONAVIRUS NEUTRALIZING MONOCLONAL ANTIBODIES TARGETING THE SPIKE PROTEIN

In previous study, our group generated a panel of 18 anti-SARS-CoV mAbs by immunization of BALB/c mice using an *Escherichia coli* (*E. coli*)-expressed gluthathione S-transferase (GST)-tagged protein consisting of amino acids 1029 to 1192 of the S2 region of the SARS-CoV S protein [363]. These neutralizing mAbs were largely grouped into four groups (Type I, II, III and IV) based on their binding sites on the S protein, which were mapped to be at four linear epitopes within the S2 subunit. Two of these binding sites were located upstream of HR2 domain and two within the HR2 domain. These mAbs exhibited *in vitro* neutralizing activities against SARS-CoV and were demonstrated to be able to inhibit cell-cell membrane fusion. Two mAbs, 1A9 and 1G10, among others, showed potent effects in neutralizing SARS-CoV infections and in preventing cell-cell membrane fusion. Both mAbs also demonstrated broadly-neutralizing capability in cross-neutralizing SARS-CoV strains from animal reservoirs [401]. In current study, we further characterized mAb 1A9 and 1G10 to gain a better understanding of their neutralizing mechanisms. Firstly, the cross-reactivity of mAb 1A9 and 1G10 against S protein of the recently emerged human coronavirus, MERS-CoV was determined. Secondly, the generation of escape mutant viruses using mAb 1A9 and 1G10 was also carried out. The selection of mAb escape mutants is a useful method that allows the characterization of antibody binding sites and enables the identification of critical residues required for antibody binding. In addition, this method allows the subsequent evaluation of escape mutant viruses that arise from the process of mAb neutralization.

3.1 Binding of mAb 1A9 and 1G10 to the S protein of MERS-CoV

The binding site of mAb 1A9 lies upstream of the HR2 domain at residues 1111-1130 of the S2 subunit, while that of mAb 1G10 is located within HR2 domain at residues 1151-1192 (Figure 3.1A). Sequence alignment showed that both binding sites of mAb 1A9 and 1G10 are highly conserved in human (HKU39849), civet SARS-CoV (SZ3) and bat SL-CoV (Rp3 and Rf1) strains (Figure 3.1B). However, the binding regions are highly variable between SARS-CoV and MERS-CoV (Figure 3.1B).

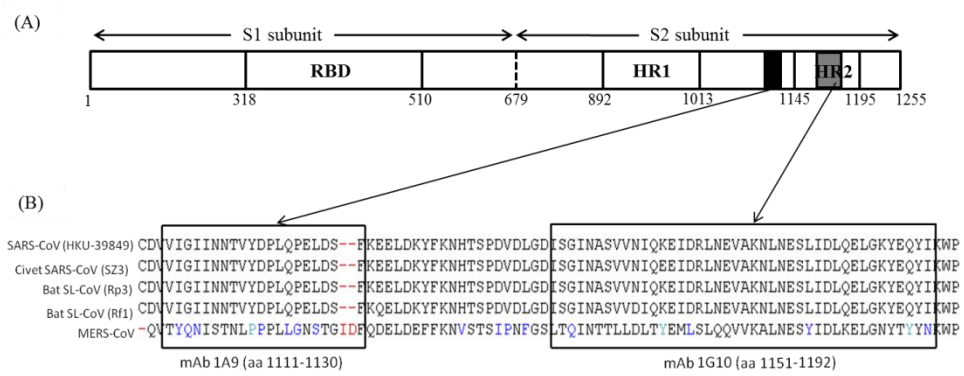

Figure 3.1. Binding sites of mAb 1A9 and 1G10 within the SARS-CoV, zoonotic SARS-CoVs and MERS-CoV S proteins. (A) Schematic diagram of the different motifs in the SARS-CoV S protein. RBD, receptor binding domain; HR1, heptad repeats 1 domain; HR2, heptad repeats 2 domain. Black box and grey box represent the domain in S that is required for the interaction with mAb 1A9 and 1G10 respectively. (B) Sequence alignment of S proteins of human SARS-CoV HKU39849 strain, civet SARS-CoV SZ3 strain, bat SL-CoV Rp3 and Rf1 strains and MERS-CoV at regions corresponding to the binding sites of mAb 1A9 and 1G10.

It has been demonstrated that mAb 1A9 and 1G10 can bind to S proteins of zoonotic SARS-CoV strains and cross-neutralize infections by these strains [401]. To check if mAbs 1A9 and 1G10 can cross-react and bind to the S protein of MERS-CoV, plasmids expressing HA-tagged S proteins of SARS-CoV and MERS-CoV were transfected in 293 FT cells and binding of the proteins to mAb 1A9 and 1G10 was determined by Western Blot analysis. Successful expression of the S proteins

was determined by anti-HA antibody (Figure 3.2, lowest panel). From the Western Blot results as shown in Figure 3.2, both SARS-CoV S protein-binding mAb 1A9 and 1G10 could not bind to MERS-CoV S protein. This indicated that mAb 1A9 and 1G10 do not exhibit cross-binding ability to MERS-CoV S, and it is likely that the two mAbs would not be able to neutralize MERS-CoV infection.

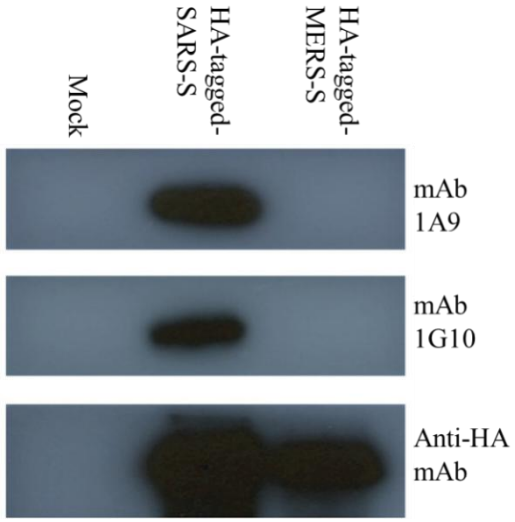

Figure 3.2. Binding of mAb 1A9 and 1G10 to wild-type S proteins of SARS-CoV and MERS-CoV. 293 FT cells were transfected with no plasmid (mock) or with plasmids expressing HA-tagged full length S of SARS-CoV (HA-tagged-SARS-S) and MERS-CoV (HA-tagged-MERS-S). Western Blot analysis was performed on the cell lysates using mAb 1A9 and 1G10 to determine binding to S proteins. Anti-HA mAb was used to detect protein expressions.

3.2 Generation of mAb 1A9 and 1G10 escape mutants and identification of S mutations in escape mutants

To identify critical residue(s) required for the interactions of mAb 1A9 and 1G10 with SARS-CoV S, escape mutants against mAb 1A9 and 1G10 were generated. SARS-CoV HKU39849 strain was first cultured in Vero E6 cells at sub-optimal levels of mAb 1A9 and 1G10 separately. The sub-optimal concentration represent the mAb selection concentrations that can reduce the virus titres by more than 3 logarithms, which was determined to be 0.25 mg/ml for mAb 1A9 and 0.1 mg/ml for

mAb 1G10. Supernatant from the wells containing cells that exhibited cytopathic effect (CPE) at the highest dilution of SARS-CoV was harvested as passage 1 and passaged 3 times in the presence of mAb, after which the virus titres gradually increased back to level higher or comparable to virus grown in the absence of mAb (Figure 3.3). Plaque purification assays were then done to isolate 5 individual SARS-CoV escape mutant clones for each mAb.

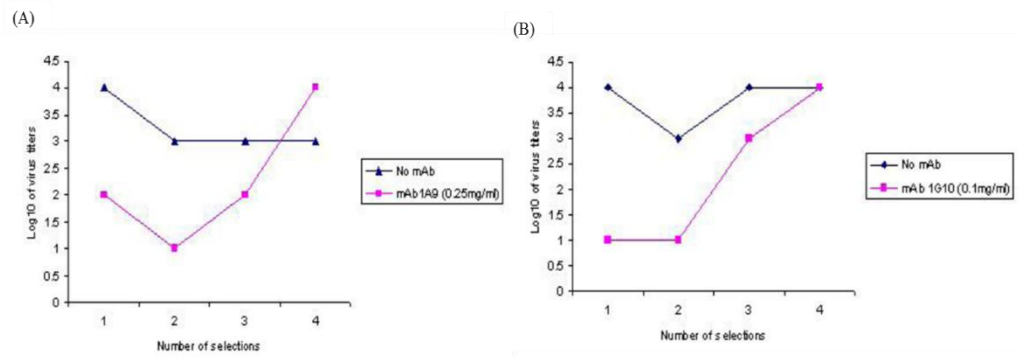

Figure 3.3. Generation of SARS-CoV escape mutants against mAb 1A9 and 1G10. Escape mutants were passaged for three rounds in the presence of (A) mAb 1A9 at 0.25 mg/ml and (B) mAb 1G10 at 0.1 mg/ml selection concentrations, after which virus titres gradually increased back to level higher or comparable to virus grown in the absence of mAb, as determined by the TCID50 assay. Figures adapted from PhD thesis of Keng Choong Tat (2011).

Neutralization assays were carried out to confirm the escape ability of the escape mutant clones, after which viral RNA was extracted and converted to cDNA by standard RT-PCR. Due to the large size of the S gene, two sets of S primers were used to amplify the cDNA into an N-terminal long fragment (residues 1-1003) and a C-terminal short fragment (residues 969-1255). This is followed by the cloning of the cDNAs into the TOPO vector and sequencing of the DNA. After the analysis of the sequences, no specific mutations were identified in mAb 1G10 escape mutants, while two escape mutations, N1056K and D1128A, were identified in the mAb 1A9 escape mutants. 2 out of 5 clones had D1128A mutation and 3 out of 5 clones had

N1056K mutation. None of the clones had both mutations. Residue D1128 lies within the mAb 1A9 binding site, while residue N1056 lies upstream of the binding site.

3.3 Difference in mAb 1A9 binding to wild-type and mutant S proteins

We further focused on the characterization of mAb 1A9 and understanding the underlying mechanism of viral escape from mAb 1A9 based on the two identified S escape mutations, N1056K and D1128A. Firstly, to check if these two mutations in S cause a change in binding efficiency to mAb 1A9, wild-type S, substitution S mutants, namely D1128A, N1056K and that containing both D1128A and N1056K, were expressed in 293 FT cells, followed by Western Blot analysis to compare the binding capabilities of the S proteins to mAb 1A9. As shown in Figure 3.4A (upper panel), S protein containing mutation D1128A (S-D1128A) showed a reduced binding to mAb 1A9 compared to the wild-type S protein (S-WT), while S protein with the N1056K mutation (S-N1056K) did not show a reduction in mAb 1A9 binding compared to S-WT. S containing double mutation (S-D1128A/N1056K) also exhibited decrease in binding to mAb 1A9 but no enhanced reduction was observed compared to S-D1128A. MAb 7G12, an anti-SARS mAb that binds to the S1 domain at amino acids 281 to 300 of S [363], was used as a control antibody to detect protein expression (Figure 3.4A, lower panel).

While Western Blot revealed the binding of mAb 1A9 to denatured epitope on S, immunoprecipitation (IP) was performed to compare the mAb 1A9 binding to native forms of S. Lysates of transfected 293 FT cells expressing S-WT, S-D1128A, S-N1056K and S-D1128A/N1056K were first subjected to IP using mAb 1A9 or 7G12 in the presence of protein A beads. The IP beads were then used for Western Blot where the immunoprecipitated S proteins were detected using a rabbit anti-S1 antibody (Rb-α-SΔ1), which targets the S1 domain at amino acids 48 to 358 [201].

Consistent with the results obtained in Western Blot analysis, S-D1128A exhibited a decrease in mAb 1A9 binding compared to S-WT while S-N1056K did not, and no synergistic effects in the reduction of binding to mAb 1A9 was observed with S-D1128A/N1056K compared to S-D1128A (Figure 3.4B, upper panel). When mAb 7G12 was used for IP, equal amount of S proteins were pulled down, indicating that equal amounts of S-WT and mutant S proteins were used for IP (Figure 3.4B, lower panel). These results suggested that D1128A mutation, but not N1056K, led to a decrease in binding of S to mAb 1A9. Once again, the presence of the double mutations did not enhance reduction in binding of S to mAb 1A9. In addition, substitution of D1128 with amino acid asparagine (N) or glutamic acid (E), which shares the same side-chain and the same charge as D respectively, also reduced interaction with mAb 1A9 to similar extent as the substitution by A (Figure 3.4C, upper panel). Thus, the amino acid D at position 1128 in S appears to play an essential role in the interaction with mAb 1A9.

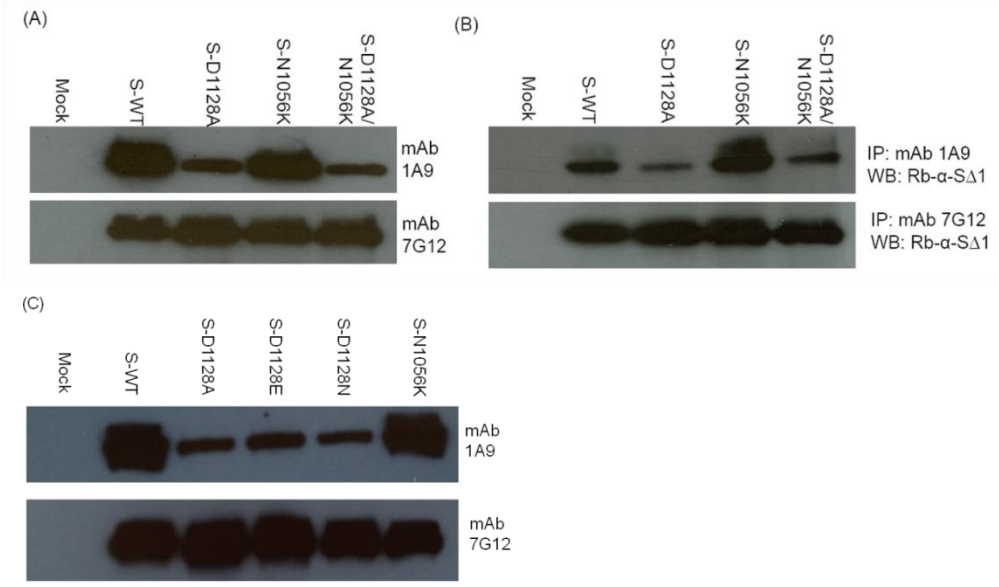

Figure 3.4. Binding of mAb 1A9 to wild-type and mutant S proteins by Western Blot and IP. 293 FT cells were transfected with no plasmid (mock) or with plasmids expressing full length wild-type S (S-WT) or mutant S (S-D1128A, S-N1056K and S-D1128A/N1056K). (A) Western Blot analysis was performed on cell lysates using mAb 1A9. MAb 7G12, which binds to S1 domain, was used as a control antibody to detect protein expression. (B) Cell lysates containing S-WT, S-D1128A, S-N1056K or S-D1128A/N1056K were subjected to IP using mAb 1A9 or 7G12 in the presence of protein A beads and immunoprecipitated S proteins were detected using Rb-α-SΔ1 antibody in Western blot (WB). (C) 293FT cells were transfected with no plasmid (mock) or with plasmids expressing full length S-WT or mutant S (S-D1128A, S-D1128E, S-D1128N and S-N1056K). Western Blot analysis was performed on the cell lysates using mAb 1A9 and 7G12.

To further confirm the binding results, ELISA was carried out using purified wild-type and mutant GST-tagged S fragments consisting of residues 1030-1188 expressed in *E. coli*. Unlike Western Blot and IP, ELISA allows a quantitative assessment and comparison of mAb 1A9 binding to WT-S and mutant S. As shown in Figure 3.5A, all GST-tagged S fragments were obtained at high amounts and good purity, with the exception of GST-tagged fragment containing N1056K mutation [GST-S(1030-1188)-N1056K], where an additional visible protein band at around 25kDa was observed (lane 4). This could be the GST protein (26 kDa) that was expressed along with the GST-fusion protein or GST protein that resulted from a

cleavage of the GST-fusion protein. Therefore, even though mAb anti-GST was used to ensure equal amount of each S fragment was used for ELISA (Figure 3.5C), the actual amount of loaded GST-S(1030-1188)-N1056K proteins could be lower. Nonetheless, similar degree of binding of mAb 1A9 to both GST-S(1030-1188)-wild-type and GST-S(1030-1188)-N1056K was observed (Figure 3.5B), in agreement with previous Western blot and IP results that the N1056K mutation is not involved in the reduction in S protein binding to mAb 1A9, thus indicating relatively equal amount of protein used for ELISA. As shown in Figure 3.5A and B, binding of both mAb 1A9 and anti-GST to the S fragments decreased in a dose-dependent manner with increase in mAb dilutions and no saturation was observed. Similar to results obtained from Western blot and IP, GST-tagged fragment containing D1128A mutation [GST-S(1030-1188)-D1128A] showed significant reduction in binding to mAb 1A9 at all concentrations tested compared to wild-type GST-S(1030-1188) (Figure 3.5B). These results further support that residue 1128 of the S protein is important in the binding to mAb 1A9.

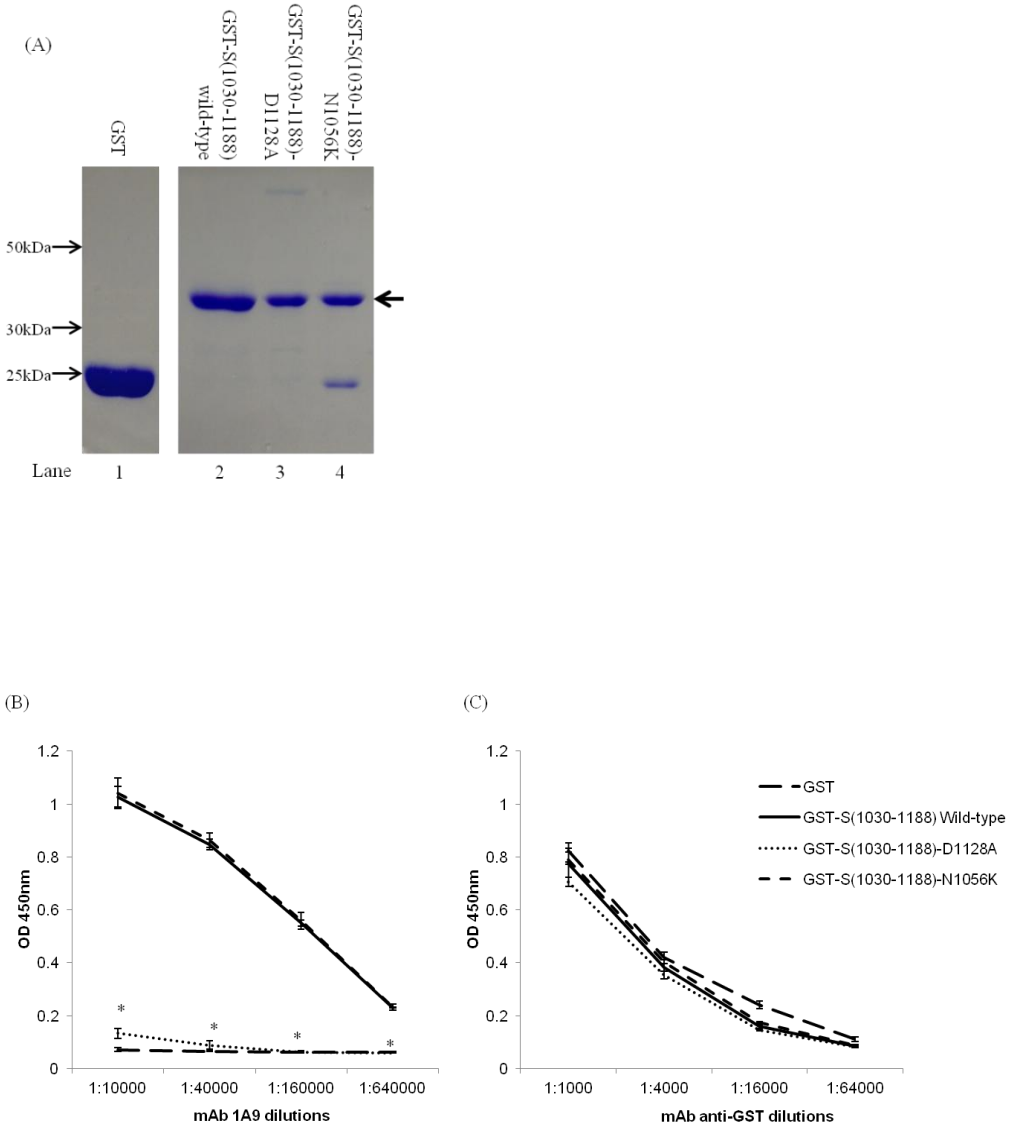

Figure 3.5. Binding of mAb 1A9 to wild-type, mutant D1128A and N1056K GST-S(1030-1188) fragments by ELISA. (A) Purified GST, GST-S(1030-1188)-wild-type, GST-S(1030-1188)-D1128A and GST-S(1030-1188)-N1056K fragments (lanes 1-4) were separated on a 12% gel by SDS-PAGE and stained using Coomassie Blue. Molecular weight markers in kDa are indicated on the left. Expected size of each GST-S(1030-1188) fragment is around 43kDa as indicated by the arrow. GST, GST-S(1030-1188) wild-type, GST-S(1030-1188)-D1128A and GST-S(1030-1188)-N1056K proteins were coated on 96-well plate at 100ng/well and detected using (A) mAb 1A9 and (B) mAb anti-GST at 4-fold serial dilutions. Optical density (OD) was measured at 450nm. Bars represent SD of the experiment carried out in triplicates. *indicates statistically significant difference (p<0.01) when compared to wild-type. MAb anti-GST was used as a control antibody to ensure that equal amounts of GST-tagged proteins were coated onto each well.

3.4 Resistance of S-pp expressing mutant D1128A S protein to neutralization by mAb 1A9

Since both D1128A and N1056K are mutations identified in escape SARS-CoV mutant clones generated against mAb 1A9, we wanted to verify if these two mutations contributed to the escape from neutralization by mAb 1A9. To do so, a lentiviral-based pseudovirus system was employed, where S-pseudotyped virus particles, or S-pps, were generated and used for mAb neutralization assays. In this pseudotyped virus system, replication incompetent lentiviral particles that express SARS-CoV S protein on the surface were used in replacement of live SARS-CoVs, permitting studies involving S-pps to be done in a biosafety level 2 (BSL2) environment, while those involving live SARS-CoV have to be done strictly in a BSL3 facility. The lentiviral backbone of the S-pps contains the luciferase reporter gene, allowing the quantification of viral entry based on luciferase activity measured in the infected cells. This system has been successfully employed in the study of highly pathogenic viruses including the Influenza A H5N1 virus [402] and SARS-CoV [403,404]. Neutralizing antibody titres measured using pseudotyped SARS-CoV correlated well with the use of replication competent SARS-CoV [405], as such, this system has been widely used in the evaluation of SARS-CoV neutralizing antibodies [358,360,406]. In this *in vitro* pseudotyped virus assay, S-pps expressing the wild-type, mutant D1128A, N1056K and D1128A/N1056K S proteins were generated and used at equal amounts to infect CHO-ACE2 cells in the absence or presence of different concentrations of mAb 1A9. The CHO-ACE2 cell line is a previously established stable cell line derived from CHO cells to express a high level of ACE2 receptor [363], thus it is susceptible to S-pps infection through the binding of S to ACE2. Equal amounts of S-pps were determined based on P24 ELISA, which measures lentiviral titres based on the amount of lentiviral P24 protein detected.

pNL43-R-E-Luc virus, the lentivirus that does not express S protein, was used as negative control. As shown in Figure 3.6A, all S-pps (S-WT-pp, S-D1128A-pp, S-N1056K-pp and S-D1128A/N1056K-pp) were able to infect CHO-ACE2 cells, with the mutant S-pps showing a slightly lower infectivity compared to the wild-type.

Next, to examine mAb 1A9 neutralization effects on the wild-type and mutant S-pps, percentages of viral entry in CHO-ACE2 cells based on luciferase activity in the presence of different mAb 1A9 concentrations (25, 50, 100 and 200 μg/ml) were compared. Luciferase activity measured from CHO-ACE2 cells in the absence of mAb 1A9 was set as 100% viral entry. MAb 7G12, an anti-S1, non-neutralizing mAb, was used as the control antibody at 200 μg/ml. As shown in Figure 3.6B, at the highest concentration of 200 μg/ml, mAb 1A9 prevented the viral entry of S-WT-pp and S-N1056K-pp in CHO-ACE2 cells by 36% and 35% respectively, while the entry of S-D1128A-pp was not significantly affected. At lower concentrations of mAb 1A9 (25, 50 and 100 μg/ml), similar results were obtained, suggesting that S-D1128-pp was resistant to mAb 1A9 neutralization. This indicated that through a reduction in binding to mAb 1A9, as observed in Western Blot, IP and ELISA, the D1128A mutation in S protein is sufficient to mediate the escape from neutralization by mAb 1A9. In addition, S-pp containing both D1128A and N1056K mutations was investigated for its resistance to mAb 1A9 neutralization and it was found that S-D1128A/N1056K-pp was also resistant to mAb 1A9 neutralization at a similar extent as the S-D1128A-pp (Figure 3.6B), indicating no synergistic effects between the D1128A and N1056K mutations in conferring mAb 1A9 resistance to the viral particles. Neutralization was observed for all S-pps at a dose-dependent manner with mAb 1G10, which binds to a separate epitope within the S2 subunit at amino acids 1151–1192, at the same concentrations tested (Figure 3.6C).

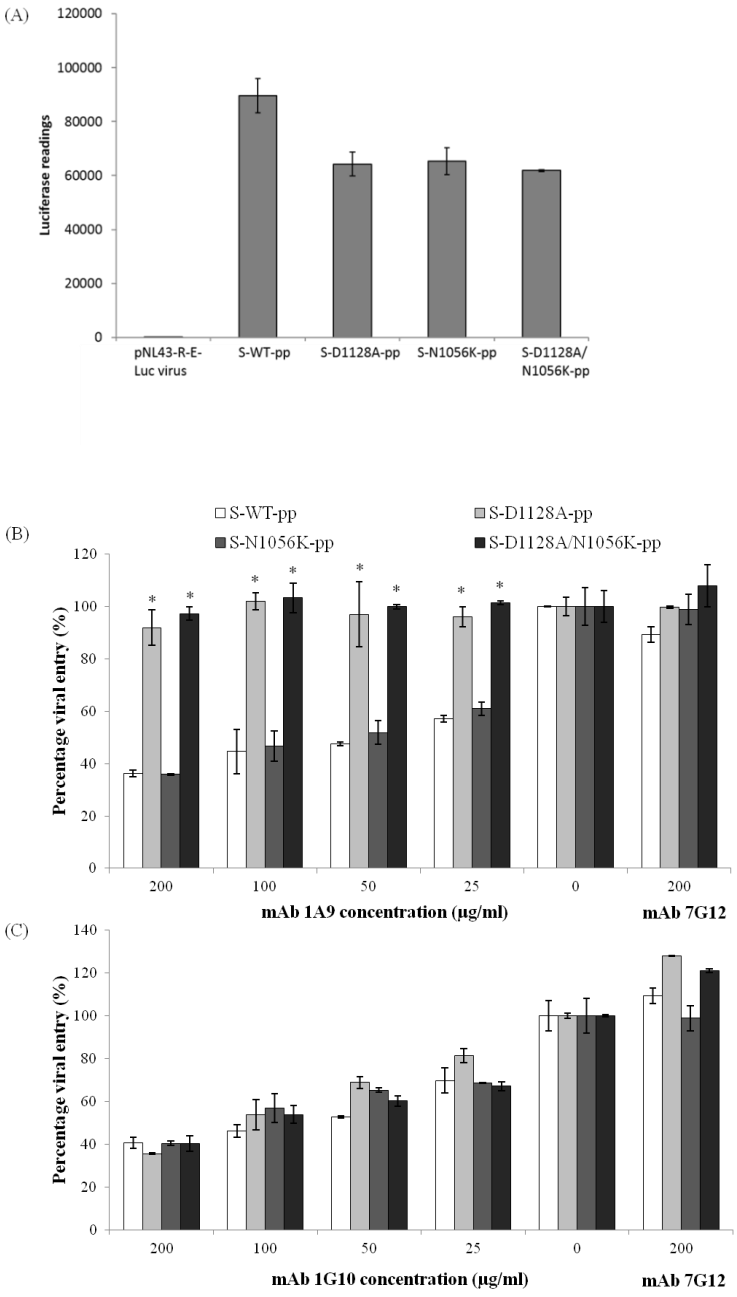

Figure 3.6. Neutralization of wild-type, mutant D1128A and N1056K S-pps by mAb 1A9. (A) S-pp containing wild-type or mutant D1128A, N1056K or D1128A/N1056K S were used to infect CHO-ACE2 cells at equal amount (as quantitated using P24 ELISA) to determine infectivity. pNL43-R-E-Luc virus, which do not express S protein, was used as negative control. S-pps were then pre-incubated with different concentrations of (B) mAb 1A9 or (C) mAb 1G10 at 25, 50, 100 and 200 µg/ml for 1 hour before infecting CHO-ACE2 cells. An anti-S1, non-neutralizing mAb 7G12 was used as control antibody at 200 µg/ml. Viral entry, as indicated by the luciferase activity, was expressed as a percentage of the reading obtained in the absence of antibody, which was set at 100%. Data shown represents that obtained from 3 independent experiments. Bars represent SD of the experiment carried out in triplicates. *indicates statistically significant difference of $p<0.01$ when compared to S-WT-pp at each specific mAb concentration.

3.5 Effects of D1128A mutation on the expression of S protein on cell surface and incorporation of S protein into S-pp

The ability of virus to escape mAb neutralization through the acquisition of mutations is a major caveat of the administration of mAb for passive immunotherapy against viral infections. This is especially true for RNA viruses, such as coronaviruses, of which mutability of viral genome is high due to the error prone nature of RdRps [188]. Escape mutants that result from mAb escape could exhibit different fitness from the wild-type virus [407,408,409,410]. We next investigated if the D1128A mutation in the S protein which arose from mAb 1A9 escape caused a change in viral fitness of the escape mutant virus. The coronavirus S protein plays essential roles in viral entry and viral-cell fusion, and its maturation and incorporation into virion particles has been shown to be an important determinant in SARS-CoV infectivity [411]. Mutations within the coronavirus S protein can have profound effects on the synthesis and maturation process of the S protein, resulting in decreased cell surface expression as well as defects in its incorporation into matured virion particles, and giving rise to viruses with lower infectivity [412]. As such, the study of the effect(s) of the D1128A mutation on S protein processing and functionality can give us an insight into the fitness and infectivity of the D1128A escape SARS-CoV mutant.

First, to evaluate the possible effects of D1128A mutation on the maturation process of the S protein during its synthesis, FACS analysis was performed to compare the cell surface expression of wild-type and mutant D1128A S proteins in transfected 293 FT cells. Vector-transfected, wild-type S- and mutant D1128A S-transfected cells were incubated with mAb 7G12 (which binds to the S1 subunit of S) followed by FITC-conjugated anti-mouse secondary antibody for FACS analysis. A positive shift in fluorescence was observed in the wild-type S-expressing cells when

compared to the vector-transfected cells due to the specific binding of mAb 7G12 to the S protein expressed on the cell surface (Figure 3.7A). In comparison, the mutant D1128A S-expressing cells showed similar degree of shift in fluorescence as those expressing wild-type S (Figure 3.7A). Thus, the D1128A mutation did not affect the surface level expression of the S protein, suggesting that this substitution at residue 1128 did not hamper the synthesis and processing of the S protein.

To determine if the mutant D1128A S protein is incorporated into the S-pps as efficiently as wild-type S, equal amount of wild-type S-pp (S-WT-pp) and S-D1128A-pp was coated onto an ELISA plate and mAb 7G12 was again used to compare the amount of S protein in the S-pps. No significant difference was observed in the expression of wild-type and mutant D1128A S protein in the S-pps at all four different dosages of mAb 7G12 (Figure 3.7B, top). This indicated that the mutation did not cause any change in the efficiency of S protein incorporation into viral particles. An anti-HIV-1 P24 mAb was used instead of mAb 7G12 to confirm equal amounts of S-pp viruses were used for ELISA (Figure 3.7B, bottom). Based on these observations, it is likely that the mAb 1A9 escape SARS-CoV mutant virus containing the D1128A mutation in S protein have comparable viral fitness as the wild-type virus.

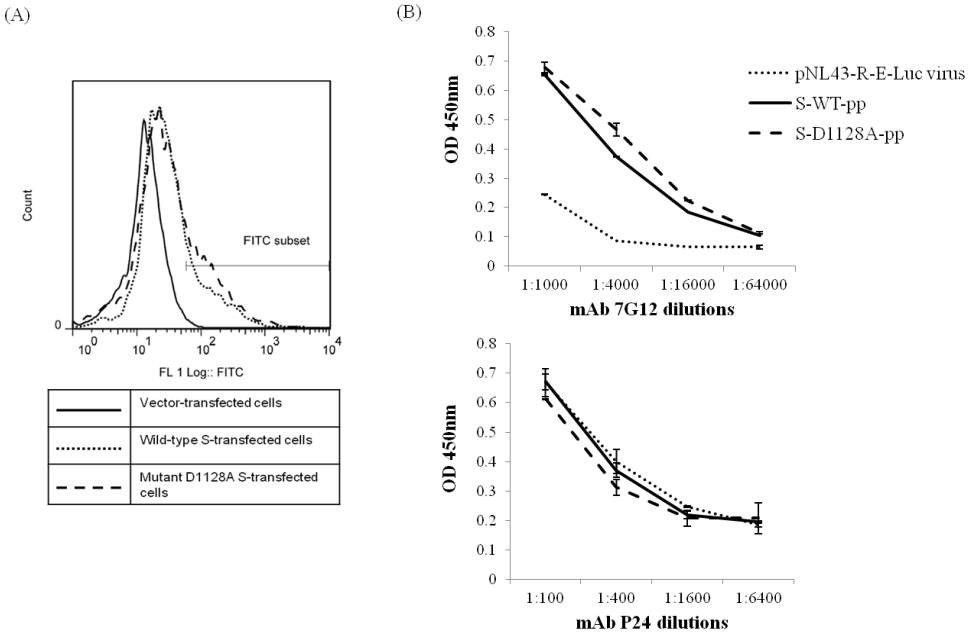

Figure 3.7. Determination of wild-type and mutant D1128A S protein expressions on cell surface and incorporation in S-pps. (A) FACS analysis of 293 FT cells transfected with empty vector (full line) or with plasmids expressing full length wild-type S (dotted line) or full length mutant D1128A S (dash line). Cells were harvested and stained with mouse mAb 7G12, followed by FITC-conjugated goat anti-mouse antibody. Result shown is representative of 3 independent experiments. (B) Pseudoviral particles not expressing S (pNL43-R-E-Luc virus), S-pp expressing wild-type S (S-WT-pp) and mutant D1128A S (S-D1128A-pp) were coated on a 96-well plate at 16 ng/well, as quantitated using P24 ELISA, and detected using mAb 7G12 (top) and mAb P24 (bottom) at 4-fold serial dilutions by ELISA. Optical density (OD) was measured at 450 nm. Bars represent SD of the experiment carried out in triplicates. MAb P24 was used as a control antibody to ensure equal S-pp coating on each well.

3.6 Discussion

Although there has been no reported case of SARS-CoV infection in humans since 2004, the development of SARS-CoV treatments and vaccines remains crucial. Human and civet SARS-CoVs are believed to have originated from SL-CoVs residing in bats [413]. As coronaviruses are known to be capable of frequent cross-species transmission, the continual persistence of SL-CoVs in animal hosts and reservoirs poses a threat to humans should a cross-species transmission occurs [149].

Neutralizing mAbs have been shown to be important in the recovery of SARS patients and protection against SARS-CoV infections [405]. Thus, the use of neutralizing mAbs is an attractive prophylactic and therapeutic strategy for the prevention and treatment of SARS-CoV infection. Given the zoonotic origin of SARS-CoV, broadly neutralizing mAbs that confer cross-protection zoonotic strains of SARS-CoV and SL-CoV are important. The putative S1 subunit of bats SL-CoVs has a low sequence homology of about 63% to that of human SARS-CoV, especially in the RBD, indicating different host cell receptor usage and tissue tropisms [414]. On the other hand, the high sequence homology in the S2 subunit of about 92-96% suggests that the fusion mechanism is well-conserved [415]. Broadly neutralizing mAbs usually target conserved epitopes required for highly conserved process, such as the post-attachment fusion process [357]. A majority of SARS-CoV-neutralizing mAbs reported bind and target the S1 protein at the RBD region [189]. Nonetheless, neutralizing mAbs that bind to the S2 subunit have been reported. The epitopes of these mAbs are located at the S2 subunit upstream of HR1 (residues 787-809, 791-805) [359,361], within the loop region in between HR1 and HR2 (residues 1023–1189) [360,363] and within the HR2 domain (residues 1151-1192) [363]. It has been shown that anti-S2 mAbs that bind to the highly conserved HR1, HR2 and ectodomain of the SARS-CoV S protein are able to neutralize a wider range of clinical isolates, including human and zoonotic strains of SARS-CoVs [188,358]. MAb 1A9 and 1G10, both of which bind to the S2 subunit at the highly conserved regions at residues 1111-1130 and 1151-1192 respectively, were demonstrated to cross-neutralize pseudotyped S-pp viruses of the human SARS-CoV, civet SARS-CoV and bat SL-CoV strains [401]. This is consistent with the sequence conservation of the mAb 1A9 and 1G10 binding epitopes in S. In addition, sequence alignment (not shown) revealed that the two binding sites are also conserved in other bat CoVs

such as the Bulgarian SARS-related CoV strain [416] as well as the bat SL-CoVs (RsSHC014 and Rs3367 strains) which recognizes the ACE2 receptor [271], indicating the potential cross-protective effect of mAb 1A9 and 1G10 against viruses highly related to the human SARS-CoV as well as those that are more distantly related.

Cross-neutralizing mAbs against human and civet SARS-CoV strains targeting the RBD have been described, with IC50 values ranging from 0.01 to 0.5 µg/ml [406,417,418,419]. The IC50 values of mAb 1A9 and 1G10 lies between 25-50 µg/ml and 100-150 µg/ml respectively, which are higher than that of RBD-targeting mAbs, indicating the lower potency of mAb 1A9 and 1G10 [401]. In general, higher IC50 values have been observed in anti-S2 mAbs [360,420]. This can possibly be attributed to the inaccessibility of the S2 subunit, which constitutes the stalk region of S, as compared to the S1 subunit that is exposed on the viral surface [421]. A major concern in the use of neutralizing mAbs for therapeutic purposes is the generation of escape viral mutants as a result of the high mutation rate of RNA viruses due to the error prone nature of genome replication by RdRps [422]. Coronaviruses are highly capable of attaining mutations, especially in the more plastic RBD region, without affecting viral infectivity. On the other hand, mutations within the highly conserved S2 subunit are more likely to be detrimental since the S2 region plays a critical role in fusion process and is less permissive to mutagenesis [152]. Therefore, although less potent in neutralization, anti-S2 mAbs are capable in preventing generation of mAb escape mutants, making them favourable passive immunotherapeutic agents.

MERS-CoV belongs to lineage C of the betacoronavirus genus and is distantly related to the SARS-CoV from lineage B. However, both share similarities in their high pathogenicity in human and causing serious respiratory disease. Similar to SARS-CoV, neutralizing antibodies targeting the S protein of MERS-CoV are

effective and promising antivirals to target the virus [423]. In a study using mouse models, the administration of camel serum containing MERS-CoV-specific antibodies for prophylactic or therapeutic treatment was able to prevent and clear MERS-CoV infections in mice [424]. Compared to the common occurrence of cross-reactive antibodies targeting conserved epitopes in N proteins across betacoronaviruses of different lineages, cross-reactive neutralizing antibodies targeting S proteins of betacoronaviruses is rare due to the highly non-conserved immunogenic epitopes within the S proteins [425]. Interestingly, Chan *et al.* demonstrated that SARS patient's sera showed significant neutralizing antibody titres against MERS-CoV, indicating the possible presence of cross-reactive anti-SARS-CoV S antibodies against MERS-CoV [426]. Therefore, we checked if mAb 1A9 and 1G10 could bind to the S protein of MERS-CoV to neutralize MERS-CoV infection. We showed that both mAbs are unable to bind to MERS-CoV S protein, thus indicating that these two mAbs, although able to neutralize infections of SARS-CoV and related zoonotic SARS-CoV and SL-CoV strains, are likely unable to cross-neutralize MERS-CoV infections. A detailed analysis of the sequence alignment of the S proteins of SARS-CoV and MERS-CoV (Figure 3.8) revealed that the mAb 1A9 and 1G10 binding sites are highly variable, with 4 out of 20 (20%) and 18 out of 42 (43%) amino acid residues similarity respectively. This is consistent with the observation that the conservation of amino acids within neutralizing epitopes in the S proteins of various SARS-CoV strains determines cross-neutralization of mAbs. Nonetheless, sequence alignment of the full S2 subunits of SARS-CoV and MERS-CoV revealed presence of several highly conserved regions (Figure 3.8), and antibodies could be developed to target these conserved regions to achieve cross-neutralization between SARS-CoV and MERS-CoV.

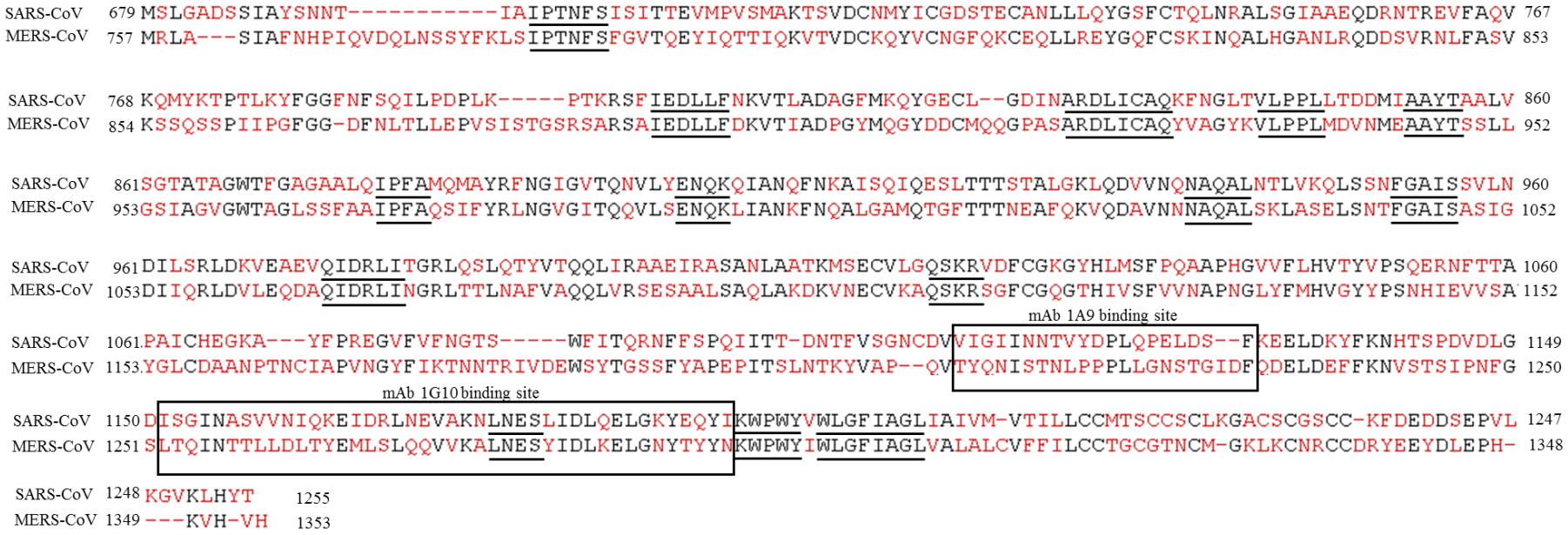

Figure 3.8. Sequence alignment of the S2 regions of SARS-CoV and MERS-CoV. Identical residues are indicated in black. Fully conserved regions of 4 amino acids or more are as underlined. Binding sites of mAb 1A9 and 1G10 are as boxed.

The generation and study of mAb escape mutant is important in identifying critical residues within viral protein important for mAb binding and defining mAb neutralization mechanism. In addition, it can be useful in the evaluation of any altered phenotypic features, including replicative fitness and virulence, of the escape viral mutants which may arise during mAb neutralization. Several studies have investigated SARS-CoV mutant escape viruses that resulted from neutralization by mAbs targeting the more heterogeneous RBD domain [409,410], but none has been done for mAbs targeting the highly conserved S2 domain. In current study, the generation of escape SARS-CoV mutants *in vitro* using mAbs 1A9 and 1G10 was carried out. Although mAb 1G10 escape mutants were successfully generated, no specific mutations were identified in mAb 1G10 escape mutants within its binding site. While no specific mutations were identified in mAb 1G10 escape mutants within its binding site, 3 mutations located far upstream within HR1 domain, H641Y, T706I and W869L, were identified. However, neutralization experiments using mAb 1G10 on S-pps containing these 3 individual mutations showed no resistance to mAb 1G10 neutralization (data not shown). This may suggest that the binding of 1G10 to HR2 could require these distant residues (e.g. upstream of HR1) in the 3D conformational structure of the S protein, hence mutations at these residues away from the mapped binding site abolished binding to mAb 1G10, leading to viral escape. However, mAb resistance conferred by these single mutations could be low and inefficient, such that viral escape activity could not be observed using S-pps, but could still allow escape of infectious SARS-CoVs. Alternatively, selection pressure of mAb 1G10 may have driven mutations in other viral proteins other than the S protein, thereby leading to the escape of virus in the presence of mAb 1G10. However, full genome sequencing of the 1G10 escape mutants was not carried out due to high cost.

Based on the crystal structure resolved for the SARS-CoV S protein fusion core consisting of the six-helical bundle of HR1 and HR2 domains [427], the binding site of mAb 1G10 was found to be located in the region of HR2 that comes into direct contact with HR1. Since the HR1 and HR2 regions are highly conserved and critical for the formation of the fusion core during the SARS-CoV viral entry process, mutations within the 1G10 binding site may not be well-tolerated in mAb 1G10 escape viruses, which could be a reason why there were no 1G10 escape mutants with mutations within its binding site.

On the other hand, through the successful generation of mAb 1A9 escape mutants, it was found that the escape mutation D1128A in the S protein resulted in diminished binding to mAb 1A9 and S-pp containing the D1128A mutation was resistant to neutralization by mAb 1A9. In addition, the substitution of D1128 by either N (having same side-chain as D) or E (having same charge as D) also led to reduction of interaction with mAb 1A9 to similar extent as the A substitution. Thus, the D residue at position 1128 in the S protein plays an essential role in the interaction with mAb 1A9. Another mutation, N1056K, also identified in mAb 1A9 escape virus, was found to have no effects on mAb 1A9 binding and neutralization, indicating that it is most likely a random mutation that arose during the generation of escape mutants. No significant synergistic effect was observed between the D1128A and N1056K mutations in decreasing mAb 1A9 binding and conferring resistance to mAb 1A9 neutralization, further supporting that residue N1056 is not involved in mAb 1A9 binding to S and neutralization of SARS-CoV infections.

Escape viral mutants that attained mutation(s) which allows its escape from mAb neutralization could exhibit changed or unchanged fitness compared to the wild-type virus. Viral fitness generally refers to the replicative capability of a virus, and is usually associated with virulence which is regulated by numerous factors including viral entry and shedding [428]. Changes in viral fitness are dependent on the role and importance of the mutated residue(s) in determining viral replication and infectivity. For SARS-CoV, it was demonstrated that escape mutants of RBD-targeting mAbs were found to replicate to similar titres as the wild-type virus *in vitro* but at a delayed rate, and caused attenuated disease in aged mouse model [410]. In another study, SARS-CoV escape mutants generated using a combination of mAbs targeting the RBD also exhibited delayed but comparable replication as wild-type virus *in vitro*, but *in vivo* studies showed that the escape mutants displayed either attenuated or enhanced virulence [409]. Due to the lack of access to a BSL3 facility, we were unable to carry out direct *in vitro* or *in vivo* infection studies to determine the fitness of the D1128A escape SARS-CoV mutant. Mutations in the S protein can have effects on the fundamental processing of the S protein, which can affect SARS-CoV viral entry and infectivity [411]. The coronavirus S protein is first co-translationally N-glycosylated and oligomerized in the ER, followed by further glycosylation and acquisition of endoglycosidase H resistance in the Golgi apparatus, before assembling into virion particles [429]. It has been demonstrated that a single amino acid mutation in the S protein of the infectious bronchitis coronavirus was capable in hampering S protein maturation and incorporation into virion particles [412]. As there is currently no information on the possible functional role of mAb 1A9 binding epitope or the residue D1128, the effects of D1128A mutation on the cell surface expression of S and its incorporation into viral-like particles were investigated in present

study. The results showed that S-D1128A is similar to wild-type S in these aspects, suggesting that viral entry property, as mediated by S protein, of the escape virus was not changed and it is likely that the mutant D1128A SARS-CoV escape mutant retained similar fitness as the wild-type virus. The ability of the SARS-CoV to mutate to escape neutralization without a loss in fitness represent a caveat of mAb 1A9 passive immunotherapy, as with that observed for other viruses and antibodies [340]. Since mAb 1A9 and 1G10 bind to separate, non-overlapping amino acid regions within the S2 subunit, and mAb 1G10 is able to neutralize mutant D1128A escape SARS-CoV mutant generated from mAb 1A9 escape at similar level as wild-type virus (see Figure 3.6C), the combined use of mAb 1A9 and 1G10 could prevent the generation of viral escape mutants, although this has not been demonstrated in current study. In addition, the administration of a combination of mAbs consisting of mAb 1A9 and 1G10 with other SARS-CoV mAbs targeting the RBD could also be used to achieve efficacious virus neutralization through synergism as well as eliminate immune escape of viruses.

A major obstacle to overcome involving the use of mAbs is the high costs associated with mAb bioproduction and usage. To mitigate the high cost associated with the use of a cocktail of mAbs, the combination of mAbs with other existing anti-infective drugs, which are cheaper in cost than mAbs, could also be explored to achieve synergistic effects. In addition, improvements in antibody affinities and specificities to enhance efficacies, as well as advancements in mAb bioproduction methods, are ways to reduce cost of passive immunotherapy in the future. Much research has focused on improving antibody efficacies through enhancing binding affinity to antigens via antibody engineering [430]. Alterations in the antibody Fc regions to prolong half-life [431] and to enhance Fc region-mediated effector functions, such as ADCC and CDC, have also

been pursued [432,433]. Through the generation of bispecific or muiltispecific mAbs, which are mAbs capable of binding to 2 or more epitopes, the number of mAbs used in combination immunotherapy could be reduced with increased efficacies [434]. Besides the use of mammalian cell culture systems in mAb production, alternative biological systems could be used, including bacteria, yeast and plant-based systems, which are cheaper and easily scalable to increase production yields [435,436,437]. Cell line engineering to create highly productive cell lines and optimization of cell culture process conditions is also another approach to improve mAb production yields [438].

In summary, we characterized two SARS-CoV-neutralizing mAbs 1A9 and 1G10 that bind to novel epitopes located within the loop region located in between HR1 and HR2 at a position directly upstream of HR2 at residues 1111-1130, and within the HR2 domain at residues 1151-1192 of the S protein respectively. These neutralizing epitopes have not been previously identified and were found to be important in determining mAb cross-reactivity and cross-neutralization between human SARS-CoV strains and those from zoonotic reservoirs. The loop region in between HR1 and HR2 in the S2 subunit is believed to be a region required for viral-cell membrane fusion, as peptides analogous to the loop region were found to inhibit SARS-CoV infection [439]. Although D1128 residue has not been shown to be directly involved in membrane fusion, it is probable that the binding of mAb 1A9 to the D1128 residue in the loop region causes steric hindrance that prevents the association of HR1 and HR2 to form the six-helical fusion bundle core. Similarly, the direct association of mAb 1G10 to HR2 domain could inhibit fusion by preventing the successful formation of the six-helical bundle structure that is required for membrane fusion. Although residues important for binding to mAb 1G10 were not identified via escape mutant study, other methods, such as site-directed mutagenesis,

could be carried out in the future to identify critical residues involved in mAb 1G10 binding. On the other hand, by escape mutant generation, the aspartic acid at residue 1128 is found to mediate the interaction of S protein with mAb 1A9 and a substitution to alanine in the escape virus is sufficient to abolish neutralization by mAb 1A9 but has little effect on viral entry property. Consistently, while a detailed study on the fitness of the escape virus has not been performed, it was observed that the virus titre of the escape virus after 3 passages in presence of mAb 1A9 reached similar level as the wild-type virus (see Figure 3.3). Combination immunotherapy, involving the use of a cocktail of anti-S1 and anti-S2 SARS-CoV mAbs, represents an attractive strategy to be explored in the future to achieve neutralization synergism, increase in breadth of protection and the prevention of immune escape.

CHAPTER 4: MEMORY T CELL RESPONSES IN SARS-RECOVERED INDIVIDUALS

Besides the development of antiviral agents and strategies for prophylaxis and treatment of SARS, like that based on mAb immunotherapy as described in Chapter 3, the availability of vaccines is equally important in an event of a SARS outbreak to protect the general population and to prevent further spread of the virus. The SARS outbreak broke out in late 2002 to mid 2003, followed by a few sporadic cases in late 2003 to early 2004, after which no subsequent cases of SARS cases in humans were reported, with the exception of a few laboratory-acquired cases. As such, it is not known if memory immune responses against SARS-CoV in recovered individuals are able to protect against re-infection. The identification of SARS-specific humoral and cellular immune responses from SARS convalescent patients not only allows for the understanding of SARS-specific protective immunity that have contributed to the recovery of these patients, but also have important implications in development of treatment and vaccine strategies against the virus in the event of its re-emergence. While SARS-specific antibody in SARS-recovered individuals was found to decrease in level over time and eventually became undetectable at 6 years post-infection, SARS-specific memory T cells persisted in SARS convalescent subjects up to 6 years following recovery [142]. The long-term persistence of memory T cell immunity could play an important role in protection against SARS-CoV re-infection, and the characterization of these SARS-specific T cells may reveal the kind of immune responses responsible for viral clearance and protection.

In our previous study, memory T cell responses against the SARS-CoV structural N protein and the accessory 3a protein were examined in a group of 16 Asian SARS convalescent subjects 6 years post-infection. Using peptides spanning the N and 3a

proteins, T cell responses specific against these proteins were detected, indicating the persistence of memory T cells after 6 years post-infection [142]. In current study, we continue to look into the presence and persistence of SARS-specific T cells targeting all SARS-CoV structural and accessory proteins in 3 Asian SARS-recovered individuals up to 11 years post-infection. We further focused on the characterization of the identified $CD8^+$ T cell responses against the structural M and N proteins, including the determination of HLA restriction and the minimal epitope region.

4.1 Screening of memory T cell responses against SARS-CoV structural and accessory proteins in SARS-recovered individuals

Peptides used for the screening of SARS-specific memory T cells consisted of a total of 550 15-mer peptides of 10 overlapping amino acids spanning the SARS-CoV structural (S, N, M and E) and accessory (3a, 3b, 6, 7a,7b, 8a, 8b, 9b) proteins, which comprise of 1/3 of the entire SARS-CoV proteome. Due to the limited amount of SARS subject PBMCs obtained for study, we could not carry out T cell screening using peptides spanning the full SARS-CoV proteome including the replicase protein. Based on current literature, the SARS-CoV replicase protein is considered less immunogenic compared to the structural and accessory proteins, as most SARS-CoV T cell epitopes reported so far were located within the SARS-CoV structural and accessory proteins. Particularly, in a study looking at T cell responses against all SARS-CoV proteins in 128 SARS-recovered patients, 7 out of a total of 55 T cell epitopes identified (13%) were located in the replicase protein despite it covering 2/3 of the SARS-CoV proteome, while the rest of the 48 epitopes (87%) were located in the structural and accessory proteins [140]. In addition, the frequencies and magnitudes of T cell responses specific against the replicase protein

were lower than that against the structural and accessory proteins, suggesting that the T cell responses against the replicase protein is less immunodominant and possibly play a less important role in protective cellular immunity against SARS-CoV infections. Therefore, we focused on identifying SARS-specific T cell responses targeting the structural and accessory proteins.

PBMCs from 3 Asian SARS convalescent subjects were collected at either 9 or 11 years post-infection and tested for SARS-specific T cells using the IFNγ ELISpot assay. After 10 days of *in vitro* expansion using the mixture of SARS-CoV peptides, the PBMCs were subjected to stimulation by peptide pools arranged in alphabetic and numeric matices (Table 4.1) in IFNγ ELISpot assay, which measures the frequency of IFNγ-producing T cells based on spot forming unit (SFU), of which each spot represents an $IFN\gamma^+$ T cell after peptide pool stimulation.

Protein	Matrix (number of numeric pools + number of alphabetic pools)	Number of pools	Total number of peptides in matrix
S	16 + 16	32	249
E / M	7 + 9	16	57 (14 E peptides; 43 M peptides)
N	9 + 9	18	82
3a	7 + 8	15	53
3b / 6	6 + 7	13	40 (29 3b peptides; 11 6 peptides)
7a / 7b	5 + 6	11	30 (23 7a peptides; 7b peptides)
8a / 8b / 9b	6 + 7	13	39 (6 8a pepitides; 15 8b peptides; 18 ORF9 peptides)

Table 4.1. Pooling of 550 SARS-CoV peptides spanning the entire proteome of the structural (S, N, M and E) and accessory (3a, 3b, 6, 7a, 7b, 8a, 8b, 9b) proteins. Peptides are 15-mer peptides of 10 overlapping amino acids. Peptides within each protein were arranged in a matrix consisting of numeric and alphabetic pools.

Analysis of the ELISpot results was performed with the positive threshold set as the number of SFU two times above the mean SFU of unstimulated cells. Memory T cell responses were detected in all the SARS-recovered subjects, but not in a healthy individual with no prior medical history of SARS, indicating that the responses are SARS-specific (Figure 4.1). The common peptide in both the alphabetic pool and numeric pool that gave positive IFNγ responses was identified as the positive peptide that is capable of eliciting T cell IFNγ production. For example, as illustrated in Figure 4.2, in SARS subject 1, both E/M numeric pool 5 and alphabetic pool G were found to induce IFNγ response (Figure 4.2A), and the common peptide found in these two pools was M29 (Figure 4.2B). Hence, M29 was determined to be the peptide capable in inducing the T cell IFNγ response.

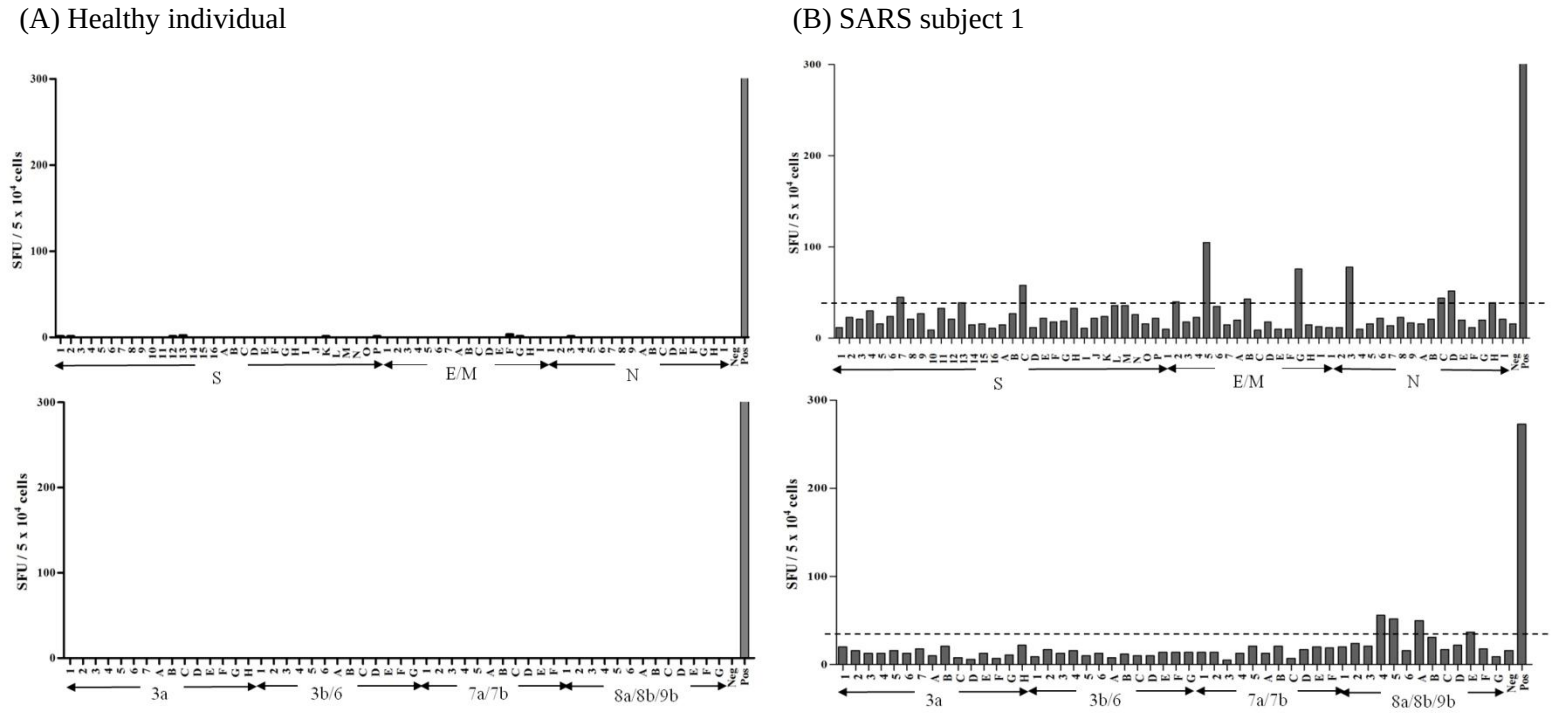

Figure 4.1. IFNγ ELISpot results for SARS-specific T cell screening. PBMCs from (A) a healthy individual and (B) a representative SARS-recovered individual (SARS subject 1) were expanded *in vitro* using a mixture of SARS-CoV peptides, followed by IFNγ ELISpot assay using SARS peptide matrix pools of the structural (top panels) and accessory proteins (lower panels). Each bar represents the IFNγ-producing response to an individual peptide matrix pool (numeric or alphabetic) in SFU per 5 x 10^4 cells. The threshold for a positive response was set as two times above the mean SFU of unstimulated cells (Neg), as indicated by the dotted line in the right panels. Cells stimulated with PMA/ionomycin were included as positive control.

(A)

(B)

E/M Alphabetic pools →

E/M Numeric pools ↓

	A	B	C	D	E	F	G	H	I
1	E1	E2	E3	E4	E5	E6	E7	E8	E9
2	E10	E11	E12	E13	E14	M1	M2	M3	M4
3	M5	M6	M7	M8	M9	M10	M11	M12	M13
4	M14	M15	M16	M17	M18	M19	M20	M21	M22
5	M23	M24	M25	M26	M27	M28	M29	M30	M31
6	M32	M33	M34	M35	M36	M37	M38	M39	M40
7	M41	M42	M43						

Figure 4.2. Example of ELISpot data analysis. (A) Picture of a portion of the ELISpot plate with wells showing positive IFNγ production following stimulation by numeric E/M-5 pool and alphabetic E/M-G pool (boxed in red). (B) 9 x 7 matrix arrangement of E/M numeric and alphabetic pools of the E and M peptides. Based on matrix arrangement, common peptide in positive wells E/M-5 and E/M-G was identified as the M29 peptide, as highlighted in yellow.

4.2 SARS-specific $CD8^+$ and $CD4^+$ T cell responses in SARS convalescent subjects

The positive peptides identified from ELISpot were further tested by intracellular cytokine staining (ICS) and flow cytometry to confirm their abilities to activate specific T

cell IFNγ response. *In vitro* expanded PBMCs were stimulated with the specific peptide in the presence of brefeldin A for 5 hours or overnight, followed by staining of cells for CD8, IFNγ and CD107a expression and analysis by flow cytometry. Not all peptides identified in ELISpot were positive in eliciting T cell response. This could be attributed to non-specific activation of other immune cells by the peptide pools. A summary of all identified SARS-specific memory $CD4^+$ and $CD8^+$ T cell responses in the 3 SARS subjects after confirmation by ICS is provided in Table 4.2. HLA class I haplotype of each SARS subject was determined by PCR and sequencing method (done by BGI Clinical laboratories, ShenZhen, China), as also indicated in Table 4.2. A total of 5 SARS-specific memory T cell responses were identified and they were specific for the SARS-CoV structural S, N and M proteins. No T cell responses against the E protein and the accessory proteins were detected. 4 of the responses were $CD4^+$ T cell responses, of which 3 recognized the S protein (S104, S109, S217) and 1 recognized the N protein (N21). 2 of the SARS subjects (SARS subject 1 and 2) presented the N21 $CD4^+$ T cell response. A $CD8^+$ memory T cell response specific for the SARS-CoV M protein (M29) was identified in two out of three SARS subjects (SARS subject 1 and 3).

	HLA Class I	Years post-SARS infection	Peptide	Amino acid position	Type of T cell response
SARS subject 1	A*2402 A*0206 B*1502 B*1525 C*0801 C*0403	9 years	S104	516 - 530	$CD4^+$
			S109	541 - 555	$CD4^+$
			N21	101 -115	$CD4^+$
			M29	141 - 155	$CD8^+$
SARS subject 2	A*1101 A*3303 B*5502 B*5801 C*0302 C*0303	9 years	N21	101 -115	$CD4^+$
SARS subject 3	A*0201 A*1101 B*1502 B*4001 C*0801 C*1502	11 years	S217	1081 - 1095	$CD4^+$
			M29	141 - 155	$CD8^+$

Table 4.2 Summary of T cell responses in three SARS recovered individuals identified from screening by ELISpot and confirmation by ICS.

4.3 Characterization of SARS-specific M29 $CD8^+$ T cell response in SARS-recovered subjects

We focused on the further characterization of the $CD8^+$ T cell response specific for the SARS peptide M29, which was detected in 2 out of the 3 SARS convalescent subjects (SARS subject 1 and 3) employed in this study. The M29 peptide corresponds to amino acid residues 141-155 of the SARS-CoV M protein. From ICS and flow cytomerty analysis of *in vitro* expanded PBMCs, M29 induced $CD8^+IFN\gamma^+$ T cell response at a low frequency of 1.0% (0.8% in unstimulated cells) and 0.4% (0.1% in unstimulated cells) in SARS subject 1 and 3 respectively (results not shown). To enrich the population of M29-specific T cells, *in vitro* expanded cells were further restimulated using M29 peptide in

the presence of IL-2, IL-7 and IL-15 for 10 days. Flow cytometry analysis of the restimulated cells showed increase in M29-specific $CD8^+IFN\gamma^+$ T cell responses at 27.6% (unstimulated cells at 0.1%) in SARS subject 1 and 1.7% (unstimulated cells at 0.3%) in SARS subject 3 (Figure 4.3). The marked difference in the M29-specific $CD8^+IFN\gamma^+$ T cell responses observed in the 2 SARS subjects was noted, which could be attributed to a much lower frequency of M29-specific T cells in SARS subject 3 compared to SARS subject 1. Additionally, staining for CD107a, a marker for degranulation of T cells [440], was also done to assess the level of T cell degranulation and cytotoxicity. As shown in Figure 4.3, CD107a expression of the $CD8^+$ T cells induced by M29 in both SARS subject 1 and 3 was determined to be 12.7% (unstimulated cells at 0.2%) and 0.5% (unstimulated cells at 0.1%) respectively. Similar to the production of IFNγ, M29-specific $CD8^+$ T cells of SARS subject 1 showed higher CD107a expression upon M29 peptide stimulation compared to that in SARS subject 3. These results indicated the presence of M29-specific SARS memory $CD8^+$ T cells in SARS subject 1 and 3 at 9 years and 11 years post-infection respectively. Furthermore, the T cells were capable to be activated for degranulation and cytotoxicity upon stimulation by M29 peptide as indicated by the increase in CD107a expression.

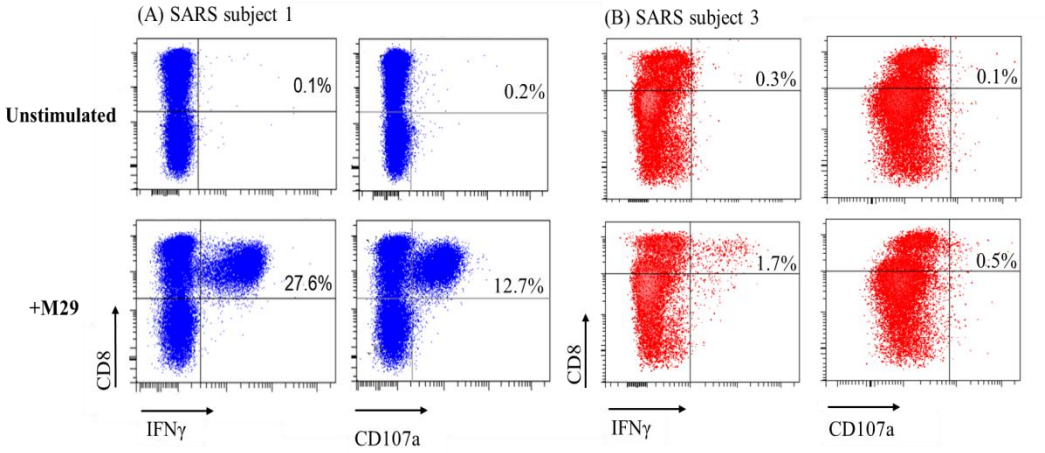

Figure 4.3. ICS and flow cytometry analysis of unstimulated and M29-stimulated T cells after restimulation using M29 peptide. As indicated in the upper right quadrant of each dot plot, the percentages of $CD8^+$ $IFN\gamma^+$ and $CD8^+CD107a^+$ T cells shown represent the percentage of the T cells in total T cell population after gating the $CD3^+$ cells of the PBMCs from (A) SARS subject 1 and (B) SARS subject 3.

Next, we investigated the HLA class I restriction of the M29-specific $CD8^+$ T cell response. To do so, Epstein-Barr virus-transformed lymphoblastoid B cell lines (EBV-LCLs) expressing the matching allele(s) of each SARS-recovered subject's HLA class I haplotype were used as antigen-presenting cells to present the M29 peptide to the T cells. Only the EBV-LCL which possesses the correct HLA allele is able to present the peptide to the T cells to elicit the $CD8^+IFN\gamma^+$ response, hence allowing the determination of the HLA restriction. The combination of EBV-LCLs used for each SARS subject was carefully chosen based on the HLA class I haplotype so that the single allele responsible for the $CD8^+$ T cell response could be determined. Since both SARS subject 1 and 3 possess the HLA-B*1502 and HLA-C*0801 alleles, it is expected that the $CD8^+$ T cell response should be restricted by one of these two alleles. As shown in Figure 4.4A, four EBV-LCLs were tested for SARS subject 1, of which two cell lines (EBV-LCL 2 and 3) gave positive $CD8^+$ T cell response in the presence of M29 peptide. Both EBV-LCL2 and 3 had the HLA-B*1502 and HLA-C*0801 alleles in common as SARS subject 1, but

EBV-LCL1, which also contained the HLA-C*0801 allele, was unable to induce the M29-specific T cell response. As such, it could be drawn that the HLA-B*1502 allele is responsible for the M29-specific T cell response.

Similarly, for SARS subject 3, a combination of 5 EBV-LCLs were tested for their ability to present M29 peptide to the T cells, and it was observed that only EBV-LCL5 was able to induce the M29 $CD8^+$ T cell response. EBV-LCL5 had three common HLA class I alleles, HLA-A*0201, HLA-B*1502 and HLA-C*0801, as SARS subject 3. Since EBV-LCL6 (expressing HLA-A*0201) and EBV-LCL7 (expressing HLA-C*0801) were both unable to induce T cell response, this indicated that HLA-B*1502 is the HLA restriction of the M29 $CD8^+$ T cell response in SARS subject 3. This is the same as that determined for SARS subject 1. Consistent with previous results of M29-specific T cell responses determined using the SARS subjects' autologous PBMCs for antigen-presenting (Figure 4.3), the percentage $CD8^+IFN\gamma^+$ T cell response induced by positive EBV-LCL5 in the presence of M29 (1.3%, absence of M29 at 0.8%) in SARS subject 3 was much lower than that found in SARS subject 1 induced by positive EBV-LCL 2 and 3 (29.2% and 9% respectively, absence of M29 at 0.2%) (Figure 4.4).

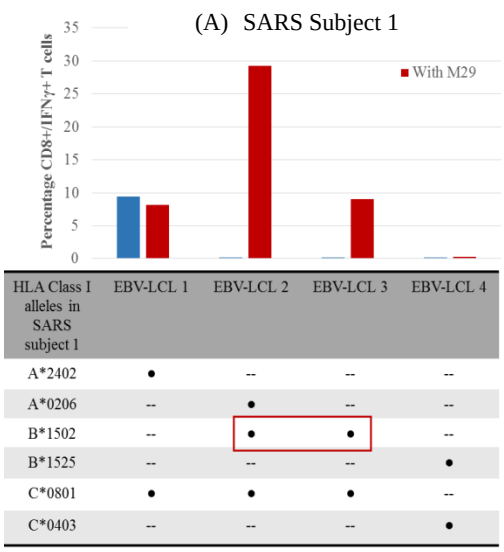

HLA Class I alleles in SARS subject 1	EBV-LCL 1	EBV-LCL 2	EBV-LCL 3	EBV-LCL 4
A*2402	•	--	--	--
A*0206	--	•	--	--
B*1502	--	•	•	--
B*1525	--	--	--	•
C*0801	•	•	•	--
C*0403	--	--	--	•

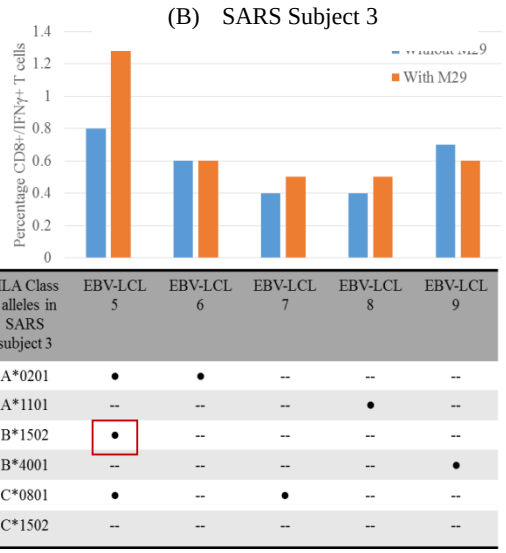

HLA Class I alleles in SARS subject 3	EBV-LCL 5	EBV-LCL 6	EBV-LCL 7	EBV-LCL 8	EBV-LCL 9
A*0201	•	•	--	--	--
A*1101	--	--	--	•	--
B*1502	•	--	--	--	--
B*4001	--	--	--	--	•
C*0801	•	--	•	--	--
C*1502	--	--	--	--	--

Figure 4.4. HLA class I determination of M29-specific CD8$^+$ T cell responses. Graphs show the percentages of CD8$^+$IFNγ$^+$ T cells using different EBV-LCLs pulsed with and without M29 peptide for (A) SARS subject 1 and (B) SARS subject 3. Each EBV-LCL used possesses HLA allele(s) that match the HLA class I haplotypes of the SARS subjects. ● indicates the HLA allelle each EBV-LCL possesses in common with the SARS subjects.

HLA class I molecules preferentially bind and present peptides of 8 to 11 amino acids in length to be recognized by HLA receptors on CD8$^+$ cytotoxic T cells during T cell activation [441]. Since the M29 peptide is a 15-mer peptide, we sought to identify the position and the minimal number of amino acids within the M29 region, known as the minimal epitope region, capable in eliciting the M29-specific CD8$^+$ T cell response. To do so, truncated peptides within the M29 region ranging from 8- to 12-mers were tested for their abilities to induce IFNγ secretion by the M29-restimulated T cells using ICS. As shown in Table 4.3, 9-mer peptide, $M29_{147\text{-}155}$, corresponding to amino acid residues 147-155 of the M protein was most efficient in the activation of CD8$^+$ T cells in both SARS subject 1 and 3, inducing the highest percentage of IFNγ-producing cells of 32.9% and 1.7% out of the total T cell population respectively. This 9-mer peptide also represents

the minimal epitope region of M29-specific $CD8^+$ T-cell response, as the removal of either the N-terminus histidine (H) residue ($M29_{148-155}$) or the C-terminus leucine (L) residue ($M29_{145-154}$) completely abolished IFNγ production. It was also observed that other 12-mer, 11-mer and 10-mer peptides ($M29_{144-155,}$ $M29_{145-155,}$ $M29_{146-155}$) containing residues 147-155 were all capable in inducing the M29 T cell response, though at lower efficiencies compared to the 9-mer minimal peptide, further supporting that this region is the minimal T cell epitope for the M29-specific $CD8^+$ T cell response.

Although our sample number is very small, it is interesting to note that M29-specific $CD8^+$ T cell response was observed in subject 1 and 3 but not subject 2 who does not have the HLA-B*1502 allele needed to present this epitope. A previous study has also reported a 9% prevalence of the SARS-specific $CD8^+$ T cell response with epitope at residues 146-160 of the M protein in SARS-recovered patients [140], and this region contains the M29 minimal epitope of residues 147-155 as identified in current study. However, the HLAs of the patients were not determined in that study. Taken together, our results suggest the dominance of the M29 T cell response in SARS convalescent subjects possessing the HLA-B*1502 allele.

Peptide	Peptide Length	Amino acid position	Peptide Sequence	Percentage of $CD8^+IFN\gamma^+$ T cells	
				SARS subject 1	SARS subject 3
M29	15-mer	141 - 155	AVIIR G**HLRM AGHSL**	5.3%	1.1%
$M29_{144-155}$	12-mer	144 - 155	IR GHLRM AGHSL	14.8%	1.5%
$M29_{143-154}$	12-mer	143 - 154	IIR GHLRM AGHS	0.2%	0%
$M29_{145-155}$	11-mer	145 - 155	R GHLRM AGHSL	17.8%	1.6%
$M29_{146-155}$	10-mer	146 -155	GHLRM AGHSL	22.8%	1.6%
$M29_{145-154}$	10-mer	145 - 154	R GHLRM AGHS	0.2%	0.1%
$M29_{147-155}$	9-mer	147 -155	**HLRM AGHSL**	32.9%	1.7%
$M29_{148-155}$	8-mer	148 - 155	LRM AGHSL	0.3%	0%
Unstimulated cells				0.2%	0.1%
PMA/Ionomycin-stimulated cells				11.1%	5.8%

Table 4.3. Summary of percentage $CD8^+$ $IFN\gamma^+$ responses in SARS subject 1 and 3 induced by truncated peptides within M29 region. Results of positive peptides (M29, $M29_{144-155}$, $M29_{145-155}$, $M29_{146-155}$, $M29_{147-155}$) and selected negative peptides ($M29_{143-154}$, $M29_{145-154}$, $M29_{148-155}$) are shown. Percentage $CD8^+IFN\gamma^+$ cells shown represents the percentage of IFNγ-producing $CD8^+$ T cells in the total T cell population. Minimal T cell epitope is highlighted in red.

4.4 Characterization of SARS-specific N53 $CD8^+$ T cell response in SARS subject 1

In our previous study, several SARS-specific $CD8^+$ memory T cell epitopes within the SARS-CoV N protein were detected at 6 years post-infection [142]. A HLA-B*1525-restricted memory $CD8^+$ T cell response specific for the SARS-CoV N53 peptide, corresponding to the amino acid residues 261-275 of the N protein, was identified at 6 years post-infection in SARS subject 1, who was also enrolled in the past study. However, at 9 years post-infection, the N53-specific memory $CD8^+$ T cell response was not detected in the screening of memory T cell responses of SARS subject 1 by IFNγ ELISpot assay (Figure 4.1B and Table 4.2). Similarly, no $CD8^+$ T cell activation was observed via ICS when *in vitro* expanded PBMCs were stimulated with the specific N53 peptide (data not shown). We speculated that the response might have decreased over time to a level no longer detectable by our screening protocol which uses 15-mer peptides. Since peptides consisting the minimal peptide region are more efficient in inducing T cell

activation, the use of a peptide corresponding to the N53 minimal epitope, instead of the 15-mer N53 peptide, could allow the detection of N53-specific $CD8^+$ T cell response if it is present. To determine the minimal epitope region responsible for the N53-specific $CD8^+$ T cell response, truncated peptides of the N53 region were tested in ICS using PBMCs collected from SARS subject 1 and frozen down at 6 years post-infection. The truncated peptides consist of 8- to 10-mers within the 10 overlapping amino acids between N53 and N54 minimal peptides, as the N54 peptide was also capable in eliciting the $CD8^+$ T cell response (data not shown). Results as summarized in Table 4.4 showed that the 10-mer peptide, $N53_{266\text{-}275}$, corresponding to residues 266-275 of the N protein, was the most efficient inducer of N53 T cell response (12.7%) compared to other peptides tested. Deletion of the N-terminal threonine (T) residue and the C-terminal phenylalanine (F) residue from $N53_{266\text{-}275}$ decreased the percentage of IFNγ-producing $CD8^+$ T cells to 10.9% and 8.0% respectively. This indicated that amino acids 266-275 of the N protein is the minimal epitope required for the N53-specific $CD8^+$ T cell response. In a study based on bioinformatics prediction using the NetMHCpan algorithm, the predicted minimal epitope for the SARS N53 region was determined to be 9 amino acids at position 267-275 [442], which is within the 10-mer region as identified in current study.

Peptide	Peptide Length	Amino acid position	Sequence	Percentage $CD8^+IFN\gamma^+$ T cells
N53	15-mer	261 - 275	QKRTA **TKQYN VTQAF**	8.8%
$N53_{266-275}$	10-mer	266 - 275	**TKQYN VTQAF**	12.7%
$N53_{266-274}$	9-mer	266 - 274	TKQYN VTQA	8.0%
$N53_{267-275}$	9-mer	267 -275	KQYN VTQAF	10.9%
$N53_{266-273}$	8-mer	266 - 273	TKQYN VTQ	2.2%
$N53_{267-274}$	8-mer	267 - 274	KQYN VTQA	2.3%
$N53_{268-275}$	8-mer	268 - 275	QYN VTQAF	2.2%
Unstimulated cells				1.6%
PMA/Ionomycin-stimulated cells				15.3%

Table 4.4. Summary of percentage $CD8^+IFN\gamma^+$ responses induced by truncated peptides within N53 region. T cells used were obtained from SARS subject 1 at 6 years post-infection. Percentage of $CD8^+IFN\gamma^+$ cells shown represent the percentage of IFNγ-producing $CD8^+$ cells in the total T cell population. Minimal T cell epitope is highlighted in red.

After identification of the N53 minimal epitope region, we performed *in vitro* expansion of the PBMCs collected from SARS subject 1 at 9 years post-infection using the $N53_{266-275}$ peptide for 10 days followed by the determination of IFNγ response induced by N53 and $N53_{266-275}$ in ICS and flow cytometry analysis. No significant $CD8^+IFN\gamma^+$ T cell response was observed when the cells were stimulated with N53, while a slightly higher $CD8^+IFN\gamma^+$ response of 0.4% was observed with $N53_{266-275}$ peptide compared to 0% in unstimulated cells (data not shown). Further restimulation of the T cells using $N53_{266-275}$ enriched the population of N53-specific $CD8^+$ T cells, with $N53_{266-275}$ peptide stimulation resulting in a $CD8^+IFN\gamma^+$ response of 7.1% (unstimulated cells at 0.3%), while the $CD8^+IFN\gamma^+$ response resulted from N53 stimulation was much lower at 0.8% (Figure 4.5, left panel). This indicated the presence of N53-specific $CD8^+$ T cell response in SARS subject 1 at 9 years after SARS-CoV infection, but this response was low and not identified using N53 15-mer peptide, and could only be detected when the $N53_{266-275}$ minimal peptide was used for *in vitro* T cell expansion and restimulation. This

further confirmed that residues 266-275 of the N protein constitutes the minimal epitope region and was more efficient than the N53 15-mer in eliciting a $CD8^+IFN\gamma^+$ T cell response. In addition, staining for CD107a was done to assess the level of T cell degranulation and cytotoxicity. CD107a expression of the $CD8^+$ T cells induced by N53 and $N53_{266\text{-}275}$ peptides were 2.0% and 10.5% respectively, compared to unstimulated cells at 1.1% (Figure 4.5, right panel), indicating that the T cells were activated for cytotoxicity upon stimulation by the peptides.

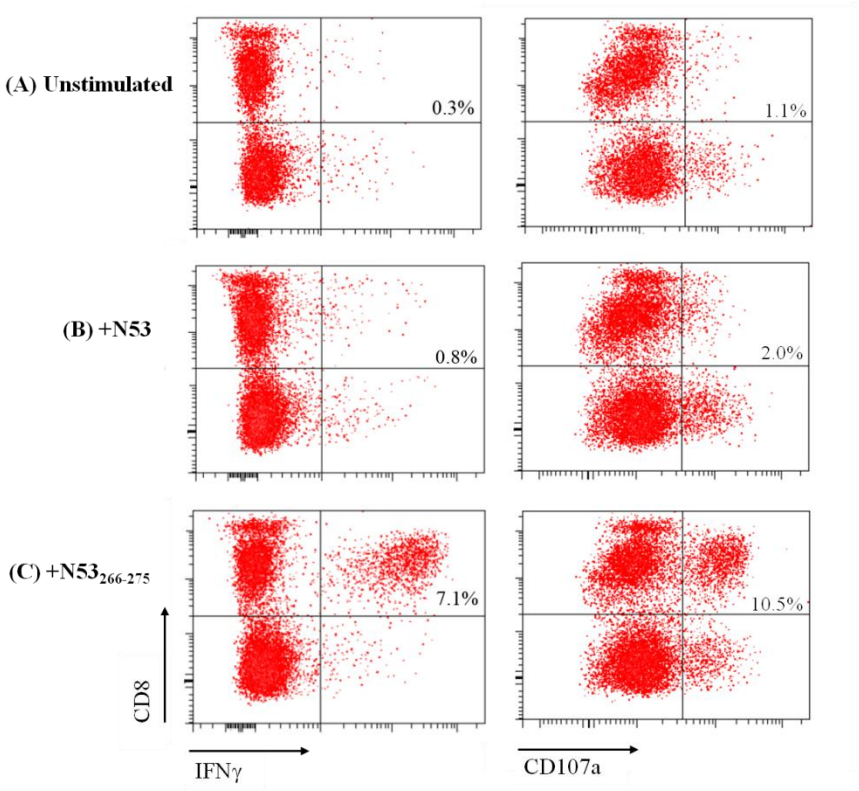

Figure 4.5. ICS and flow cytometry analysis of $N53_{266\text{-}275}$-restimulated T cells from SARS subject 1 at 9 years post-infection. Percentages of $CD8^+IFN\gamma^+$ responses (left panel) and $CD8^+CD107a^+$ responses (right panel) of (A) unstimulated, (B) N53-stimulated, (C) $N53_{266\text{-}275}$-stimulated T cells are indicated in the upper right quadrant of each dot plot. Percentage $CD8^+$ $IFN\gamma^+$ cells shown represent the percentage of IFNγ-producing cells in the total T cell population.

4.5 Persistence of memory SARS-specific M29 and N53 $CD8^+$ T cell responses at 11 years post-infection

We continued to explore the fate of the SARS-specific M29 and N53 $CD8^+$ T cell responses in SARS subject 1 at 11 years post-infection. PBMCs from SARS subject 1 were collected at 11 years after infection, expanded *in vitro* using both M29 and N53 minimal peptides for 10 days and tested for M29- and N53-specific $CD8^+IFN\gamma^+$ T cell responses using ICS and flow cytometry. As shown in Figure 4.6 (left panel), when the T cells were stimulated with M29 minimal peptide, $M29_{147\text{-}155}$, and the NP53 minimal peptide, $N53_{266\text{-}275}$, $CD8^+IFN\gamma^+$ T cell responses of 0.4% and 0.9% were observed respectively, compared to 0% in unstimulated cells. These results suggested the presence of SARS-specific T cell at 11 year after recovery. When cells were stimulated by M29 and N53 15-mer peptides, no significant T cell responses were detected (data not shown). This indicated that the level of T cell response has further decreased over the years and could only be identified using minimal peptides. In addition, CD107a expressions of $CD8^+$ T cells at 0.6% and 1.3% were observed when cells were stimulated with $M29_{147\text{-}155}$ and $N53_{266\text{-}275}$ peptides respectively, compared to 0.2% in unstimulated cells (Figure 4.6, right), indicating the increase of CD107a expression and degranulation of T cells upon peptide stimulation.

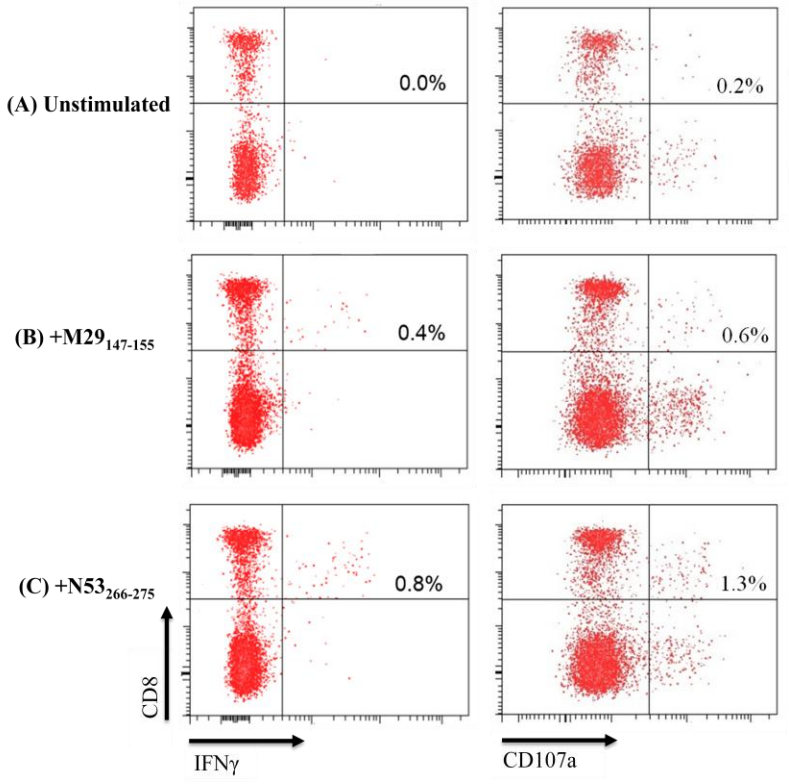

Figure 4.6. ICS and flow cytometry analysis of restimulated T cells from SARS subject 1 at 11 years post-infection. Percentages of $CD8^+IFN\gamma^+$ responses (left panel) and $CD8^+CD107a^+$ responses (right panel) of (A) unstimulated, (B) $M29_{147\text{-}155}$-stimulated, (C) $N53_{266\text{-}275}$-stimulated T cells are indicated in the upper right quadrant of each dot plot. Percentage $CD8^+$ $IFN\gamma^+$ cells shown represent the percentage of IFNγ-producing cells in the total T cell population.

4.6 Cross-reactivity of SARS-specific M29 and N53 $CD8^+$ T cell responses against MERS-CoV

We further investigated if the SARS-CoV M29- and N53-specific $CD8^+$ T cells can cross-react with the corresponding peptides of the MERS-CoV. To do so, sequence alignments of the SARS-CoV and MERS-CoV M and N proteins were done to identify the corresponding SARS-CoV M29 and N53 minimal epitope regions on the MERS-CoV M and N protein respectively (Figure 4.7A and B). Sequence alignments revealed that 5

out of 9 amino acid residues are in common between the M29 minimal epitope regions of SARS-CoV and MERS-CoV (Figure 4.7A). For the N53 minimal epitope regions, 6 out of 10 residues are conserved (Figure 4.7B). The civet SARS-CoV SZ3 and bat SL-CoV Rp3, Rf1 and Rs3367 strains were also aligned and they showed 100% conservation at both M29 and N53 minimal epitope regions. When M29- and N53-specific T cells were stimulated with peptides corresponding to the MERS-CoV M29 minimal epitope (HLKMAGMHF) and N53 minimal epitope (TKSFNMVQAF) respectively, no $CD8^{+}IFN\gamma^{+}$ T cell responses were observed (Figure 4.7C), indicating the inability of these SARS-CoV-specific T cells to be activated by MERS-CoV peptides and the absence of cross-reactivity against the corresponding MERS-CoV M29 and N53 epitopes.

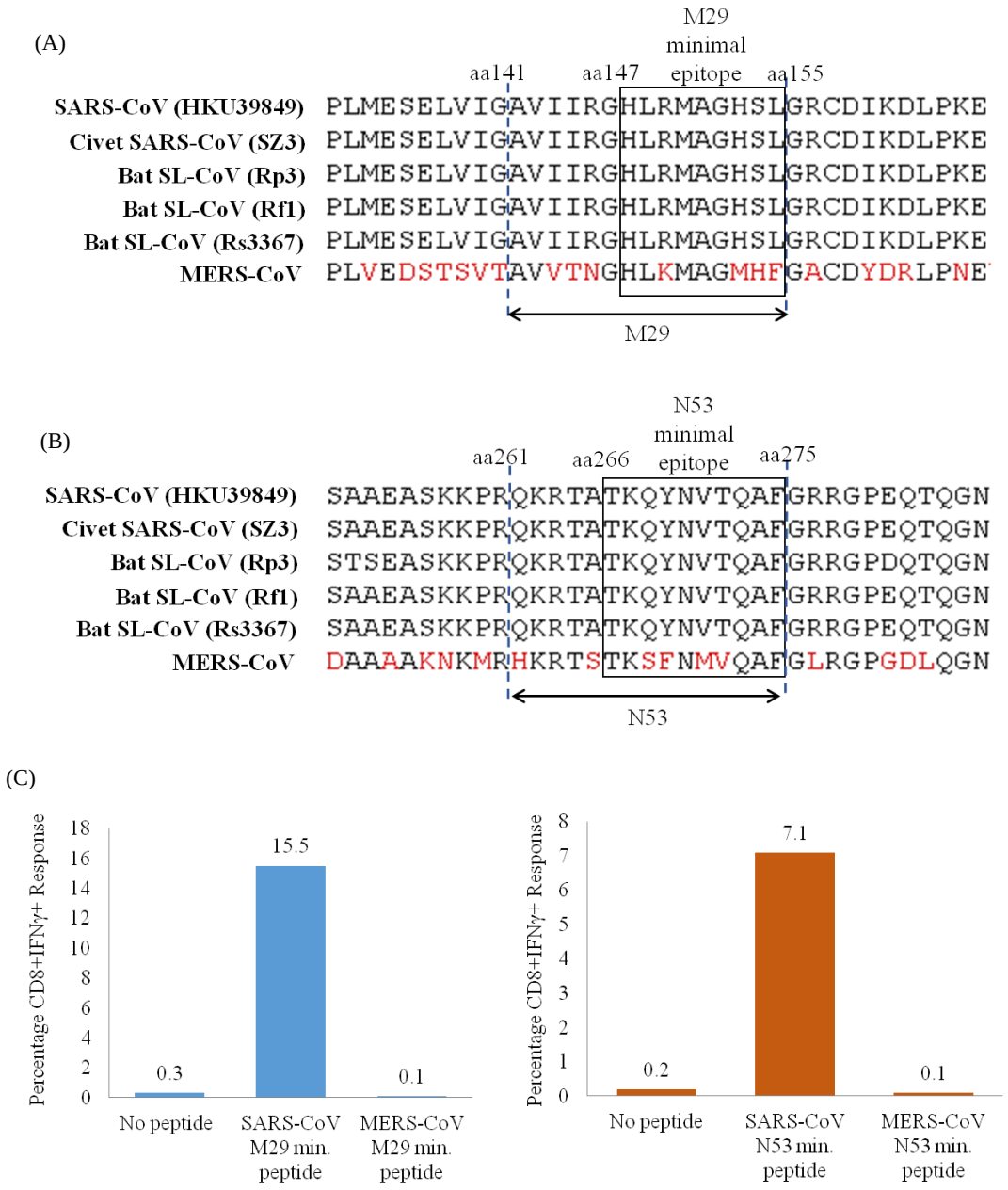

Figure 4.7. Cross-reactivity of SARS-specific M29 and N53 T cells against civet SARS-CoV, bat SL-CoVs and MERS-CoV. Sequence alignment of (A) M29 and (B) N53 regions of human SARS-CoV (HKU39849), civet SARS-CoV (SZ3), bat SL-CoVs (Rp3, Rf1 and Rs3367) and MERS-CoV was done. (C) Percentages of $CD8^{+}IFN\gamma^{+}$ T cell responses induced by SARS-CoV and MERS-CoV M29 and N53 minimal peptides in SARS-M29-specific and SARS-N53-specific T cells from SARS subject 1 at 9 years post-infection.

4.7 Discussion

This study represents the first report on the identification and characterization of SARS-CoV-specific memory T cell responses in SARS-recovered individuals at 9 to 11 years post-infection. T cell responses against a total of 5 T cell epitopes located within the SARS-CoV structural S, N and M proteins (4 $CD4^+$ and 1 $CD8^+$ T cell epitopes) were detected in 3 SARS convalescent individuals who have recovered from SARS ranging from 9 to 11 years ago. This provides evidence that SARS-specific memory T cells persist in SARS-recovered individuals up to 11 years post-infection, even though the level of response is low and *in vitro* expansion of PBMCs using SARS peptide mixtures was required for detection. This is in agreement with previous reports that SARS-specific cytotoxic T lymphocyte (CTL) responses declined over time in convalescent SARS individuals after recovery and that *in vitro* expansion of PBMCs, but not direct *ex vivo* stimulation, allowed detection of SARS-specific T cell responses at 6 years post-infection [142,443]. Because PBMCs isolated from convalescent SARS subjects were used for screening and identification of T cell epitopes, all identified epitopes represent naturally processed antigens capable in eliciting T cell responses that played a part in the recovery from SARS. Compared to other methods of epitope discovery, such as the use of bioinformatics predicting tools to predict peptide sequences with high binding affinity to a given HLA allele followed by verification of peptide using functional assays [444], our method of using a large panel of overlapping peptides is more labour-intensive, but it allows for the unbiased, HLA-independent recognition of all T cell epitopes, rather than restricting to a few peptides which could under-represent that epitopes engaged by the full T cell repertoire.

All 5 T cells epitopes identified in present study were located in the structural proteins (3 in the S protein, 1 in N protein and 1 in M protein). This is consistent with the knowledge that SARS-CoV structural proteins are highly immunogenic in eliciting cellular protective responses and that immunodominant SARS-specific T cell responses usually target structural proteins. Out of the 5 T cell epitopes identified here, 4 were $CD4^+$ T cell epitopes while one was $CD8^+$. Overlaps of T cell epitopes identified in current study with those reported in previous studies were noted. The $CD4^+$ T cell epitopes identified here, which are specific against S104 (S protein residues 516-530), S109 (S protein residues 541-555), S217 (S protein residues 1081-1095) and N21 (N protein residues 101-115), have been previously reported from a cohort of SARS patients in China, [140], suggesting the immunoprevalence and dominance of these responses in convalescent SARS patients. Notably, among the 5 T cell epitopes identified here, 3 (60%) localized within the S protein. A majority of SARS-CoV T cell epitopes were found to lie in the S protein (summarized in Chapter 1, Table 1.4), suggesting that S protein is the major target of immunodominant T cell responses against SARS-CoV. No T cell epitopes within the accessory proteins were identifed in current study, although these T cell epitopes have been identified in other studies (summarized in Chapter 1, Table 1.4). In a study focused on identifying human T cell responses against the full SARS-CoV proteome, a $CD8^+$ T cell epitope in the accessory 3a protein was found to be most frequently recognized alongside with two other T cell epitopes within the S protein [140]. In our previous study, we also reported 7 T cell epitopes recognizing the 3a protein in convalescent SARS patients at 6 years post-infection, suggesting the importance of the 3a accessory protein in eliciting SARS-specific T cell immunity [142]. The absence of T cell responses against the accessory proteins in the three SARS-recovered volunteers in

present study could be due to the lack of these responses or low frequencies of these responses beyond the detection limit of current method used based on 15-mer peptides. Nonetheless, the identification of T cell responses against the structural proteins at 9 to 11 years post-infection strongly suggests the long persistence and dominance of these responses in convalescent SARS individuals.

The in-depth characterization of a $CD8^+$ T cell response identified in 2 out of 3 SARS subjects, which is specific for the M29 epitope located within the SARS-CoV M protein, was carried out. In both SARS subjects, the HLA restriction was determined to be HLA-B*1502 and the minimal epitope region is located at amino acids 147-155 of the M protein. Based on bioinformatic NetMHCpan prediction method [445], this region of the SARS-CoV M protein was also predicted to bind to HLA-B*1502, confirming that experimental results obtained. In a large cohort study involving 128 SARS convalescent patients from China at 1 year post-infection, $CD8^+$ T cell response against the region of amino acid 146-160 of the M protein was present in 9% of the study subjects, although the minimal epitope and the HLA-restriction of the response(s) were not determined [140]. The M29 minimal epitope (residues 147-155) identified in present study lies within this reported region. Numerous other T cell epitopes, both $CD4^+$ and $CD8^+$, within the SARS-CoV M protein have also been reported [140,379,446]. In a study looking at SARS-specific memory T cell responses in fully recovered SARS individuals at 4 years post-infection, 28.75% of them presented T cell responses to M peptides [375]. Therefore, besides its structural role, the M protein plays an important part in eliciting dominant cellular immunity during SARS-CoV infection. In present study, it was noted that the magnitudes of M29 $CD8^+$ T cell response detected in SARS subject 1 and 3 were markedly different. It was observed that the percentages of IFNγ-secreting and CD107a-

expressing M29-specific $CD8^+$ T cells upon peptide stimulation in SARS subject 3 were consistently lower than that observed in subject 1, indicating a less robust T cell response in subject 3 compared to subject 1. Since the level of memory $CD8^+$ T cell responses significantly decrease over the years after recovery from SARS infection, the difference in frequency of M29-specific T cells in SARS subject 1 and 3 could be attributed to the difference in time of analysis of M29-specific T cell responses, which was done 2 years later for SARS subject 3 (11 years post-infection) compared to subject 1 (9 year post-infection). Alternatively, the difference could be due to variations in the state and severity of SARS-CoV infection between the 2 individuals, leading to different degree of robustness of $CD8^+$ T cell responses. Unfortunately, clinical data on these two SARS subjects are not available for this study.

The SARS-CoV N protein is considered to be another highly immunogenic protein in eliciting protective T cell responses during SARS-CoV infections. It has been shown to be capable in eliciting immunodominant T cell responses in SARS-recovered individuals and involved in protection against SARS-CoV infections in animal models [141,142,447]. Here, we characterized another HLA-B*1525-restricted $CD8^+$ T cell response against the N53 region, identified in a SARS convalescent patient in our previous study at 6 years post-infection [142]. We experimentally determined the N53 minimal epitope to be at amino acids 266-275 of the SARS-CoV N protein. Thus far, no other T cell studies involving SARS-CoV have reported the identification of the N53 $CD8^+$ T cell epitope. In addition, in our previous study involving 16 SARS convalescent individuals, only 1 subject presented this particular memory $CD8^+$ T cell response [142]. This suggests the rarity of this response in the T cell repertoire of SARS-infected individuals. As mentioned, the N53-specific T cell response was first identified in SARS

subject 1 at 6 years post-infection in our previous study. However, it was not detected at 9 years post-infection in the same individual using the N53 15-mer peptide for *in vitro* expansion and restimulation (see Table 4.2). Subsequently, the use of a 10-mer peptide corresponding to the N53 minimal epitope region allowed the detection of the response, indicating its presence at 9 years post-SARS-CoV exposure but at a lower magnitude compared to that at 6 years post-infection. This is in agreement with the fact that HLA I molecules ideally recognize and accommodate peptides of 8-11 amino acids during T cell activation. Peptides longer than 11 amino acids are required at higher concentrations compared to shorter peptides to induce the same level of T cell response [448]. As clearly demonstrated in this study, the M29 and N53 15-mer peptides are less efficient in inducing $CD8^+$ T cell responses compared to shorter peptides comprising of the minimal epitope region. In current study, as screening of T cell epitopes was done using 15-mer peptide mixtures, $CD8^+$ T cell responses of low avidity could be missed as a consequence of lower efficiency of T cell activation by 15-mers peptides. Therefore, it is possible that some $CD8^+$ T cell responses present in the SARS subjects were not identified. In the case of $CD4^+$ T cell activation, HLA class II molecules bind to longer peptides, typically ranging from 12-25 amino acids in length [449]. Shorter peptides of 8- to 10-mers in length, though able to elicit effective $CD8^+$ T cell responses, do not stimulate efficient $CD4^+$ T cell responses [450]. As such, the use of 15-mer peptides in our experiments perhaps favors the activation and identification of $CD4^+$ T cell responses as compared to $CD8^+$ responses.

To our knowledge, there are currently no reports on the persistence of memory T cells in SARS-recovered individuals beyond 6 years following infection, therefore, the longevity of SARS-CoV cellular immunity remains a question. Following the detection

of M29- and N53-specific $CD8^+$ T cell responses in SARS subject 1 at 9 years post-infection, we continued to trace the persistence of these SARS-specific memory $CD8^+$ T cell responses in the same individual at 11 years post-infection. Using peptides corresponding to the M29 and N53 minimal epitope for *in vitro* expansion of PBMCs, we showed that SARS-specific memory M29 and N53 $CD8^+$ T cell responses persist in SARS subject 1 up to 11 years post-infection in the absence of the antigen. In addition, the M29-specific response was also detected in another one of our SARS subjects, i.e. subject 3, at 11 year post-infection. This suggests the long-lived nature of SARS-CoV cellular immunity. To rule out the possibility that the T cell responses observed were a result of cross-reactive T cells that arose from infections by other HCoVs, protein alignment of the M and N proteins of HCoV-229E, OC43, NL63, HKU1 and SARS-CoV was carried out to determine the level of amino acid conservation (not shown). It was found that the M29 and N53 minimal regions of these HCoVs share a low level of amino acid conservation with SARS-CoV, indicating the unlikelihood that the M29 and N53 T cell responses identified in current study were a result of cross-reactive T cells specific for other HCoVs. Due to the absence of SARS-CoV infections in humans, it is unclear if the persistence of T cell responses could contribute to the protection of SARS-CoV re-infection. Nonetheless, understanding memory SARS-specific T cell persistence has important implications in the design of SARS vaccines, which should target to induce dominant, potent and long-lived memory protective cellular responses. Although a direct cytotoxic effect of the M29- and N53-specific memory $CD8^+$ T cells was not demonstrated, the production of IFNγ by the $CD8^+$ T cells upon specific peptide stimulation indicated activation of T cell effector functions. IFNγ, an inflammatory cytokine, besides being able to directly inhibit viral replication, has multiple important

immunomodulatory functions leading to killing of infected cells, such as the upregulation of HLA I molecules expression on target cells to enhance $CD8^+$ T cell-mediated killing, activation of macrophages for phagocytosis of target cells, as well as enhancement of production of other cytokines and anti-microbial chemicals such as hydrogen peroxide and superoxide radicals [451]. Additionally, the observed increase in CD107a expression by the $CD8^+$ T cells upon specific peptide stimulation indicated T cell degranulation and target cell killing function. Degranulation of $CD8^+$ T cells, a requisite for cytotoxic T cell-mediated killing via the perforin-granzyme pathway, is associated with cell surface accumulation of the granule membrane protein, CD107a [452]. The measurement of surface expression of CD107a of responding antigen-specific $CD8^+$ T cells therefore provides assessment of T cell-mediated target cell killing [440]. Future experiments involving the use of M29- and N53-specific $CD8^+$ T cells in *in vitro* target cell killing assays as well as in SARS animal models would allow for the more direct demonstration of cytotoxic and protective effects. Furthermore, the detection of M29- and N53-specific $CD8^+$ T cell responses in a larger number of SARS-recovered individuals would allow a stronger correlation of these responses to SARS recovery.

Most SARS $CD8^+$ T cell epitopes reported in the literature do not have their HLA class I restrictions defined. Those with defined HLA class I restrictions were focused on the human HLA-A*0201 allele, which is expressed in approximately 4-21% of individuals in South Asia [453]. All HLA-A*0201-restricted SARS $CD8^+$ T cell responses reported so far are specific against the S and N proteins, suggesting the critical roles of both proteins in $CD8^+$ T cell immunity in recovery from SARS-CoV infections in HLA-A*0201 individuals [141,192]. Here, we identified two $CD8^+$ T cell responses specific against the SARS-CoV M and N proteins that are both restricted by HLA-B

subtype. In our previous study on 16 SARS convalescent patients, all identified $CD8^+$ T cell responses specific against the N and 3a proteins were also restricted by the HLA-B subtype (data not shown), suggesting the possible protective effects of HLA-B in SARS-CoV infections and its association with SARS recovery. HLA-B has been found to be associated with numerous acute and chronic viral infections, including Influenza virus, HCV, herpes simplex virus and HIV [454,455,456,457]. With regards to SARS-CoV infection, HLA-B subtypes HLA-B*4601 and HLA-B*0703 are reported to have an association with the development of SARS [458,459]. Therefore, HLA-B subtype could have important roles in the protection as well as immunopathogenesis in SARS-CoV infections, which are yet to be fully understood. The small number of individuals (n=3) enrolled in current study is a limitation which significantly decreased the strength of conclusions drawn. To better determine whether HLA-B subtypes indeed have protective role in SARS-CoV infection, larger cohort study involving more SARS-recovered volunteers is needed to assess the correlations of HLA-B subtypes with SARS infection and recovery.

Heterologous immunity involving cross-reactive $CD8^+$ T cells has been well-documented. Heterologous immunity is defined as the immunity that can be developed to a pathogen after the host has been exposed to a non-identical pathogen [460]. This is due to the fact that T cell recognition is degenerate − they are able to bind to a specific range of peptides based on certain amino acid specificities, allowing T cells to cross-react with peptides from heterologous pathogens [461]. During T cell activation, the engagement of the T cell receptor (TCR) with the peptide-MHC (pMHC) complex usually requires direct contact with no more than three amino acids found on the peptide, hence allowing amino acid substitutions on the peptide without affecting interaction between TCR and pMHC

complex [462]. Cross-reactivity of $CD8^+$ T cells between closely related viruses have been identified, including that between different dengue virus serotypes [463]. Cross-reactive $CD8^+$ T cells also exist between heterologous viruses, such as HCV and Influenza virus, HCV and HIV, as well as human papillomavirus and HCoV-OC43 [464,465,466]. It is thought that heterologous immunity has important implications in the cross-protection against different viruses as well as alterations in pathogenesis of viral infections. In current study, we demonstrated the absence of cross-reactivity of SARS-specific M29 and N53 $CD8^+$ T cells against MERS-CoV M29 and N53 peptides. The M and N proteins between the two viruses are partially conserved at 42% and 48.5% sequence similarity respectively. Specifically, the M29 and N53 minimal epitopes are 55.6% (5 out of 9 residues) and 60% (6 out of 10 residues) conserved between SARS-CoV and MERS-CoV (See Figure 4.7A and B) respectively. Our results indicate that the substitutions of 4 amino acids in the SARS-CoV M29 and N53 regions abolished the $CD8^+$ T cell responses. This could be due to the disruption of the recognition of the peptide by the HLA molecule, or the failure in engagement of the TCR with the HLA molecule in complex with the peptides. In conclusion, SARS-specific T cell immunity is highly specific and SARS-specific M29 and N53 $CD8^+$ T cell responses are likely to be unable to provide cross-protection against MERS-CoV infections. Nonetheless, as also shown in Figures 4.7A and B, sequence alignments of the M29 and N53 minimal epitope regions revealed that they are fully conserved in human SARS-CoV and zoonotic strains including the civet SARS-CoV SZ3, bat SL-CoVs Rp3 and Rf1 and the recently discovered bat SARS-CoV Rs3367 which is capable of utilizing both the human and bat ACE2 receptors for cell entry [467]. Therefore, it is very likely that the SARS-specific

M29 and N53 $CD8^+$ T cells will be able to confer cross-protection against infections of these zoonotic SARS-CoV and SL-CoV strains.

To conclude, the dominance and long-lived nature of memory T cell responses against the SARS-CoV structural proteins (S, M and N proteins) are demonstrated. The in-depth characterization of $CD8^+$ memory T cell responses against the M and N proteins allows the future development of these two proteins as potential SARS vaccine candidates. Defining critical immunodominant viral-specific T cell epitopes and HLA restrictions have been important in the development of peptide-based vaccines that are recognized by all HLA haplotypes widely present in human population to effectively induce T cell responses required to prevent infections [468]. Given that SARS-CoV originates from a heterogeneous pool of viruses from zoonotic sources [3], efforts in identifying highly invariant T cell epitopes that exist in different SARS-CoV and SL-CoV strains can facilitate the development of universal, broadly protective epitope-based vaccines to induce cross-protection against multiple viral variants. In addition, such studies pave ways for the advancement of adoptive T cell immunotherapy, involving the re-targeting of T cells through expression of TCR genes in autologous naïve T cells to re-direct their antigen specificity [469]. The feasibility of this has been demonstrated for SARS-CoV and HBV [142,470]. More recently, the engineering of T cells based on the expression of a synthetic receptor, known as the chimeric antigen receptor (CAR), has shown promising clinical results in adoptive immunotherapy for the treatment of cancer [471]. Because CAR is derived from the single chain variable fragment (scFv) of an antigen-specific mAb, the CAR-expressing T cells are able to bind antigen directly and function independently of HLA. Several studies have demonstrated that CAR-engineered T cells redirected against viral proteins, such as the HCV E2 glycoprotein, the influenza

M2 protein and the HBV envelope protein, are capable in controlling viral infection *in vitro* and *in vivo* [472,473,474]. This highlights the potential use of engineered T cell adoptive immunotherapy to achieve effective therapeutic results against viral infections.

CHAPTER 5: EFFECTS OF MERS CORONAVIRUS NUCLEOCAPSID PROTEIN ON CELLULAR FUNCTIONS IN COMPARISON TO SARS CORONAVIRUS

In Chapter 3 and 4 of this thesis, we examined the interaction of SARS-CoV viral proteins with the host immune system, in terms of the antibody and T cell immune responses. Such immune response lead to the elimination of viruses from the host system, but the virus can evolve through mutations to escape from such detrimental viral-host interactions. In addition, viruses also interact with various host factors for its own benefits to modulate host responses for enhancing its own replication and survival, and this has been shown for numerous viruses, including coronaviruses [475,476,477,478,479]. In this aspect, much research has been done on the SARS-CoV N protein, which has been shown to interact with multiple host factors [480,481], but thus far, little is known about how the MERS-CoV N protein interacts with the host cell machinery. In this chapter, we focus on determining if MERS-CoV N protein shares similar properties as the SARS-CoV N protein. The SARS-CoV N protein has been previously shown to interact with the host factor, eukaryotic elongation factor 1 alpha (eEF1A) and inhibit cell protein translation, cell cytokinesis and proliferation [137]. Here, three main aspects were investigated for MERS-CoV N protein in comparison to SARS-CoV N: (i) ability to interact with eEF1A; (ii) effects on cellular protein translation and (iii) cellular F-actin arrangement.

5.1 Interaction of N protein of MERS-CoV with eEF1A

Interaction between SARS-N and eEF1A was demonstrated by co-immunoprecipitation (co-IP) through the over-expression of proteins in 293T cells in a previous publication by Zhou and colleagues [137]. In current study, we chose to study

MERS-CoV/SARS-CoV N protein and eEF1A interaction using the Vero E6 cell line since it is a cell line that supports both SARS-CoV and MERS-CoV replication [324,482]. To check if the interaction of SARS-CoV N protein and eEF1A could be reproduced in our experimental setup using Vero E6 cells, the cells were transfected to co-express FLAG-tagged full length SARS-CoV N protein (FLAG-SARS-N) and myc-tagged eEF1A (myc-eEF1A). Myc-tagged dihydrofolate reductase (myc-DHFR) was used as negative control to rule out any non-specific binding. The transfected cells were harvested and probed with anti-myc or anti-FLAG antibodies in Western blot analysis to determine expression of each protein before being subjected to co-IP. As seen in Figure 5.1A, the proteins were successfully expressed in Vero E6 cells. It was noted that an additional protein band was detected for SARS-N protein (Figure 5.1A[i]), suggesting the occurrence of a cleavage of the protein. However, this cleavage of SARS-N was not observed in 293 FT cells (see Figure 5.3A[i]), suggesting that this phenomenon is cell line-specific.

As shown in Figure 5.1B(iv), in co-IP using anti-myc antibody and protein A beads, FLAG-SARS-N was co-immunoprecipitated by myc-eEF1A and detected in Western blot. Similarly, as shown in Figure 5.1B(v), when FLAG beads, which contain anti-FLAG antibody, were used for co-IP, myc-eEF1A protein was pulled down by FLAG-SARS-N protein as detected in Western blot. This confirmed that SARS-N protein interacts with eEF1A.

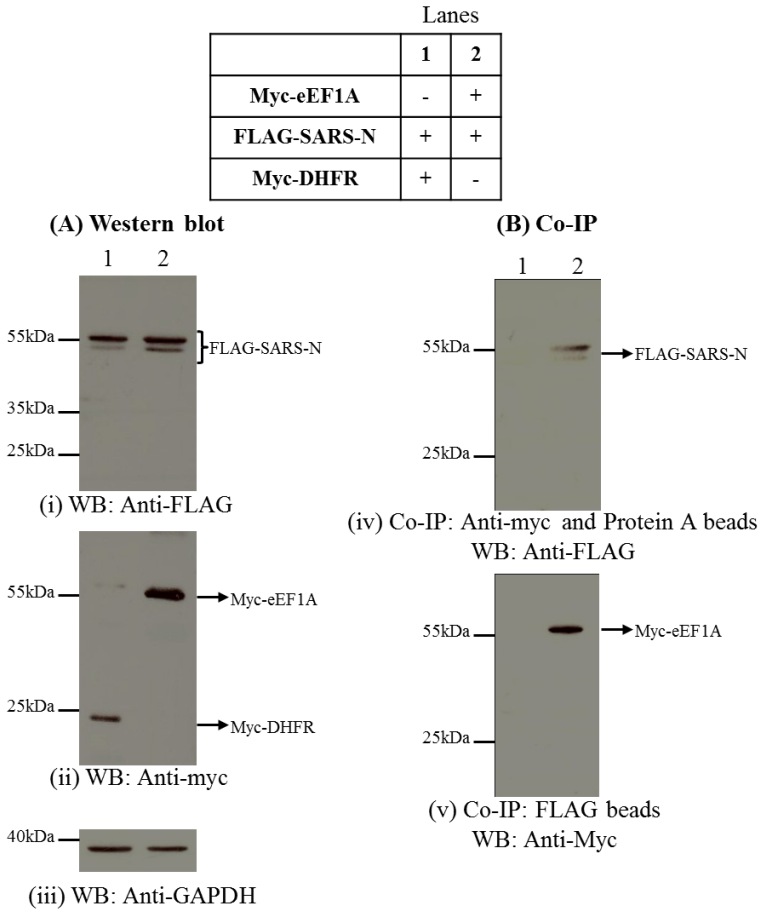

Figure 5.1. Association of SARS-CoV N with over-expressed eEF1A in Vero E6 cells. (A) Western blot analysis to determine the expressions of myc-eEF1A, myc-DHFR and FLAG-SARS-N proteins in transfected Vero E6 cell using [i] anti-FLAG and [ii] anti-myc antibodies. [iii] Anti-GAPDH antibody was used to detect GAPDH as the loading control to ensure equal loading of proteins. (B) Transfected Vero E6 cell lysates were subjected to co-IP using [iv] anti-myc antibody in the presence of protein A beads followed by detection of co-immunoprecipitated proteins using anti-FLAG antibody in Western blot (WB), or [v] FLAG beads followed by detection of co-immunoprecipitated proteins using anti-myc antibody in WB.

To investigate whether MERS-CoV N protein also interacts with eEF1A, Vero E6 cells were co-transfected with plasmids expressing FLAG-tagged full-length MERS-CoV N (FLAG-MERS-N), FLAG-tagged N-terminal residues 1-195 of MERS-CoV N

(FLAG-MERS-N-1-195), FLAG-tagged C-terminal residues 196-414 of MERS-CoV N (FLAG-MERS-N-196-414) and myc-eEF1A. Similarly, FLAG-DHFR and myc-DHFR were expressed as negative controls. Successful expressions of the proteins were checked by Western blot analysis as shown in Figure 5.2(A). Similar to that observed with SARS-N, an additional protein band was observed with the full-length FLAG-MERS-N protein (Figure 5.2B[i]), indicating the cleavage of MERS-N protein. Protein cleavage was also observed with C-terminal FLAG-MERS-N-196-414 but not the N-terminal FLAG-MERS-N-1-195, suggesting that the site of cleavage is present in the C-terminal end. Consistent with the SARS-N protein, the cleavage of MERS-N was not observed in 293 FT cells (see Figure 5.3A[i]).

In co-IP using anti-myc antibody and protein A beads, FLAG-MERS-N was co-immunoprecipitated by myc-eEF1A (Figure 5.1B[iv, lane 3]). Similarly, myc-eEF1A co-immunoprecipitated with FLAG-MERS-N protein in co-IP using FLAG beads (Figure 5.1B[v, lane 3]). These results gave evidence for the interaction of the full length MERS-N and eEF1A proteins, in consistent with that observed for full length SARS-N and eEF1A. As seen in Figure 5.1B(iv, lanes 4 and 5), co-immunoprecipitation of the C-terminal FLAG-MERS-N-196-414 protein with myc-eEF1A was observed but not for the N-terminal FLAG-MERS-N-1-195. Similarly, co-immunoprecipitation of myc-eEF1A was also achieved only with FLAG-MERS-N-196-414 but not with FLAG-MERS-N-1-195 (Figure 5.1B[v, lanes 4 and 5]). These results further suggested that the C-terminal of the MERS-N protein, but not the N-terminal region, is responsible for the interaction with eEF1A. No protein pull-down was observed with negative controls myc-tagged and FLAG-tagged DHFR proteins (Figure 5.1B, lanes 1 and 2).

Lanes

	1	2	3	4	5
Myc-eEF1A	-	+	+	+	+
FLAG-MERS-N	+	-	+	-	-
FLAG-MERS-N-1-195	-	-	-	+	-
FLAG-MERS-N-196-414	-	-	-	-	+
Myc-DHFR	+	-	-	-	-
FLAG-DHFR	-	+	-	-	-

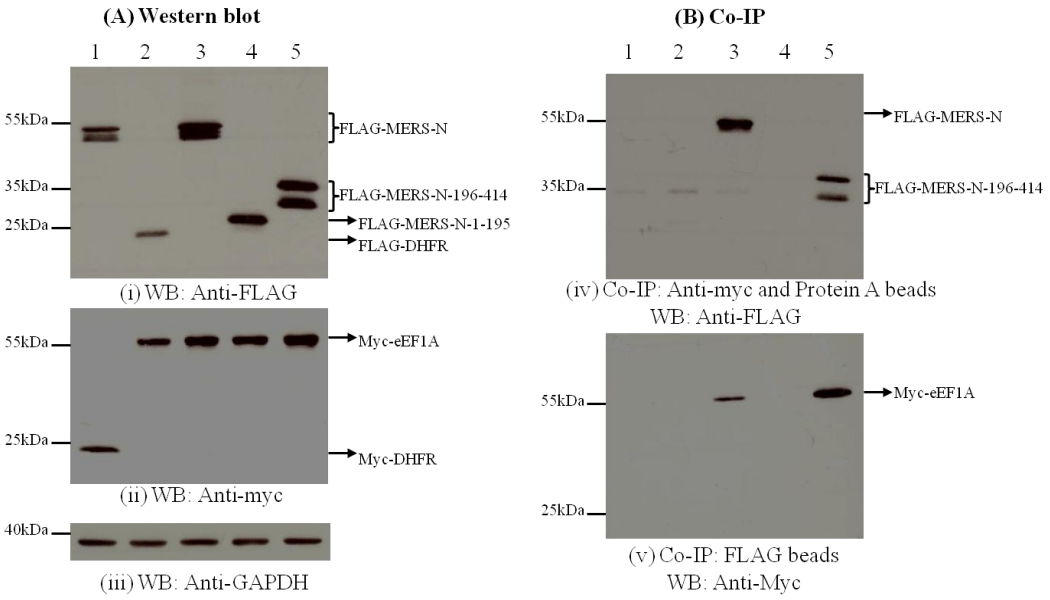

Figure 5.2. Association of MERS-CoV N with over-expressed eEF1A in Vero E6 cells. (A) Western blot analysis was done to determine the expressions of myc-eEF1A, FLAG-MERS-N, FLAG-MERS-N-1-195, FLAG-MERS-N-196-414 proteins as well as myc-DHFR and FLAG-DHFR proteins in transfected Vero E6 cells using [i] anti-FLAG and [ii] anti-myc antibodies. [iii] Anti-GAPDH antibody was used to detect GAPDH as the loading control to ensure equal loading of proteins. (B) The transfected Vero E6 cell lysates were then subjected to co-IP using [iv] anti-myc antibody in the presence of protein A beads followed by detection of co-immunoprecipitated proteins using anti-FLAG antibody in WB, or [v] FLAG beads followed by detection of co-immunoprecipitated proteins using anti-myc antibody in WB.

Since the interaction of SARS-N/MERS-N and eEF1A as demonstrated above was based on the over-expression of eEF1A in Vero E6 cells, we further determined the interaction of MERS-N protein with endogenous eEF1A in a human cell line. MERS-CoV infection is capable of causing acute renal failure, and the virus has been shown to

lytically infect human embryonic kidney (HEK) cell line and a human kidney cell line, 769P [324,325]. Using the HEK 293 FT cells, transfection of plasmids expressing FLAG-tagged full-length MERS-N, N-terminal MERS-N-1-195, C-terminal MERS-N-196-414 as well as full-length SARS-N was carried out. In Western blot analysis, single protein band were detected for FLAG-SARS-N, FLAG-MERS-N and FLAG-MERS-N-196-414 proteins (Figure 5.3A[i]), unlike in Vero E6 cells where double bands were observed. This suggested the absence of N protein cleavage in 293 FT cells.

For co-IP experiment, anti-eEF1A antibody was used for the immunoprecipitation of endogenous eEF1A proteins and anti-FLAG antibody was used to detect co-immunoprecipitated FLAG-tagged N proteins in Western blot analysis. As shown in Figure 5.3, interactions between eEF1A and full-length MERS-N, C-terminal MERS-N-196-414 and full-length SARS-N were observed, consistent with the results obtained in the over-expression of eEF1A in Vero E6 cells (Figures 5.1 and 5.2). This further confirmed that, similar to SARS-N, MERS-N protein interacts with eEF1A and that the C-terminal 196-414 amino acid residues of MERS-N, but not the N-terminal, is required for the interaction.

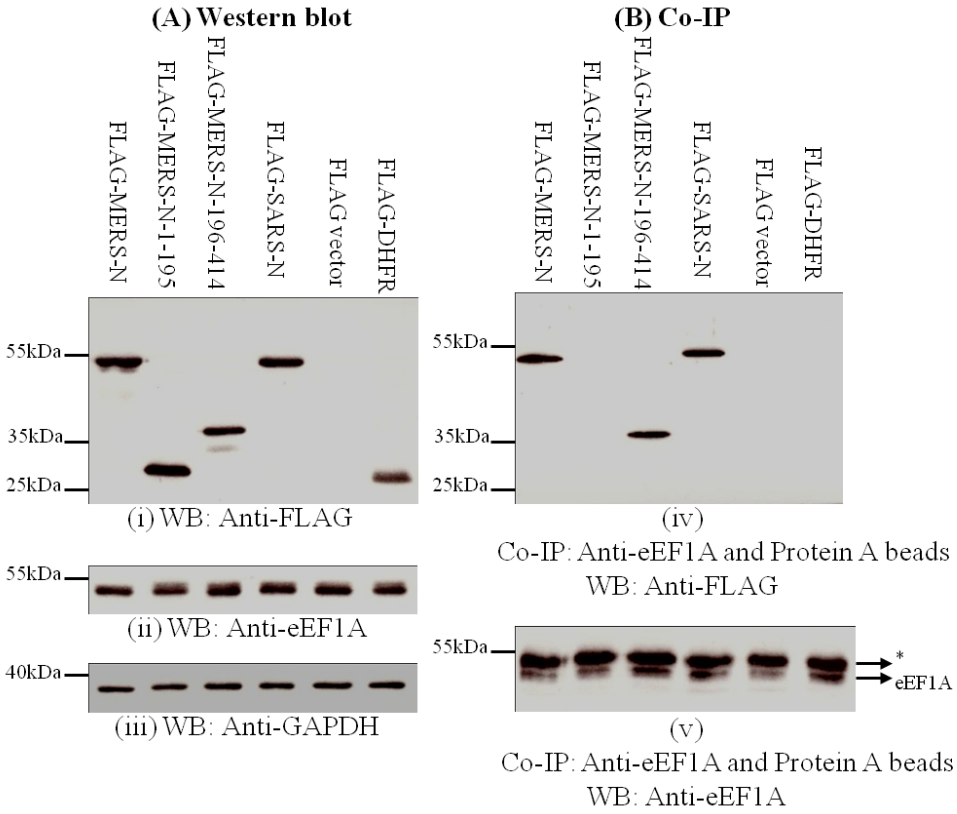

Figure 5.3. Association of MERS-CoV N with endogenous eEF1A in 293 FT cells. (A) Western blot analysis was done to determine the expressions of FLAG-MERS-N, FLAG-MERS-N-1-195, FLAG-MERS-N-196-414, FLAG-SARS-N and FLAG-DHFR proteins in transfected 293FT cells using [i] anti-FLAG antibody, [ii] anti-eEF1A and [iii] anti-GAPDH antibody, which was used to detect GAPDH as the loading control. (B) Transfected 293 FT cell lysates were then subjected to co-IP using anti-eEF1A antibody in the presence of protein A beads followed by detection of co-immunoprecipitated proteins using (iv) anti-FLAG antibody or (v) anti-eEF1A antibody in WB. * indicates the heavy chain of the anti-eEF1A antibody used in co-IP that was detected in WB.

5.2 Further mapping of region in MERS-CoV N protein required for interaction with eEF1A

To further delineate the region within the C-terminal MERS-N protein (residues 196-414) necessary for the interaction with eEF1A, 4 truncated mutants of the C-terminal MERS-N protein were designed, cloned into the FLAG-vector and expressed in Vero E6

cells with myc-eEF1A. They consist of amino acid residues 196-349, 196-312, 196-250 and 196-285 of the MERS-CoV N protein. A schematic diagram of the truncated MERS-N proteins is provided in Figure 5.4A. Although the different truncated MERS-N proteins were expressed at different levels in Vero E6 cells as revealed by Western blot analysis (Figure 5.4B[i]), it was observed that truncated MERS-N proteins containing residues 196-349, 196-312 and 196-285 were able to associate with eEF1A in co-IP experiment, while MERS-N protein containing residues 196-250 was unable to (Figure 5.4B[iv]). Taking these results together, it can be drawn that residues 251-285 located within the C-terminal MERS-CoV N protein is required for the interaction with eEF1A (Figure 5.4A).

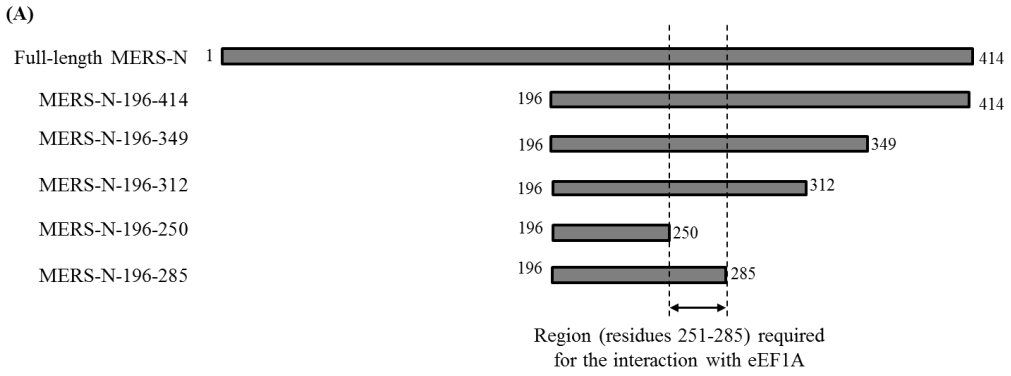

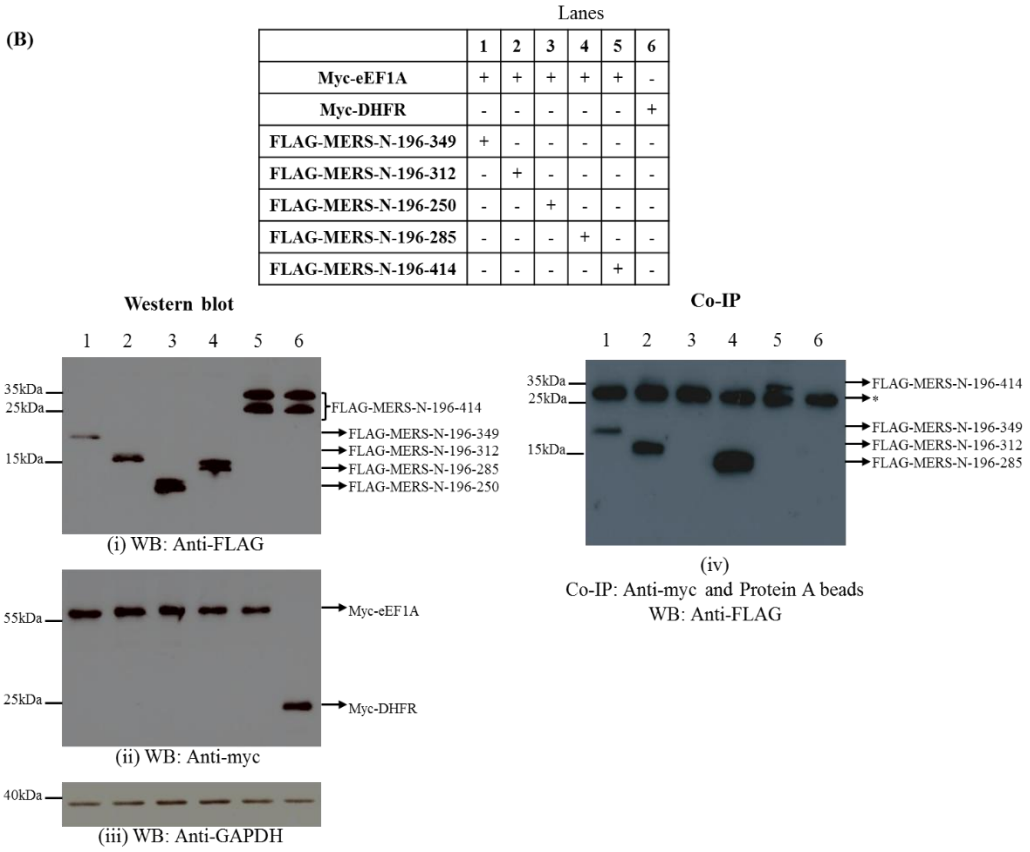

Figure 5.4. Mapping of MERS-N and eEF1A binding site. (A) Schematic diagram of the full length MERS-N and truncated MERS-N proteins consisting of residues 196-414, 196-349, 196-312, 196-285 and 196-250. (B) Association of truncated MERS-N proteins with eEF1A in Vero E6 cells. Western blot analysis was carried out to determine the expressions of myc-eEF1A, myc-DHFR, FLAG-MERS-N and FLAG-tagged truncated MERS-N proteins in transfected Vero E6 cell using [i] anti-FLAG, [ii] anti-myc and [ii] anti-GAPDH antibody, which was used to detect GAPDH as loading control. Transfected Vero E6 cell lysates were then subjected to co-IP using [iv] anti-myc antibody in the presence of protein A beads followed by detection of co-immunoprecipitated proteins using anti-FLAG antibody in WB. * indicates the light chain of the anti-myc antibody used in co-IP that was detected in WB.

5.3 Co-localization of MERS-CoV N protein and eEF1A in cells

We next investigated the subcellular co-localization of MERS-CoV and SARS-CoV N proteins with endogenous eEF1A protein in human cells by immunofluoresence assay (IFA). 293 FT cells were transiently transfected with the empty FLAG-vector and

plasmids expressing FLAG-tagged MERS-N and SARS-N for 24 hours, after which the cells were fixed, permeabilized and stained with anti-FLAG and anti-eEF1A primary antibodies followed by Alexa Fluor® 488- and Alexa Fluor® 568-conjugated secondary antibodies. The cells were then analyzed using confocal microscopy. As shown in Figure 5.5, eEF1A, MERS-N and SARS-N proteins localized in the cytoplasm of the cells (column 2 and 3). Based on the overlay images, it was observed that MERS-N co-localized with eEF1A in the cytoplasm of the cells, similar to that observed with SARS-N (Figure 5.5B and C, column 4).

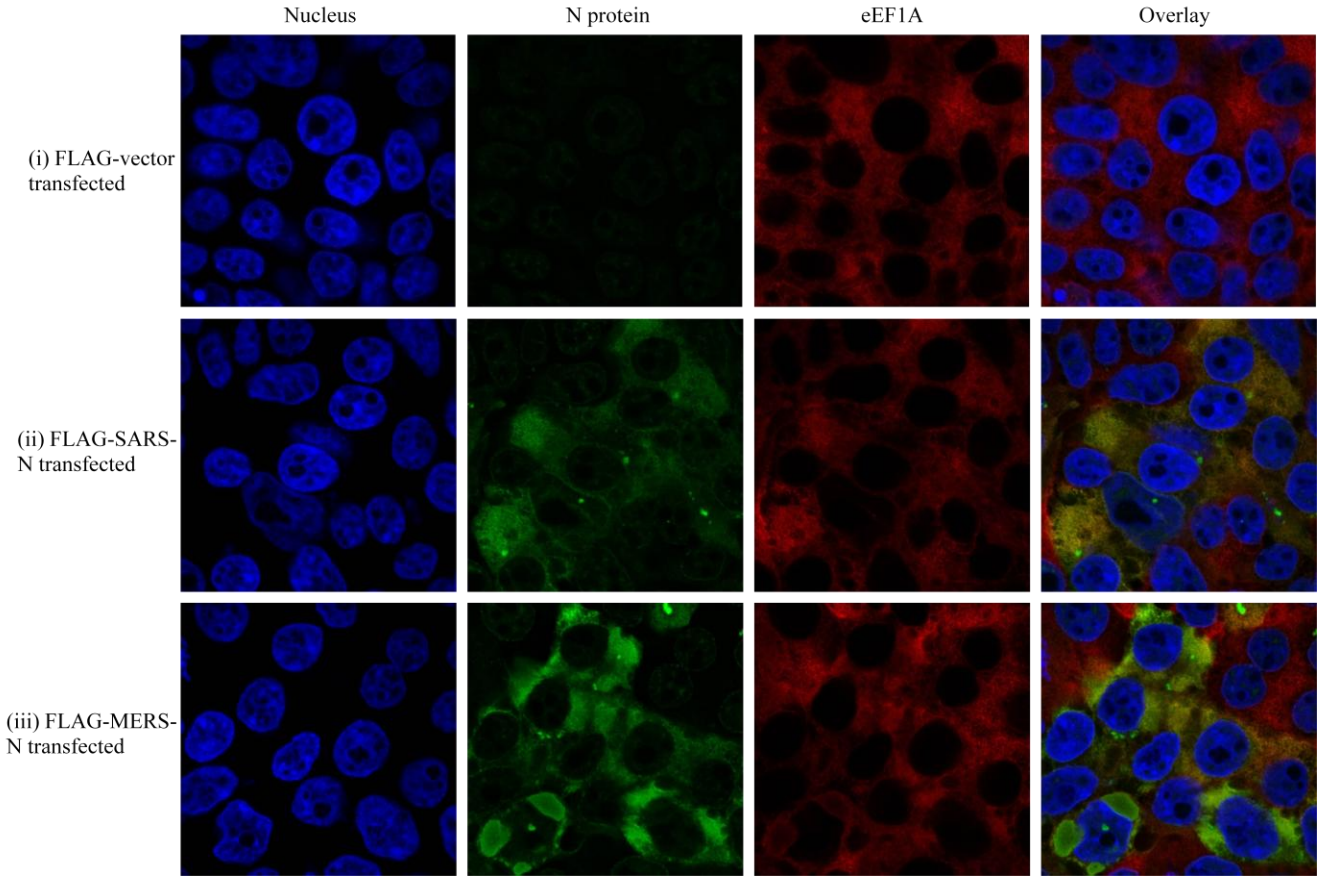

Figure 5.5. Co-localization of MERS-CoV and SARS-CoV N protein with eEF1A in 293 FT cells. 293 FT cells were transiently transfected with (i) FLAG-vector, (ii) FLAG-SARS-N or (iii) FLAG-MERS-N plasmids for 24 hours after which the cells were fixed and permeabilized. FLAG-SARS-N and FLAG-MERS-N proteins were stained using anti-FLAG primary antibody followed by Alexa Fluor® 488-conjugated secondary antibody (green) and endogenous eEF1A was stained using anti-eEF1A antibody followed by Alexa Fluor® 568-conjugated secondary antibody (red). Nucleus was stained using DAPI (blue). Cells were then mounted onto microscopy glass slides and visualized by confocal microscopy at 100x magnification with 2x zoom.

5.4 Effects of MERS-CoV N protein on cellular protein translation

The SARS-CoV N protein has been demonstrated to have an inhibitory effect on protein translation [137]. Therefore, we investigated if the N protein of MERS-CoV also exhibit similar function in suppressing protein translation. To do so, RNA coding for the luciferase gene was first synthesized from luciferase DNA by *in vitro* transcription. The resultant luciferase-coding RNA was used for *in vitro* translation in the presence of purified bacterially-expressed GST and GST-tagged N proteins. Any effect on protein translation by N proteins is reflected from the level of luciferase activity as compared to the negative control, GST protein. A Coomassie Blue-stained SDS-PAGE gel of the purified GST, full-length GST-tagged SARS-N (GST-SARS-N), full-length MERS-N (GST-MERS-N), truncated MERS-N proteins including N-terminal MERS-N (GST-MERS-N-1-195), C-terminal MERS-N (GST-MERS-N-196-414), full-length and C-terminal MERS-N with eEF1A binding region at residues 251-285 deleted (GST-MERS-N-Δ251-285, GST-MERS-N-196-414-Δ251-285) is provided in Figure 5.6A.

As shown in Figure 5.6B, both GST-MERS-N and GST-SARS-N inhibited translation of luciferase-coding RNA in a dose-dependent manner and at significantly lower levels ($p<0.01$) at all four concentrations (0.25, 0.5, 1.0 and 1.5 μM) tested compared to the GST protein. A 50% inhibition of protein translation was observed for GST-MERS-N protein at a concentration of approximately 0.25-0.5 μM, while that for GST-SARS-N protein was higher at approximately 0.5-1.0 μM. At the highest concentration of 1.5 μM tested, an inhibitory effect on translation of approximately 98% was achieved for both GST-SARS-N and GST-MERS-N. These results suggest that similar to SARS-N, MERS-N is capable of inhibiting protein translation. However, at the

same concentrations of 0.25, 0.5 and 1.0 μM, GST-MERS-N exhibited greater inhibitory effects on protein synthesis compared to SARS-N.

As eEF1A is an important component in the mammalian cell translation apparatus, we checked if the inhibition on translation of MERS-N was due to the interaction with eEF1A. To do so, the effects on translation suppression for purified GST-tagged N-terminal MERS-N (GST-MERS-N-1-195), C-terminal MERS-N (GST-MERS-N-196-414), full length and C-terminal MERS-N proteins with the eEF1A binding site removed (GST-MERS-N-Δ251-285 and GST-MERS-N-196-414-Δ251-285) were determined. All proteins were used at 1.5 μM. As shown in Figure 5.6C, both N-terminal GST-MERS-N-1-195 and C-terminal GST-MERS-N-196-414 proteins significantly inhibited translation compared to GST protein (p<0.01). It was noted that the level of inhibition of translation observed for N-terminal GST-MERS-N-1-195 was greater than that of full-length GST-MERS-N and C-terminal GST-MERS-N-196-414. Since the N-terminal residues 1-195 of MERS-N is not involved in eEF1A interaction, the ability of this region to inhibit protein translation suggests other eEF1A-independent mechanisms for its activity. Nonetheless, full length GST-MERS-N-Δ251-285 displayed less significant effects on translation inhibition when compared to full-length GST-MERS-N (p<0.01) (Figure 5.6C). Furthermore, protein translation in the presence of GST-MERS-N-196-414-Δ251-285 was significantly higher in comparison to the C-terminal GST-MERS-N-196-414 (p<0.01) (Figure 5.6C). This indicated that the binding to eEF1A contributes to MERS-N-mediated inhibition of cellular protein translation.

(A)

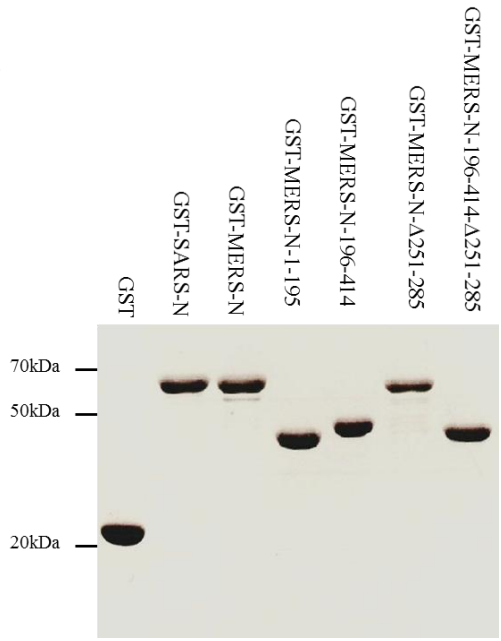
GST
GST-SARS-N
GST-MERS-N
GST-MERS-N-1-195
GST-MERS-N-196-414
GST-MERS-N-Δ251-285
GST-MERS-N-196-414-Δ251-285
70kDa
50kDa
20kDa

(B)

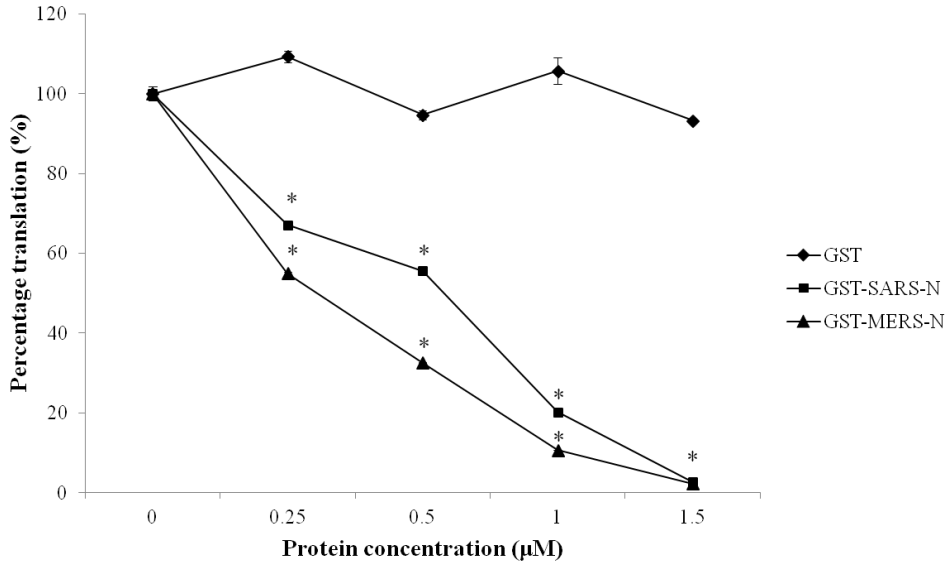
Percentage translation (%)
120
100
80
60
40
20
0
0
0.25
0.5
1
1.5
Protein concentration (μM)
GST
GST-SARS-N
GST-MERS-N

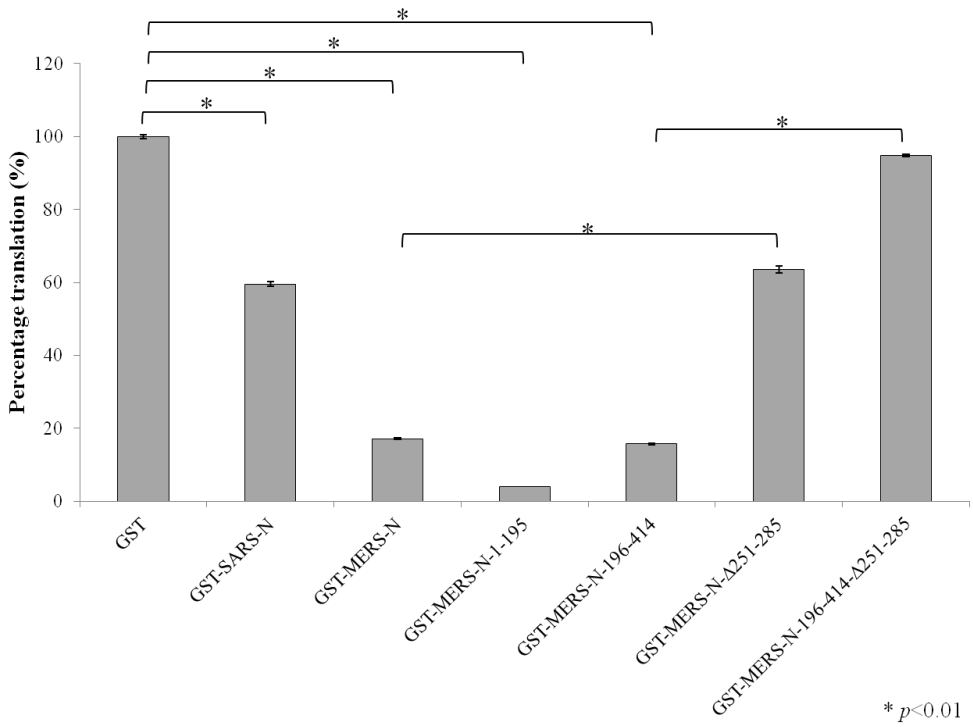

Figure 5.6. Effects of GST-tagged SARS-N, MERS-N and truncated MERS-N proteins on *in vitro* translation. (A) SDS-PAGE of purified bacterially-expressed GST and GST-fusion proteins, including GST-SARS-N, GST-tagged full length and truncated MERS-N proteins stained using Coomassie Blue. (B) GST, GST-SARS-N and GST-MERS-N proteins were added at the indicated concentrations into rabbit reticulocyte lysate reaction mixture containing 1µg of luciferase-coding RNA, followed by the measurement of luciferase activity based on relative light units (RLU). Percentage translation was calculated using 100% translation set at RLU determined in the absence of proteins. (C) GST, GST-SARS-N, GST-MERS-N, and truncated GST-MERS-N proteins were used at 1.5 µM and incubated with rabbit reticulocyte lysate reaction mixture containing 1µg of luciferase-coding RNA, followed by the measurement of luciferase activity. Percentage translation was calculated based on 100% translation set at RLU determined in the presence of negative control, GST protein. Bars represent SD of the experiment carried out in triplicates. * indicates statistically significant difference (p<0.01).

5.5 Effects of MERS-CoV N protein on F-actin bundling and activity

It has been previously shown that SARS-N, through its interaction with eEF1A, an actin-binding protein, inhibits filamentous actin (F-actin) bundling and cytokinesis of

cells [137]. To assess whether MERS-N also affects F-actin bundling and arrangement, phalloidin, which selectively binds F-actin, was used to visualize F-actin distribution in the presence of MERS-N protein by IFA. Both 293 FT and HeLa cells were transfected with expression vector and plasmids expressing FLAG-tagged MERS-N and FLAG-tagged SARS-N proteins. As shown in Figure 5.7A and B, fewer F-actin bundles were observed in transfected 293 FT cells and HeLa cells in the presence of both full length FLAG-SARS-N and FLAG-MERS-N (Figure 5.7A[ii, iii] and B[ii, iii]) compared to vector-transfected cells that did not express N protein (Figure 5.7A[i] and B[i]). Furthermore, the presence of SARS-N and MERS-N appeared to cause the re-organization of F-actin to concentrate at the outer membrane of the cells, instead of being distributed throughout the cytoplasmic region as observed in vector-transfected cells. Reduction in cell sizes was also observed, which was more obvious in HeLa cells compared to 293 FT cells. These results showed that MERS-N protein behaves similarly to the SARS-N protein in inhibiting F-actin bundling and inducing F-actin re-arrangement.

EEF1A is a F-actin-binding protein and regulates cell cytoskeleton activity. To check if the interaction with eEF1A is responsible for this phenomenon of F-actin re-arrangement induced by MERS-N, F-actin arrangement and cell morphology of transfected HeLa cells expressing FLAG-MERS-N-1-195, FLAG-MERS-N-196-414, FLAG-MERS-N-Δ251-285 and FLAG-MERS-N-196-414-Δ251-285 were compared. HeLa cells, but not 293 FT cells, were used for the studies of these truncated MERS-N proteins as the morphology of HeLa cells is more ideal for microscopy analysis. As shown in Figure 5.7B (iv) and (v), fewer F-actin bundles and reduced cell size was observed in cells expressing the C-terminal FLAG-MERS-N-196-414, but not in cells

expressing the N-terminal FLAG-MERS-N-1-195, which is not involved in eEF1A interaction. Moreover, cells expressing full-length and C-terminal MERS-N proteins with the eEF1A binding site removed (FLAG-MERS-N-Δ251-285 and FLAG-MERS-N-196-414-Δ251-285) showed less obvious effects on F-actin re-arrangement and decrease in cell size compared to full length MERS-N and C-terminal MERS-N (Figure 5.7B [vi] and [vii]). These results suggest that the interaction of MERS-N and eEF1A resulted in the reduction of F-actin bundle formation and the re-arrangement of F-actin.

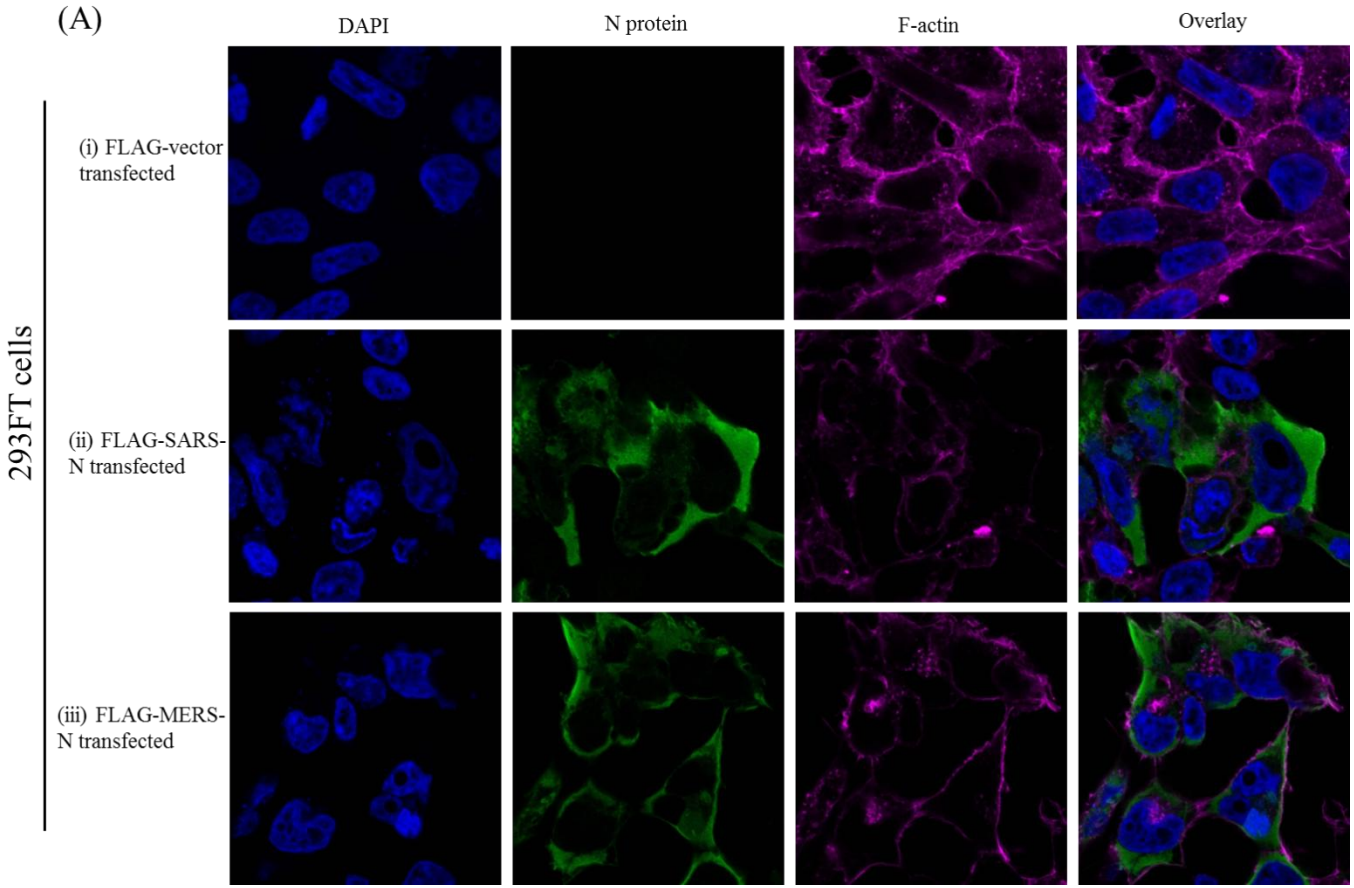
(A)
DAPI
N protein
F-actin
Overlay
293FT cells
(i) FLAG-vector transfected
(ii) FLAG-SARS-N transfected
(iii) FLAG-MERS-N transfected

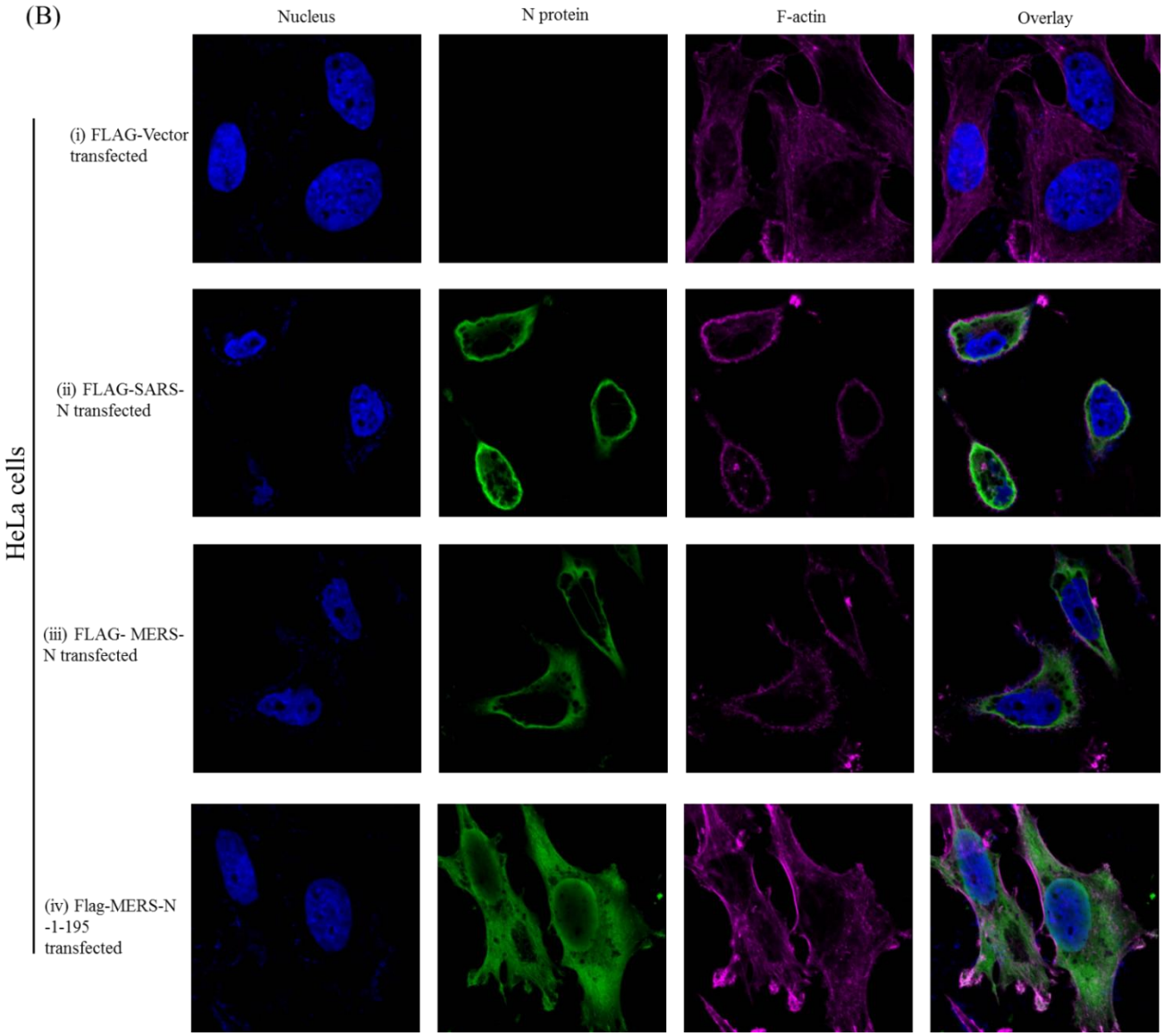
(B)
Nucleus
N protein
F-actin
Overlay
HeLa cells
(i) FLAG-Vector transfected
(ii) FLAG-SARS-N transfected
(iii) FLAG- MERS-N transfected
(iv) Flag-MERS-N -1-195 transfected

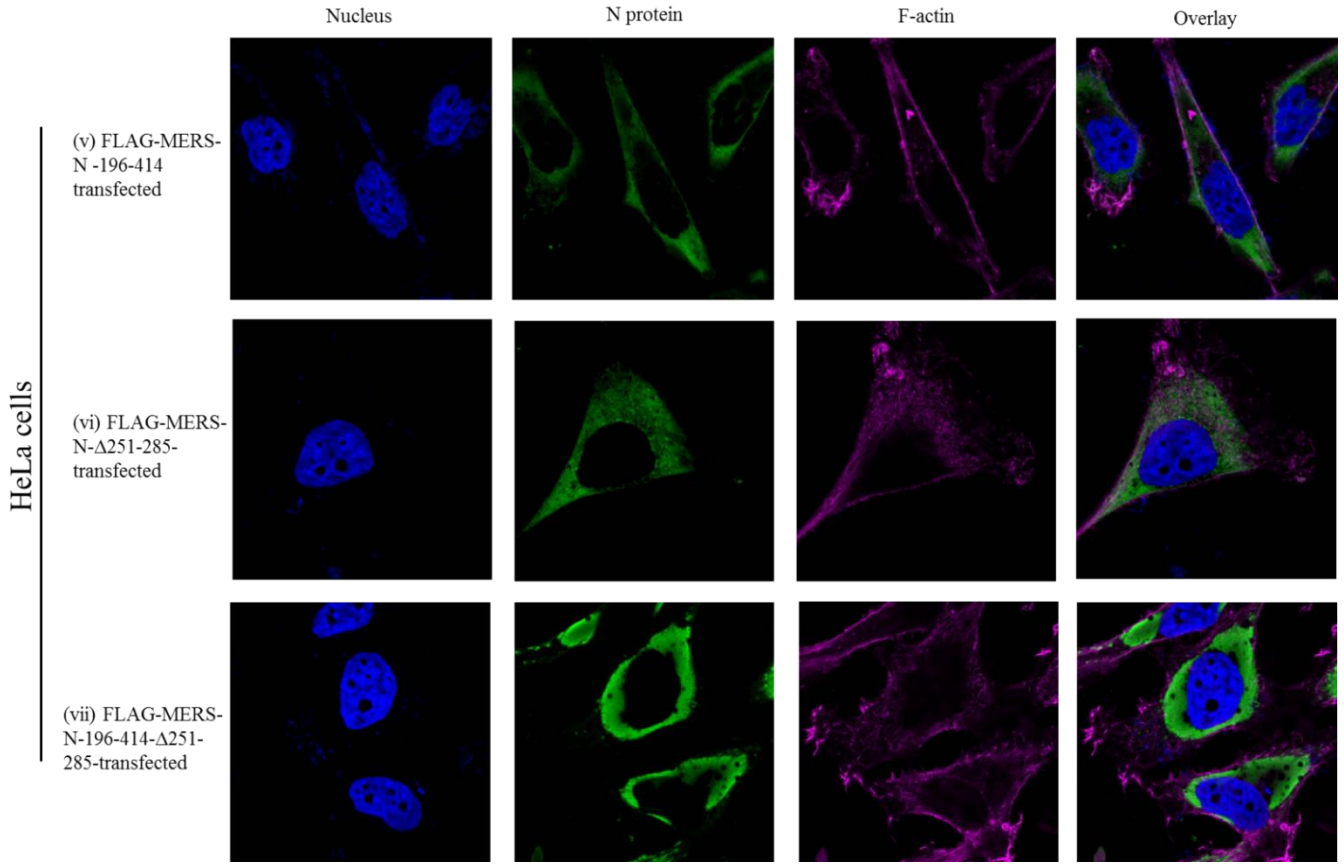

Figure 5.7. Visualization of F-actin bundling and arrangement in the presence of SARS-N and MERS-N proteins. (A) 293 FT cells were transiently transfected with [i] FLAG-vector, [ii] FLAG-SARS-N and [iii] FLAG-MERS-N for 48 hours followed by IFA. (B) HeLa cells were transiently transfected with [i] FLAG-vector, [ii] FLAG-SARS-N, [iii] FLAG-MERS-N and [iv-vii] truncated FLAG-MERS-N proteins for 72 hours followed by IFA. Cells were fixed and permeabilized followed by staining with anti-FLAG primary antibody and Alexa Fluor® 488-conjugated secondary antibody (green). F-actin was stained using Alexa Fluor® 647-conjugated phalloidin (purple) and nucleus with DAPI (blue). Cells were then mounted onto microscope glass slides and visualized by confocal microscopy. All images were taken at 100x magnification with 2x zoom.

5.6 Discussion

Current knowledge on the N protein of MERS-CoV is limited. Having a sequence homology of 48.5% as the SARS-CoV N protein, the MERS-CoV N protein is expected to have some similar functions as the SARS-CoV N protein. Therefore, in present study, we investigated whether the MERS-CoV N protein exhibit similar or different properties as the SARS-CoV N protein. We demonstrated that the 2 proteins share some common features, in terms of the processing (cleavage) in cells, interaction with host factor eEF1A, and the ability to inhibit protein translation and induce F-actin re-arrangement.

In transfected Vero E6 cells expressing the N proteins of MERS-CoV and SARS-CoV, it was found that the N proteins undergo cleavage as double protein bands were observed in Western blot analysis. The SARS-CoV N protein has been reported to induce the intrinsic apoptotic pathway during SARS-CoV infection and activate caspase 6 and potentially caspase 3, leading to cleavage of the N protein [483]. This cleavage was shown to be cell-type specific, as it was observed in certain cell lines such as Vero E6, but not in other cell types like Caco-2. In addition, cleavage site by caspase 6 was determined to be at the C-terminal aspartic acid residues at position 400 and 403 of the SARS-CoV N protein. The physiological function of this cleavage of the SARS-CoV N protein is unclear. It has been reported that the SARS-CoV N protein localized to the nucleus in serum starved cells [480]; localization of various deletion mutants of the N protein to the nucleus and nucleolus has also been observed [116,117]. It is possible that the production of truncated N proteins from caspase cleavage leads to the exposure of active nuclear localization signals (NLSs) or nucleolus localization signals (NuLS) which

allows translocation of N to the nucleus or nucleolus, where it exhibits certain cellular functions important for viral replication and pathogenesis [480]. Additionally, N protein of the transmissible gastroenteritis virus (TGEV), an alphacoronavirus that causes acute and fatal diarrhea in newborn pigs, has also been shown to be cleaved by caspase 6 and 7, and to a lesser extent, caspase 3 [484]. The site of cleavage of the TGEV N protein is also located in the C-terminus at the aspartic acid residue at position 359. Similar to the SARS-CoV N protein, cell type-specific cleavage of MERS-CoV N protein was observed in current study, occurring in Vero E6 cells. Moreover, the cleavage site of MERS-CoV N was also found to be located at the C-terminal region, although the exact position was not determined. Therefore, it seems that MERS-CoV N protein share similar processing in terms of protein cleavage as the SARS-CoV N protein. However, based on sequence alignment, the caspase cleavage sites of SARS-CoV N protein (residues 400 and 403), as well as that of the TGEV N protein (residue 359), are not conserved in the MERS-CoV N protein. Further investigation is needed to determine if the cleavage of MERS-CoV N is also a result of caspase activation.

The eEF1A protein exists in abundance in mammalian cells, constituting about 1 to 4% of the total soluble proteins [485] and functions as an important elongation factor during the protein translation elongation step [486]. In humans, there are two isoforms of eEF1A, eEF1A1 and eEF1A2, which share a sequence homology of 92%. EEF1A1 is ubiquitously expressed in all tissues, while eEF1A2 is only expressed in certain cells such as muscle, cardiac and large motor neurons [487]. Both isoforms were thought to share similar functions and exhibit similar activities, but may have differential roles in different cell and tissue types [488]. Besides the canonical function of eEF1A in protein elongation, numerous studies have shed light into its non-canonical functions, including protein

degradation, nuclear export of tRNAs, regulation of cytoskeleton activity, apoptosis, cell proliferation and oncogenesis, highlighting its important involvements in diverse cellular processes [486,489]. Given this, it is no surprise that viruses take advantage of host cell machinery to enhance its own survival through interaction with eEF1A. EEF1A has been implicated in various processes in viral replication and life cycle, as it is a regular binding target of many viral RNA and proteins [490]. For instance, the West Nile virus interacts with eEF1A through viral RNA and the replication complex NS3 and NS5 proteins to facilitate minus-strand viral RNA synthesis [491]. EEF1A associates with HIV-1 reverse transcriptase and significantly enhanced late DNA synthesis of HIV-1 during reverse transcription, possibly through the eEF1A-related stabilization of the reverse transcription complex [492]. In addition, the HIV-1 Gag protein and the Nef-1 protein were reported to interact with eEF1A, leading to reduced protein synthesis to redirect release of viral RNA to be packaged into nascent virions [493,494] and enhanced resistance to stress-induced apoptosis in human macrophages [495]. Other viral proteins that have been shown to interact with eEF1A include the human papillovirus type 38 (HPV38) E7 protein, HBV X protein and the SARS-CoV N protein [137,496,497].

In current study, N protein of MERS-CoV was shown to bind to eEF1A (eEF1A1 isoform), be it over-expressed eEF1A in Vero E6 cells or endogenous eEF1A in 293 FT cells. The region required for the interaction was mapped at residues 251-285 on the MERS-CoV N protein. The C-terminus residues 251-422 of the SARS-CoV N protein has been previously proven to be essential for the interaction with eEF1A, however, a shorter region necessary for the interaction has not been identified [137]. While the direct interaction between SARS-CoV and eEF1A has been demonstrated by Zhou *et al* [137], a direct interaction of MERS-CoV and eEF1A has not been proven in our current study.

More experiments, such as the use of surface plasmon resonance, could be used to address this. The interaction of MERS-CoV N and eEF1A was retained in co-IP experiments carried out in the presence of RNase (data not shown), suggesting that the association between the 2 proteins is not mediated by RNA. Besides the SARS-CoV N protein, the eEF1A protein has also been shown to interact with N protein of another coronavirus, TGEV [498]. Sequence alignment of the MERS-CoV, SARS-CoV and TGEV N proteins at the region determined for MERS-CoV N interaction with eEF1A (residues 251-285), as shown in Figure 5.8A, revealed 60% amino acid sequence identity between MERS-CoV and SARS-CoV and 31% identity between MERS-CoV and TGEV. The lower degree of sequence conservation between TGEV and MERS-CoV is expected, since TGEV is an alphacoronavirus and MERS-CoV is a betacoronavirus. Future work could focus on further mapping the eEF1A binding site on N proteins of MERS-CoV, SARS-CoV and TGEV to determine if the interaction site is identical within these coronaviruses. Sequence alignment of the N proteins of all known human coronaviruses at the eEF1A binding region is also provided in Figure 5.8B. Sequence homologies at the region between MERS-CoV and HCoV-229E, HCoV-OC43, HCoV-HKU1 and HCoV-NL63 are 31%, 40%, 46% and 37% respectively. Given that the N proteins of all human coronaviruses share some degree of conservation at this region, it is worth exploring whether the N proteins of other human coronaviruses also interact with eEF1A.

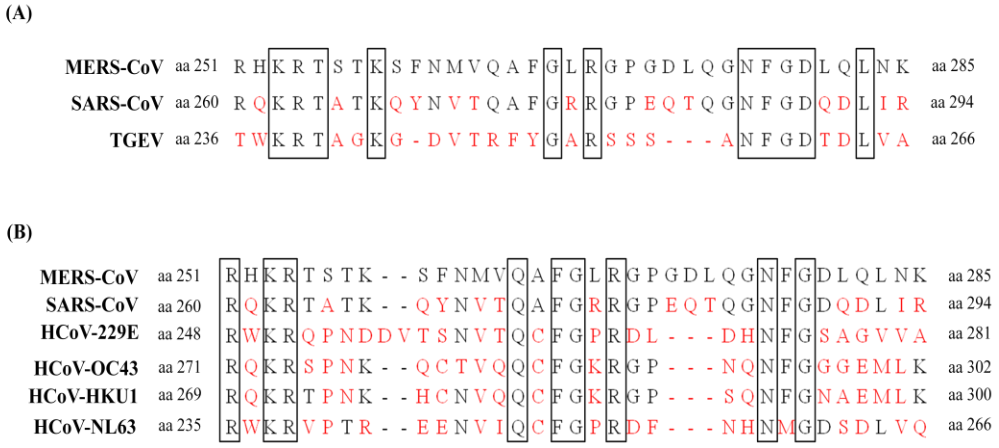

Figure 5.8. Sequence alignment of coronavirus N proteins. N proteins between (A) coronaviruses known to interact with eEF1A (MERS-CoV, SARS-CoV and TGEV) and (B) all known human coronaviruses (MERS-CoV, SARS-CoV, HCoV-229E, HCoV-OC43, HCoV-HKU1 and HCoV-NL63) were aligned at the region required for interaction between MERS-CoV N and eEF1A (residues 251-285 of MERS-CoV N). Non-identical amino acid residues to the MERS-CoV N protein are highlighted in red. Amino acid residues that are conserved among the viruses are boxed up.

By IFA, both SARS-CoV and MERS-CoV N proteins were found to co-localize with the endogenous eEF1A in the cytoplasm of transfected 293 FT cells, indicating that the site of interaction occurs in the cytoplasm. This is expected since both eEF1A and coronavirus N proteins are commonly present in the cell cytoplasm. Although eEF1A possesses the ability to shuttle between the nucleus and cytoplasm for the nuclear export of tRNAs, studies showed that eEF1A predominantly localizes in the cytoplasm [499,500]. Nonetheless, presence of eEF1A in the nucleus has been demonstrated in *Saccharomyces cerevisiae* [501]. In current study, endogenous eEF1A was found mainly in the cytoplasm of 293 FT and no presence in the nucleus was observed (see Figure 5.5). In the case of coronaviruses, it is generally believed that N proteins localize in the cytoplasm of cells but presence in nucleus and nucleolus is also possible [502]. It is reported that coronavirus N proteins can interact with certain nucleolar proteins in the

nucleolus to control and disrupt cell division and proliferation [502,503]. However, unlike other coronaviruses, the N protein of the SARS-CoV seems to localize exclusively in the cytoplasm of SARS-CoV-infected cells [116]. Similarly, over-expressed SARS-CoV N protein also localized predominantly in the cytoplasm with some degree of localization in the nucleolus [116]. As observed in current study, over-expressed full-length SARS-CoV N protein was present in the cytoplasm of transfected 293 FT and HeLa cells (see Figure 5.5[ii] and Figure 5.7B[ii]), supporting the findings of previous reports. Similar to SARS-CoV, over-expressed full length N protein of MERS-CoV also mainly localized in the cell cytoplasm and no localization in the nucleus or nucleolus was detected (see Figure 5.5[iii] and Figure 5.7B[iii]). However, it was noted that over-expressed N-terminal of MERS-CoV N (residues 1-195) localized both to the cytoplasm and the nucleus of transfected HeLa cells, but not in the nucleolus (see Figure 5.7[iv]). This is in agreement with previous report on SARS-CoV N, which demonstrated the predominant localization of N-terminal residues 1-156 in the nucleus of transfected COS-1 cells [116,504]. It is likely that the N-terminal of both the SARS-CoV and MERS-CoV N proteins contain nuclear localization signals (NLSs) that lead to nucleus localization of the proteins. The major nuclear export signals (NESs) responsible for the cytoplasmic localization of the SARS-CoV and MERS-CoV N proteins could therefore be located in the C-terminal end. Indeed, it has been suggested that a NES is located in the C-terminal end of the SARS-CoV between residues 300-422 and it acts as a dominant signal for the cytoplasmic retention of the whole N protein [116,504]. Our observations suggest that the MERS-CoV N protein behaves in a similar way as the SARS-CoV N protein in terms of subcellular localization. The physiological relevance of the different subcellular localization of the N proteins remains to be addressed, although, it has been proposed that

cleavage of SARS-CoV N protein by activated caspases from SARS-CoV N-induced apoptosis during stressed conditions could result in the formation of truncated forms of N proteins with an active NLS, leading to nuclear translocation and disruptions in nuclear functions [480].

Although viruses rely on the host cell translation machinery to complete its life cycle, the inhibition of translation and the shutoff of host protein synthesis have been known to be a common strategy employed by viruses to promote efficient viral replication. Viral suppression of translation can be achieved by multiple mechanisms, with the aim to retard the production of host cellular proteins related to the host defence system to ensure successful viral replication, survival and pathogenesis [505]. For example, enterovirus infection is capable in inhibiting host cell translation through the viral 2A and 3C protease-mediated cleavage of eukaryotic translation initiation factors eIF4GI, eIFGII and eIF5B [506,507]. The measles virus N protein, rabies virus M protein, SARS-CoV S protein and avian coronavirus infectious bronchitis virus (IBV) S protein have also been shown to bind eIF3 and have a negative impact on host cell translation [508,509,510]. Alphavirus Semliki Forest virus (SFV) and mouse hepatitis coronavirus infections also result in host protein synthesis shutoff via the phosphorylation of the eIF2A [511,512]. The SARS-CoV N protein has been shown to inhibit *in vitro* cellular protein translation through its interaction with eEF1A, as the addition of purified eEF1A proteins reversed this effect [137]. Here, by using *in vitro* translation assay, we found that similar to SARS-CoV N, MERS-CoV N inhibited protein translation, but at a significantly higher level compared to SARS-CoV N, with a 50% inhibition of protein translation at approximately 0.25-0.5 μM of MERS-CoV N protein compared to 0.5-1.0 μM of SARS-CoV N. To delineate the mechanism and the involvement of eEF1A in

MERS-CoV N-induced protein translation inhibition, the full length and C-terminal MERS-CoV N with eEF1A binding site (residues 251-285) removed were assessed for their abilities to inhibit protein translation. The removal of the eEF1A binding site (residues 251-285) from the full-length and C-terminal MERS-CoV N protein led to reduced level of protein translation inhibition compared to the proteins containing the eEF1A binding site. This strongly suggests that the binding of MERS-CoV N protein and eEF1A plays a role in suppressing protein translation, since the deletion of the eEF1A binding site significantly affected this function of MERS-CoV N protein. Interestingly, the N-terminal MERS-CoV N (residues 1-195) also displayed ability to suppress protein translation at a level higher than the full length and C-terminal MERS-CoV N. This indicates that the N-terminal MERS-CoV N protein can also mediate inhibition of cellular protein translation through other mechanisms that are independent of eEF1A. It has been demonstrated that a single protein, the p17 protein of the avian reovirus achieves the shutoff of its host protein translation system through the suppression of several translation factors like the eIF2α, eIF4B, eIF4E, eIF4G and eEF2 [513,514]. Based on our results, we conclude that the MERS-CoV N protein is capable in suppressing protein translation like the SARS-CoV N protein, and this is possibly achieved through multiple mechanisms, involving the interaction with eEF1A as well as other host factors and mechanisms which are yet to be identified.

The re-organization and re-configuration of cellular actin is yet another frequent approach used by viruses for efficacious replication at many stages of the viral life cycle, ranging from viral entry, subcellular localization, genomic transcription, viral assembly to dissemination [515,516]. Filamentous actin (F-actin), which is composed of two parallel strands of globular actin (G-actin) monomers, forms the primary structural

components of the eukaryotic cytoskeleton and plays key roles in the regulation of various cellular processes, including cell morphology, cytokinesis, cell division and migration. Proper actin function is dependent on the polymerization or the bundling of F-actin, which involves the interplay of a vast number of protein factors [517]. The SARS-CoV N is capable of inducing actin re-organization during cellular stress condition in the absence of growth factors through the activation of the p38 MAPK pathway, which may serve to redirect interactions between host and viral proteins to prevent viral clearance by the host immune system, thereby ensuring persistent viral replication and infection [135]. In another study, the SARS-CoV N protein was shown to prevent F-actin bundling via its interaction with eEF1A, leading to the inhibition of cytokinesis and a slower transition of cell cycle from the S phase to G_2/M phase, which may represent another way in which the virus prevent rapid cell proliferation and attenuate host anti-viral immune responses so as to enhance viral replication, survival and pathogenesis [137]. In addition to its canonical role in protein translation, eEF1A is an important regulator of the cell cytoskeleton network. A significant amount of more than 60% of cellular eEF1A is estimated to associate with F-actin, functioning to cross-link F actin and promote F-actin polymerization and bundling, thereby contributing to F-actin functions [518,519]. Studies have shown that eEF1A mutants resulted in severe defects in F-actin bundling, cell morphology and reduction of translation activity *in vitro* [518,520,521]. Several other viral proteins, including the human papillovirus type 38 (HPV38) E7 protein and HBV X protein, have also been demonstrated to induce a change in actin organization through the interaction with eEF1A, indicating that this is a common mechanism employed by viruses in viral infection and pathogenesis [496,497]. In current study, we determined that the presence of MERS-CoV N protein lead to a reduction of F-actin bundle

formation and the re-organization of actin structure within cells in ways similar to the SARS-CoV N protein. We also provided evidence that these changes are possibly linked to MERS-CoV N protein interaction with eEF1A. This is because the degree of F-actin bundling reduction and re-arrangement was not as pronounced in the presence of mutant N proteins that lacked the ability to interact with eEF1A as compared to the full length and C-terminal MERS-CoV N protein.

To conclude, in present study, we compared some cellular activities and functions of the MERS-CoV N protein with the SARS-CoV N protein and found that the two proteins share common properties. We demonstrated the ability of the MERS-CoV N protein to undergo cellular processing and cleavage, interact with host factor eEF1A and inhibit cellular translation and F-actin bundling, as also seen with the SARS-CoV N protein [137]. Furthermore, it was determined that the association of MERS-CoV N and eEF1A played a part in the suppression of cellular translation machinery and the inhibition of F-actin bundling in cells. It was also noted that the inhibition of cellular protein synthesis by MERS-CoV N was greater than that of SARS-CoV N at low concentrations, suggesting that differences exist between the two viral proteins although they share similar functions. Being the most abundantly expressed viral protein, extensive studies have been done on SARS-CoV N protein, and it is recognized as not only an important structural protein of the SARS-CoV, but also a multipurpose viral protein capable in interfering with different cellular pathways, thus implying its critical roles in influencing viral replication and mediating pathogenesis [481]. Much less is understood for the N protein of MERS-CoV, since MERS-CoV is a newly emerged virus identified not too long ago. Identifying similarities and differences between SARS-CoV and MERS-CoV, such as that of N proteins as shown in current study, could allow the

understanding of the underlying factors that may be attributed to the higher pathogenicity of these viruses.

CHAPTER 6: CONCLUSION AND FUTURE WORK

The SARS epidemic in 2003 was successfully controlled due to the implementations of effective public health measures rather than the availability of antiviral treatments or vaccines. The continual zoonotic persistence of highly similar and related SL-CoVs as well as other genetically diverse coronavirus strains in the natural wildlife reservoirs suggests that a re-emergence of SARS or emergence of novel coronaviruses in humans is highly possible. The emergence of MERS-CoV, another zoonotic coronavirus that has crossed the species barrier to infect human, ten years after SARS certainly proves this. While the SARS epidemic occurred swiftly and ended within 4 months, the MERS epidemic is slow-progressing and has been ongoing for 3 years with no signs of dwindling. Both the SARS-CoV and MERS-CoV are classified as highly pathogenic human coronaviruses due to their high fatality rates as compared to other endemic human coronaviruses which usually cause mild cold-like symptoms. It is clear that newly emerged zoonotic coronaviruses can cause severe diseases in humans and pose significant public health threats and challenges. While continual surveillance coupled with effective infection control measures are important in addressing these threats and challenges, research efforts focusing on elucidating the mechanisms of replication and pathogenesis is essential for the identification of potential drug targets and development of antiviral agents and vaccine strategies.

In this thesis, we focused on the understanding of the viral and host interactions of newly emerged and highly pathogenic human coronaviruses, the SARS-CoV (Chapter 3 and 4) and the MERS-CoV (Chapter 5). Firstly, the generation of escape SARS-CoV mutants against two SARS-CoV-neutralizing mAbs targeting the S protein was carried

out to better characterize the neutralizing epitopes involved in binding to S protein and to understand the neutralization mechanism of the mAbs. Next, we looked into identifying long-term memory SARS-specific T cell responses from SARS-convalescent patients and defining the T cell epitopes on viral proteins that are necessary to elicit these responses. Finally, we investigated the effects of the MERS-CoV N protein on host cell activities in comparison to the SARS-CoV N protein, with the aim to elucidate the role of the N protein in MERS-CoV infection and pathogenesis. The important findings from the chapters are as summarized below:

a) MAb 1A9 and 1G10 bind to S protein of SARS-CoV at the S2 subunit and neutralize SARS-CoV infection *in vitro*, but are unable to bind to the S protein of MERS-CoV, hence unlikely to cross-neutralize MERS-CoV infection.
b) Through the generation of SARS-CoV escape mutants, two mutations, N1056K and D1128A, were identified in the S protein of mAb 1A9 escape mutants. No specific mutations were identified in escape mutants generated using mAb 1G10.
c) Aspartic acid (D) at residue 1128 of the SARS-CoV S protein, but not lysine (N) at residue 1056, was found to be important in mAb 1A9 binding to S protein and mAb 1A9 neutralization of SARS-CoV.
d) Aspartic acid (D) residue at position 1128 of SARS-CoV S protein does not play a role in S protein synthesis and maturation as mutant D1128A S protein functioned similarly to wild-type S protein, indicating that the mutant D1128A SARS-CoV escape virus likely exhibits similar virus fitness as the wild-type virus.
e) SARS-specific memory T cell responses persist in 3 SARS-convalescent subjects at 9-11 years post-infection in the absence of antigen.

f) A total of five T cell responses were identified: four $CD4^+$ T cell responses targeting the SARS-CoV S (S104, S109, S217) and N (N21) proteins, and one $CD8^+$ T cell response targeting the M (M29) protein.

g) M29-specific $CD8^+$ T cell response is a dominant T cell response identified in 2 out of 3 SARS subjects, and it targets the SARS-CoV M protein at residues 147-155 and is restricted by HLA-B*1502 allele.

h) A previously identified SARS-specific $CD8^+$ T cell response from a SARS subject at 6 years post-infection targeting the SARS-CoV N53 region was undetectable at 9 years post-infection using N53 15-mer peptide, but could be detected using 10-mer peptide corresponding to its minimal epitope, suggesting the decrease in magnitude of the response over the years.

i) The N53-specific $CD8^+$ T cell response targets the SARS-CoV N protein at residues 266-275 and is HLA-B*1525-restricted.

j) Both the SARS-specfic M29 and N53 $CD8^+$ T cell responses persist in the SARS subject up to 11 years post-infection.

k) Both M29 and N53 $CD8^+$ T cells were unable to cross-react with corresponding MERS-CoV M29 and N53 minimal peptides, indicating that T cell responses are SARS-specific and unlikely to provide cross-protection against MERS-CoV infection.

l) M29 and N53 minimal epitope regions are fully conserved in human SARS-CoV, civet SARS-CoV (SZ3) and bat SL-CoV (Rp3, Rf1, Rs3367), suggesting cross-reactivity and cross-protection of the $CD8^+$ T cell responses against zoonotic SARS-CoV and SL-CoV infections.

m) The MERS-CoV N protein shares some common activities and cellular functions as the SARS-CoV N protein, in terms of the protein processing/cleavage in transfected cells, interaction with host cell factor eEF1A, inhibition of cellular protein translation and induction of F-actin re-organization.

n) N protein of MERS-CoV interacts with host protein eEF1A via its C-terminal end at residues 251-285, and co-localizes with eEF1A in the cytoplasm of cells.

o) Similar to SARS-CoV N, MERS-CoV N protein suppressed cellular protein translation, and its effect was greater compared to SARS-CoV N protein. This effect was found to be mediated via eEF1A dependent and independent manners.

p) MERS-CoV N protein resulted in decreased F-actin bundling and F-actin re-arrangement in cells in similar way as the SARS-CoV N protein.

q) The association of MERS-CoV N and eEF1A possibly plays a role in the inhibition of total cellular protein translation and F-actin re-arrangement in cells.

Neutralizing mAbs are proposed to be a promising new class of antivirals to confer broad protection against SARS-CoV variants in the therapeutic and prophylactic treatment of SARS. In Chapter 3, we described the in-depth characterization of 2 mAbs previously generated by our group, mAb 1A9 and 1G10, which target the highly conserved S2 domain of the SARS-CoV S protein and exhibit neutralization activity against humans SARS-CoV as well as zoonotic civet SARS-CoV and bat SL-CoV strains [401]. To gain a better understanding of their neutralizing mechanisms, escape SARS-CoV mutants against mAb 1A9 and 1G10 were generated with the aim to identify critical residues required for antibody binding. Overall, this work has contributed to the understanding of the viral-host interplay involving S protein and the neutralizing antibodies and the mechanism of anti-S2 mAb neutralization of SARS-CoV. The degree

of amino acid conservation of neutralizing epitopes located within the S proteins of various coronaviruses determines mAb cross-binding and cross-reactivity, and the S protein is capable of mutation to escape neutralization by neutralizing mAbs without affecting viral fitness. This has implications in the development of mAbs for the field of therapy and prophylaxis against SARS-CoV infection. It also allows the design of novel coronavirus vaccines, such as epitope-based vaccines capable of eliciting effective neutralizing antibody responses against coronavirus infection. The broadly-neutralizing capability of mAb 1A9 and 1G10 makes them attractive candidates for passive immunotherapy over other mAbs, as future re-emergence of SARS-CoV or SL-CoV threats would most likely result from a cross-species transmission from a zoonotic source. For future studies, structural analysis of the interaction between the mAb 1A9/1G10 and S could be pursued in order to clearly define the inhibition mechanisms of the mAbs. Although we demonstrated that the D1128A mutant S protein is functional like the wild-type S and that the D1128A escape mutant most likely shares similar virus fitness as the wild-type virus, future work is necessary to clearly demonstrate the viral fitness of mutant D1128A escape virus, in terms of replicative capabilities and virulence of the live virus in *in vitro* and *in vivo* systems. In addition, humanization of the mAbs is required and the binding profiles and effects of the resultant chimeric human-mouse mAbs would need to be re-assessed. Given the low neutralization potencies of mAb 1A9 and 1G10, which target the membrane-embedded S2 region of the S protein, the effects of combining these two mAbs to increase neutralization efficacy could be examined. Since escape mutants can arise from using mAb 1A9 and 1G10 individually as demonstrated in current study, a combined passive immunotherapy could be a wiser approach to minimize the risk of emergence of viral escape variants, as these 2 mAbs bind to separate epitopes on the S

protein. In addition, the combined use of mAb 1A9 and 1G10, which are anti-S2 mAbs, with other anti-S1 mAbs could be explored for the development of a more effective combination therapy against SARS-CoV infections.

Besides neutralizing antibodies, helper $CD4^+$ and cytotoxic $CD8^+$ T cells are also important in the clearance and protection against SARS-CoV infections. In Chapter 4, we looked into the identification of long-lived SARS-specific memory T cell responses from SARS-convalescent individuals at 9 to 11 years after SARS-CoV infection. The knowledge of the type of T cell responses that have contributed to the recovery of SARS patients and the length of their persistence after SARS recovery not only allow a better understanding of the role of cellular immunity in SARS-CoV infection, but also provides valuable information for the development of SARS vaccines, which should be able to induce effective and long-lived protective cellular immunity. In addition, the in-depth characterizations of two SARS-specific $CD8^+$ T cell responses targeting the M and N proteins through defining their epitope regions and HLA restrictions, revealed the importance of these two viral proteins in inducing dominant and long-lived host cellular immune responses in addition to their basic structural functions. Future research efforts could focus on the development of a SARS vaccine composed of the SARS-CoV M and N proteins. This knowledge can also be further harnessed for the development of a T cell adoptive immunotherapy for SARS-CoV infections, which make use of engineered T cells expressing SARS peptide-specific TCR to specifically target SARS-infected cells. Future work includes the determination of cytokine profiles of the SARS-specific $CD4^+$ and $CD8^+$ T cells identified in this study to better characterize their functions.

Although most MERS-CoV infections occur in the Middle East, the epidemic threatens to spread to other countries due to high frequency of air travel. In the last 3 years since its emergence, MERS-CoV has been exported to numerous countries, including Asian countries like The Phillipines, Malaysia, Thailand and South Korea [274]. The recent MERS outbreak in May 2015 that occurred in Republic of Korea, the largest outbreak reported outside of the Middle East, affected a total of 186 people with 36 deaths as of 15th July 2015 [274]. This significantly highlights the worldwide threat of MERS-CoV, prompting the urgent need for antivirals and vaccines targeting the virus which are currently unavailable. Being a relatively new virus, the MERS-CoV is currently poorly understood. Understanding the interplay between viral and host proteins and delineating the effects on cellular functions and viral replication/pathogenesis is an important basis for identifying potential drug targets and developing antiviral strategies. Besides its primary role in encapsidating viral RNA, extensive research revealed that the SARS-CoV N protein also interacts with numerous host factors, exhibits various cellular functions and is thus believed to be an important modulator of SARS-CoV replication and disease pathogenesis. In Chapter 5, we demonstrated that several characteristics and cellular functions of the MERS-CoV N protein are in common as the SARS-CoV N protein. This study provides insights into the alternative functions of the MERS-CoV N protein on top of its viral RNA-packaging role. Future work includes to further evaluate the effects of MERS-CoV N on other cellular processes, such as cell cycle, cell death, IFN antagonism and the suppression of RNA silencing, which have been reported for the SARS-CoV N protein. The effects of MERS-CoV N and eEF1A protein interaction on virus replication and pathogenesis should also be further explored to determine the significance of this interaction. This can be done through the use of RNA interference

(RNAi) technology and reverse genetic technique. Finer mapping of the region on MERS-CoV N required for interaction with eEF1A and whether the site of interaction is conserved in MERS-CoV and SARS-CoV N proteins could be investigated. The conservation of this interaction with eEF1A could also be further examined in other HCoVs to determine if this interaction is universal among HCoVs or exclusive in highly pathogenic HCoVs. Furthermore, the screening and identification of more host factors that MERS-CoV N protein can potentially interact with and the delineation of the molecular pathways involved is an area of research to explore in the future.

REFERENCES

1. Parrish CR, Holmes EC, Morens DM, Park EC, Burke DS, et al. (2008) Cross-species virus transmission and the emergence of new epidemic diseases. Microbiol Mol Biol Rev 72: 457-470.

2. Berry M, Gamieldien J, Fielding BC (2015) Identification of new respiratory viruses in the new millennium. Viruses 7: 996-1019.

3. Woo PC, Lau SK, Huang Y, Yuen KY (2009) Coronavirus diversity, phylogeny and interspecies jumping. Exp Biol Med (Maywood) 234: 1117-1127.

4. Peiris JS, Guan Y, Yuen KY (2004) Severe acute respiratory syndrome. Nat Med 10: S88-97.

5. Ksiazek TG, Erdman D, Goldsmith CS, Zaki SR, Peret T, et al. (2003) A novel coronavirus associated with severe acute respiratory syndrome. N Engl J Med 348: 1953-1966.

6. Normile D (2004) Infectious diseases. Mounting lab accidents raise SARS fears. Science 304: 659-661.

7. Yu IT, Li Y, Wong TW, Tam W, Chan AT, et al. (2004) Evidence of airborne transmission of the severe acute respiratory syndrome virus. N Engl J Med 350: 1731-1739.

8. Poon LL, Guan Y, Nicholls JM, Yuen KY, Peiris JS (2004) The aetiology, origins, and diagnosis of severe acute respiratory syndrome. Lancet Infect Dis 4: 663-671.

9. Lee N, Hui D, Wu A, Chan P, Cameron P, et al. (2003) A major outbreak of severe acute respiratory syndrome in Hong Kong. N Engl J Med 348: 1986-1994.

10. Cheng VC, Chan JF, To KK, Yuen KY (2013) Clinical management and infection control of SARS: lessons learned. Antiviral Res 100: 407-419.

11. Leung GM, Hedley AJ, Ho LM, Chau P, Wong IO, et al. (2004) The epidemiology of severe acute respiratory syndrome in the 2003 Hong Kong epidemic: an analysis of all 1755 patients. Ann Intern Med 141: 662-673.

12. Perlman S, Netland J (2009) Coronaviruses post-SARS: update on replication and pathogenesis. Nat Rev Microbiol 7: 439-450.

13. Masters PS (2006) The molecular biology of coronaviruses. Adv Virus Res 66: 193-292.

14. Snijder EJ, van der Meer Y, Zevenhoven-Dobbe J, Onderwater JJ, van der Meulen J, et al. (2006) Ultrastructure and origin of membrane vesicles associated with the severe acute respiratory syndrome coronavirus replication complex. J Virol 80: 5927-5940.

15. Knoops K, Kikkert M, Worm SH, Zevenhoven-Dobbe JC, van der Meer Y, et al. (2008) SARS-coronavirus replication is supported by a reticulovesicular network of modified endoplasmic reticulum. PLoS Biol 6: e226.

16. Sawicki SG, Sawicki DL, Siddell SG (2007) A contemporary view of coronavirus transcription. J Virol 81: 20-29.

17. Stadler K, Masignani V, Eickmann M, Becker S, Abrignani S, et al. (2003) SARS--beginning to understand a new virus. Nat Rev Microbiol 1: 209-218.

18. Ziebuhr J (2006) The coronavirus replicase: insights into a sophisticated enzyme machinery. Adv Exp Med Biol 581: 3-11.

19. Wathelet MG, Orr M, Frieman MB, Baric RS (2007) Severe acute respiratory syndrome coronavirus evades antiviral signaling: role of nsp1 and rational design of an attenuated strain. J Virol 81: 11620-11633.

20. Brierley I, Dos Ramos FJ (2006) Programmed ribosomal frameshifting in HIV-1 and the SARS-CoV. Virus Res 119: 29-42.

21. Thiel V, Ivanov KA, Putics A, Hertzig T, Schelle B, et al. (2003) Mechanisms and enzymes involved in SARS coronavirus genome expression. J Gen Virol 84: 2305-2315.

22. Almeida MS, Johnson MA, Herrmann T, Geralt M, Wuthrich K (2007) Novel beta-barrel fold in the nuclear magnetic resonance structure of the replicase nonstructural protein 1 from the severe acute respiratory syndrome coronavirus. J Virol 81: 3151-3161.

23. Prentice E, McAuliffe J, Lu X, Subbarao K, Denison MR (2004) Identification and characterization of severe acute respiratory syndrome coronavirus replicase proteins. J Virol 78: 9977-9986.

24. Narayanan K, Huang C, Lokugamage K, Kamitani W, Ikegami T, et al. (2008) Severe acute respiratory syndrome coronavirus nsp1 suppresses host gene expression, including that of type I interferon, in infected cells. J Virol 82: 4471-4479.

25. Kamitani W, Huang C, Narayanan K, Lokugamage KG, Makino S (2009) A two-pronged strategy to suppress host protein synthesis by SARS coronavirus Nsp1 protein. Nat Struct Mol Biol 16: 1134-1140.

26. Lokugamage KG, Narayanan K, Huang C, Makino S (2012) Severe acute respiratory syndrome coronavirus protein nsp1 is a novel eukaryotic translation inhibitor that represses multiple steps of translation initiation. J Virol 86: 13598-13608.

27. Li Y, Ren Z, Bao Z, Ming Z, Li X (2011) Expression, crystallization and preliminary crystallographic study of the C-terminal half of nsp2 from SARS coronavirus. Acta Crystallogr Sect F Struct Biol Cryst Commun 67: 790-793.

28. Graham RL, Sims AC, Brockway SM, Baric RS, Denison MR (2005) The nsp2 replicase proteins of murine hepatitis virus and severe acute respiratory syndrome coronavirus are dispensable for viral replication. J Virol 79: 13399-13411.

29. Cornillez-Ty CT, Liao L, Yates JR, 3rd, Kuhn P, Buchmeier MJ (2009) Severe acute respiratory syndrome coronavirus nonstructural protein 2 interacts with a host protein complex involved in mitochondrial biogenesis and intracellular signaling. J Virol 83: 10314-10318.

30. Baez-Santos YM, St John SE, Mesecar AD (2015) The SARS-coronavirus papain-like protease: structure, function and inhibition by designed antiviral compounds. Antiviral Res 115: 21-38.

31. Ratia K, Saikatendu KS, Santarsiero BD, Barretto N, Baker SC, et al. (2006) Severe acute respiratory syndrome coronavirus papain-like protease: structure of a viral deubiquitinating enzyme. Proc Natl Acad Sci U S A 103: 5717-5722.

32. Hagemeijer MC, Verheije MH, Ulasli M, Shaltiel IA, de Vries LA, et al. (2010) Dynamics of coronavirus replication-transcription complexes. J Virol 84: 2134-2149.

33. Harcourt BH, Jukneliene D, Kanjanahaluethai A, Bechill J, Severson KM, et al. (2004) Identification of severe acute respiratory syndrome coronavirus replicase products and characterization of papain-like protease activity. J Virol 78: 13600-13612.

34. Egloff MP, Malet H, Putics A, Heinonen M, Dutartre H, et al. (2006) Structural and functional basis for ADP-ribose and poly(ADP-ribose) binding by viral macro domains. J Virol 80: 8493-8502.

35. Tan J, Vonrhein C, Smart OS, Bricogne G, Bollati M, et al. (2009) The SARS-unique domain (SUD) of SARS coronavirus contains two macrodomains that bind G-quadruplexes. PLoS Pathog 5: e1000428.

36. Neuman BW, Joseph JS, Saikatendu KS, Serrano P, Chatterjee A, et al. (2008) Proteomics analysis unravels the functional repertoire of coronavirus nonstructural protein 3. J Virol 82: 5279-5294.

37. Angelini MM, Akhlaghpour M, Neuman BW, Buchmeier MJ (2013) Severe acute respiratory syndrome coronavirus nonstructural proteins 3, 4, and 6 induce double-membrane vesicles. MBio 4.

38. Oostra M, te Lintelo EG, Deijs M, Verheije MH, Rottier PJ, et al. (2007) Localization and membrane topology of coronavirus nonstructural protein 4: involvement of the early secretory pathway in replication. J Virol 81: 12323-12336.

39. Anand K, Ziebuhr J, Wadhwani P, Mesters JR, Hilgenfeld R (2003) Coronavirus main proteinase (3CLpro) structure: basis for design of anti-SARS drugs. Science 300: 1763-1767.

40. Lai CC, Jou MJ, Huang SY, Li SW, Wan L, et al. (2007) Proteomic analysis of up-regulated proteins in human promonocyte cells expressing severe acute respiratory syndrome coronavirus 3C-like protease. Proteomics 7: 1446-1460.

41. Oostra M, Hagemeijer MC, van Gent M, Bekker CP, te Lintelo EG, et al. (2008) Topology and membrane anchoring of the coronavirus replication complex: not all hydrophobic domains of nsp3 and nsp6 are membrane spanning. J Virol 82: 12392-12405.

42. Baliji S, Cammer SA, Sobral B, Baker SC (2009) Detection of nonstructural protein 6 in murine coronavirus-infected cells and analysis of the transmembrane topology by using bioinformatics and molecular approaches. J Virol 83: 6957-6962.

43. Cottam EM, Maier HJ, Manifava M, Vaux LC, Chandra-Schoenfelder P, et al. (2011) Coronavirus nsp6 proteins generate autophagosomes from the endoplasmic reticulum via an omegasome intermediate. Autophagy 7: 1335-1347.

44. Zhai Y, Sun F, Li X, Pang H, Xu X, et al. (2005) Insights into SARS-CoV transcription and replication from the structure of the nsp7-nsp8 hexadecamer. Nat Struct Mol Biol 12: 980-986.

45. Johnson MA, Jaudzems K, Wuthrich K (2010) NMR Structure of the SARS-CoV Nonstructural Protein 7 in Solution at pH 6.5. J Mol Biol 402: 619-628.

46. te Velthuis AJ, van den Worm SH, Snijder EJ (2012) The SARS-coronavirus nsp7+nsp8 complex is a unique multimeric RNA polymerase capable of both de novo initiation and primer extension. Nucleic Acids Res 40: 1737-1747.

47. Imbert I, Guillemot JC, Bourhis JM, Bussetta C, Coutard B, et al. (2006) A second, non-canonical RNA-dependent RNA polymerase in SARS coronavirus. EMBO J 25: 4933-4942.

48. Kumar P, Gunalan V, Liu B, Chow VT, Druce J, et al. (2007) The nonstructural protein 8 (nsp8) of the SARS coronavirus interacts with its ORF6 accessory protein. Virology 366: 293-303.

49. Egloff MP, Ferron F, Campanacci V, Longhi S, Rancurel C, et al. (2004) The severe acute respiratory syndrome-coronavirus replicative protein nsp9 is a single-stranded RNA-binding subunit unique in the RNA virus world. Proc Natl Acad Sci U S A 101: 3792-3796.

50. Ponnusamy R, Moll R, Weimar T, Mesters JR, Hilgenfeld R (2008) Variable oligomerization modes in coronavirus non-structural protein 9. J Mol Biol 383: 1081-1096.

51. Sutton G, Fry E, Carter L, Sainsbury S, Walter T, et al. (2004) The nsp9 replicase protein of SARS-coronavirus, structure and functional insights. Structure 12: 341-353.

52. Miknis ZJ, Donaldson EF, Umland TC, Rimmer RA, Baric RS, et al. (2009) Severe acute respiratory syndrome coronavirus nsp9 dimerization is essential for efficient viral growth. J Virol 83: 3007-3018.

53. Su D, Lou Z, Sun F, Zhai Y, Yang H, et al. (2006) Dodecamer structure of severe acute respiratory syndrome coronavirus nonstructural protein nsp10. J Virol 80: 7902-7908.

54. Joseph JS, Saikatendu KS, Subramanian V, Neuman BW, Brooun A, et al. (2006) Crystal structure of nonstructural protein 10 from the severe acute respiratory syndrome coronavirus reveals a novel fold with two zinc-binding motifs. J Virol 80: 7894-7901.

55. Ke M, Chen Y, Wu A, Sun Y, Su C, et al. (2012) Short peptides derived from the interaction domain of SARS coronavirus nonstructural protein nsp10 can suppress the 2'-O-methyltransferase activity of nsp10/nsp16 complex. Virus Res 167: 322-328.

56. Bouvet M, Lugari A, Posthuma CC, Zevenhoven JC, Bernard S, et al. (2014) Coronavirus Nsp10, a critical co-factor for activation of multiple replicative enzymes. J Biol Chem 289: 25783-25796.

57. Pan J, Peng X, Gao Y, Li Z, Lu X, et al. (2008) Genome-wide analysis of protein-protein interactions and involvement of viral proteins in SARS-CoV replication. PLoS One 3: e3299.

58. Bouvet M, Debarnot C, Imbert I, Selisko B, Snijder EJ, et al. (2010) In vitro reconstitution of SARS-coronavirus mRNA cap methylation. PLoS Pathog 6: e1000863.

59. Cheng A, Zhang W, Xie Y, Jiang W, Arnold E, et al. (2005) Expression, purification, and characterization of SARS coronavirus RNA polymerase. Virology 335: 165-176.

60. Ahn DG, Choi JK, Taylor DR, Oh JW (2012) Biochemical characterization of a recombinant SARS coronavirus nsp12 RNA-dependent RNA polymerase capable of copying viral RNA templates. Arch Virol 157: 2095-2104.

61. te Velthuis AJ, Arnold JJ, Cameron CE, van den Worm SH, Snijder EJ (2010) The RNA polymerase activity of SARS-coronavirus nsp12 is primer dependent. Nucleic Acids Res 38: 203-214.

62. Seybert A, Posthuma CC, van Dinten LC, Snijder EJ, Gorbalenya AE, et al. (2005) A complex zinc finger controls the enzymatic activities of nidovirus helicases. J Virol 79: 696-704.

63. Tanner JA, Watt RM, Chai YB, Lu LY, Lin MC, et al. (2003) The severe acute respiratory syndrome (SARS) coronavirus NTPase/helicase belongs to a distinct class of 5' to 3' viral helicases. J Biol Chem 278: 39578-39582.

64. Ivanov KA, Thiel V, Dobbe JC, van der Meer Y, Snijder EJ, et al. (2004) Multiple enzymatic activities associated with severe acute respiratory syndrome coronavirus helicase. J Virol 78: 5619-5632.

65. Adedeji AO, Marchand B, Te Velthuis AJ, Snijder EJ, Weiss S, et al. (2012) Mechanism of nucleic acid unwinding by SARS-CoV helicase. PLoS One 7: e36521.

66. Fang S, Chen B, Tay FP, Ng BS, Liu DX (2007) An arginine-to-proline mutation in a domain with undefined functions within the helicase protein (Nsp13) is lethal to the coronavirus infectious bronchitis virus in cultured cells. Virology 358: 136-147.

67. Chen P, Jiang M, Hu T, Liu Q, Chen XS, et al. (2007) Biochemical characterization of exoribonuclease encoded by SARS coronavirus. J Biochem Mol Biol 40: 649-655.

68. Chen Y, Cai H, Pan J, Xiang N, Tien P, et al. (2009) Functional screen reveals SARS coronavirus nonstructural protein nsp14 as a novel cap N7 methyltransferase. Proc Natl Acad Sci U S A 106: 3484-3489.

69. Minskaia E, Hertzig T, Gorbalenya AE, Campanacci V, Cambillau C, et al. (2006) Discovery of an RNA virus 3'->5' exoribonuclease that is critically involved in coronavirus RNA synthesis. Proc Natl Acad Sci U S A 103: 5108-5113.

70. Eckerle LD, Becker MM, Halpin RA, Li K, Venter E, et al. (2010) Infidelity of SARS-CoV Nsp14-exonuclease mutant virus replication is revealed by complete genome sequencing. PLoS Pathog 6: e1000896.

71. Bouvet M, Imbert I, Subissi L, Gluais L, Canard B, et al. (2012) RNA 3'-end mismatch excision by the severe acute respiratory syndrome coronavirus

nonstructural protein nsp10/nsp14 exoribonuclease complex. Proc Natl Acad Sci U S A 109: 9372-9377.

72. Ricagno S, Egloff MP, Ulferts R, Coutard B, Nurizzo D, et al. (2006) Crystal structure and mechanistic determinants of SARS coronavirus nonstructural protein 15 define an endoribonuclease family. Proc Natl Acad Sci U S A 103: 11892-11897.

73. Ricagno S, Coutard B, Grisel S, Bremond N, Dalle K, et al. (2006) Crystallization and preliminary X-ray diffraction analysis of Nsp15 from SARS coronavirus. Acta Crystallogr Sect F Struct Biol Cryst Commun 62: 409-411.

74. Bhardwaj K, Guarino L, Kao CC (2004) The severe acute respiratory syndrome coronavirus Nsp15 protein is an endoribonuclease that prefers manganese as a cofactor. J Virol 78: 12218-12224.

75. Ivanov KA, Hertzig T, Rozanov M, Bayer S, Thiel V, et al. (2004) Major genetic marker of nidoviruses encodes a replicative endoribonuclease. Proc Natl Acad Sci U S A 101: 12694-12699.

76. Bhardwaj K, Palaninathan S, Alcantara JM, Yi LL, Guarino L, et al. (2008) Structural and functional analyses of the severe acute respiratory syndrome coronavirus endoribonuclease Nsp15. J Biol Chem 283: 3655-3664.

77. Chen Y, Su C, Ke M, Jin X, Xu L, et al. (2011) Biochemical and structural insights into the mechanisms of SARS coronavirus RNA ribose 2'-O-methylation by nsp16/nsp10 protein complex. PLoS Pathog 7: e1002294.

78. Decroly E, Debarnot C, Ferron F, Bouvet M, Coutard B, et al. (2011) Crystal structure and functional analysis of the SARS-coronavirus RNA cap 2'-O-methyltransferase nsp10/nsp16 complex. PLoS Pathog 7: e1002059.

79. Decroly E, Imbert I, Coutard B, Bouvet M, Selisko B, et al. (2008) Coronavirus nonstructural protein 16 is a cap-0 binding enzyme possessing (nucleoside-2'O)-methyltransferase activity. J Virol 82: 8071-8084.

80. von Grotthuss M, Wyrwicz LS, Rychlewski L (2003) mRNA cap-1 methyltransferase in the SARS genome. Cell 113: 701-702.

81. Snijder EJ, Bredenbeek PJ, Dobbe JC, Thiel V, Ziebuhr J, et al. (2003) Unique and conserved features of genome and proteome of SARS-coronavirus, an early split-off from the coronavirus group 2 lineage. J Mol Biol 331: 991-1004.

82. Ho Y, Lin PH, Liu CY, Lee SP, Chao YC (2004) Assembly of human severe acute respiratory syndrome coronavirus-like particles. Biochem Biophys Res Commun 318: 833-838.

83. Huang Y, Yang ZY, Kong WP, Nabel GJ (2004) Generation of synthetic severe acute respiratory syndrome coronavirus pseudoparticles: implications for assembly and vaccine production. J Virol 78: 12557-12565.

84. Hatakeyama S, Matsuoka Y, Ueshiba H, Komatsu N, Itoh K, et al. (2008) Dissection and identification of regions required to form pseudoparticles by the interaction between the nucleocapsid (N) and membrane (M) proteins of SARS coronavirus. Virology 380: 99-108.

85. Siu YL, Teoh KT, Lo J, Chan CM, Kien F, et al. (2008) The M, E, and N structural proteins of the severe acute respiratory syndrome coronavirus are required for efficient assembly, trafficking, and release of virus-like particles. J Virol 82: 11318-11330.

86. Marra MA, Jones SJ, Astell CR, Holt RA, Brooks-Wilson A, et al. (2003) The Genome sequence of the SARS-associated coronavirus. Science 300: 1399-1404.

87. Nieto-Torres JL, Dediego ML, Alvarez E, Jimenez-Guardeno JM, Regla-Nava JA, et al. (2011) Subcellular location and topology of severe acute respiratory syndrome coronavirus envelope protein. Virology 415: 69-82.

88. DeDiego ML, Alvarez E, Almazan F, Rejas MT, Lamirande E, et al. (2007) A severe acute respiratory syndrome coronavirus that lacks the E gene is attenuated in vitro and in vivo. J Virol 81: 1701-1713.

89. Maeda J, Repass JF, Maeda A, Makino S (2001) Membrane topology of coronavirus E protein. Virology 281: 163-169.

90. Hsieh YC, Li HC, Chen SC, Lo SY (2008) Interactions between M protein and other structural proteins of severe, acute respiratory syndrome-associated coronavirus. J Biomed Sci 15: 707-717.

91. Chen SC, Lo SY, Ma HC, Li HC (2009) Expression and membrane integration of SARS-CoV E protein and its interaction with M protein. Virus Genes 38: 365-371.

92. Tseng YT, Wang SM, Huang KJ, Wang CT (2014) SARS-CoV envelope protein palmitoylation or nucleocapid association is not required for promoting virus-like particle production. J Biomed Sci 21: 34.

93. Shen X, Xue JH, Yu CY, Luo HB, Qin L, et al. (2003) Small envelope protein E of SARS: cloning, expression, purification, CD determination, and bioinformatics analysis. Acta Pharmacol Sin 24: 505-511.

94. Wilson L, McKinlay C, Gage P, Ewart G (2004) SARS coronavirus E protein forms cation-selective ion channels. Virology 330: 322-331.

95. Nieva JL, Madan V, Carrasco L (2012) Viroporins: structure and biological functions. Nat Rev Microbiol 10: 563-574.

96. Sze C, Tan YJ (2015) Viral Membrane Channels: Role and Function in the Virus Life Cycle. Viruses 7: 3261-3284.

97. Netland J, DeDiego ML, Zhao J, Fett C, Alvarez E, et al. (2010) Immunization with an attenuated severe acute respiratory syndrome coronavirus deleted in E protein protects against lethal respiratory disease. Virology 399: 120-128.

98. Nieto-Torres JL, DeDiego ML, Verdia-Baguena C, Jimenez-Guardeno JM, Regla-Nava JA, et al. (2014) Severe acute respiratory syndrome coronavirus envelope protein ion channel activity promotes virus fitness and pathogenesis. PLoS Pathog 10: e1004077.

99. DeDiego ML, Nieto-Torres JL, Jimenez-Guardeno JM, Regla-Nava JA, Alvarez E, et al. (2011) Severe acute respiratory syndrome coronavirus envelope protein regulates cell stress response and apoptosis. PLoS Pathog 7: e1002315.

100. Yang Y, Xiong Z, Zhang S, Yan Y, Nguyen J, et al. (2005) Bcl-xL inhibits T-cell apoptosis induced by expression of SARS coronavirus E protein in the absence of growth factors. Biochem J 392: 135-143.

101. Pervushin K, Tan E, Parthasarathy K, Lin X, Jiang FL, et al. (2009) Structure and inhibition of the SARS coronavirus envelope protein ion channel. PLoS Pathog 5: e1000511.

102. Torres J, Maheswari U, Parthasarathy K, Ng L, Liu DX, et al. (2007) Conductance and amantadine binding of a pore formed by a lysine-flanked transmembrane domain of SARS coronavirus envelope protein. Protein Sci 16: 2065-2071.

103. Voss D, Pfefferle S, Drosten C, Stevermann L, Traggiai E, et al. (2009) Studies on membrane topology, N-glycosylation and functionality of SARS-CoV membrane protein. Virol J 6: 79.

104. de Haan CA, Rottier PJ (2005) Molecular interactions in the assembly of coronaviruses. Adv Virus Res 64: 165-230.

105. Voss D, Kern A, Traggiai E, Eickmann M, Stadler K, et al. (2006) Characterization of severe acute respiratory syndrome coronavirus membrane protein. FEBS Lett 580: 968-973.

106. Nal B, Chan C, Kien F, Siu L, Tse J, et al. (2005) Differential maturation and subcellular localization of severe acute respiratory syndrome coronavirus surface proteins S, M and E. J Gen Virol 86: 1423-1434.

107. Luo H, Wu D, Shen C, Chen K, Shen X, et al. (2006) Severe acute respiratory syndrome coronavirus membrane protein interacts with nucleocapsid protein mostly through their carboxyl termini by electrostatic attraction. Int J Biochem Cell Biol 38: 589-599.

108. McBride CE, Machamer CE (2010) A single tyrosine in the severe acute respiratory syndrome coronavirus membrane protein cytoplasmic tail is important for efficient interaction with spike protein. J Virol 84: 1891-1901.

109. McBride CE, Li J, Machamer CE (2007) The cytoplasmic tail of the severe acute respiratory syndrome coronavirus spike protein contains a novel endoplasmic reticulum retrieval signal that binds COPI and promotes interaction with membrane protein. J Virol 81: 2418-2428.

110. Tseng YT, Chang CH, Wang SM, Huang KJ, Wang CT (2013) Identifying SARS-CoV membrane protein amino acid residues linked to virus-like particle assembly. PLoS One 8: e64013.

111. Tsoi H, Li L, Chen ZS, Lau KF, Tsui SK, et al. (2014) The SARS-Coronavirus Membrane protein induces apoptosis via interfering PDK1-PKB/Akt signaling. Biochem J.

112. Chan CM, Ma CW, Chan WY, Chan HY (2007) The SARS-Coronavirus Membrane protein induces apoptosis through modulating the Akt survival pathway. Arch Biochem Biophys 459: 197-207.

113. Siu KL, Chan CP, Kok KH, Chiu-Yat Woo P, Jin DY (2014) Suppression of innate antiviral response by severe acute respiratory syndrome coronavirus M protein is mediated through the first transmembrane domain. Cell Mol Immunol 11: 141-149.

114. Siu KL, Kok KH, Ng MH, Poon VK, Yuen KY, et al. (2009) Severe acute respiratory syndrome coronavirus M protein inhibits type I interferon production by impeding the formation of TRAF3.TANK.TBK1/IKKepsilon complex. J Biol Chem 284: 16202-16209.

115. Fang X, Gao J, Zheng H, Li B, Kong L, et al. (2007) The membrane protein of SARS-CoV suppresses NF-kappaB activation. J Med Virol 79: 1431-1439.

116. You J, Dove BK, Enjuanes L, DeDiego ML, Alvarez E, et al. (2005) Subcellular localization of the severe acute respiratory syndrome coronavirus nucleocapsid protein. J Gen Virol 86: 3303-3310.

117. Timani KA, Liao Q, Ye L, Zeng Y, Liu J, et al. (2005) Nuclear/nucleolar localization properties of C-terminal nucleocapsid protein of SARS coronavirus. Virus Res 114: 23-34.

118. Krokhin O, Li Y, Andonov A, Feldmann H, Flick R, et al. (2003) Mass spectrometric characterization of proteins from the SARS virus: a preliminary report. Mol Cell Proteomics 2: 346-356.

119. Li Q, Xiao H, Tam JP, Liu DX (2006) Sumoylation of the nucleocapsid protein of severe acute respiratory syndrome coronavirus by interaction with Ubc9. Adv Exp Med Biol 581: 121-126.

120. Surjit M, Kumar R, Mishra RN, Reddy MK, Chow VT, et al. (2005) The severe acute respiratory syndrome coronavirus nucleocapsid protein is phosphorylated and localizes in the cytoplasm by 14-3-3-mediated translocation. J Virol 79: 11476-11486.

121. Chang CK, Sue SC, Yu TH, Hsieh CM, Tsai CK, et al. (2006) Modular organization of SARS coronavirus nucleocapsid protein. J Biomed Sci 13: 59-72.

122. Saikatendu KS, Joseph JS, Subramanian V, Neuman BW, Buchmeier MJ, et al. (2007) Ribonucleocapsid formation of severe acute respiratory syndrome coronavirus through molecular action of the N-terminal domain of N protein. J Virol 81: 3913-3921.

123. Huang Q, Yu L, Petros AM, Gunasekera A, Liu Z, et al. (2004) Structure of the N-terminal RNA-binding domain of the SARS CoV nucleocapsid protein. Biochemistry 43: 6059-6063.

124. Surjit M, Liu B, Kumar P, Chow VT, Lal SK (2004) The nucleocapsid protein of the SARS coronavirus is capable of self-association through a C-terminal 209 amino acid interaction domain. Biochem Biophys Res Commun 317: 1030-1036.

125. Chen CY, Chang CK, Chang YW, Sue SC, Bai HI, et al. (2007) Structure of the SARS coronavirus nucleocapsid protein RNA-binding dimerization domain suggests a mechanism for helical packaging of viral RNA. J Mol Biol 368: 1075-1086.

126. Chang CK, Hsu YL, Chang YH, Chao FA, Wu MC, et al. (2009) Multiple nucleic acid binding sites and intrinsic disorder of severe acute respiratory syndrome coronavirus nucleocapsid protein: implications for ribonucleocapsid protein packaging. J Virol 83: 2255-2264.

127. Zhang X, Wu K, Wang D, Yue X, Song D, et al. (2007) Nucleocapsid protein of SARS-CoV activates interleukin-6 expression through cellular transcription factor NF-kappaB. Virology 365: 324-335.

128. Yan X, Hao Q, Mu Y, Timani KA, Ye L, et al. (2006) Nucleocapsid protein of SARS-CoV activates the expression of cyclooxygenase-2 by binding directly to regulatory elements for nuclear factor-kappa B and CCAAT/enhancer binding protein. Int J Biochem Cell Biol 38: 1417-1428.

129. He R, Leeson A, Andonov A, Li Y, Bastien N, et al. (2003) Activation of AP-1 signal transduction pathway by SARS coronavirus nucleocapsid protein. Biochem Biophys Res Commun 311: 870-876.

130. Kopecky-Bromberg SA, Martinez-Sobrido L, Frieman M, Baric RA, Palese P (2007) Severe acute respiratory syndrome coronavirus open reading frame (ORF) 3b, ORF 6, and nucleocapsid proteins function as interferon antagonists. J Virol 81: 548-557.

131. Lu X, Pan J, Tao J, Guo D (2011) SARS-CoV nucleocapsid protein antagonizes IFN-beta response by targeting initial step of IFN-beta induction pathway, and its C-terminal region is critical for the antagonism. Virus Genes 42: 37-45.

132. Zhao X, Nicholls JM, Chen YG (2008) Severe acute respiratory syndrome-associated coronavirus nucleocapsid protein interacts with Smad3 and modulates transforming growth factor-beta signaling. J Biol Chem 283: 3272-3280.

133. Cui L, Wang H, Ji Y, Yang J, Xu S, et al. (2015) The Nucleocapsid Protein of Coronaviruses Acts as a Viral Suppressor of RNA Silencing in Mammalian Cells. J Virol.

134. Surjit M, Liu B, Chow VT, Lal SK (2006) The nucleocapsid protein of severe acute respiratory syndrome-coronavirus inhibits the activity of cyclin-cyclin-dependent kinase complex and blocks S phase progression in mammalian cells. J Biol Chem 281: 10669-10681.

135. Surjit M, Liu B, Jameel S, Chow VT, Lal SK (2004) The SARS coronavirus nucleocapsid protein induces actin reorganization and apoptosis in COS-1 cells in the absence of growth factors. Biochem J 383: 13-18.

136. Zhao G, Shi SQ, Yang Y, Peng JP (2006) M and N proteins of SARS coronavirus induce apoptosis in HPF cells. Cell Biol Toxicol 22: 313-322.

137. Zhou B, Liu J, Wang Q, Liu X, Li X, et al. (2008) The nucleocapsid protein of severe acute respiratory syndrome coronavirus inhibits cell cytokinesis and proliferation by interacting with translation elongation factor 1alpha. J Virol 82: 6962-6971.

138. Luo H, Chen Q, Chen J, Chen K, Shen X, et al. (2005) The nucleocapsid protein of SARS coronavirus has a high binding affinity to the human cellular heterogeneous nuclear ribonucleoprotein A1. FEBS Lett 579: 2623-2628.

139. Wang Y, Chang Z, Ouyang J, Wei H, Yang R, et al. (2005) Profiles of IgG antibodies to nucleocapsid and spike proteins of the SARS-associated coronavirus in SARS patients. DNA Cell Biol 24: 521-527.

140. Li CK, Wu H, Yan H, Ma S, Wang L, et al. (2008) T cell responses to whole SARS coronavirus in humans. J Immunol 181: 5490-5500.

141. Tsao YP, Lin JY, Jan JT, Leng CH, Chu CC, et al. (2006) HLA-A*0201 T-cell epitopes in severe acute respiratory syndrome (SARS) coronavirus nucleocapsid and spike proteins. Biochem Biophys Res Commun 344: 63-71.

142. Oh HL, Chia A, Chang CX, Leong HN, Ling KL, et al. (2011) Engineering T cells specific for a dominant severe acute respiratory syndrome coronavirus CD8 T cell epitope. J Virol 85: 10464-10471.

143. Che XY, Hao W, Wang Y, Di B, Yin K, et al. (2004) Nucleocapsid protein as early diagnostic marker for SARS. Emerg Infect Dis 10: 1947-1949.

144. Li YH, Li J, Liu XE, Wang L, Li T, et al. (2005) Detection of the nucleocapsid protein of severe acute respiratory syndrome coronavirus in serum: comparison with results of other viral markers. J Virol Methods 130: 45-50.

145. Lin Y, Yan X, Cao W, Wang C, Feng J, et al. (2004) Probing the structure of the SARS coronavirus using scanning electron microscopy. Antivir Ther 9: 287-289.

146. Xiao X, Chakraborti S, Dimitrov AS, Gramatikoff K, Dimitrov DS (2003) The SARS-CoV S glycoprotein: expression and functional characterization. Biochem Biophys Res Commun 312: 1159-1164.

147. Du L, He Y, Zhou Y, Liu S, Zheng BJ, et al. (2009) The spike protein of SARS-CoV--a target for vaccine and therapeutic development. Nat Rev Microbiol 7: 226-236.

148. Lewicki DN, Gallagher TM (2002) Quaternary structure of coronavirus spikes in complex with carcinoembryonic antigen-related cell adhesion molecule cellular receptors. J Biol Chem 277: 19727-19734.

149. Li W, Wong SK, Li F, Kuhn JH, Huang IC, et al. (2006) Animal origins of the severe acute respiratory syndrome coronavirus: insight from ACE2-S-protein interactions. J Virol 80: 4211-4219.

150. Li W, Moore MJ, Vasilieva N, Sui J, Wong SK, et al. (2003) Angiotensin-converting enzyme 2 is a functional receptor for the SARS coronavirus. Nature 426: 450-454.

151. Wong SK, Li W, Moore MJ, Choe H, Farzan M (2004) A 193-amino acid fragment of the SARS coronavirus S protein efficiently binds angiotensin-converting enzyme 2. J Biol Chem 279: 3197-3201.

152. Chakraborti S, Prabakaran P, Xiao X, Dimitrov DS (2005) The SARS coronavirus S glycoprotein receptor binding domain: fine mapping and functional characterization. Virol J 2: 73.

153. Li F, Li W, Farzan M, Harrison SC (2005) Structure of SARS coronavirus spike receptor-binding domain complexed with receptor. Science 309: 1864-1868.

154. Jeffers SA, Tusell SM, Gillim-Ross L, Hemmila EM, Achenbach JE, et al. (2004) CD209L (L-SIGN) is a receptor for severe acute respiratory syndrome coronavirus. Proc Natl Acad Sci U S A 101: 15748-15753.

155. Yang ZY, Huang Y, Ganesh L, Leung K, Kong WP, et al. (2004) pH-dependent entry of severe acute respiratory syndrome coronavirus is mediated by the spike glycoprotein and enhanced by dendritic cell transfer through DC-SIGN. J Virol 78: 5642-5650.

156. Marzi A, Gramberg T, Simmons G, Moller P, Rennekamp AJ, et al. (2004) DC-SIGN and DC-SIGNR interact with the glycoprotein of Marburg virus and the S protein of severe acute respiratory syndrome coronavirus. J Virol 78: 12090-12095.

157. Gramberg T, Hofmann H, Moller P, Lalor PF, Marzi A, et al. (2005) LSECtin interacts with filovirus glycoproteins and the spike protein of SARS coronavirus. Virology 340: 224-236.

158. Colman PM, Lawrence MC (2003) The structural biology of type I viral membrane fusion. Nat Rev Mol Cell Biol 4: 309-319.

159. Tripet B, Howard MW, Jobling M, Holmes RK, Holmes KV, et al. (2004) Structural characterization of the SARS-coronavirus spike S fusion protein core. J Biol Chem 279: 20836-20849.

160. Xu Y, Zhu J, Liu Y, Lou Z, Yuan F, et al. (2004) Characterization of the heptad repeat regions, HR1 and HR2, and design of a fusion core structure model of the spike protein from severe acute respiratory syndrome (SARS) coronavirus. Biochemistry 43: 14064-14071.

161. Hofmann H, Pohlmann S (2004) Cellular entry of the SARS coronavirus. Trends Microbiol 12: 466-472.

162. McReynolds S, Jiang S, Guo Y, Celigoy J, Schar C, et al. (2008) Characterization of the prefusion and transition states of severe acute respiratory syndrome coronavirus S2-HR2. Biochemistry 47: 6802-6808.

163. Ingallinella P, Bianchi E, Finotto M, Cantoni G, Eckert DM, et al. (2004) Structural characterization of the fusion-active complex of severe acute respiratory syndrome (SARS) coronavirus. Proc Natl Acad Sci U S A 101: 8709-8714.

164. Xu Y, Lou Z, Liu Y, Pang H, Tien P, et al. (2004) Crystal structure of severe acute respiratory syndrome coronavirus spike protein fusion core. J Biol Chem 279: 49414-49419.

165. Spiga O, Bernini A, Ciutti A, Chiellini S, Menciassi N, et al. (2003) Molecular modelling of S1 and S2 subunits of SARS coronavirus spike glycoprotein. Biochem Biophys Res Commun 310: 78-83.

166. White JM, Delos SE, Brecher M, Schornberg K (2008) Structures and mechanisms of viral membrane fusion proteins: multiple variations on a common theme. Crit Rev Biochem Mol Biol 43: 189-219.

167. Hofmann H, Hattermann K, Marzi A, Gramberg T, Geier M, et al. (2004) S protein of severe acute respiratory syndrome-associated coronavirus mediates entry into hepatoma cell lines and is targeted by neutralizing antibodies in infected patients. J Virol 78: 6134-6142.

168. Simmons G, Gosalia DN, Rennekamp AJ, Reeves JD, Diamond SL, et al. (2005) Inhibitors of cathepsin L prevent severe acute respiratory syndrome coronavirus entry. Proc Natl Acad Sci U S A 102: 11876-11881.

169. Bosch BJ, Bartelink W, Rottier PJ (2008) Cathepsin L functionally cleaves the severe acute respiratory syndrome coronavirus class I fusion protein upstream of rather than adjacent to the fusion peptide. J Virol 82: 8887-8890.

170. Simmons G, Reeves JD, Rennekamp AJ, Amberg SM, Piefer AJ, et al. (2004) Characterization of severe acute respiratory syndrome-associated coronavirus (SARS-CoV) spike glycoprotein-mediated viral entry. Proc Natl Acad Sci U S A 101: 4240-4245.

171. Belouzard S, Chu VC, Whittaker GR (2009) Activation of the SARS coronavirus spike protein via sequential proteolytic cleavage at two distinct sites. Proc Natl Acad Sci U S A 106: 5871-5876.

172. Belouzard S, Madu I, Whittaker GR (2010) Elastase-mediated activation of the severe acute respiratory syndrome coronavirus spike protein at discrete sites within the S2 domain. J Biol Chem 285: 22758-22763.

173. Bottcher E, Matrosovich T, Beyerle M, Klenk HD, Garten W, et al. (2006) Proteolytic activation of influenza viruses by serine proteases TMPRSS2 and HAT from human airway epithelium. J Virol 80: 9896-9898.

174. Glowacka I, Bertram S, Muller MA, Allen P, Soilleux E, et al. (2011) Evidence that TMPRSS2 activates the severe acute respiratory syndrome coronavirus spike protein for membrane fusion and reduces viral control by the humoral immune response. J Virol 85: 4122-4134.

175. Bertram S, Glowacka I, Muller MA, Lavender H, Gnirss K, et al. (2011) Cleavage and activation of the severe acute respiratory syndrome coronavirus spike protein by human airway trypsin-like protease. J Virol 85: 13363-13372.

176. Kawase M, Shirato K, van der Hoek L, Taguchi F, Matsuyama S (2012) Simultaneous treatment of human bronchial epithelial cells with serine and cysteine protease inhibitors prevents severe acute respiratory syndrome coronavirus entry. J Virol 86: 6537-6545.

177. Simmons G, Zmora P, Gierer S, Heurich A, Pohlmann S (2013) Proteolytic activation of the SARS-coronavirus spike protein: cutting enzymes at the cutting edge of antiviral research. Antiviral Res 100: 605-614.

178. Bosch BJ, Martina BE, Van Der Zee R, Lepault J, Haijema BJ, et al. (2004) Severe acute respiratory syndrome coronavirus (SARS-CoV) infection inhibition using spike protein heptad repeat-derived peptides. Proc Natl Acad Sci U S A 101: 8455-8460.

179. Sainz B, Jr., Rausch JM, Gallaher WR, Garry RF, Wimley WC (2005) Identification and characterization of the putative fusion peptide of the severe acute respiratory syndrome-associated coronavirus spike protein. J Virol 79: 7195-7206.

180. Madu IG, Roth SL, Belouzard S, Whittaker GR (2009) Characterization of a highly conserved domain within the severe acute respiratory syndrome coronavirus spike protein S2 domain with characteristics of a viral fusion peptide. J Virol 83: 7411-7421.

181. Belouzard S, Millet JK, Licitra BN, Whittaker GR (2012) Mechanisms of coronavirus cell entry mediated by the viral spike protein. Viruses 4: 1011-1033.

182. Howard MW, Travanty EA, Jeffers SA, Smith MK, Wennier ST, et al. (2008) Aromatic amino acids in the juxtamembrane domain of severe acute respiratory syndrome coronavirus spike glycoprotein are important for receptor-dependent virus entry and cell-cell fusion. J Virol 82: 2883-2894.

183. Broer R, Boson B, Spaan W, Cosset FL, Corver J (2006) Important role for the transmembrane domain of severe acute respiratory syndrome coronavirus spike protein during entry. J Virol 80: 1302-1310.

184. Petit CM, Chouljenko VN, Iyer A, Colgrove R, Farzan M, et al. (2007) Palmitoylation of the cysteine-rich endodomain of the SARS-coronavirus spike glycoprotein is important for spike-mediated cell fusion. Virology 360: 264-274.

185. Lu Y, Neo TL, Liu DX, Tam JP (2008) Importance of SARS-CoV spike protein Trp-rich region in viral infectivity. Biochem Biophys Res Commun 371: 356-360.

186. Dosch SF, Mahajan SD, Collins AR (2009) SARS coronavirus spike protein-induced innate immune response occurs via activation of the NF-kappaB pathway in human monocyte macrophages in vitro. Virus Res 142: 19-27.

187. Chen IY, Chang SC, Wu HY, Yu TC, Wei WC, et al. (2010) Upregulation of the chemokine (C-C motif) ligand 2 via a severe acute respiratory syndrome coronavirus spike-ACE2 signaling pathway. J Virol 84: 7703-7712.

188. Coughlin MM, Prabhakar BS (2012) Neutralizing human monoclonal antibodies to severe acute respiratory syndrome coronavirus: target, mechanism of action, and therapeutic potential. Rev Med Virol 22: 2-17.

189. Coughlin MM, Babcook J, Prabhakar BS (2009) Human monoclonal antibodies to SARS-coronavirus inhibit infection by different mechanisms. Virology 394: 39-46.

190. Wang YD, Sin WY, Xu GB, Yang HH, Wong TY, et al. (2004) T-cell epitopes in severe acute respiratory syndrome (SARS) coronavirus spike protein elicit a specific T-cell immune response in patients who recover from SARS. J Virol 78: 5612-5618.

191. Channappanavar R, Zhao J, Perlman S (2014) T cell-mediated immune response to respiratory coronaviruses. Immunol Res 59: 118-128.

192. Zhao K, Yang B, Xu Y, Wu C (2010) CD8+ T cell response in HLA-A*0201 transgenic mice is elicited by epitopes from SARS-CoV S protein. Vaccine 28: 6666-6674.

193. Struck AW, Axmann M, Pfefferle S, Drosten C, Meyer B (2012) A hexapeptide of the receptor-binding domain of SARS corona virus spike protein blocks viral entry into host cells via the human receptor ACE2. Antiviral Res 94: 288-296.

194. Han DP, Penn-Nicholson A, Cho MW (2006) Identification of critical determinants on ACE2 for SARS-CoV entry and development of a potent entry inhibitor. Virology 350: 15-25.

195. Ujike M, Nishikawa H, Otaka A, Yamamoto N, Matsuoka M, et al. (2008) Heptad repeat-derived peptides block protease-mediated direct entry from the cell surface of severe acute respiratory syndrome coronavirus but not entry via the endosomal pathway. J Virol 82: 588-592.

196. Liu S, Xiao G, Chen Y, He Y, Niu J, et al. (2004) Interaction between heptad repeat 1 and 2 regions in spike protein of SARS-associated coronavirus: implications for virus fusogenic mechanism and identification of fusion inhibitors. Lancet 363: 938-947.

197. Zheng BJ, Guan Y, Hez ML, Sun H, Du L, et al. (2005) Synthetic peptides outside the spike protein heptad repeat regions as potent inhibitors of SARS-associated coronavirus. Antivir Ther 10: 393-403.

198. Adedeji AO, Severson W, Jonsson C, Singh K, Weiss SR, et al. (2013) Novel inhibitors of severe acute respiratory syndrome coronavirus entry that act by three distinct mechanisms. J Virol 87: 8017-8028.

199. Elshabrawy HA, Fan J, Haddad CS, Ratia K, Broder CC, et al. (2014) Identification of a broad-spectrum antiviral small molecule against severe acute respiratory syndrome coronavirus and Ebola, Hendra, and Nipah viruses by using a novel high-throughput screening assay. J Virol 88: 4353-4365.

200. Ho TY, Wu SL, Chen JC, Li CC, Hsiang CY (2007) Emodin blocks the SARS coronavirus spike protein and angiotensin-converting enzyme 2 interaction. Antiviral Res 74: 92-101.

201. Keng CT, Zhang A, Shen S, Lip KM, Fielding BC, et al. (2005) Amino acids 1055 to 1192 in the S2 region of severe acute respiratory syndrome coronavirus S protein induce neutralizing antibodies: implications for the development of vaccines and antiviral agents. J Virol 79: 3289-3296.

202. Coughlin M, Lou G, Martinez O, Masterman SK, Olsen OA, et al. (2007) Generation and characterization of human monoclonal neutralizing antibodies with distinct binding and sequence features against SARS coronavirus using XenoMouse. Virology 361: 93-102.

203. Traggiai E, Becker S, Subbarao K, Kolesnikova L, Uematsu Y, et al. (2004) An efficient method to make human monoclonal antibodies from memory B cells: potent neutralization of SARS coronavirus. Nat Med 10: 871-875.

204. He Y, Zhou Y, Siddiqui P, Jiang S (2004) Inactivated SARS-CoV vaccine elicits high titers of spike protein-specific antibodies that block receptor binding and virus entry. Biochem Biophys Res Commun 325: 445-452.

205. Czub M, Weingartl H, Czub S, He R, Cao J (2005) Evaluation of modified vaccinia virus Ankara based recombinant SARS vaccine in ferrets. Vaccine 23: 2273-2279.

206. Du L, Zhao G, Lin Y, Sui H, Chan C, et al. (2008) Intranasal vaccination of recombinant adeno-associated virus encoding receptor-binding domain of severe acute respiratory syndrome coronavirus (SARS-CoV) spike protein induces strong mucosal immune responses and provides long-term protection against SARS-CoV infection. J Immunol 180: 948-956.

207. Yang ZY, Kong WP, Huang Y, Roberts A, Murphy BR, et al. (2004) A DNA vaccine induces SARS coronavirus neutralization and protective immunity in mice. Nature 428: 561-564.

208. Huang J, Cao Y, Du J, Bu X, Ma R, et al. (2007) Priming with SARS CoV S DNA and boosting with SARS CoV S epitopes specific for CD4+ and CD8+ T cells promote cellular immune responses. Vaccine 25: 6981-6991.

209. Du L, Zhao G, He Y, Guo Y, Zheng BJ, et al. (2007) Receptor-binding domain of SARS-CoV spike protein induces long-term protective immunity in an animal model. Vaccine 25: 2832-2838.

210. Li J, Ulitzky L, Silberstein E, Taylor DR, Viscidi R (2013) Immunogenicity and protection efficacy of monomeric and trimeric recombinant SARS coronavirus spike protein subunit vaccine candidates. Viral Immunol 26: 126-132.

211. Bai B, Lu X, Meng J, Hu Q, Mao P, et al. (2008) Vaccination of mice with recombinant baculovirus expressing spike or nucleocapsid protein of SARS-like coronavirus generates humoral and cellular immune responses. Mol Immunol 45: 868-875.

212. Tan YJ, Lim SG, Hong W (2006) Understanding the accessory viral proteins unique to the severe acute respiratory syndrome (SARS) coronavirus. Antiviral Res 72: 78-88.

213. McBride R, Fielding BC (2012) The role of severe acute respiratory syndrome (SARS)-coronavirus accessory proteins in virus pathogenesis. Viruses 4: 2902-2923.

214. Curtis KM, Yount B, Baric RS (2002) Heterologous gene expression from transmissible gastroenteritis virus replicon particles. J Virol 76: 1422-1434.

215. de Haan CA, Masters PS, Shen X, Weiss S, Rottier PJ (2002) The group-specific murine coronavirus genes are not essential, but their deletion, by reverse genetics, is attenuating in the natural host. Virology 296: 177-189.

216. Yount B, Roberts RS, Sims AC, Deming D, Frieman MB, et al. (2005) Severe acute respiratory syndrome coronavirus group-specific open reading frames encode nonessential functions for replication in cell cultures and mice. J Virol 79: 14909-14922.

217. Narayanan K, Huang C, Makino S (2008) SARS coronavirus accessory proteins. Virus Res 133: 113-121.

218. Oostra M, de Haan CA, de Groot RJ, Rottier PJ (2006) Glycosylation of the severe acute respiratory syndrome coronavirus triple-spanning membrane proteins 3a and M. J Virol 80: 2326-2336.

219. Ito N, Mossel EC, Narayanan K, Popov VL, Huang C, et al. (2005) Severe acute respiratory syndrome coronavirus 3a protein is a viral structural protein. J Virol 79: 3182-3186.

220. Yuan X, Li J, Shan Y, Yang Z, Zhao Z, et al. (2005) Subcellular localization and membrane association of SARS-CoV 3a protein. Virus Res 109: 191-202.

221. Yu CJ, Chen YC, Hsiao CH, Kuo TC, Chang SC, et al. (2004) Identification of a novel protein 3a from severe acute respiratory syndrome coronavirus. FEBS Lett 565: 111-116.

222. Tan YJ, Teng E, Shen S, Tan TH, Goh PY, et al. (2004) A novel severe acute respiratory syndrome coronavirus protein, U274, is transported to the cell surface and undergoes endocytosis. J Virol 78: 6723-6734.

223. Tan YJ (2005) The Severe Acute Respiratory Syndrome (SARS)-coronavirus 3a protein may function as a modulator of the trafficking properties of the spike protein. Virol J 2: 5.

224. Sharma K, Surjit M, Satija N, Liu B, Chow VT, et al. (2007) The 3a accessory protein of SARS coronavirus specifically interacts with the 5'UTR of its genomic RNA, Using a unique 75 amino acid interaction domain. Biochemistry 46: 6488-6499.

225. Lu W, Zheng BJ, Xu K, Schwarz W, Du L, et al. (2006) Severe acute respiratory syndrome-associated coronavirus 3a protein forms an ion channel and modulates virus release. Proc Natl Acad Sci U S A 103: 12540-12545.

226. von Brunn A, Teepe C, Simpson JC, Pepperkok R, Friedel CC, et al. (2007) Analysis of intraviral protein-protein interactions of the SARS coronavirus ORFeome. PLoS One 2: e459.

227. Lu B, Tao L, Wang T, Zheng Z, Li B, et al. (2009) Humoral and cellular immune responses induced by 3a DNA vaccines against severe acute respiratory syndrome (SARS) or SARS-like coronavirus in mice. Clin Vaccine Immunol 16: 73-77.

228. Kanzawa N, Nishigaki K, Hayashi T, Ishii Y, Furukawa S, et al. (2006) Augmentation of chemokine production by severe acute respiratory syndrome coronavirus 3a/X1 and 7a/X4 proteins through NF-kappaB activation. FEBS Lett 580: 6807-6812.

229. Minakshi R, Padhan K, Rani M, Khan N, Ahmad F, et al. (2009) The SARS Coronavirus 3a protein causes endoplasmic reticulum stress and induces ligand-independent downregulation of the type 1 interferon receptor. PLoS One 4: e8342.

230. Chan CM, Tsoi H, Chan WM, Zhai S, Wong CO, et al. (2009) The ion channel activity of the SARS-coronavirus 3a protein is linked to its pro-apoptotic function. Int J Biochem Cell Biol 41: 2232-2239.

231. Yuan X, Yao Z, Wu J, Zhou Y, Shan Y, et al. (2007) G1 phase cell cycle arrest induced by SARS-CoV 3a protein via the cyclin D3/pRb pathway. Am J Respir Cell Mol Biol 37: 9-19.

232. Law PT, Wong CH, Au TC, Chuck CP, Kong SK, et al. (2005) The 3a protein of severe acute respiratory syndrome-associated coronavirus induces apoptosis in Vero E6 cells. J Gen Virol 86: 1921-1930.

233. Padhan K, Minakshi R, Towheed MA, Jameel S (2008) Severe acute respiratory syndrome coronavirus 3a protein activates the mitochondrial death pathway through p38 MAP kinase activation. J Gen Virol 89: 1960-1969.

234. Rota PA, Oberste MS, Monroe SS, Nix WA, Campagnoli R, et al. (2003) Characterization of a novel coronavirus associated with severe acute respiratory syndrome. Science 300: 1394-1399.

235. Yuan X, Shan Y, Yao Z, Li J, Zhao Z, et al. (2006) Mitochondrial location of severe acute respiratory syndrome coronavirus 3b protein. Mol Cells 21: 186-191.

236. Freundt EC, Yu L, Park E, Lenardo MJ, Xu XN (2009) Molecular determinants for subcellular localization of the severe acute respiratory syndrome coronavirus open reading frame 3b protein. J Virol 83: 6631-6640.

237. Yuan X, Yao Z, Shan Y, Chen B, Yang Z, et al. (2005) Nucleolar localization of non-structural protein 3b, a protein specifically encoded by the severe acute respiratory syndrome coronavirus. Virus Res 114: 70-79.

238. Guo JP, Petric M, Campbell W, McGeer PL (2004) SARS corona virus peptides recognized by antibodies in the sera of convalescent cases. Virology 324: 251-256.

239. Khan S, Fielding BC, Tan TH, Chou CF, Shen S, et al. (2006) Over-expression of severe acute respiratory syndrome coronavirus 3b protein induces both apoptosis and necrosis in Vero E6 cells. Virus Res 122: 20-27.

240. Spiegel M, Pichlmair A, Martinez-Sobrido L, Cros J, Garcia-Sastre A, et al. (2005) Inhibition of Beta interferon induction by severe acute respiratory syndrome coronavirus suggests a two-step model for activation of interferon regulatory factor 3. J Virol 79: 2079-2086.

241. Yuan X, Shan Y, Zhao Z, Chen J, Cong Y (2005) G0/G1 arrest and apoptosis induced by SARS-CoV 3b protein in transfected cells. Virol J 2: 66.

242. Huang C, Peters CJ, Makino S (2007) Severe acute respiratory syndrome coronavirus accessory protein 6 is a virion-associated protein and is released from 6 protein-expressing cells. J Virol 81: 5423-5426.

243. Geng H, Liu YM, Chan WS, Lo AW, Au DM, et al. (2005) The putative protein 6 of the severe acute respiratory syndrome-associated coronavirus: expression and functional characterization. FEBS Lett 579: 6763-6768.

244. Zhao J, Falcon A, Zhou H, Netland J, Enjuanes L, et al. (2009) Severe acute respiratory syndrome coronavirus protein 6 is required for optimal replication. J Virol 83: 2368-2373.

245. Nelson CA, Pekosz A, Lee CA, Diamond MS, Fremont DH (2005) Structure and intracellular targeting of the SARS-coronavirus Orf7a accessory protein. Structure 13: 75-85.

246. Huang C, Ito N, Tseng CT, Makino S (2006) Severe acute respiratory syndrome coronavirus 7a accessory protein is a viral structural protein. J Virol 80: 7287-7294.

247. Tan YJ, Fielding BC, Goh PY, Shen S, Tan TH, et al. (2004) Overexpression of 7a, a protein specifically encoded by the severe acute respiratory syndrome coronavirus, induces apoptosis via a caspase-dependent pathway. J Virol 78: 14043-14047.

248. Kopecky-Bromberg SA, Martinez-Sobrido L, Palese P (2006) 7a protein of severe acute respiratory syndrome coronavirus inhibits cellular protein synthesis and activates p38 mitogen-activated protein kinase. J Virol 80: 785-793.

249. Yuan X, Wu J, Shan Y, Yao Z, Dong B, et al. (2006) SARS coronavirus 7a protein blocks cell cycle progression at G0/G1 phase via the cyclin D3/pRb pathway. Virology 346: 74-85.

250. Schaecher SR, Mackenzie JM, Pekosz A (2007) The ORF7b protein of severe acute respiratory syndrome coronavirus (SARS-CoV) is expressed in virus-infected cells and incorporated into SARS-CoV particles. J Virol 81: 718-731.

251. Guan Y, Zheng BJ, He YQ, Liu XL, Zhuang ZX, et al. (2003) Isolation and characterization of viruses related to the SARS coronavirus from animals in southern China. Science 302: 276-278.

252. Chen CY, Ping YH, Lee HC, Chen KH, Lee YM, et al. (2007) Open reading frame 8a of the human severe acute respiratory syndrome coronavirus not only promotes viral replication but also induces apoptosis. J Infect Dis 196: 405-415.

253. Law PY, Liu YM, Geng H, Kwan KH, Waye MM, et al. (2006) Expression and functional characterization of the putative protein 8b of the severe acute respiratory syndrome-associated coronavirus. FEBS Lett 580: 3643-3648.

254. Keng CT, Choi YW, Welkers MR, Chan DZ, Shen S, et al. (2006) The human severe acute respiratory syndrome coronavirus (SARS-CoV) 8b protein is distinct from its counterpart in animal SARS-CoV and down-regulates the expression of the envelope protein in infected cells. Virology 354: 132-142.

255. Le TM, Wong HH, Tay FP, Fang S, Keng CT, et al. (2007) Expression, post-translational modification and biochemical characterization of proteins encoded by subgenomic mRNA8 of the severe acute respiratory syndrome coronavirus. FEBS J 274: 4211-4222.

256. Moshynskyy I, Viswanathan S, Vasilenko N, Lobanov V, Petric M, et al. (2007) Intracellular localization of the SARS coronavirus protein 9b: evidence of active export from the nucleus. Virus Res 127: 116-121.

257. Meier C, Aricescu AR, Assenberg R, Aplin RT, Gilbert RJ, et al. (2006) The crystal structure of ORF-9b, a lipid binding protein from the SARS coronavirus. Structure 14: 1157-1165.

258. Qiu M, Shi Y, Guo Z, Chen Z, He R, et al. (2005) Antibody responses to individual proteins of SARS coronavirus and their neutralization activities. Microbes Infect 7: 882-889.

259. Liang G, Chen Q, Xu J, Liu Y, Lim W, et al. (2004) Laboratory diagnosis of four recent sporadic cases of community-acquired SARS, Guangdong Province, China. Emerg Infect Dis 10: 1774-1781.

260. Li W, Zhang C, Sui J, Kuhn JH, Moore MJ, et al. (2005) Receptor and viral determinants of SARS-coronavirus adaptation to human ACE2. EMBO J 24: 1634-1643.

261. Qu XX, Hao P, Song XJ, Jiang SM, Liu YX, et al. (2005) Identification of two critical amino acid residues of the severe acute respiratory syndrome coronavirus spike protein for its variation in zoonotic tropism transition via a double substitution strategy. J Biol Chem 280: 29588-29595.

262. Li F (2008) Structural analysis of major species barriers between humans and palm civets for severe acute respiratory syndrome coronavirus infections. J Virol 82: 6984-6991.

263. Kan B, Wang M, Jing H, Xu H, Jiang X, et al. (2005) Molecular evolution analysis and geographic investigation of severe acute respiratory syndrome coronavirus-like virus in palm civets at an animal market and on farms. J Virol 79: 11892-11900.

264. Song HD, Tu CC, Zhang GW, Wang SY, Zheng K, et al. (2005) Cross-host evolution of severe acute respiratory syndrome coronavirus in palm civet and human. Proc Natl Acad Sci U S A 102: 2430-2435.

265. Li W, Shi Z, Yu M, Ren W, Smith C, et al. (2005) Bats are natural reservoirs of SARS-like coronaviruses. Science 310: 676-679.

266. Lau SK, Woo PC, Li KS, Huang Y, Tsoi HW, et al. (2005) Severe acute respiratory syndrome coronavirus-like virus in Chinese horseshoe bats. Proc Natl Acad Sci U S A 102: 14040-14045.

267. Ren W, Li W, Yu M, Hao P, Zhang Y, et al. (2006) Full-length genome sequences of two SARS-like coronaviruses in horseshoe bats and genetic variation analysis. J Gen Virol 87: 3355-3359.

268. Ren W, Qu X, Li W, Han Z, Yu M, et al. (2008) Difference in receptor usage between severe acute respiratory syndrome (SARS) coronavirus and SARS-like coronavirus of bat origin. J Virol 82: 1899-1907.

269. Drexler JF, Corman VM, Drosten C (2014) Ecology, evolution and classification of bat coronaviruses in the aftermath of SARS. Antiviral Res 101: 45-56.

270. Bolles M, Donaldson E, Baric R (2011) SARS-CoV and emergent coronaviruses: viral determinants of interspecies transmission. Curr Opin Virol 1: 624-634.

271. Ge XY, Li JL, Yang XL, Chmura AA, Zhu G, et al. (2013) Isolation and characterization of a bat SARS-like coronavirus that uses the ACE2 receptor. Nature 503: 535-538.

272. Zaki AM, van Boheemen S, Bestebroer TM, Osterhaus AD, Fouchier RA (2012) Isolation of a novel coronavirus from a man with pneumonia in Saudi Arabia. N Engl J Med 367: 1814-1820.

273. de Groot RJ, Baker SC, Baric RS, Brown CS, Drosten C, et al. (2013) Middle East respiratory syndrome coronavirus (MERS-CoV): announcement of the Coronavirus Study Group. J Virol 87: 7790-7792.

274. (2015) Middle East respiratory syndrome coronavirus (MERS-CoV) http://www.wpro.who.int/outbreaks_emergencies/wpro_coronavirus/en/. World Health Organization

275. Al-Tawfiq JA, Memish ZA (2015) An update on Middle East respiratory syndrome: 2 years later. Expert Rev Respir Med 9: 327-335.

276. Assiri A, McGeer A, Perl TM, Price CS, Al Rabeeah AA, et al. (2013) Hospital outbreak of Middle East respiratory syndrome coronavirus. N Engl J Med 369: 407-416.

277. Drosten C, Meyer B, Muller MA, Corman VM, Al-Masri M, et al. (2014) Transmission of MERS-coronavirus in household contacts. N Engl J Med 371: 828-835.

278. Hui DS, Memish ZA, Zumla A (2014) Severe acute respiratory syndrome vs. the Middle East respiratory syndrome. Curr Opin Pulm Med 20: 233-241.

279. Assiri A, Al-Tawfiq JA, Al-Rabeeah AA, Al-Rabiah FA, Al-Hajjar S, et al. (2013) Epidemiological, demographic, and clinical characteristics of 47 cases of Middle East respiratory syndrome coronavirus disease from Saudi Arabia: a descriptive study. Lancet Infect Dis 13: 752-761.

280. Arabi YM, Arifi AA, Balkhy HH, Najm H, Aldawood AS, et al. (2014) Clinical course and outcomes of critically ill patients with Middle East respiratory syndrome coronavirus infection. Ann Intern Med 160: 389-397.

281. Al-Abdallat MM, Payne DC, Alqasrawi S, Rha B, Tohme RA, et al. (2014) Hospital-associated outbreak of Middle East respiratory syndrome coronavirus: a serologic, epidemiologic, and clinical description. Clin Infect Dis 59: 1225-1233.

282. Breban R, Riou J, Fontanet A (2013) Interhuman transmissibility of Middle East respiratory syndrome coronavirus: estimation of pandemic risk. Lancet 382: 694-699.

283. de Wilde AH, Raj VS, Oudshoorn D, Bestebroer TM, van Nieuwkoop S, et al. (2013) MERS-coronavirus replication induces severe in vitro cytopathology and is strongly inhibited by cyclosporin A or interferon-alpha treatment. J Gen Virol 94: 1749-1760.

284. Falzarano D, de Wit E, Martellaro C, Callison J, Munster VJ, et al. (2013) Inhibition of novel beta coronavirus replication by a combination of interferon-alpha2b and ribavirin. Sci Rep 3: 1686.

285. Spanakis N, Tsiodras S, Haagmans BL, Raj VS, Pontikis K, et al. (2014) Virological and serological analysis of a recent Middle East respiratory syndrome coronavirus infection case on a triple combination antiviral regimen. Int J Antimicrob Agents 44: 528-532.

286. de Wilde AH, Jochmans D, Posthuma CC, Zevenhoven-Dobbe JC, van Nieuwkoop S, et al. (2014) Screening of an FDA-approved compound library identifies four small-molecule inhibitors of Middle East respiratory syndrome coronavirus replication in cell culture. Antimicrob Agents Chemother 58: 4875-4884.

287. Chan JF, Lau SK, To KK, Cheng VC, Woo PC, et al. (2015) Middle East respiratory syndrome coronavirus: another zoonotic betacoronavirus causing SARS-like disease. Clin Microbiol Rev 28: 465-522.

288. van Boheemen S, de Graaf M, Lauber C, Bestebroer TM, Raj VS, et al. (2012) Genomic characterization of a newly discovered coronavirus associated with acute respiratory distress syndrome in humans. MBio 3.

289. Kilianski A, Mielech AM, Deng X, Baker SC (2013) Assessing activity and inhibition of Middle East respiratory syndrome coronavirus papain-like and 3C-like proteases using luciferase-based biosensors. J Virol 87: 11955-11962.

290. Yang X, Chen X, Bian G, Tu J, Xing Y, et al. (2014) Proteolytic processing, deubiquitinase and interferon antagonist activities of Middle East respiratory syndrome coronavirus papain-like protease. J Gen Virol 95: 614-626.

291. Bailey-Elkin BA, Knaap RC, Johnson GG, Dalebout TJ, Ninaber DK, et al. (2014) Crystal structure of the Middle East respiratory syndrome coronavirus (MERS-CoV) papain-like protease bound to ubiquitin facilitates targeted disruption of deubiquitinating activity to demonstrate its role in innate immune suppression. J Biol Chem 289: 34667-34682.

292. Baez-Santos YM, Mielech AM, Deng X, Baker S, Mesecar AD (2014) Catalytic function and substrate specificity of the papain-like protease domain of nsp3 from the Middle East respiratory syndrome coronavirus. J Virol 88: 12511-12527.

293. Tomar S, Johnston ML, St John SE, Osswald HL, Nyalapatla PR, et al. (2015) Ligand-induced dimerization of MERS coronavirus nsp5 protease (3CLpro): implications for nsp5 regulation and the development of antivirals. J Biol Chem.

294. Wu A, Wang Y, Zeng C, Huang X, Xu S, et al. (2015) Prediction and biochemical analysis of putative cleavage sites of the 3C-like protease of Middle East respiratory syndrome coronavirus. Virus Res 208: 56-65.

295. Du L, Zhao G, Kou Z, Ma C, Sun S, et al. (2013) Identification of a receptor-binding domain in the S protein of the novel human coronavirus Middle East respiratory syndrome coronavirus as an essential target for vaccine development. J Virol 87: 9939-9942.

296. Qian Z, Dominguez SR, Holmes KV (2013) Role of the spike glycoprotein of human Middle East respiratory syndrome coronavirus (MERS-CoV) in virus entry and syncytia formation. PLoS One 8: e76469.

297. Raj VS, Mou H, Smits SL, Dekkers DH, Muller MA, et al. (2013) Dipeptidyl peptidase 4 is a functional receptor for the emerging human coronavirus-EMC. Nature 495: 251-254.

298. Mou H, Raj VS, van Kuppeveld FJ, Rottier PJ, Haagmans BL, et al. (2013) The receptor binding domain of the new Middle East respiratory syndrome coronavirus maps to a 231-residue region in the spike protein that efficiently elicits neutralizing antibodies. J Virol 87: 9379-9383.

299. Du L, Kou Z, Ma C, Tao X, Wang L, et al. (2013) A truncated receptor-binding domain of MERS-CoV spike protein potently inhibits MERS-CoV infection and induces strong neutralizing antibody responses: implication for developing therapeutics and vaccines. PLoS One 8: e81587.

300. Kim E, Okada K, Kenniston T, Raj VS, AlHajri MM, et al. (2014) Immunogenicity of an adenoviral-based Middle East Respiratory Syndrome coronavirus vaccine in BALB/c mice. Vaccine 32: 5975-5982.

301. Millet JK, Whittaker GR (2014) Host cell entry of Middle East respiratory syndrome coronavirus after two-step, furin-mediated activation of the spike protein. Proc Natl Acad Sci U S A 111: 15214-15219.

302. Shirato K, Kawase M, Matsuyama S (2013) Middle East respiratory syndrome coronavirus infection mediated by the transmembrane serine protease TMPRSS2. J Virol 87: 12552-12561.

303. Xia S, Liu Q, Wang Q, Sun Z, Su S, et al. (2014) Middle East respiratory syndrome coronavirus (MERS-CoV) entry inhibitors targeting spike protein. Virus Res 194: 200-210.

304. Lu L, Liu Q, Zhu Y, Chan KH, Qin L, et al. (2014) Structure-based discovery of Middle East respiratory syndrome coronavirus fusion inhibitor. Nat Commun 5: 3067.

305. Surya W, Li Y, Verdia-Baguena C, Aguilella VM, Torres J (2015) MERS coronavirus envelope protein has a single transmembrane domain that forms pentameric ion channels. Virus Res 201: 61-66.

306. Almazan F, DeDiego ML, Sola I, Zuniga S, Nieto-Torres JL, et al. (2013) Engineering a replication-competent, propagation-defective Middle East respiratory syndrome coronavirus as a vaccine candidate. MBio 4: e00650-00613.

307. Yang Y, Zhang L, Geng H, Deng Y, Huang B, et al. (2013) The structural and accessory proteins M, ORF 4a, ORF 4b, and ORF 5 of Middle East respiratory syndrome coronavirus (MERS-CoV) are potent interferon antagonists. Protein Cell 4: 951-961.

308. Papaneri AB, Johnson RF, Wada J, Bollinger L, Jahrling PB, et al. (2015) Middle East respiratory syndrome: obstacles and prospects for vaccine development. Expert Rev Vaccines 14: 949-962.

309. Siu KL, Yeung ML, Kok KH, Yuen KS, Kew C, et al. (2014) Middle east respiratory syndrome coronavirus 4a protein is a double-stranded RNA-binding protein that suppresses PACT-induced activation of RIG-I and MDA5 in the innate antiviral response. J Virol 88: 4866-4876.

310. Matthews KL, Coleman CM, van der Meer Y, Snijder EJ, Frieman MB (2014) The ORF4b-encoded accessory proteins of Middle East respiratory syndrome coronavirus and two related bat coronaviruses localize to the nucleus and inhibit innate immune signalling. J Gen Virol 95: 874-882.

311. Gierer S, Hofmann-Winkler H, Albuali WH, Bertram S, Al-Rubaish AM, et al. (2013) Lack of MERS coronavirus neutralizing antibodies in humans, eastern province, Saudi Arabia. Emerg Infect Dis 19: 2034-2036.

312. Aburizaiza AS, Mattes FM, Azhar EI, Hassan AM, Memish ZA, et al. (2014) Investigation of anti-middle East respiratory syndrome antibodies in blood donors and slaughterhouse workers in Jeddah and Makkah, Saudi Arabia, fall 2012. J Infect Dis 209: 243-246.

313. Woo PC, Wang M, Lau SK, Xu H, Poon RW, et al. (2007) Comparative analysis of twelve genomes of three novel group 2c and group 2d coronaviruses reveals unique group and subgroup features. J Virol 81: 1574-1585.

314. Woo PC, Lau SK, Li KS, Tsang AK, Yuen KY (2012) Genetic relatedness of the novel human group C betacoronavirus to Tylonycteris bat coronavirus HKU4 and Pipistrellus bat coronavirus HKU5. Emerg Microbes Infect 1: e35.

315. Lau SK, Li KS, Tsang AK, Lam CS, Ahmed S, et al. (2013) Genetic characterization of Betacoronavirus lineage C viruses in bats reveals marked sequence divergence in the spike protein of pipistrellus bat coronavirus HKU5 in Japanese pipistrelle: implications for the origin of the novel Middle East respiratory syndrome coronavirus. J Virol 87: 8638-8650.

316. Lelli D, Papetti A, Sabelli C, Rosti E, Moreno A, et al. (2013) Detection of coronaviruses in bats of various species in Italy. Viruses 5: 2679-2689.

317. Ithete NL, Stoffberg S, Corman VM, Cottontail VM, Richards LR, et al. (2013) Close relative of human Middle East respiratory syndrome coronavirus in bat, South Africa. Emerg Infect Dis 19: 1697-1699.

318. Corman VM, Ithete NL, Richards LR, Schoeman MC, Preiser W, et al. (2014) Rooting the phylogenetic tree of middle East respiratory syndrome coronavirus by characterization of a conspecific virus from an African bat. J Virol 88: 11297-11303.

319. Annan A, Baldwin HJ, Corman VM, Klose SM, Owusu M, et al. (2013) Human betacoronavirus 2c EMC/2012-related viruses in bats, Ghana and Europe. Emerg Infect Dis 19: 456-459.

320. Goes LG, Ruvalcaba SG, Campos AA, Queiroz LH, de Carvalho C, et al. (2013) Novel bat coronaviruses, Brazil and Mexico. Emerg Infect Dis 19: 1711-1713.

321. Yang Y, Du L, Liu C, Wang L, Ma C, et al. (2014) Receptor usage and cell entry of bat coronavirus HKU4 provide insight into bat-to-human transmission of MERS coronavirus. Proc Natl Acad Sci U S A 111: 12516-12521.

322. Wang Q, Qi J, Yuan Y, Xuan Y, Han P, et al. (2014) Bat origins of MERS-CoV supported by bat coronavirus HKU4 usage of human receptor CD26. Cell Host Microbe 16: 328-337.

323. Yang Y, Liu C, Du L, Jiang S, Shi Z, et al. (2015) Two mutations were critical for bat-to-human transmission of MERS coronavirus. J Virol.

324. Chan JF, Chan KH, Choi GK, To KK, Tse H, et al. (2013) Differential cell line susceptibility to the emerging novel human betacoronavirus 2c EMC/2012: implications for disease pathogenesis and clinical manifestation. J Infect Dis 207: 1743-1752.

325. Muller MA, Raj VS, Muth D, Meyer B, Kallies S, et al. (2012) Human coronavirus EMC does not require the SARS-coronavirus receptor and maintains broad replicative capability in mammalian cell lines. MBio 3.

326. Eckerle I, Corman VM, Muller MA, Lenk M, Ulrich RG, et al. (2014) Replicative Capacity of MERS Coronavirus in Livestock Cell Lines. Emerg Infect Dis 20: 276-279.

327. Cai Y, Yu SQ, Postnikova EN, Mazur S, Bernbaum JG, et al. (2014) CD26/DPP4 cell-surface expression in bat cells correlates with bat cell susceptibility to Middle East respiratory syndrome coronavirus (MERS-CoV) infection and evolution of persistent infection. PLoS One 9: e112060.

328. van Doremalen N, Miazgowicz KL, Milne-Price S, Bushmaker T, Robertson S, et al. (2014) Host species restriction of Middle East respiratory syndrome coronavirus through its receptor, dipeptidyl peptidase 4. J Virol 88: 9220-9232.

329. Reusken CB, Haagmans BL, Muller MA, Gutierrez C, Godeke GJ, et al. (2013) Middle East respiratory syndrome coronavirus neutralising serum antibodies in dromedary camels: a comparative serological study. Lancet Infect Dis 13: 859-866.

330. Haagmans BL, Al Dhahiry SH, Reusken CB, Raj VS, Galiano M, et al. (2014) Middle East respiratory syndrome coronavirus in dromedary camels: an outbreak investigation. Lancet Infect Dis 14: 140-145.

331. Meyer B, Muller MA, Corman VM, Reusken CB, Ritz D, et al. (2014) Antibodies against MERS coronavirus in dromedary camels, United Arab Emirates, 2003 and 2013. Emerg Infect Dis 20: 552-559.

332. Alexandersen S, Kobinger GP, Soule G, Wernery U (2014) Middle East respiratory syndrome coronavirus antibody reactors among camels in Dubai, United Arab Emirates, in 2005. Transbound Emerg Dis 61: 105-108.

333. Muller MA, Corman VM, Jores J, Meyer B, Younan M, et al. (2014) MERS coronavirus neutralizing antibodies in camels, Eastern Africa, 1983-1997. Emerg Infect Dis 20: 2093-2095.

334. Memish ZA, Cotten M, Meyer B, Watson SJ, Alsahafi AJ, et al. (2014) Human infection with MERS coronavirus after exposure to infected camels, Saudi Arabia, 2013. Emerg Infect Dis 20: 1012-1015.

335. Azhar EI, El-Kafrawy SA, Farraj SA, Hassan AM, Al-Saeed MS, et al. (2014) Evidence for camel-to-human transmission of MERS coronavirus. N Engl J Med 370: 2499-2505.

336. Muller MA, Meyer B, Corman VM, Al-Masri M, Turkestani A, et al. (2015) Presence of Middle East respiratory syndrome coronavirus antibodies in Saudi Arabia: a nationwide, cross-sectional, serological study. Lancet Infect Dis 15: 559-564.

337. Alagaili AN, Briese T, Mishra N, Kapoor V, Sameroff SC, et al. (2014) Middle East respiratory syndrome coronavirus infection in dromedary camels in Saudi Arabia. MBio 5: e00884-00814.

338. Yusof MF, Eltahir YM, Serhan WS, Hashem FM, Elsayed EA, et al. (2015) Prevalence of Middle East respiratory syndrome coronavirus (MERS-CoV) in dromedary camels in Abu Dhabi Emirate, United Arab Emirates. Virus Genes 50: 509-513.

339. Ma C, Li Y, Wang L, Zhao G, Tao X, et al. (2014) Intranasal vaccination with recombinant receptor-binding domain of MERS-CoV spike protein induces much stronger local mucosal immune responses than subcutaneous immunization: Implication for designing novel mucosal MERS vaccines. Vaccine 32: 2100-2108.

340. Both L, Banyard AC, van Dolleweerd C, Wright E, Ma JK, et al. (2013) Monoclonal antibodies for prophylactic and therapeutic use against viral infections. Vaccine 31: 1553-1559.

341. Forthal DN, Moog C (2009) Fc receptor-mediated antiviral antibodies. Curr Opin HIV AIDS 4: 388-393.

342. Michaud HA, Gomard T, Gros L, Thiolon K, Nasser R, et al. (2010) A crucial role for infected-cell/antibody immune complexes in the enhancement of endogenous antiviral immunity by short passive immunotherapy. PLoS Pathog 6: e1000948.

343. Nasser R, Pelegrin M, Michaud HA, Plays M, Piechaczyk M, et al. (2010) Long-lasting protective antiviral immunity induced by passive immunotherapies requires both neutralizing and effector functions of the administered monoclonal antibody. J Virol 84: 10169-10181.

344. Hsueh PR, Huang LM, Chen PJ, Kao CL, Yang PC (2004) Chronological evolution of IgM, IgA, IgG and neutralisation antibodies after infection with SARS-associated coronavirus. Clin Microbiol Infect 10: 1062-1066.

345. Xu X, Gao X (2004) Immunological responses against SARS-coronavirus infection in humans. Cell Mol Immunol 1: 119-122.

346. Grant PR, Garson JA, Tedder RS, Chan PK, Tam JS, et al. (2003) Detection of SARS coronavirus in plasma by real-time RT-PCR. N Engl J Med 349: 2468-2469.

347. Nie Y, Wang G, Shi X, Zhang H, Qiu Y, et al. (2004) Neutralizing antibodies in patients with severe acute respiratory syndrome-associated coronavirus infection. J Infect Dis 190: 1119-1126.

348. Tang F, Quan Y, Xin ZT, Wrammert J, Ma MJ, et al. (2011) Lack of peripheral memory B cell responses in recovered patients with severe acute respiratory syndrome: a six-year follow-up study. J Immunol 186: 7264-7268.

349. Buchholz UJ, Bukreyev A, Yang L, Lamirande EW, Murphy BR, et al. (2004) Contributions of the structural proteins of severe acute respiratory syndrome coronavirus to protective immunity. Proc Natl Acad Sci U S A 101: 9804-9809.

350. Casadevall A, Dadachova E, Pirofski LA (2004) Passive antibody therapy for infectious diseases. Nat Rev Microbiol 2: 695-703.

351. Zhu Z, Prabakaran P, Chen W, Broder CC, Gong R, et al. (2013) Human monoclonal antibodies as candidate therapeutics against emerging viruses and HIV-1. Virol Sin 28: 71-80.

352. Soo YO, Cheng Y, Wong R, Hui DS, Lee CK, et al. (2004) Retrospective comparison of convalescent plasma with continuing high-dose methylprednisolone treatment in SARS patients. Clin Microbiol Infect 10: 676-678.

353. Wong VW, Dai D, Wu AK, Sung JJ (2003) Treatment of severe acute respiratory syndrome with convalescent plasma. Hong Kong Med J 9: 199-201.

354. Peiris JS, Chu CM, Cheng VC, Chan KS, Hung IF, et al. (2003) Clinical progression and viral load in a community outbreak of coronavirus-associated SARS pneumonia: a prospective study. Lancet 361: 1767-1772.

355. Domingo E (1998) Quasispecies and the implications for virus persistence and escape. Clin Diagn Virol 10: 97-101.

356. ter Meulen J, van den Brink EN, Poon LL, Marissen WE, Leung CS, et al. (2006) Human monoclonal antibody combination against SARS coronavirus: synergy and coverage of escape mutants. PLoS Med 3: e237.

357. Dimitrov DS (2004) Virus entry: molecular mechanisms and biomedical applications. Nat Rev Microbiol 2: 109-122.

358. Elshabrawy HA, Coughlin MM, Baker SC, Prabhakar BS (2012) Human monoclonal antibodies against highly conserved HR1 and HR2 domains of the SARS-CoV spike protein are more broadly neutralizing. PLoS One 7: e50366.

359. Miyoshi-Akiyama T, Ishida I, Fukushi M, Yamaguchi K, Matsuoka Y, et al. (2011) Fully human monoclonal antibody directed to proteolytic cleavage site in severe acute respiratory syndrome (SARS) coronavirus S protein neutralizes the virus in a rhesus macaque SARS model. J Infect Dis 203: 1574-1581.

360. Duan J, Yan X, Guo X, Cao W, Han W, et al. (2005) A human SARS-CoV neutralizing antibody against epitope on S2 protein. Biochem Biophys Res Commun 333: 186-193.

361. Zhong X, Yang H, Guo ZF, Sin WY, Chen W, et al. (2005) B-cell responses in patients who have recovered from severe acute respiratory syndrome target a dominant site in the S2 domain of the surface spike glycoprotein. J Virol 79: 3401-3408.

362. Lai SC, Chong PC, Yeh CT, Liu LS, Jan JT, et al. (2005) Characterization of neutralizing monoclonal antibodies recognizing a 15-residues epitope on the spike protein HR2 region of severe acute respiratory syndrome coronavirus (SARS-CoV). J Biomed Sci 12: 711-727.

363. Lip KM, Shen S, Yang X, Keng CT, Zhang A, et al. (2006) Monoclonal antibodies targeting the HR2 domain and the region immediately upstream of the HR2 of the S protein neutralize in vitro infection of severe acute respiratory syndrome coronavirus. J Virol 80: 941-950.

364. Hua R, Zhou Y, Wang Y, Hua Y, Tong G (2004) Identification of two antigenic epitopes on SARS-CoV spike protein. Biochem Biophys Res Commun 319: 929-935.

365. Swain SL, McKinstry KK, Strutt TM (2012) Expanding roles for CD4(+) T cells in immunity to viruses. Nat Rev Immunol 12: 136-148.

366. Doherty PC, Christensen JP (2000) Accessing complexity: the dynamics of virus-specific T cell responses. Annu Rev Immunol 18: 561-592.

367. Kagi D, Vignaux F, Ledermann B, Burki K, Depraetere V, et al. (1994) Fas and perforin pathways as major mechanisms of T cell-mediated cytotoxicity. Science 265: 528-530.

368. Chen J, Lau YF, Lamirande EW, Paddock CD, Bartlett JH, et al. (2010) Cellular immune responses to severe acute respiratory syndrome coronavirus (SARS-CoV) infection in senescent BALB/c mice: CD4+ T cells are important in control of SARS-CoV infection. J Virol 84: 1289-1301.

369. Zhao J, Perlman S (2010) T cell responses are required for protection from clinical disease and for virus clearance in severe acute respiratory syndrome coronavirus-infected mice. J Virol 84: 9318-9325.

370. Channappanavar R, Fett C, Zhao J, Meyerholz DK, Perlman S (2014) Virus-specific memory CD8 T cells provide substantial protection from lethal severe acute respiratory syndrome coronavirus infection. J Virol 88: 11034-11044.

371. Chen H, Hou J, Jiang X, Ma S, Meng M, et al. (2005) Response of memory CD8+ T cells to severe acute respiratory syndrome (SARS) coronavirus in recovered SARS patients and healthy individuals. J Immunol 175: 591-598.

372. Li T, Qiu Z, Zhang L, Han Y, He W, et al. (2004) Significant changes of peripheral T lymphocyte subsets in patients with severe acute respiratory syndrome. J Infect Dis 189: 648-651.

373. Cameron MJ, Bermejo-Martin JF, Danesh A, Muller MP, Kelvin DJ (2008) Human immunopathogenesis of severe acute respiratory syndrome (SARS). Virus Res 133: 13-19.

374. Li T, Qiu Z, Han Y, Wang Z, Fan H, et al. (2003) Rapid loss of both CD4+ and CD8+ T lymphocyte subsets during the acute phase of severe acute respiratory syndrome. Chin Med J (Engl) 116: 985-987.

375. Fan YY, Huang ZT, Li L, Wu MH, Yu T, et al. (2009) Characterization of SARS-CoV-specific memory T cells from recovered individuals 4 years after infection. Arch Virol 154: 1093-1099.

376. Yang LT, Peng H, Zhu ZL, Li G, Huang ZT, et al. (2006) Long-lived effector/central memory T-cell responses to severe acute respiratory syndrome coronavirus (SARS-CoV) S antigen in recovered SARS patients. Clin Immunol 120: 171-178.

377. Zhou M, Xu D, Li X, Li H, Shan M, et al. (2006) Screening and identification of severe acute respiratory syndrome-associated coronavirus-specific CTL epitopes. J Immunol 177: 2138-2145.

378. Lv Y, Ruan Z, Wang L, Ni B, Wu Y (2009) Identification of a novel conserved HLA-A*0201-restricted epitope from the spike protein of SARS-CoV. BMC Immunol 10: 61.

379. Yang L, Peng H, Zhu Z, Li G, Huang Z, et al. (2007) Persistent memory CD4+ and CD8+ T-cell responses in recovered severe acute respiratory syndrome (SARS) patients to SARS coronavirus M antigen. J Gen Virol 88: 2740-2748.

380. Peng H, Yang LT, Li J, Lu ZQ, Wang LY, et al. (2006) Human memory T cell responses to SARS-CoV E protein. Microbes Infect 8: 2424-2431.

381. van den Brand JM, Smits SL, Haagmans BL (2015) Pathogenesis of Middle East respiratory syndrome coronavirus. J Pathol 235: 175-184.

382. Nicholls JM, Poon LL, Lee KC, Ng WF, Lai ST, et al. (2003) Lung pathology of fatal severe acute respiratory syndrome. Lancet 361: 1773-1778.

383. Cheung OY, Chan JW, Ng CK, Koo CK (2004) The spectrum of pathological changes in severe acute respiratory syndrome (SARS). Histopathology 45: 119-124.

384. Hui DS, Chan MC, Wu AK, Ng PC (2004) Severe acute respiratory syndrome (SARS): epidemiology and clinical features. Postgrad Med J 80: 373-381.

385. Hui DS, Wong PC, Wang C (2003) SARS: clinical features and diagnosis. Respirology 8 Suppl: S20-24.

386. Cunha CB, Opal SM (2014) Middle East respiratory syndrome (MERS): a new zoonotic viral pneumonia. Virulence 5: 650-654.

387. Al-Tawfiq JA, Hinedi K, Ghandour J, Khairalla H, Musleh S, et al. (2014) Middle East respiratory syndrome coronavirus: a case-control study of hospitalized patients. Clin Infect Dis 59: 160-165.

388. Nie Y, Wang P, Shi X, Wang G, Chen J, et al. (2004) Highly infectious SARS-CoV pseudotyped virus reveals the cell tropism and its correlation with receptor expression. Biochem Biophys Res Commun 321: 994-1000.

389. Sutton TC, Subbarao K (2015) Development of animal models against emerging coronaviruses: From SARS to MERS coronavirus. Virology 479-480C: 247-258.

390. Gu J, Korteweg C (2007) Pathology and pathogenesis of severe acute respiratory syndrome. Am J Pathol 170: 1136-1147.

391. Cheng VC, Lau SK, Woo PC, Yuen KY (2007) Severe acute respiratory syndrome coronavirus as an agent of emerging and reemerging infection. Clin Microbiol Rev 20: 660-694.

392. Faure E, Poissy J, Goffard A, Fournier C, Kipnis E, et al. (2014) Distinct immune response in two MERS-CoV-infected patients: can we go from bench to bedside? PLoS One 9: e88716.

393. Lau SK, Lau CC, Chan KH, Li CP, Chen H, et al. (2013) Delayed induction of proinflammatory cytokines and suppression of innate antiviral response by the novel Middle East respiratory syndrome coronavirus: implications for pathogenesis and treatment. J Gen Virol 94: 2679-2690.

394. Scheuplein VA, Seifried J, Malczyk AH, Miller L, Hocker L, et al. (2015) High secretion of interferons by human plasmacytoid dendritic cells upon recognition of Middle East respiratory syndrome coronavirus. J Virol 89: 3859-3869.

395. Reuss A, Litterst A, Drosten C, Seilmaier M, Bohmer M, et al. (2014) Contact investigation for imported case of Middle East respiratory syndrome, Germany. Emerg Infect Dis 20: 620-625.

396. Kapoor M, Pringle K, Kumar A, Dearth S, Liu L, et al. (2014) Clinical and laboratory findings of the first imported case of Middle East respiratory syndrome coronavirus to the United States. Clin Infect Dis 59: 1511-1518.

397. Janice Oh HL, Ken-En Gan S, Bertoletti A, Tan YJ (2012) Understanding the T cell immune response in SARS coronavirus infection. Emerg Microbes Infect 1: e23.

398. Zhao J, Li K, Wohlford-Lenane C, Agnihothram SS, Fett C, et al. (2014) Rapid generation of a mouse model for Middle East respiratory syndrome. Proc Natl Acad Sci U S A 111: 4970-4975.

399. (2003) Case Definitions for Surveillance of Severe Acute Respiratory Syndrome (SARS). http://www.who.int/csr/sars/casedefinition/en/. World Health Organization.

400. Sayer D, Whidborne R, Brestovac B, Trimboli F, Witt C, et al. (2001) HLA-DRB1 DNA sequencing based typing: an approach suitable for high throughput typing including unrelated bone marrow registry donors. Tissue Antigens 57: 46-54.

401. Ng OW, Keng CT, Leung CS, Peiris JS, Poon LL, et al. (2014) Substitution at aspartic acid 1128 in the SARS coronavirus spike glycoprotein mediates escape from a S2 domain-targeting neutralizing monoclonal antibody. PLoS One 9: e102415.

402. Garcia JM, Lai JC (2011) Production of influenza pseudotyped lentiviral particles and their use in influenza research and diagnosis: an update. Expert Rev Anti Infect Ther 9: 443-455.

403. Giroglou T, Cinatl J, Jr., Rabenau H, Drosten C, Schwalbe H, et al. (2004) Retroviral vectors pseudotyped with severe acute respiratory syndrome coronavirus S protein. J Virol 78: 9007-9015.

404. Moore MJ, Dorfman T, Li W, Wong SK, Li Y, et al. (2004) Retroviruses pseudotyped with the severe acute respiratory syndrome coronavirus spike protein efficiently infect cells expressing angiotensin-converting enzyme 2. J Virol 78: 10628-10635.

405. Temperton NJ, Chan PK, Simmons G, Zambon MC, Tedder RS, et al. (2005) Longitudinally profiling neutralizing antibody response to SARS coronavirus with pseudotypes. Emerg Infect Dis 11: 411-416.

406. He Y, Li J, Li W, Lustigman S, Farzan M, et al. (2006) Cross-neutralization of human and palm civet severe acute respiratory syndrome coronaviruses by antibodies targeting the receptor-binding domain of spike protein. J Immunol 176: 6085-6092.

407. Pal P, Fox JM, Hawman DW, Huang YJ, Messaoudi I, et al. (2014) Chikungunya viruses that escape monoclonal antibody therapy are clinically attenuated, stable, and not purified in mosquitoes. J Virol 88: 8213-8226.

408. O'Donnell CD, Vogel L, Wright A, Das SR, Wrammert J, et al. (2012) Antibody pressure by a human monoclonal antibody targeting the 2009 pandemic H1N1 virus hemagglutinin drives the emergence of a virus with increased virulence in mice. MBio 3.

409. Sui J, Deming M, Rockx B, Liddington RC, Zhu QK, et al. (2014) Effects of human anti-spike protein receptor binding domain antibodies on severe acute respiratory syndrome coronavirus neutralization escape and fitness. J Virol 88: 13769-13780.

410. Rockx B, Donaldson E, Frieman M, Sheahan T, Corti D, et al. (2010) Escape from human monoclonal antibody neutralization affects in vitro and in vivo fitness of severe acute respiratory syndrome coronavirus. J Infect Dis 201: 946-955.

411. Fukushi M, Yoshinaka Y, Matsuoka Y, Hatakeyama S, Ishizaka Y, et al. (2012) Monitoring of S protein maturation in the endoplasmic reticulum by calnexin is important for the infectivity of severe acute respiratory syndrome coronavirus. J Virol 86: 11745-11753.

412. Shen S, Law YC, Liu DX (2004) A single amino acid mutation in the spike protein of coronavirus infectious bronchitis virus hampers its maturation and incorporation into virions at the nonpermissive temperature. Virology 326: 288-298.

413. Vijaykrishna D, Smith GJ, Zhang JX, Peiris JS, Chen H, et al. (2007) Evolutionary insights into the ecology of coronaviruses. J Virol 81: 4012-4020.

414. Graham RL, Baric RS (2010) Recombination, reservoirs, and the modular spike: mechanisms of coronavirus cross-species transmission. J Virol 84: 3134-3146.

415. Shi Z, Hu Z (2008) A review of studies on animal reservoirs of the SARS coronavirus. Virus Res 133: 74-87.

416. Drexler JF, Gloza-Rausch F, Glende J, Corman VM, Muth D, et al. (2010) Genomic characterization of severe acute respiratory syndrome-related coronavirus in European bats and classification of coronaviruses based on partial RNA-dependent RNA polymerase gene sequences. J Virol 84: 11336-11349.

417. Rockx B, Corti D, Donaldson E, Sheahan T, Stadler K, et al. (2008) Structural basis for potent cross-neutralizing human monoclonal antibody protection against lethal human and zoonotic severe acute respiratory syndrome coronavirus challenge. J Virol 82: 3220-3235.

418. Sui J, Li W, Roberts A, Matthews LJ, Murakami A, et al. (2005) Evaluation of human monoclonal antibody 80R for immunoprophylaxis of severe acute respiratory syndrome by an animal study, epitope mapping, and analysis of spike variants. J Virol 79: 5900-5906.

419. Zhu Z, Chakraborti S, He Y, Roberts A, Sheahan T, et al. (2007) Potent cross-reactive neutralization of SARS coronavirus isolates by human monoclonal antibodies. Proc Natl Acad Sci U S A 104: 12123-12128.

420. Mitsuki YY, Ohnishi K, Takagi H, Oshima M, Yamamoto T, et al. (2008) A single amino acid substitution in the S1 and S2 Spike protein domains determines the neutralization escape phenotype of SARS-CoV. Microbes Infect 10: 908-915.

421. Bosch BJ, van der Zee R, de Haan CA, Rottier PJ (2003) The coronavirus spike protein is a class I virus fusion protein: structural and functional characterization of the fusion core complex. J Virol 77: 8801-8811.

422. Saylor C, Dadachova E, Casadevall A (2009) Monoclonal antibody-based therapies for microbial diseases. Vaccine 27 Suppl 6: G38-46.

423. Sakamoto S, Tanaka H, Morimoto S (2015) Towards the prophylactic and therapeutic use of human neutralizing monoclonal antibodies for Middle East respiratory syndrome coronavirus (MERS-CoV). Ann Transl Med 3: 35.

424. Zhao J, Perera RA, Kayali G, Meyerholz D, Perlman S, et al. (2015) Passive immunotherapy with dromedary immune serum in an experimental animal model for middle East respiratory syndrome coronavirus infection. J Virol 89: 6117-6120.

425. Agnihothram S, Gopal R, Yount BL, Jr., Donaldson EF, Menachery VD, et al. (2014) Evaluation of serologic and antigenic relationships between middle eastern

respiratory syndrome coronavirus and other coronaviruses to develop vaccine platforms for the rapid response to emerging coronaviruses. J Infect Dis 209: 995-1006.

426. Chan KH, Chan JF, Tse H, Chen H, Lau CC, et al. (2013) Cross-reactive antibodies in convalescent SARS patients' sera against the emerging novel human coronavirus EMC (2012) by both immunofluorescent and neutralizing antibody tests. J Infect 67: 130-140.

427. Supekar VM, Bruckmann C, Ingallinella P, Bianchi E, Pessi A, et al. (2004) Structure of a proteolytically resistant core from the severe acute respiratory syndrome coronavirus S2 fusion protein. Proc Natl Acad Sci U S A 101: 17958-17963.

428. Wargo AR, Kurath G (2011) In vivo fitness associated with high virulence in a vertebrate virus is a complex trait regulated by host entry, replication, and shedding. J Virol 85: 3959-3967.

429. Luo Z, Matthews AM, Weiss SR (1999) Amino acid substitutions within the leucine zipper domain of the murine coronavirus spike protein cause defects in oligomerization and the ability to induce cell-to-cell fusion. J Virol 73: 8152-8159.

430. Presta LG (2008) Molecular engineering and design of therapeutic antibodies. Curr Opin Immunol 20: 460-470.

431. Kontermann RE (2009) Strategies to extend plasma half-lives of recombinant antibodies. BioDrugs 23: 93-109.

432. Jefferis R (2009) Glycosylation as a strategy to improve antibody-based therapeutics. Nat Rev Drug Discov 8: 226-234.

433. Beck A, Wagner-Rousset E, Bussat MC, Lokteff M, Klinguer-Hamour C, et al. (2008) Trends in glycosylation, glycoanalysis and glycoengineering of therapeutic antibodies and Fc-fusion proteins. Curr Pharm Biotechnol 9: 482-501.

434. Mabry R, Snavely M (2010) Therapeutic bispecific antibodies: The selection of stable single-chain fragments to overcome engineering obstacles. IDrugs 13: 543-549.

435. Mazor Y, Van Blarcom T, Mabry R, Iverson BL, Georgiou G (2007) Isolation of engineered, full-length antibodies from libraries expressed in Escherichia coli. Nat Biotechnol 25: 563-565.

436. Li H, Sethuraman N, Stadheim TA, Zha D, Prinz B, et al. (2006) Optimization of humanized IgGs in glycoengineered Pichia pastoris. Nat Biotechnol 24: 210-215.

437. Ko K (2014) Expression of recombinant vaccines and antibodies in plants. Monoclon Antib Immunodiagn Immunother 33: 192-198.

438. Rodrigues ME, Costa AR, Henriques M, Azeredo J, Oliveira R (2010) Technological progresses in monoclonal antibody production systems. Biotechnol Prog 26: 332-351.

439. Sainz B, Jr., Mossel EC, Gallaher WR, Wimley WC, Peters CJ, et al. (2006) Inhibition of severe acute respiratory syndrome-associated coronavirus (SARS-CoV) infectivity by peptides analogous to the viral spike protein. Virus Res 120: 146-155.

440. Betts MR, Brenchley JM, Price DA, De Rosa SC, Douek DC, et al. (2003) Sensitive and viable identification of antigen-specific CD8+ T cells by a flow cytometric assay for degranulation. J Immunol Methods 281: 65-78.

441. Harding CV, Geuze HJ (1993) Antigen processing and intracellular traffic of antigens and MHC molecules. Curr Opin Cell Biol 5: 596-605.

442. Rivino L, Tan AT, Chia A, Kumaran EA, Grotenbreg GM, et al. (2013) Defining CD8+ T cell determinants during human viral infection in populations of Asian ethnicity. J Immunol 191: 4010-4019.

443. Li T, Xie J, He Y, Fan H, Baril L, et al. (2006) Long-term persistence of robust antibody and cytotoxic T cell responses in recovered patients infected with SARS coronavirus. PLoS One 1: e24.

444. Patronov A, Doytchinova I (2013) T-cell epitope vaccine design by immunoinformatics. Open Biol 3: 120139.

445. Hoof I, Peters B, Sidney J, Pedersen LE, Sette A, et al. (2009) NetMHCpan, a method for MHC class I binding prediction beyond humans. Immunogenetics 61: 1-13.

446. Liu J, Sun Y, Qi J, Chu F, Wu H, et al. (2010) The membrane protein of severe acute respiratory syndrome coronavirus acts as a dominant immunogen revealed by a clustering region of novel functionally and structurally defined cytotoxic T-lymphocyte epitopes. J Infect Dis 202: 1171-1180.

447. Kim TW, Lee JH, Hung CF, Peng S, Roden R, et al. (2004) Generation and characterization of DNA vaccines targeting the nucleocapsid protein of severe acute respiratory syndrome coronavirus. J Virol 78: 4638-4645.

448. Tobery TW, Wang S, Wang XM, Neeper MP, Jansen KU, et al. (2001) A simple and efficient method for the monitoring of antigen-specific T cell responses using peptide pool arrays in a modified ELISpot assay. J Immunol Methods 254: 59-66.

449. Rammensee HG (1995) Chemistry of peptides associated with MHC class I and class II molecules. Curr Opin Immunol 7: 85-96.

450. Gammon G, Geysen HM, Apple RJ, Pickett E, Palmer M, et al. (1991) T cell determinant structure: cores and determinant envelopes in three mouse major histocompatibility complex haplotypes. J Exp Med 173: 609-617.

451. Schoenborn JR, Wilson CB (2007) Regulation of interferon-gamma during innate and adaptive immune responses. Adv Immunol 96: 41-101.

452. Barry M, Bleackley RC (2002) Cytotoxic T lymphocytes: all roads lead to death. Nat Rev Immunol 2: 401-409.

453. Gonzalez-Galarza FF, Christmas S, Middleton D, Jones AR (2011) Allele frequency net: a database and online repository for immune gene frequencies in worldwide populations. Nucleic Acids Research 39: D913-D919.

454. Akram A, Inman RD (2013) Co-expression of HLA-B7 and HLA-B27 alleles is associated with B7-restricted immunodominant responses following influenza infection. Eur J Immunol 43: 3254-3267.

455. Kuniholm MH, Anastos K, Kovacs A, Gao X, Marti D, et al. (2013) Relation of HLA class I and II supertypes with spontaneous clearance of hepatitis C virus. Genes Immun 14: 330-335.

456. Samandary S, Kridane-Miledi H, Sandoval JS, Choudhury Z, Langa-Vives F, et al. (2014) Associations of HLA-A, HLA-B and HLA-C alleles frequency with prevalence of herpes simplex virus infections and diseases across global populations: implication for the development of an universal CD8+ T-cell epitope-based vaccine. Hum Immunol 75: 715-729.

457. Schellens IM, Spits HB, Navis M, Westerlaken GH, Nanlohy NM, et al. (2014) Differential characteristics of cytotoxic T lymphocytes restricted by the protective HLA alleles B*27 and B*57 in HIV-1 infection. J Acquir Immune Defic Syndr 67: 236-245.

458. Ng MH, Lau KM, Li L, Cheng SH, Chan WY, et al. (2004) Association of human-leukocyte-antigen class I (B*0703) and class II (DRB1*0301) genotypes with susceptibility and resistance to the development of severe acute respiratory syndrome. J Infect Dis 190: 515-518.

459. Lin M, Tseng HK, Trejaut JA, Lee HL, Loo JH, et al. (2003) Association of HLA class I with severe acute respiratory syndrome coronavirus infection. BMC Med Genet 4: 9.

460. Welsh RM, Selin LK (2002) No one is naive: the significance of heterologous T-cell immunity. Nat Rev Immunol 2: 417-426.

461. Frankild S, de Boer RJ, Lund O, Nielsen M, Kesmir C (2008) Amino acid similarity accounts for T cell cross-reactivity and for "holes" in the T cell repertoire. PLoS One 3: e1831.

462. Welsh RM, Che JW, Brehm MA, Selin LK (2010) Heterologous immunity between viruses. Immunol Rev 235: 244-266.

463. Bashyam HS, Green S, Rothman AL (2006) Dengue virus-reactive CD8+ T cells display quantitative and qualitative differences in their response to variant epitopes of heterologous viral serotypes. J Immunol 176: 2817-2824.

464. Nilges K, Hohn H, Pilch H, Neukirch C, Freitag K, et al. (2003) Human papillomavirus type 16 E7 peptide-directed CD8+ T cells from patients with cervical cancer are cross-reactive with the coronavirus NS2 protein. J Virol 77: 5464-5474.

465. Wedemeyer H, Mizukoshi E, Davis AR, Bennink JR, Rehermann B (2001) Cross-reactivity between hepatitis C virus and Influenza A virus determinant-specific cytotoxic T cells. J Virol 75: 11392-11400.

466. Vali B, Tohn R, Cohen MJ, Sakhdari A, Sheth PM, et al. (2011) Characterization of cross-reactive CD8+ T-cell recognition of HLA-A2-restricted HIV-Gag (SLYNTVATL) and HCV-NS5b (ALYDVVSKL) epitopes in individuals infected with human immunodeficiency and hepatitis C viruses. J Virol 85: 254-263.

467. He B, Zhang Y, Xu L, Yang W, Yang F, et al. (2014) Identification of diverse alphacoronaviruses and genomic characterization of a novel severe acute respiratory syndrome-like coronavirus from bats in China. J Virol 88: 7070-7082.

468. Castelli M, Cappelletti F, Diotti RA, Sautto G, Criscuolo E, et al. (2013) Peptide-based vaccinology: experimental and computational approaches to target hypervariable viruses through the fine characterization of protective epitopes recognized by monoclonal antibodies and the identification of T-cell-activating peptides. Clin Dev Immunol 2013: 521231.

469. Themeli M, Riviere I, Sadelain M (2015) New Cell Sources for T Cell Engineering and Adoptive Immunotherapy. Cell Stem Cell 16: 357-366.

470. Gehring AJ, Xue SA, Ho ZZ, Teoh D, Ruedl C, et al. (2011) Engineering virus-specific T cells that target HBV infected hepatocytes and hepatocellular carcinoma cell lines. J Hepatol 55: 103-110.

471. Lipowska-Bhalla G, Gilham DE, Hawkins RE, Rothwell DG (2012) Targeted immunotherapy of cancer with CAR T cells: achievements and challenges. Cancer Immunol Immunother 61: 953-962.

472. Sautto GA, Wisskirchen K, Clementi N, Castelli M, Diotti RA, et al. (2015) Chimeric antigen receptor (CAR)-engineered T cells redirected against hepatitis C virus (HCV) E2 glycoprotein. Gut.

473. Krebs K, Bottinger N, Huang LR, Chmielewski M, Arzberger S, et al. (2013) T cells expressing a chimeric antigen receptor that binds hepatitis B virus envelope proteins control virus replication in mice. Gastroenterology 145: 456-465.

474. Talbot SJ, Blair NF, McGill N, Ligertwood Y, Dutia BM, et al. (2013) An Influenza Virus M2 Protein Specific Chimeric Antigen Receptor Modulates Influenza A/WSN/33 H1N1 Infection In Vivo. Open Virol J 7: 28-36.

475. Dube M, Bego MG, Paquay C, Cohen EA (2010) Modulation of HIV-1-host interaction: role of the Vpu accessory protein. Retrovirology 7: 114.

476. Hofmann-Winkler H, Kaup F, Pohlmann S (2012) Host cell factors in filovirus entry: novel players, new insights. Viruses 4: 3336-3362.

477. Li K, Phoo WW, Luo D (2014) Functional interplay among the flavivirus NS3 protease, helicase, and cofactors. Virol Sin 29: 74-85.

478. Shaw ML (2011) The host interactome of influenza virus presents new potential targets for antiviral drugs. Rev Med Virol 21: 358-369.

479. Zhong Y, Tan YW, Liu DX (2012) Recent progress in studies of arterivirus- and coronavirus-host interactions. Viruses 4: 980-1010.

480. Surjit M, Lal SK (2008) The SARS-CoV nucleocapsid protein: a protein with multifarious activities. Infect Genet Evol 8: 397-405.

481. Chang CK, Hou MH, Chang CF, Hsiao CD, Huang TH (2014) The SARS coronavirus nucleocapsid protein--forms and functions. Antiviral Res 103: 39-50.

482. Ng ML, Tan SH, See EE, Ooi EE, Ling AE (2003) Proliferative growth of SARS coronavirus in Vero E6 cells. J Gen Virol 84: 3291-3303.

483. Diemer C, Schneider M, Seebach J, Quaas J, Frosner G, et al. (2008) Cell type-specific cleavage of nucleocapsid protein by effector caspases during SARS coronavirus infection. J Mol Biol 376: 23-34.

484. Eleouet JF, Slee EA, Saurini F, Castagne N, Poncet D, et al. (2000) The viral nucleocapsid protein of transmissible gastroenteritis coronavirus (TGEV) is cleaved by caspase-6 and -7 during TGEV-induced apoptosis. J Virol 74: 3975-3983.

485. Condeelis J (1995) Elongation factor 1 alpha, translation and the cytoskeleton. Trends Biochem Sci 20: 169-170.

486. Sasikumar AN, Perez WB, Kinzy TG (2012) The many roles of the eukaryotic elongation factor 1 complex. Wiley Interdiscip Rev RNA 3: 543-555.

487. Lund A, Knudsen SM, Vissing H, Clark B, Tommerup N (1996) Assignment of human elongation factor 1alpha genes: EEF1A maps to chromosome 6q14 and EEF1A2 to 20q13.3. Genomics 36: 359-361.

488. Soares DC, Barlow PN, Newbery HJ, Porteous DJ, Abbott CM (2009) Structural models of human eEF1A1 and eEF1A2 reveal two distinct surface clusters of sequence variation and potential differences in phosphorylation. PLoS One 4: e6315.

489. Mateyak MK, Kinzy TG (2010) eEF1A: thinking outside the ribosome. J Biol Chem 285: 21209-21213.

490. Li D, Wei T, Abbott CM, Harrich D (2013) The unexpected roles of eukaryotic translation elongation factors in RNA virus replication and pathogenesis. Microbiol Mol Biol Rev 77: 253-266.

491. Davis WG, Blackwell JL, Shi PY, Brinton MA (2007) Interaction between the cellular protein eEF1A and the 3'-terminal stem-loop of West Nile virus genomic RNA facilitates viral minus-strand RNA synthesis. J Virol 81: 10172-10187.

492. Warren K, Wei T, Li D, Qin F, Warrilow D, et al. (2012) Eukaryotic elongation factor 1 complex subunits are critical HIV-1 reverse transcription cofactors. Proc Natl Acad Sci U S A 109: 9587-9592.

493. Cimarelli A, Luban J (1999) Translation elongation factor 1-alpha interacts specifically with the human immunodeficiency virus type 1 Gag polyprotein. J Virol 73: 5388-5401.

494. Abbas W, Dichamp I, Herbein G (2012) The HIV-1 Nef protein interacts with two components of the 40S small ribosomal subunit, the RPS10 protein and the 18S rRNA. Virol J 9: 103.

495. Abbas W, Khan KA, Kumar A (2014) Blockade of BFA-mediated apoptosis in macrophages by the HIV-1 Nef protein. 5: e1080.

496. Yue J, Shukla R, Accardi R, Zanella-Cleon I, Siouda M, et al. (2011) Cutaneous human papillomavirus type 38 E7 regulates actin cytoskeleton structure for increasing cell proliferation through CK2 and the eukaryotic elongation factor 1A. J Virol 85: 8477-8494.

497. Lin WS, Jiao BY, Wu YL, Chen WN, Lin X (2012) Hepatitis B virus X protein blocks filamentous actin bundles by interaction with eukaryotic translation elongat ion factor 1 alpha 1. J Med Virol 84: 871-877.

498. Zhang X, Shi H, Chen J, Shi D, Li C, et al. (2014) EF1A interacting with nucleocapsid protein of transmissible gastroenteritis coronavirus and plays a role in virus replication. Vet Microbiol 172: 443-448.

499. Bohnsack MT, Regener K, Schwappach B, Saffrich R, Paraskeva E, et al. (2002) Exp5 exports eEF1A via tRNA from nuclei and synergizes with other transport pathways to confine translation to the cytoplasm. EMBO J 21: 6205-6215.

500. Calado A, Treichel N, Muller EC, Otto A, Kutay U (2002) Exportin-5-mediated nuclear export of eukaryotic elongation factor 1A and tRNA. EMBO J 21: 6216-6224.

501. Murthi A, Shaheen HH, Huang HY, Preston MA, Lai TP, et al. (2010) Regulation of tRNA bidirectional nuclear-cytoplasmic trafficking in Saccharomyces cerevisiae. Mol Biol Cell 21: 639-649.

502. Wurm T, Chen H, Hodgson T, Britton P, Brooks G, et al. (2001) Localization to the nucleolus is a common feature of coronavirus nucleoproteins, and the protein may disrupt host cell division. J Virol 75: 9345-9356.

503. Chen H, Wurm T, Britton P, Brooks G, Hiscox JA (2002) Interaction of the coronavirus nucleoprotein with nucleolar antigens and the host cell. J Virol 76: 5233-5250.

504. Timani KA, Liao Q, Ye L, Zeng Y, Liu J, et al. (2005) Nuclear/nucleolar localization properties of C-terminal nucleocapsid protein of SARS coronavirus. Virus Res 114: 23-34.

505. Walsh D, Mohr I (2011) Viral subversion of the host protein synthesis machinery. Nat Rev Microbiol 9: 860-875.

506. Hsu YY, Liu YN, Lu WW, Kung SH (2009) Visualizing and quantifying the differential cleavages of the eukaryotic translation initiation factors eIF4GI and eIF4GII in the enterovirus-infected cell. Biotechnol Bioeng 104: 1142-1152.

507. de Breyne S, Bonderoff JM, Chumakov KM, Lloyd RE, Hellen CU (2008) Cleavage of eukaryotic initiation factor eIF5B by enterovirus 3C proteases. Virology 378: 118-122.

508. Komarova AV, Real E, Borman AM, Brocard M, England P, et al. (2007) Rabies virus matrix protein interplay with eIF3, new insights into rabies virus pathogenesis. Nucleic Acids Res 35: 1522-1532.

509. Sato H, Masuda M, Kanai M, Tsukiyama-Kohara K, Yoneda M, et al. (2007) Measles virus N protein inhibits host translation by binding to eIF3-p40. J Virol 81: 11569-11576.

510. Xiao H, Xu LH, Yamada Y, Liu DX (2008) Coronavirus spike protein inhibits host cell translation by interaction with eIF3f. PLoS One 3: e1494.

511. McInerney GM, Kedersha NL, Kaufman RJ, Anderson P, Liljestrom P (2005) Importance of eIF2alpha phosphorylation and stress granule assembly in alphavirus translation regulation. Mol Biol Cell 16: 3753-3763.

512. Raaben M, Groot Koerkamp MJ, Rottier PJ, de Haan CA (2007) Mouse hepatitis coronavirus replication induces host translational shutoff and mRNA decay, with concomitant formation of stress granules and processing bodies. Cell Microbiol 9: 2218-2229.

513. Chulu JL, Huang WR, Wang L, Shih WL, Liu HJ (2010) Avian reovirus nonstructural protein p17-induced G(2)/M cell cycle arrest and host cellular protein translation shutoff involve activation of p53-dependent pathways. J Virol 84: 7683-7694.

514. Ji WT, Wang L, Lin RC, Huang WR, Liu HJ (2009) Avian reovirus influences phosphorylation of several factors involved in host protein translation including eukaryotic translation elongation factor 2 (eEF2) in Vero cells. Biochem Biophys Res Commun 384: 301-305.

515. Taylor MP, Koyuncu OO, Enquist LW (2011) Subversion of the actin cytoskeleton during viral infection. Nat Rev Microbiol 9: 427-439.

516. Spear M, Wu Y (2014) Viral exploitation of actin: force-generation and scaffolding functions in viral infection. Virol Sin 29: 139-147.

517. Winder SJ (2003) Structural insights into actin-binding, branching and bundling proteins. Curr Opin Cell Biol 15: 14-22.

518. Gross SR, Kinzy TG (2005) Translation elongation factor 1A is essential for regulation of the actin cytoskeleton and cell morphology. Nat Struct Mol Biol 12: 772-778.

519. Yang F, Demma M, Warren V, Dharmawardhane S, Condeelis J (1990) Identification of an actin-binding protein from Dictyostelium as elongation factor 1a. Nature 347: 494-496.

520. Gross SR, Kinzy TG (2007) Improper organization of the actin cytoskeleton affects protein synthesis at initiation. Mol Cell Biol 27: 1974-1989.

521. Perez WB, Kinzy TG (2014) Translation elongation factor 1A mutants with altered actin bundling activity show reduced aminoacyl-tRNA binding and alter initiation via eIF2alpha phosphorylation. J Biol Chem 289: 20928-20938.